UNIVERSITÁ DEGLI STUDI DI PADOVA

Dipartimento di Fisica e Astronomia "Galileo Galilei"

Master Degree in Astrophysics and Csomology

Final Dissertation

Quantum Decoherence in Axion Models of Inflation

Thesis supervisor

Prof. Nicola Bartolo

Candidate

Shota Khetsuriani

Academic Year 2024/2025

Dedication

I dedicate this thesis to my late beloved grandmother, Nargiza, who was an inspiration both in my personal and academic life.

A philologist and devoted researcher for over 65 years, Nargiza's love for her work deeply inspired me to pursue a master's degree. Sadly, she will not be able to witness my graduation, but her devotion to research continues to influence my academic path.

Abstract

Cosmic inflation predicts the production of quantum fluctuations that seed all the structures present in the universe today. However, these structures (such as Cosmic Microwave Background anisotropies or the large-scale distribution of galaxies) are classical objects and show no sign of quantumness. The problem of quantum-to-classical transition arises - how did fluctuations, initially quantum in nature, become classical? Quantum decoherence is considered the leading mechanism of classicalization of the primordial perturbations. In the framework of decoherence, the primordial perturbations are viewed as an open quantum system interacting with a surrounding environment. The Lindblad equation can model the evolution of these perturbations, which will lead to decoherence and possibly to corrections to cosmological observables, such as the power spectrum of inflationary perturbations. This mechanism has been extensively studied in the recent literature in the context of single scalar field-driven inflation. We apply the Lindblad formalism to the axion models of inflation that involve the coupling $\phi \tilde{F}^{\mu\nu} F_{\mu\nu}$ to some gauge fields. In our construction, these gauge fields become the environment that decoheres the inflaton perturbations. This process is modeled using the Lindblad equation, and we study how decoherence affects the power spectrum of primordial perturbations in axion models of inflation. We also calculate the rate of decoherence in the said model.

Additionally, we calculate the quantum discord as a measure of quantumness and find that on observable scales, we get both high and negligibly small values of discord. We also motivate the need to complement the study of quantum discord with other measures of quantumness, such as the Bell inequality violation or state separability.

"What we observe is not nature itself, but nature exposed to our method of questioning"

Werner Heisenberg

Contents

1 Introduction

Inflation, first introduced by A. Guth [1] to circumvent the shortcomings of the standard hot Big Bang model, has become paradigmatic in recent decades, given that it is consistent up to now with a variety of cosmological data. Implementation of inflation into the standard hot Big Bang scenario goes as follows: before the universe was radiation-dominated and the Robertson-Walker scale factor $a(t)$ grew as $\sqrt{t}$, there was a period when the energy density of the universe was dominated by vacuum energy of the inflaton - the field driving inflation - leading to a quasi-exponential growth of the scale factor. Inflation ends when the inflaton starts to oscillate about the minimum of the potential, decaying into Standard Model particles and initiating the radiation-dominated epoch of the universe.

Imposing inflation solved some of the outstanding problems in standard cosmology. Namely, homogeneity and isotropy of the Cosmic Microwave Background (CMB) on scales that were not in causal contact according to the hot Big Bang can be explained by an early epoch of accelerated expansion. It also explains why the universe is observed to be consistent with spatial flatness. Otherwise, achieving this would require fine-tuning cosmological parameters, which is generally considered a shortcoming of any physical theory.

In any consistent models of inflation arguably the most profound insight is that all structures in the universe originated from quantum fluctuations produced during inflation and amplified to cosmic significance by gravitational instability. This scenario is favored by data, namely the observed nearly scale-invariant power spectrum of curvature perturbations (explained in detail below).

Even though the inflationary perturbations are quantum in nature, all the cosmic structures we observe today seem to possess no trace of "quantumness". The problem of quantum-to-classical transition in the early universe arises. The answer to this problem is still not conclusive and is the subject of recent studies [2, 3, 4, 5, 6, 7, 8]. We have no concrete evidence on what causes classicalization of inherently quantum fluctuations. Moreover, it has been shown, that by replacing quantum fluctuations of a free scalar field with classical stochastic perturbations, at least in the lowest order of correlation functions, we obtain essentially the same results, meaning, that if we stick to the power spectrum of cosmological perturbations, the two scenarios are indistinguishable.

The most probable cause of the classicalization, however, is the effect of quantum decoherence, which is an experimentally observed phenomenon.

Quantum decoherence in the context of inflation has been studied extensively in recent years [2, 4, 5, 6]. Decoherence implies that the inflaton is an open quantum system, interacting with its environment. The two main types of environments studied so far are i) sub-horizon tensor and scalar modes, that decohere the super-horizon modes of observational interest [7, 9, 10] and ii) other fields coupled with the inflaton field [2]. We will mostly be interested in the second type of environment since other fields are bound to exist during inflation, at least the ones resulting in the reheating and subsequent radiation-dominated epoch.

The evolution of an open quantum system can be described by the Lindblad equation [11, 12], however, some assumptions are required that will be discussed in this thesis. The Lindblad equation

captures how the interaction with the environment modifies the off-diagonal elements of the quantum density operator, sometimes referred to as the density matrix in the literature, defined simply by $\rho = |\psi\rangle \langle\psi|$. This modification makes the off-diagonal terms go to zero in a preferred basis chosen by the interaction form.

Decoherence can also change the diagonal terms in the density matrix, which means that probabilities of the possible outcomes of measurements may be modified. This leads to an important point studied in Refs. [2, 3, 4, 13, 14, 15]: in the cosmological context, applying decoherence to the perturbations in the early universe can modify their statistical properties significantly. Since the latter are well-constrained by data from CMB observations [16, 17, 18], this opens up a new window to study cosmic decoherence and compare the obtained statistics with observations. This has recently been done in [2, 4] for the case of a single field scalar inflaton coupled with massive scalar fields.

Despite the success of the inflationary paradigm throughout the years, there remain open questions of fundamental importance. Namely, one important caveat is that we do not know what the inflaton actually is. Therefore we cannot conclusively assume that the inflaton is a scalar field. In fact, a compelling particle physics scenario is lacking. The problem arises due to the flatness of a scalar potential $V(\phi)$ required to maintain inflation for a sufficient amount of time. In order to have a successful inflation the slow-roll parameters must obey $\epsilon_V, |\eta_V| \ll 1$, with

$$\epsilon_V \equiv \frac{M_{\rm P}}{2}\left(\frac{V_\phi}{V}\right)^2 \qquad \eta_V \equiv M_{\rm P}^2 \frac{V_{\phi\phi}}{V}, \tag{1.1}$$

where the subscript denotes a derivative by ϕ, $M_{\rm P} = \sqrt{1/8\pi G}$ is the reduced Planck mass with G being the Newton's constant. These parameters are UV-sensitive, meaning, that quantum corrections can contribute substantially and possibly ruin inflation.

Generally, these corrections require fine-tuning, which, as mentioned before signals a problem in the theory. However, these corrections are handled in a natural way by imposing symmetries. The simplest way to circumvent this problem is to identify the inflaton as a pseudo-scalar field, such as the axion, and realize inflation naturally. The first proposal by [19], called the "natural inflation' is in disagreement with the current precision measurements, e.g. [17, 18, 20]. Axions enjoy the continuous shift symmetry $\phi \longrightarrow \phi + const.$ This symmetry must be slightly broken, so that $\epsilon, \eta \neq 0$, but it must still protect the flatness of the potential and hence ensure sufficient expansion[1]. There have been various proposals to this end [19, 21, 22, 23, 24, 25, 26].

Precisely to avoid the UV corrections in the slow-roll parameters, different modifications of axion inflation models have been proposed and studied extensively. These models enjoy a rich phenomenology and are well-constrained by data [17, 18, 27].

This thesis aims to apply the concepts of open quantum systems to axion models of inflation where an axion is coupled with U(1) gauge sector and explore the modified parameter space. In our construction of the problem, the gauge fields are identified as the environment, while the axion field

[1] Here sufficient corresponds to at least $N \simeq 60$, where $N = \ln(a_f/a_i)$ is called the number of e-foldings and a_i, a_f correspond to the scale factor at the beginning and the end of inflation in this case.

is the system of interest.

Outline. In chapter 2 we review the standard setup and introduce important notions of early universe cosmology in Sec. 2.1, then in Sec. 2.2 we outline the shortcomings of the standard cosmological model only to set the stage for introducing inflation in Sec. 2.3. The mechanism for the standard scalar field-driven slow-roll inflation is presented, which we conclude by the inevitable generation of scalar quantum fluctuations. The Sec. 2.4 is devoted to explaining the squeezing formalism and the apparent emergence of classicality within that framework. In 2.5 we summarize some of the most important features of axion inflation with the coupling $\phi F\tilde{F}$. We show how the gauge fields are produced and amplified by tachyonic instability and provide the derivation of the power spectrum, present in the literature [27].

We assess the quantum decoherence in the early universe in Chapter 3. After a brief introduction to quantum decoherence in Sec. 3.1, we define formal tools that are used to study decoherence in Sec. 3.2. Equipped with the necessary toolkit, we proceed by introducing quantum master equations in Sec. 3.3. Here we apply the Born-Markov approximation, a key assumption required by the Lindblad formalism. In Sec. 3.4 we apply the ideas of the previous chapter to cosmology, as done in [2]. While the formalism is developed for general environments, a special case of heavy scalar environment is considered in 3.4.6. The Lindblad formalism allows us to study the power spectrum and quantify decoherence. We apply the same reasoning to the axion models of inflation in Sec. 3.5 where the gauge fields are treated as the environment, while the axion field is the system. We assess the validity of the Lindblad formalism in this scenario and see how the quantum state of the system is decohered by the presence of the gauge field environment.

In Chapter 4 we delve deeper into the question of detecting the traces of quantumness from inflation. In Sec. 4.1 we study the CMB Bell experiments and the obstructions one comes across when trying to observe the Bell inequality violation in cosmology. We provide a comparison between the different measures of quantumness for Gaussian states in Sec. 4.2. In Sec. 4.3 we calculate the quantum discord for axion models of inflation. We include the effect of the environment and compare the results with quantum decoherence obtained before.

A series of technical calculations are presented in the appendices. Appendix A shows the connection between the Heisenberg and the Schrödinger pictures. Namely, we relate the squeezing parameters used in the Schrödinger picture with the Heisenberg picture mode functions [28, 29]. In Appendix B we complement chapter 2.5 by providing a detailed derivation of the equations of motion for the axion and the gauge fields. In Appendix C we derive the Lindblad equation, which we use in the main text [2]. In Appendix D the environment correlation function is derived. The obtained result is not tractable analytically so we make a numerical fit and extract the correlation length and the effective correlation time of the environment. Finally, Appendix E is devoted to computing the integrals that pop up in the solution of the Lindblad equation 3.80 in the slow-roll approximation.

Notation

Natural units will be used throughout the manuscript as much as possible

$$c = \hbar = 1. \tag{1.2}$$

We will use the reduced Planck mass

$$M_{\rm Pl} = \sqrt{\frac{1}{8\pi G_N}} \tag{1.3}$$

where G_N is the Newton's constant. We also choose the metric signature (- + + +).

When using the Fourier transformation, to make it symmetric with the inverse transform, we will adopt the following convention

$$\mathcal{F}(\mathbf{x}) = \int \frac{d^3k}{(2\pi)^{3/2}} \mathcal{F}(\mathbf{k}) e^{i\mathbf{k}\cdot\mathbf{x}}. \tag{1.4}$$

The letter τ will denote the conformal time $dt = a(\tau)d\tau$ and finally, the Greek indices (e.g. $\mu, \nu ...$) take values $0, 1, 2, 3$, wile the latin indices $i, j, ... = 1, 2, 3$.

2 The Inflationary Paradigm

First introduced by A. Guth [1] inflation is supposedly an early epoch of exponential cosmic acceleration. The original motivation for introducing inflation was solving the flatness and horizon problems. However, as it turns out inflation also enables us to describe tiny deviations from isotropy observed on CMB and LSS. According to inflation, these anisotropies arise naturally during inflation through quantum fluctuations, which subsequently get stretched to cosmic significance as the universe expands.

In the simplest models, inflation is driven by a single minimally coupled scalar field. While solving the flatness and horizon problems, this simple model also produces nearly scale-invariant density perturbations, whose spectrum is close to that required by the observation of the large scale structure.

This chapter is dedicated to a (brief) overview of cosmic inflation, with a focus on the primordial scalar perturbations. For further reading the reader is referred to [30, 31, 32, 33].

2.1 The Standard Cosmological Setup

Modern cosmology is based on Einstein's theory of General Relativity (GR). GR is one of the well-tested theories in existence (e.g. [34]) and hence provides a very natural and reliable framework for building cosmological models.

The central proposition in modern cosmology is that the universe is homogeneous and isotropic. This is also known as the *cosmological principle* and it was introduced in the early 20th century without any observational evidence. One of the key reasons was that in order to study cosmology in the framework of general relativity, it is rather difficult to work with an arbitrary distribution of matter. The cosmological principle drastically simplifies the problem.

Modern ground and spaceborne missions are designed to detect a variety of fields (e.g. IceCube is a ground-based neutrino observatory, Ligo/Virgo detects gravitational waves, while Planck space observatory specializes in photons) and wavelengths of those fields (e.g. Fermi observatory is used to detect γ-rays, Chandra can detect x-rays, JWST detects near-visible and infrared radiation). The obtained data from measurements favor the cosmological principle. One obvious piece of evidence lies in the Cosmic Microwave Background (CMB), which is nearly isotropic. The measure of anisotropies in the CMB is one part in 10^{-5} (see figure 1). However, to maintain homogeneity, isotropy must be complemented with the *Copernican principle* which means that the universe must be isotropic for observers at any point in space. This seems like a reasonable assumption since disregarding the Copernican principle will amount to a fine-tuning related to our position in the universe.

The small perturbations on CMB mentioned above are the matter density fluctuations, that stem the large-scale structure observed today.

It is usually convenient to separate the dynamics of the universe into the large-scale homogeneous background and short-scale irregularities evolving on that background. These irregularities can be considered as small perturbations on the unperturbed universe. The metric describing the

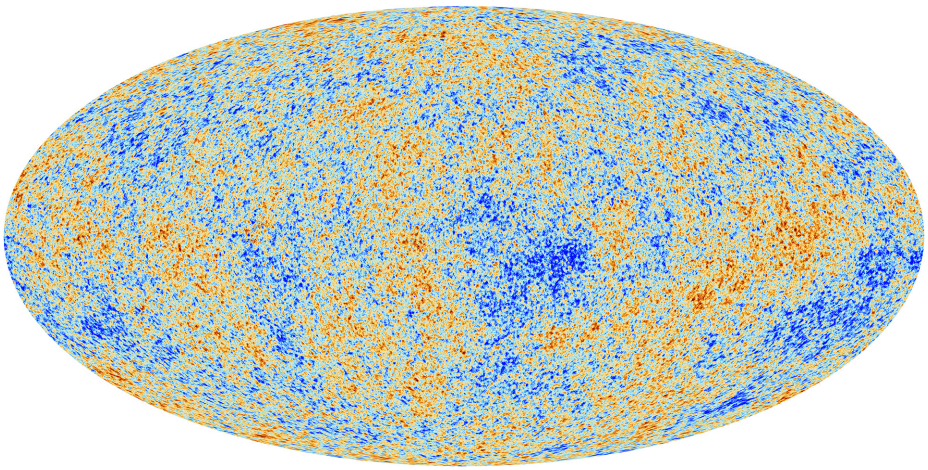

Figure 1: Anisotropies of the Cosmic Microwave Background as seen by the Planck satellite.

unperturbed universe is called the Friedman-Lemaître-Robertson-Walker (FLRW) metric, discussed below.

2.1.1 Einstein Equations and the FLRW Metric

The Einstein field equations (EFE) can be written as

$$G_{\mu\nu} = 8\pi G_N T_{\mu\nu}, \tag{2.1}$$

where $G_{\mu\nu} = R_{\mu\nu} - g_{\mu\nu}R/2$ is the Einstein tensor. $T_{\mu\nu}$ is the stress-energy tensor that describes the matter content. $g_{\mu\nu}$ (the metric), $R_{\mu\nu}$ (Ricci tensor), and R (Ricci scalar) describe the geometry of spacetime

$$R_{\mu\nu} = \Gamma^{\alpha}_{\mu\nu,\alpha} - \Gamma^{\alpha}_{\mu\alpha,\nu} + \Gamma^{\alpha}_{\beta\alpha}\Gamma^{\beta}_{\mu\nu} - \Gamma^{\alpha}_{\beta\nu}\Gamma^{\beta}_{\mu\alpha}, \qquad R = g^{\mu\nu}R_{\mu\nu}, \tag{2.2}$$

where commas denote a derivative (e.g. $(...)_{,\mu} = \partial/\partial x^{\mu}$) and Γ are the Christoffel symbols

$$\Gamma^{\gamma}_{\rho\sigma} = \frac{1}{2}g^{\gamma\lambda}\left(g_{\lambda\sigma,\rho} + g_{\rho\lambda,\sigma} - g_{\rho\sigma,\lambda}\right). \tag{2.3}$$

One can obtain the EFE by varying the action $S_{\rm tot} = S_{\rm HE} + S_{\rm m}$, where

$$S_{\rm HE} = \int d^4\sqrt{-g}\frac{R}{16\pi G_N} \tag{2.4}$$

is the Hilbert-Einstein action,

$$S_{\rm m} = \int d^4x\sqrt{-g}\mathcal{L}_{\rm m} \tag{2.5}$$

and $\mathcal{L}_{\rm m}$ denotes the matter Lagrangian density.

The stress-energy tensor can be constructed by taking the functional derivative of the matter

part of the action

$$T_{\mu\nu} = -\frac{2}{\sqrt{-g}}\frac{\delta S_{\mathrm{m}}}{\delta g^{\mu\nu}}. \tag{2.6}$$

For a perfect fluid, the energy-momentum tensor takes the form

$$T_{\mu\nu} = (P+\rho)u_\mu u_\nu + P g_{\mu\nu}, \tag{2.7}$$

where u_μ is the fluid 4-velocity.

When expressing the Einstein equations, one must also take into account the Bianchi identities, which fix

$$\nabla_\mu G^{\mu\nu} = 0, \qquad \nabla_\mu T^{\mu\nu} = 0, \tag{2.8}$$

where ∇_μ denotes the covariant derivative.

It can be shown from simple geometric arguments, that the most general metric describing the universe where the cosmological principle holds is of the following form:

$$ds^2 = -c^2dt^2 + a^2(t)\left[\frac{dr^2}{1-\kappa r^2} + r^2 d\Omega^2\right], \tag{2.9}$$

where t is the cosmic time and we have used the conformal coordinates r, ϕ, θ. $a(t)$ is the time-dependent scale factor that encodes the expansion of the universe and $d\Omega^2 = d\theta^2 + sin^2\theta d\phi^2$. The curvature κ may take positive, negative, or null values. These values will correspond to closed, open and flat universes respectively

$$\kappa = \begin{cases} +1 & \text{closed} \\ -1 & \text{open} \\ 0 & \text{flat} \end{cases} \tag{2.10}$$

So far all evidence suggests a flat universe ($\kappa = 0$).

Notice that FLRW metric (2.9) is not invariant under time translations and hence changes with time. On the other hand, as guaranteed by the cosmological principle, it is symmetric with respect to spatial translations and rotations. Using the conformal time and putting $\kappa = 0$, we can write

$$ds^2 = a^2(\tau)(-c^2d\tau^2 + dr^2 + r^2 d\Omega^2). \tag{2.11}$$

2.1.2 Dynamics

To study the dynamics of an expanding universe we need to solve Einstein equations

$$R_{\mu\nu} - \frac{1}{2}g_{\mu\nu}R = 8\pi G_N T_{\mu\nu} + g_{\mu\nu}\Lambda, \tag{2.12}$$

where for completeness, we have added the cosmological constant term. This is the most general form of the Einstein field equations. The new term acts as an additional form of the stress-energy

tensor with a constant energy density and an isotropic pressure

$$\rho_\Lambda = \frac{\Lambda}{8\pi G}, \qquad P_\Lambda = -\frac{\Lambda}{8\pi G}. \tag{2.13}$$

Hence the equation of state for the vacuum energy reads $w = p/\rho = -1$.

If we write down the 00 and ij components of the Einstein equations explicitly for the metric (2.9) and use the conservation law $\nabla_\mu T^{\mu\nu} = 0$ we obtain the Friedmann equations

$$H^2 = \frac{8\pi G}{3}\rho + \frac{\Lambda}{3} - \frac{\kappa}{a^2}, \tag{2.14}$$

$$\frac{\ddot{a}}{a} = -\frac{4\pi G}{3}(\rho + 3P) + \frac{\Lambda}{3}, \tag{2.15}$$

$$\dot{\rho} = -3H(\rho + P), \tag{2.16}$$

where dots denote the derivative with respect to cosmic time and a is the scale factor[2]. Only two of these equations are actually independent and describe the dynamics of the universe.

2.2 Problems of the Standard Cosmological Model

While the standard setup appears to describe the dynamics of our universe accurately and describes a wide range of phenomena that characterize our universe, like the abundance of light elements or the large-scale structure, there remain problems. Let us briefly consider some of the fundamental shortcomings of the standard model; More examples can be found in ref. [31], for instance.

The horizon problem. We define the comoving particle horizon, which expresses the maximum comoving distance light can travel in an FLRW expanding universe from time τ_i to τ

$$d_{\mathrm{H}} \equiv \int_0^t \frac{dt'}{a(t')} = \int_0^a (aH)^{-1} d\ln a \tag{2.17}$$

where $(aH)^{-1}$ is, by definition, the comoving Hubble radius, corresponding roughly to the distance light can travel as the scale factor doubles. The comoving Hubble radius grows in the FLRW universe:

$$r_H \equiv (aH)^{-1} = \dot{a}^{-1} \qquad \Rightarrow \qquad \dot{r}_H = -\frac{\ddot{a}}{\dot{a}^2}, \tag{2.18}$$

which is always positive for an ordinary-field-dominated universe, since in that case, the equation of state $w = p/\rho$ is such, that $w > -1/3$. Then using the standard FLRW solution for the scale factor

$$a(t) \propto t^{\frac{2}{3(w+1)}} \tag{2.19}$$

therefore, it is clear that r_H increases with time for matter-dominated ($w = 0$) and radiation-dominated universe ($w = 1/3$), implying that the causal connection around the observer increases. However, the issue stemming from observations is that all CMB regions share almost the same

[2]Notice we kept the curvature ($\kappa \neq 0$)

statistical properties without ever being in causal contact with one another[3]. This marks the first caveat in the standard hot Big Bang model.

The flatness problem. Since the standard cosmological model is based on the general theory of relativity, spacetime must be dynamic, curving in the presence of matter in the universe. If we recall the first Friedmann equation without the cosmological constant term,

$$H^2 = \frac{8\pi G}{3}\rho - \frac{\kappa}{a^2}, \tag{2.20}$$

we recognize, that since for the matter and radiation-dominated epochs, the energy density scales as a^{-3} and a^{-4} respectively, at some point, unless κ=0, the curvature term must overcome the energy density part since its dependence on the scale factor is a^{-2}. We mentioned the possibility of $\kappa = 0$, however, on general grounds, there is no reason for this condition to hold. In fact, κ may take any value.

To appreciate the gravity of the problem, let us introduce the density parameter $\Omega(t) = \rho(t)/\rho_c(t)$ and $\Omega_\kappa = \Omega(t) - 1 = \kappa r_H^2(t)$, where $\rho_c(t) = 3M_{\rm Pl}H^2(t)$ is the critical energy density, i.e. the total energy density of a completely flat universe. If we go backward in time, the scale factor will start to decrease, resulting in the energy density ρ increasing rapidly compared to the curvature term, hence we may neglect the curvature at very early times $\Omega = 1$. Then for $\kappa \neq 0$ [4], it is evident, that $\Omega(t)$ will start to depart from the value 1 at an ever increasing rate.

The obstruction arises from comparing the theoretical prediction with observations. Namely, from observations $|\Omega(t_0) - 1| < 10^{-3}$ at 95% CL. To obtain our present universe, at nucleosynthesis for example, we would need to require $|\Omega(t_{\rm nuc}) - 1| \lesssim 10^{-16}$. If we go further into the past this value decreases dramatically, leading to an initial value (at Planck epoch) $|\Omega(t_{\rm Pl}) - 1| \simeq 10^{-60}$. In principle, this is not a paradox, because there is no reason to exclude this initial condition, however, we evidently came across a fine-tuning problem that we would like to explain.

2.3 The Idea of Inflation

Both the flatness and horizon problems can be traced back to the fact that within the standard Big Bang framework, the comoving Hubble radius increases. Then an elegant way out of this conundrum is to invert the behavior of the comoving Hubble radius, making it decrease sufficiently in the very early universe.

Inflation, proposed by A. Guth [1] in 1981, extends the hot Big Bang model by adding a brief initial period when the universe expanded exponentially. Shrinking the comoving horizon leads to an expanding universe

$$\frac{d}{dt}\left(\frac{1}{aH}\right) < 0 \qquad \Rightarrow \qquad \frac{d^2a}{dt^2} > 0, \tag{2.21}$$

[3] In fact on CMB temperature fluctuations are very small $\delta T/T \simeq 10^{-5}$.
[4] As mentioned in sec. 2.1.1, κ may take positive or negative values

which, using the Friedmann equations, leads to

$$\omega = \frac{p}{\rho} < -\frac{1}{3}. \tag{2.22}$$

This requires physical justification, as ordinary matter and radiation do not obey this relation. But first, let us see how inflation solves the horizon and flatness problems.

Let us recall the FLRW metric (2.9). Introducing the conformal time $d\tau = dt/a$ and defining

$$r = f_\kappa(\chi) = \begin{cases} \arcsin\chi & \text{for} \quad \kappa = +1 \\ \chi & \text{for} \quad \kappa = 0 \\ \sinh^{-1}\chi & \text{for} \quad \kappa = -1 \end{cases} \tag{2.23}$$

so that (2.9) becomes

$$ds^2 = a^2(\tau)\left(-d\tau^2 + d\chi^2 + f_\kappa^2(\chi)d\Omega^2\right). \tag{2.24}$$

In these coordinates, the causal structure of the universe looks the same as in flat Minkowski space. This is fundamentally because the FLRW metric is conformally flat. We consider null geodesics ($d\tau^2 = d\chi^2$) which form lines at angle 45° on the conformal diagram, as shown in figure 2. The upper half of the diagram shows, that the universe started off at $\tau = 0$, two different regions during recombination would not have had enough time to communicate in the past, so there is no obvious reason why they share statistical properties to such a great extent unless we impose some very specific initial conditions for the Big Bang. On the other hand, if inflation were to take place, it would effectively push the initial singularity to $-\infty$. This mechanism allows for a causal connection for radiation in the far past, explaining the high levels of isotropy in the CMB. This effectively cures the horizon problem.

Let us now define the *number of e-folds* as

$$N = \ln\left(\frac{a_f}{a_i}\right), \tag{2.25}$$

where a_i, a_f correspond to the beginning and the end of inflation respectively. Then in order to solve the horizon problem, the universe must have expanded by at least $N \simeq 60 \div 70$ e-foldings.

As for the flatness problem, recalling that

$$\Omega_\kappa = \Omega(t) - 1 = \frac{\kappa}{(aH)^2}, \tag{2.26}$$

it is evident, that the decreasing Hubble radius decreases Ω_κ, allowing the universe to stay sufficiently flat.

During inflation the Hubble parameter $H \approx const.$. The scale factor is

$$a(\tau) = -\frac{1}{\tau H}, \tag{2.27}$$

so while the initial singularity ($a = 0$) is pushed to $-\infty$, we also see that at $\tau = 0$ the scale factor becomes infinite, which means, that the inflation goes on forever. This is because we assumed the Hubble parameter is constant, however, this is not exactly the case. The Hubble parameter is actually varying, albeit slowly. Hence at some point inflation concludes and reheating takes place as we enter the radiation-dominated epoch.

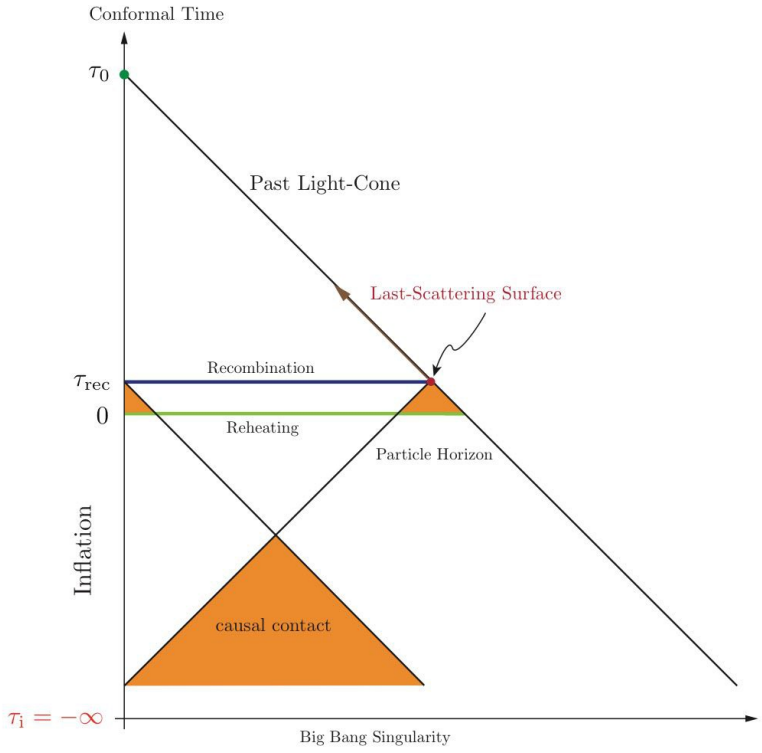

Figure 2: Inflationary solution to the horizon problem [35]. Without inflation, the universe is assumed to have started at $\tau = 0$. Then between the Big Bang and the Recombination epoch, not enough (conformal) time has passed for all scales observed on CMB to be causally connected. Inflation effectively pushes the initial singularity towards $\tau \to -\infty$, leaving time for all the currently observed CMB scales to have been in causal contact in the past.

2.3.1 Scalar Field Dynamics

The inflationary behavior is an unusual one, primarily in the sense that in the standard GR formalism, it requires a negative pressure source (2.22). This can be realized by a simple scalar field ϕ whose dynamics is governed by the action

$$S_{\rm tot} = S_{\rm HE} + S_\phi + S_{\rm fields} = \int d^4x\sqrt{-g}\left[\frac{1}{2}R + \frac{1}{2}g^{\mu\nu}\partial_\mu\phi\partial_\nu\phi - V(\phi)\right] + S_{\rm fields}, \tag{2.28}$$

where S_{HE} denotes the Hilbert-Einstein action, R is the Ricci scalar, and we have included a term S_{fields} describing all fields present during inflation[5].

The energy-momentum tensor of the scalar field reads

$$T^{\varphi}_{\mu\nu} = -\frac{2}{\sqrt{-g}}\frac{\delta S_\phi}{\delta g^{\mu\nu}} = \partial_\mu\phi\partial_\nu\phi - g_{\mu\nu}\left(\frac{1}{2}\partial_\alpha\phi\partial^\alpha\phi + V(\phi)\right), \tag{2.29}$$

while the equation of motion is

$$\frac{\delta S_\phi}{\delta\phi} = \frac{1}{\sqrt{-g}}\partial_\mu(\sqrt{-g}\partial^\mu\phi) + V_{,\phi} = 0, \tag{2.30}$$

where $V_{,\varphi}$ denotes $dV/d\phi$. The equation for the dynamics of the scalar field ϕ is the Klein-Gordon equation for a quantum scalar field in FLRW universe[6]

$$\ddot{\phi} + 3H\dot{\phi} - \frac{\nabla^2\phi}{a^2} + V_{,\phi} = 0, \tag{2.31}$$

where the second term acts as friction due to the expansion of the universe.

ϕ can be expressed as the sum of a classical background value and small fluctuations

$$\phi(\mathbf{x}, t) = \phi_0(t) + \delta\phi(\mathbf{x}, t) \tag{2.32}$$

then focusing on the dominant background value $\phi_0(t)$ components of the energy-momentum tensor (2.29) read

$$T^0_0 = -\left[\frac{1}{2}\dot{\phi}_0^2 + V(\phi_0)\right] = -\rho_\phi, \tag{2.33}$$

$$T^i_j = \delta^i_j\left[\frac{1}{2}\dot{\phi}_0^2(t) - V(\phi_0)\right] = \delta^i_j P_\phi(t). \tag{2.34}$$

Then the equation of state is

$$w^\phi = \frac{P_\phi}{\rho_\phi} = \frac{\frac{1}{2}\dot{\phi}_0^2(t) - V(\phi_0)}{\frac{1}{2}\dot{\phi}_0^2 + V(\phi_0)}, \tag{2.35}$$

which shows that the scalar field may lead to an accelerated expansion if the potential energy dominates the kinetic term. In fact we effectively get a negative pressure dynamics ($w_\phi < 0$) with an accelerated expansion ($\omega_\phi < -1/3$) if the scalar potential is sufficiently larger than the kinetic term.

As for the background dynamics, using equation (2.30) we get

$$\ddot{\phi} + 3H\dot{\phi} + V_{,\phi} = 0 \qquad \text{and} \qquad H^2 = \frac{8\pi G}{3}\rho_\phi = \frac{8\pi G}{3}\left[\frac{1}{2}\dot{\phi}_0^2 + V(\phi_0)\right], \tag{2.36}$$

[5]It is notable, that this is a minimal setup that allows inflationary dynamics. In practice, the scalar field could have a non-minimal coupling to the gravity sector, like $\lambda\varphi^2 R$.

[6]We are considering a flat FLRW metric ($\kappa = 0$) since the only difference we would get by including curvature would be in ∇^2, however, the equation would look exactly the same.

where we have neglected other contributions to the Hubble rate like $\rho_m \propto a^{-3}$, $\rho_r \propto a^{-4}$ and $\rho_\kappa \propto a^{-2}$ which are dominated by $\rho_\phi \simeq V(\phi) \simeq const.$

2.3.2 Slow-Roll

Notice, that we have already identified one of the slow-roll conditions. Namely, this was done when we imposed that the kinetic term is dominated by the potential energy

$$V(\phi) \gg \dot{\phi}^2. \tag{2.37}$$

This implies that the scalar potential is sufficiently flat.

The second slow roll condition is formulated by imposing that inflation lasts for a sufficiently long time, then the equation of motion (2.36) tells us that

$$|\ddot{\phi}| \ll |3H\dot{\phi}|, |V_{,\phi}|, \tag{2.38}$$

so the background dynamics is governed by

$$\dot{\phi} \approx -\frac{V_{,\phi}}{3H}, \qquad H^2 \approx \frac{1}{3M_{\rm Pl}^2} V(\phi), \tag{2.39}$$

and spacetime is approximately de Sitter

$$a(t) \sim e^{Ht}. \tag{2.40}$$

To quantify the slow-roll behavior we introduce the slow-roll parameters ε and η. The first slow-roll parameter quantifies how much the Hubble parameter changes during inflation

$$\varepsilon = -\frac{\dot{H}}{H^2} \tag{2.41}$$

Then using equation (2.36) we get

$$\varepsilon = 4\pi G \frac{\dot{\phi}^2}{H^2} \overset{\text{SR}}{\simeq} \frac{3}{2} \frac{\dot{\phi}^2}{V(\phi)}, \tag{2.42}$$

where the last equation holds only in the slow-roll regime since it is derived by neglecting the kinetic term in H^2 in equation (2.36). This inherently implies that during slow-roll

$$\varepsilon \ll 1. \tag{2.43}$$

Moreover, the first slow-roll parameter can also be expressed in a way that determines the shape of the inflationary potential

$$\varepsilon = \frac{M_{\rm Pl}}{2} \left(\frac{V_{,\phi}}{V} \right)^2 \ll 1, \tag{2.44}$$

meaning that $V_{,\phi}$ is small so the potential is flat.

The second slow roll parameter is defined as

$$\eta = -\frac{\ddot{\phi}}{H\dot{\phi}} \tag{2.45}$$

Recalling equation (2.39) implies $\dot{\phi} \simeq -V_{,\phi}/3H$, resulting in

$$\eta = \frac{V_{,\phi\phi}}{3H^2} - \frac{\dot{H}}{H^2}\frac{V_{,\phi}}{3H\dot{\phi}} = \eta_V - \varepsilon. \tag{2.46}$$

Since we have already imposed $\varepsilon \ll 1$, then to keep the second slow-roll parameter small, we need $\eta_V \ll 1$. Then since the dominant contribution in H^2 comes from the potential, we get

$$\eta_V \simeq M_{\rm Pl}^2 \frac{V_{,\phi\phi}}{V} \ll 1. \tag{2.47}$$

Let us recall the definition of the number of e-foldings during inflation which for any interval (t_i, t_f) can be written as

$$N = \ln\left[\frac{a(t_f)}{a(t_i)}\right] = \int_{t_i}^{t_f} H dt = \int_{\phi_i}^{\phi_f} \frac{H}{\dot{\phi}} \overset{SR}{\approx} \int_{\phi_f}^{\phi_i} \frac{V}{V_{,\phi}} d\phi. \tag{2.48}$$

We can also rewrite this using equation (2.44) to obtain

$$N = \int_{\phi_{\rm f}}^{\phi_{\rm i}} \frac{d\phi}{\sqrt{2\varepsilon}}. \tag{2.49}$$

In order to solve the flatness and the horizon problems, we need inflation to last at least $\gtrsim 60$ e-folds

$$N_{tot} = \ln\left[\frac{a(t_{\rm end})}{a(t_{\rm start})}\right], \tag{2.50}$$

where $|t_{\rm start} - t_{\rm end}|$ is the total time it takes for inflation to end. The CMB fluctuations are generated around $40 \div 60$ before inflation terminates, so using equation (2.49) we obtain a constraint on the field value when the aforementioned fluctuations were generated $\phi_{\rm CMB}$

$$\int_{\phi_{\rm end}}^{\phi_{\rm CMB}} \frac{d\phi}{\sqrt{2\varepsilon}} \approx 40 \div 60. \tag{2.51}$$

2.3.3 Scalar Perturbations from Inflation

Certainly one of the most promising predictions of inflation is the generation of quantum fluctuations which later seed the cosmic structure and the measured anisotropies on CMB. In fact, it has been shown [1, 36, 37, 38] that even the simplest realizations of inflation can account not only for galaxy formation but also their statistics. The idea behind this premise is that quantum fluctuations of

the light scalar field will "freeze" at the horizon exit (See fig. 3). This process is independent of the theory of gravity and has to do with the fact that the timescale of the given mode that crosses the horizon a/k becomes larger than the Hubble time H^{-1}. In this section, we will consider the

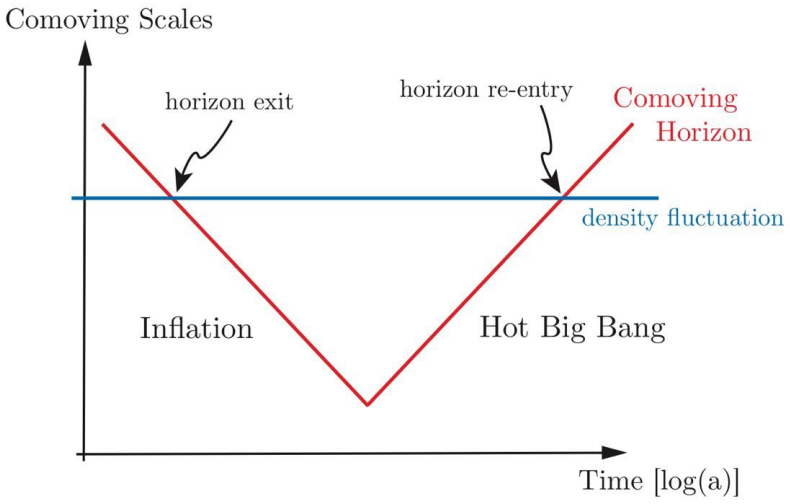

Figure 3: Fluctuations are generated in the sub-horizon scales and cross the horizon as the Hubble radius $(aH)^{-1}$ shrinks during inflation. In the super-horizon regime causal physics is non-existent and the fluctuations freeze until later, when they reenter the horizon.

first-order perturbation of the light scalar field in near de Sitter spacetime. We will ignore the metric perturbation and allow the scalar field perturbation to evolve on an unperturbed background.

Notoriously any model of inflation also predicts a generation of tensor perturbations, i.e., primordial gravitational waves (see [39] for a review of the topic). In this thesis, however, we will focus mainly on scalar perturbations. We can do this because the scalar and tensor perturbations are decoupled in the first order. In the case of the matter sector, we make the usual decomposition of the inflaton into the homogeneous background part $\phi(\tau)$ and fluctuations $\delta\phi(\tau, \mathbf{x})$

$$\phi(t, \mathbf{x}) = \phi(t) + \delta\phi(t, \mathbf{x}). \tag{2.52}$$

and solve the Klein-Gordon equation (2.31). It is convenient to move to Fourier space, where

$$\delta\phi(\mathbf{x}, t) = \int \frac{d^3k}{(2\pi)^{3/2}} e^{i\mathbf{k}\cdot\mathbf{x}} \delta\phi_{\mathbf{k}}(t), \tag{2.53}$$

where at the linear level separate modes evolve independently. The Klein-Gordon equation for $\delta\phi$ in Fourier space then reads

$$\ddot{\delta\phi}_{\mathbf{k}} + 3H\dot{\delta\phi}_{\mathbf{k}} + a^{-2}k^2\delta\phi_{\mathbf{k}} + V_{,\phi\phi}\delta\phi_{\mathbf{k}} = 0. \tag{2.54}$$

We proceed by quantizing the rescaled field $\delta\varphi = a(t)\delta\phi$:

$$\delta\varphi = \int \frac{d^3k}{(2\pi)^{3/2}} \left[u_k(\tau)\hat{a}_{\mathbf{k}} e^{-i\mathbf{k}\cdot\mathbf{x}} + u_k^*(\tau)\hat{a}_{\mathbf{k}}^\dagger e^{i\mathbf{k}\cdot\mathbf{x}} \right], \tag{2.55}$$

where $\hat{a}^\dagger$ and $\hat{a}$ are the creation and annihilation operators respectively and $\tau(= -1/aH)$ is the conformal time. $u_{\mathbf{k}}(\tau)$ satisfies the following normalization condition $u_k^*(\tau)u_k'(\tau) - u_k(\tau)u_k^*(\tau) = -i$, that guarantees the canonical quantization relations for the creation and annihilation operators

$$[\hat{a}_{\mathbf{k}}, \hat{a}_{\mathbf{k}'}^\dagger] = \delta^{(3)}(\mathbf{k} - \mathbf{k}'), \qquad [\hat{a}_{\mathbf{k}}, \hat{a}_{\mathbf{k}'}] = 0. \tag{2.56}$$

Using conformal time, the equation of motion for the rescaled field perturbation writes

$$\delta\varphi'' - \frac{a''}{a}\delta\varphi - \nabla^2\delta\varphi = -a^2 V_{,\varphi\varphi}\delta\varphi. \tag{2.57}$$

So The Fourier mode functions u_k satisfy

$$u_k''(\tau) + \left[k^2 - \frac{a''}{a} + a^2 V_{,\varphi\varphi} \right] u_k(\tau) = 0. \tag{2.58}$$

Since heavy scalar field perturbations are suppressed, we only consider light fields so we will neglect $V_{,\varphi\varphi} = m_\varphi^2$ and solve the equation at first order in slow-roll[7]

$$u_k''(\tau) + \left[k^2 - \frac{\nu^2 - \frac{1}{4}}{\tau^2} \right] u_k(\tau) = 0. \tag{2.60}$$

In this form, this equation is equivalent to the Bessel equation, whose solution can be written using the Hankel functions

$$u_k(\tau) = \sqrt{-\tau} \left[c_1(k) H_\nu^{(1)}(-k\tau) + c_2(k) H_\nu^{(2)}(-k\tau) \right], \tag{2.61}$$

where (1) and (2) denote the kinds of the Hankel function (first and the second kind respectively). We require that deep sub-horizon modes ($-k\tau \to \infty$) correspond to Bunch-Davies vacuum states

$$u_k(\tau) \approx \frac{e^{-ik\tau}}{\sqrt{2k}}. \tag{2.62}$$

This condition is satisfied by imposing $c_2(k) = 0$ and $c_1(k) = \frac{\sqrt{\pi}}{2} \exp\left[i(\nu + \frac{1}{2})\frac{\pi}{2} \right]$. Then the final

[7] During slow-roll

$$\tau \simeq -\frac{1}{aH(1-\varepsilon)}, \qquad \frac{a''}{a} = \frac{2}{\tau^2}\left(1 + \frac{3}{2}\varepsilon\right) \tag{2.59}$$

solution is[8]

$$u_k(\tau) = \frac{1}{2}\sqrt{\frac{\pi}{k}}\sqrt{-k\tau}e^{i\left(\nu+\frac{1}{2}\right)\frac{\pi}{2}}H_\nu^{(1)}(-k\tau). \tag{2.63}$$

If we had retained the mass m_φ, the form of the equation (2.60) would stay the same, only with $\nu^2 = 9/4 + 3\varepsilon - 3\eta_V$, where $\eta_V = m_\varphi^2/H^2$. Thus, if the scalar field is massive enough $m_\varphi \gtrsim H$, then $\eta \gtrsim 1$, which violates the condition necessary to have "enough" inflation.

We now go beyond the homogeneous Friedmann-Lemaitre-Robertson-Walker (FLRW) metric. This step is necessary for the complete treatment of inflationary perturbations. We write down the perturbed FLRW metric

$$ds^2 = a^2(\tau)\{-(1-2\Phi)d\tau^2 + 2\partial_i B dx^i d\tau + [(1-2\psi)\delta_{ij} + \partial_{ij}E]dx^i dx^j\}, \tag{2.64}$$

where a is the usual FLRW scale factor, τ is the conformal time and Φ, ψ, B, E generally depend on space and time. Gauge freedom allows us to decrease the number of degrees of freedom in such a way that the scalar metric perturbations can be encoded into two gauge-invariant[9] Bardeen potentials. The Bardeen potential corresponding to spatial perturbations is

$$\Psi = \psi - \frac{a'}{a}(B - E'), \tag{2.65}$$

where primes denote the derivative by conformal time $\partial_\tau = a\partial_t$, where t is the cosmic time. The inflaton field perturbations can be represented analogously using a gauge-invariant field

$$\delta\varphi_{\mathrm{GI}}(\tau, \mathbf{x}) = \delta\varphi(\tau, \mathbf{x}) + \phi'(\tau)(B - E'). \tag{2.66}$$

Conveniently, the gauge-invariant field and the Bardeen potential are combined into another gauge-invariant field, the Mukhanov-Sasaki variable

$$v(\tau, \mathbf{x}) = a\left(\delta\varphi_{\mathrm{GI}}(\tau, \mathbf{x}) + \frac{\varphi'(\tau)}{\mathcal{H}}\Psi\right), \tag{2.67}$$

which is related to the comoving curvature perturbation through

$$v = -\frac{a\varphi'(\tau)\zeta}{\mathcal{H}}, \tag{2.68}$$

where $\mathcal{H} = a'/a = aH$, H is the Hubble parameter. One could equivalently replace the conformal time with cosmic time $v = -a\dot{\phi}\zeta/H$.

[8] Note that we could have taken $c_1(k) = 0$ and present the final result using the Hankel function of the second kind $H_\nu^{(2)}$. The only difference would be the sign in front of the phase factor.

[9] Gauge freedom can lead to confusion. Namely, due to the spacetime geometry ambiguities between the real and fake perturbations may arise. This is primarily why gauge-invariant quantities are useful since perturbations in gauge-invariant quantities cannot be removed by a coordinate transformation.

It can be shown, that the Mukhanov-Sasaki variable v_k also satisfies the Bessel equation

$$v_k''(\tau) + \left[k^2 - \frac{\nu^2 - \frac{1}{4}}{\tau^2}\right] v_k(\tau) = 0 \tag{2.69}$$

and has solutions similar to (2.61).

2.4 Quantum-to-classical transition

The great advantage of cosmic inflation is that through quantum fluctuations discussed in the previous section, we obtain an elegant mechanism for generating the initial seeds of structure in the universe. Primordial perturbations are created deep into the horizon at every length scale. Figure 3 shows that at some point during inflation, the fluctuations cross the Hubble radius, becoming super-horizon, until later, when the comoving radius starts to increase. Eventually, all of the perturbations that had crossed the horizon during inflation will reenter the horizon.

However, there is a caveat in understanding how exactly the quantum-to-classical transition occurs. Specifically, how do the quantum fluctuations seed classical objects like CMB or LSS? We need a mechanism that allows for classicalization of the primordial fluctuations. Indeed, one of the most prominent ways to tackle this question is by invoking decoherence [28]. Decoherence, first proposed by Zeh [40] has been studied extensively and is an experimentally proven phenomenon [41]. The basic idea is that a quantum system interacts with its environment and this interaction changes the probabilities of possible outcomes of the measurement and suppresses the interference between them. Applying these concepts to cosmology leads to understanding the classicalization of primordial perturbations. On the other hand, since decoherence changes the statistics of the system, while the statistics of the primordial perturbations are well constrained, this opens a new window to constrain cosmic decoherence observationally. Decoherence will be the main topic of Chapter 3.

However, there is another mechanism, by which one could explain the apparent classicality of the observables. The key idea is that the primordial quantum fluctuations are placed in a highly squeezed state by the end of inflation. Paradoxically, the squeezed states are highly non-classical, however as we shall see, the very large squeezing also obscures the "quantumness" of the state.

2.4.1 The squeezing formalism for inflationary perturbations

The evolution of the quantum state during inflation is important to understand the late-time predictions associated with the state. In this section we will introduce the squeezing formalism, applied to vacuum fluctuations evolving during inflation, producing the so-called two-mode squeezed state [28, 29, 42], although this mechanism is subject to the same types of ambiguities as particle creation during inflation (see [43]). State squeezing is a well-established concept and in a way a cornerstone of quantum optics (see [44] for a review), but also in other fields of physics. We shall work in the Schrödinger picture, however in Appendix A we derive a simple relation between the two pictures.

On the one hand the produced squeezed state is expected to be highly classical [28, 29, 42, 45, 46, 47, 48], but on the other, squeezing due to inflation also entangles the modes with $\vec{k}$ and $-\vec{k}$,

making the final state highly quantum [49].

To understand the squeezing formalism, we start by taking the action for the curvature perturbations [35]

$$S = \int d^4x a^2 \varepsilon M_{\rm Pl}^2 \left[\zeta'^2 - (\partial_i \zeta)^2\right]. \tag{2.70}$$

Using the relation (2.68), we can rewrite this action in terms of the Mukhanov-Sasaki variable $v(\tau, \mathbf{x}) = z(\tau)\zeta(\tau, \beta x)$, where $z^2(\tau) = a^2 M_{\rm Pl}^2 2\varepsilon$ is a time-dependent variable. The action reads

$$S_v = \frac{1}{2}\int d\tau d^3\mathbf{x} \left[(v')^2 - (\partial_i v)^2 + \frac{z''}{z}v^2\right], \tag{2.71}$$

which is the action of a free scalar field with a time-dependent mass term $m^2 = -z''/z$ [50]. It will prove convenient to add a total derivative term, obtaining the following equivalent action [29, 51]

$$S_v = \frac{1}{2}\int d\tau d^3\mathbf{x} \left[(v')^2 - (\partial_i v)^2 - 2\frac{z'}{z}vv' + \left(\frac{z'}{z}\right)^2 v^2\right]. \tag{2.72}$$

The Hamiltonian of the system now reads

$$H_v = \frac{1}{2}\int d^3\mathbf{x} \left[p^2 + (\partial_i v)^2 + 2\frac{z'}{z}vp\right], \tag{2.73}$$

where p is the conjugate momentum corresponding to v. In order to proceed with the standard quantization procedure we promote the field variables to operators and perform Fourier decomposition

$$\begin{aligned} \hat{v} &= \int \frac{d^3k}{(2\pi)^{3/2}} \hat{v}_{\mathbf{k}} e^{i\mathbf{k}\cdot\mathbf{x}}, \\ \hat{p} &= \int \frac{d^3k}{(2\pi)^{3/2}} \hat{p}_{\mathbf{k}} e^{i\mathbf{k}\cdot\mathbf{x}}. \end{aligned} \tag{2.74}$$

We obtain a two-mode Hamiltonian in k-space

$$\hat{\mathcal{H}}_{\mathbf{k}} = \hat{p}_{-\mathbf{k}}\hat{p}_{\mathbf{k}} + k^2 \hat{v}_{-\mathbf{k}}\hat{v}_{\mathbf{k}} + \frac{z'}{z}(\hat{p}_{-\mathbf{k}}\hat{v}_{\mathbf{k}} + \hat{v}_{-\mathbf{k}}\hat{p}_{\mathbf{k}}). \tag{2.75}$$

We continue to work in the Schrödinger picture, where the operators are fixed at the initial time. The creation and annihilation operators can be introduced in the usual way

$$\begin{aligned} \hat{v}_{\mathbf{k}} &= \frac{1}{\sqrt{2k}}\left(\hat{a}_{\mathbf{k}} + \hat{a}^\dagger_{-\mathbf{k}}\right), \\ \hat{p}_{\mathbf{k}} &= -i\sqrt{\frac{k}{2}}\left(\hat{a}_{\mathbf{k}} - \hat{a}^\dagger_{-\mathbf{k}}\right). \end{aligned} \tag{2.76}$$

The two-mode Hamiltonian operator can be rewritten in terms of the creation-annihilation operators

$$\hat{\mathcal{H}}_{\mathbf{k}} = \hat{\mathcal{H}}^{(0)}_{\mathbf{k}} + \hat{\mathcal{H}}^{\rm int}_{\mathbf{k}} = F_{\mathbf{k}}\left(\hat{a}^\dagger_{\mathbf{k}}\hat{a}_{\mathbf{k}} + \hat{a}^\dagger_{-\mathbf{k}}\hat{a}_{-\mathbf{k}} + 1\right) + i\Lambda_{\mathbf{k}}\left(e^{-2i\Phi_{\mathbf{k}}}\hat{a}_{\mathbf{k}}\hat{a}_{-\mathbf{k}} - \text{h.c.}\right), \tag{2.77}$$

where in case of the inflaton (see ref. [29])

$$F_{\mathbf{k}} = k, \qquad \Lambda_{\mathbf{k}} = \frac{z'}{z}, \qquad \Phi_{\mathbf{k}} = -\pi/2. \tag{2.78}$$

So the generic quadratic Hamiltonian is comprised of a harmonic part, proportional to the *frequency* F_k and a *parametric amplification* (or the *squeezing*) part proportional to R_k. The amplification is attributed to the time-dependent background which results in the effective time-dependent mass discussed above. The Hamiltonian above generates the following time evolution operator

$$\hat{\mathcal{U}}(\tau, \tau_0) = \hat{\mathcal{S}}[r_{\mathbf{k}}, \varphi_{\mathbf{k}}]\hat{\mathcal{R}}[\theta_{\mathbf{k}}], \tag{2.79}$$

where $\hat{\mathcal{R}}_k$ is the two-mode rotation operator defined as

$$\hat{\mathcal{R}} = \exp\left[-i\theta_{\mathbf{k}}\left(\hat{a}^\dagger_{\mathbf{k}}\hat{a}_{\mathbf{k}} + \hat{a}^\dagger_{-\mathbf{k}}\hat{a}_{-\mathbf{k}} + 1\right)\right] \tag{2.80}$$

and $\hat{\mathcal{S}}_k$ is the two-mode squeeze operator

$$\hat{\mathcal{S}} = \exp\Big[\frac{r_{\mathbf{k}}}{2}\left(e^{-2i\varphi_{\mathbf{k}}}\hat{a}_{-\mathbf{k}}\hat{a}_{\mathbf{k}} - \text{h.c.}\right)\Big], \tag{2.81}$$

where r_k is the squeezing parameter, φ_k is the squeezing angle and θ_k is the squeezing phase, which are determined by the details of the studied dynamics and are generally time-dependent. In order to study the said dynamics for the case of inflation, we need to set the initial conditions of our quantum field theory. First, we impose, that the modes inside the horizon today, were also inside the horizon during the initial stages of inflation. It means that $k|\tau| \gg 1$ $F_k = k$ and $z'/z \simeq \mathcal{H} = Ha \propto 1/|\tau|$. The total Hamiltonian (2.77) reduces to the free Hamiltonian $\hat{\mathcal{H}}^{(0)}_{\mathbf{k}}$. We choose the ground state of this Hamiltonian as the initial state, which is defined by

$$\hat{a}_{\mathbf{k}}\left|0\right\rangle_{\hat{\mathcal{H}}^{(0)}_{\mathbf{k}}} = 0, \qquad \forall\mathbf{k}. \tag{2.82}$$

Acting on this state by the rotation operator $\hat{\mathcal{R}}$ gives an irrelevant phase

$$\hat{\mathcal{R}}[\theta_{\mathbf{k}}]\left|0\right\rangle_{\hat{\mathcal{H}}^{(0)}_{\mathbf{k}}} = e^{i\theta_{\mathbf{k}}}\left|0\right\rangle_{\hat{\mathcal{H}}^{(0)}_{\mathbf{k}}}, \tag{2.83}$$

however, when we act on the initial vacuum state by the squeeze operator $\hat{S}$, it becomes a two-mode squeezed state

$$\left|2MSS_{\mathbf{k}}\right\rangle = \hat{\mathcal{S}}[r_{\mathbf{k}}, \varphi_{\mathbf{k}}]\left|0\right\rangle_{\hat{\mathcal{H}}^{(0)}_{\mathbf{k}}} = \frac{1}{\cosh r_{\mathbf{k}}}\sum_{n=0}^{\infty}(-1)^n(e^{2i\varphi_{\mathbf{k}}}\tanh r_{\mathbf{k}})^n\left|n, \mathbf{k}; n, -\mathbf{k}\right\rangle, \tag{2.84}$$

where

$$\left|n, \mathbf{k}; n, -\mathbf{k}\right\rangle = \sum_{n=0}^{\infty}\frac{1}{n!}\left(\hat{a}^\dagger_{\mathbf{k}}\hat{a}_{-\mathbf{k}}\right)^n\left|0\right\rangle_{\hat{\mathcal{H}}^{(0)}_{\mathbf{k}}} \tag{2.85}$$

is the two-mode occupation number state. This part of the evolution operator defined above is responsible for the amplification of the fluctuations.

In order to assess squeezing, the evolution equations for the squeezing parameters $r_{\mathbf{k}}, \varphi_{\mathbf{k}}$ and $\theta_{\mathbf{k}}$ must be derived. We start by recalling the definition of the evolution operator[10]

$$\begin{aligned}\hat{\mathcal{U}}(\tau,\tau_0) &= \hat{\mathcal{T}}\exp\left[-i\int_{\tau_0}^{\tau} d\tau' \hat{\mathcal{H}}_{\mathbf{k}}(\tau')\right] \\ &= \hat{\mathcal{T}}\exp\left[-i\int_{\tau_0}^{\tau} d\tau' \Omega_{\mathbf{k}}\left(\hat{a}^{\dagger}_{\mathbf{k}}\hat{a}_{\mathbf{k}} + \hat{a}^{\dagger}_{-\mathbf{k}}\hat{a}_{-\mathbf{k}} + 1\right) + \int_{\tau_0}^{\tau} d\tau' \Lambda_{\mathbf{k}}\left(e^{-2i\Phi_{\mathbf{k}}}\hat{a}_{\mathbf{k}}\hat{a}_{-\mathbf{k}} - \text{h.c.}\right)\right].\end{aligned} \tag{2.86}$$

We divide the evolution into infinitesimal time steps ϵ. The evolution operators satisfy the following composite property

$$\hat{\mathcal{U}}(\tau+\epsilon,\tau_0) = \hat{\mathcal{U}}(\tau+\epsilon,\tau)\hat{\mathcal{U}}(\tau,\tau_0). \tag{2.87}$$

Then according to our definition of the evolution operator (2.79),

$$\hat{\mathcal{S}}[r_{\mathbf{k}},\varphi_{\mathbf{k}}]\hat{\mathcal{R}}[\theta_{\mathbf{k}}] = \hat{\mathcal{S}}[\delta r_{\mathbf{k}},\delta\varphi_{\mathbf{k}}]\hat{\mathcal{R}}[\delta\theta_{\mathbf{k}}]\hat{\mathcal{S}}[r^{(0)}_{\mathbf{k}},\varphi^{(0)}_{\mathbf{k}}]\hat{\mathcal{R}}[\theta^{(0)}_{\mathbf{k}}]. \tag{2.88}$$

We now infer, that for small ϵ, $\delta r_{\mathbf{k}} = \Lambda_{\mathbf{k}}$, $\delta\varphi_{\mathbf{k}} = \Phi_{\mathbf{k}}$ and $\delta\theta_{\mathbf{k}} = \Omega_{\mathbf{k}}$. The properties of the squeeze operators allow us to rewrite the right-hand side of the equation as

$$RHS = \hat{\mathcal{S}}[\delta r_{\mathbf{k}},\delta\varphi_{\mathbf{k}}]\hat{\mathcal{S}}[r^{(0)}_{\mathbf{k}},\varphi^{(0)}_{\mathbf{k}} - \delta\theta_{\mathbf{k}}]\hat{\mathcal{R}}[\theta^{(0)}_{\mathbf{k}} + \delta\theta^{(0)}_{\mathbf{k}}] = \hat{\mathcal{S}}[r_{\mathbf{k}},\varphi_{\mathbf{k}}]\hat{\mathcal{R}}[\bar{\theta}_{\mathbf{k}}], \tag{2.89}$$

where

$$e^{i\bar{\theta}_{\mathbf{k}}}\cosh r_{\mathbf{k}} = \cosh r^{(0)}_{\mathbf{k}}\cosh\delta r_{\mathbf{k}} + e^{-2i(\varphi^{(0)}_{\mathbf{k}} - \delta\varphi_{\mathbf{k}} - \delta\theta_{\mathbf{k}})}\cosh r^{(0)}_{\mathbf{k}}\sinh\delta r_{\mathbf{k}}, \tag{2.90}$$

and

$$2e^{i(2(\varphi_{\mathbf{k}} - \varphi^{(0)}_{\mathbf{k}} + \delta\theta_{\mathbf{k}}) + \bar{\theta}_{\mathbf{k}})}\sinh r_{\mathbf{k}} = \sinh r^{(0)}_{\mathbf{k}}\cosh\delta r_{\mathbf{k}} + e^{-2i(\varphi^{(0)}_{\mathbf{k}} - \delta\varphi_{\mathbf{k}} - \delta\theta_{\mathbf{k}})}\sinh\delta r_{\mathbf{k}}\cosh r^{(0)}_{\mathbf{k}}. \tag{2.91}$$

For small ε one obtains recursion relations for $r_{\mathbf{k}}$, $\varphi_{\mathbf{k}}$ and $\theta_{\mathbf{k}}$, whose differential form reads [29]

$$\begin{aligned} r'_{\mathbf{k}} &= \Lambda_{\mathbf{k}}\cos 2(\Phi_{\mathbf{k}} - \varphi_{\mathbf{k}}), \\ \varphi'_{\mathbf{k}} &= -F_{\mathbf{k}} + \frac{\Lambda_{\mathbf{k}}}{2}(\tanh r_{\mathbf{k}} + \coth R_{\mathbf{k}})\sin 2(\Phi_{\mathbf{k}} - \varphi_{\mathbf{k}}), \\ \theta'_{\mathbf{k}} &= F_{\mathbf{k}} - \Lambda_{\mathbf{k}}\tanh r_{\mathbf{k}}\sin 2(\Phi_{\mathbf{k}} - \varphi_{\mathbf{k}}). \end{aligned} \tag{2.92}$$

Note, that we have provided a simplified version of the parameters in (2.78) (see [29]), since we are interested in a (nearly) exponentially expanding universe, initially placed in a Bunch-Davies

[10] Note, that throughout this section, we have been using the Schrödinger picture variables, however, as it is well-known, Heisenberg and Schrödinger pictures are equivalent in terms of the physics they describe, so we expect to reproduce the same results in both cases. To see the connection between the two pictures see Appendix A

vacuum [52]. In this case, the equations of motion can be solved exactly and one obtains

$$\begin{aligned} r_{\mathbf{k}} &= \sinh^{-1}\frac{1}{2k\tau}, \\ \varphi_{\mathbf{k}} &= -\frac{\pi}{4} - \frac{1}{2}\arctan\frac{1}{2k\tau}, \\ \theta_{\mathbf{k}} &= k\tau + \arctan\frac{1}{2k\tau}. \end{aligned} \tag{2.93}$$

Initially, the perturbations start at subhorizon scales ($k|\tau| \gg 1$), where $r_{\mathbf{k}} \to 0$, (and $\varphi_{\mathbf{k}} \to -\pi/4$ and $\theta_{\mathbf{k}} \to \infty$) meaning that there is no squeezing. On the other hand at the superhorizon scales ($k|\tau| \ll 1$), $r_{\mathbf{k}} \to \infty$ the state is highly squeezed.

2.4.2 How does classicality emerge?

In the previous section, we have introduced the formalism of state squeezing. The question at hand is, why do we observe a classical universe when the initial fluctuations are of a quantum nature? As we have mentioned before, there are actually two main problems when talking about observing any type of imprint of "quantumness" from the very early universe. First, the final inflation puts the initial quantum state into a very special state - the squeezed state. Second, decoherence - the main focus of this thesis (see section 3) - caused by interactions is ubiquitous and erases quantum correlations.

Let us understand why squeezing leads to classical observables. The dynamical evolution of the quantum modes is governed by the time-dependent Schrödinger equation [46],

$$i\hbar\psi'(\tau, v) = \hat{H}\psi(\tau, v). \tag{2.94}$$

Since the initial adiabatic ground state is a Gaussian state, for the wavefunction Gaussianity will be preserved throughout the entire time-evolution. However, the accelerated expansion of the universe squeezes the state. The Solution for equation (2.94) reads

$$\psi(\tau, v) = \left(\frac{2\,\mathrm{Re}\,\Omega_{\mathbf{k}}(\tau)}{\pi}\right)^{\frac{1}{4}} \exp\left[-\Omega_{\mathbf{k}}(\tau)v^2(\tau)\right], \tag{2.95}$$

with [28]

$$\Omega_{\mathbf{k}}(\tau) = k\frac{1 - i\sin 2\varphi_{\mathbf{k}}\sinh 2r_{\mathbf{k}}}{\cosh 2r_{\mathbf{k}} + \cos 2\phi_{\mathbf{k}}\sinh 2r_{\mathbf{k}}} \tag{2.96}$$

where we can clearly see, that in the limit of large squeezing $\mathrm{Im}\,\Omega_{\mathbf{k}} \gg \mathrm{Re}\,\Omega_{\mathbf{k}}$.

Claim: for $\mathrm{Im}\,\Omega_{\mathbf{k}} \gg \mathrm{Re}\,\Omega_{\mathbf{k}}$ the state (2.95) becomes classical in the WKB sense [29].

Proof: Let us consider a simple inverted harmonic oscillator. The Hamiltonian reads

$$\hat{H} = \frac{\hat{p}^2}{2} - \frac{\hat{q}^2}{2} = i\frac{\hbar}{2}\left[\hat{a}^2 e^{2i\frac{\pi}{4}} + \text{h.c.}\right], \tag{2.97}$$

where $\hat{a}$ is as usual the annihilation operator. The q-representation of a squeezed state for this system writes

$$\psi(q) = N \exp\left[-\frac{q^2}{2\hbar}(B + iC)\right], \tag{2.98}$$

where

$$N = \left(\frac{B}{\hbar\pi}\right)^{\frac{1}{4}}, \qquad B = \frac{1}{\cosh 2r}, \qquad C = \tanh 2r, \tag{2.99}$$

where r is the squeezing parameter. We can rewrite the wavefunction as

$$\psi(q) = \rho(q)e^{iS(q)}. \tag{2.100}$$

WKB condition: if $S(q)$ varies more rapidly with q than $\rho(q)$ the state can be identified as a WKB state for which

$$\hat{p} \simeq \hbar\partial_q S(q)\,|\psi\rangle\,. \tag{2.101}$$

When this condition holds the state assigns the position and the momentum simultaneously with

$$p(q) = \hbar\partial_q S(q) \tag{2.102}$$

representing classical evolution in the phase space. In the case considered $\rho(q) = Ne^{-Bq^2/2\hbar}$ and $S(q) = -Cq^2/2\hbar$. The WKB condition is met when $\rho(\partial_q S(q)/\partial_q\rho_q)$ is large. One easily obtains

$$\partial_q S(q) = -C\frac{q}{\hbar}, \qquad \partial_q\rho(q) = -N\frac{Bq}{\hbar}\exp\left[-\frac{Bq^2}{2\hbar}\right], \tag{2.103}$$

so finally

$$\left|\rho\frac{\partial_q S}{\partial_q\rho}\right| = \frac{C}{B} = \sinh 2r. \tag{2.104}$$

Thus in the limit of large squeezing ($r \gg 1$), the state (2.98) is classical in the WKB sense. The argument can be generalized for (2.95).

The state (2.95) is definitely different from a classical state, however, the reason why we are unable to find any quantum signatures is because, for example, the CMB observations measure field amplitudes. In the large squeezing limit the corresponding expectation values of the state (2.95) cannot be distinguished from a classical Gaussian phase space distribution.

However, as we have noticed above, the field modes are not an isolated system. They interact with their environment (at least gravitationally) which in turn decoheres the system. A great example of how ubiquitous decoherence is in the universe is a dust particle in the interstellar medium. Simply

due to the (weak) coupling with the CMB photons they follow a classical trajectory.

There are many viable models of inflation [53], of which some are distinguished by the types of couplings with other sectors. In the framework of quantum decoherence, these sectors can be regarded as environments. We will focus on *axion inflation*, where axions play the role of the inflaton and are coupled with a *U(1) gauge field*, which we will identify as the environment.

2.5 Axion inflation

A somewhat distinguished model of inflation involves a Pseudo-Nambu-Goldstone-Boson (PGNB), which enjoys a shift symmetry $\varphi \to \varphi + const$, protecting the slow-roll parameters from dangerous corrections (see e.g. [19, 24, 54]). In this scenario, the shift symmetry is slightly broken either explicitly or by quantum effects. This allows the slow-roll parameters to maintain values $\varepsilon, \eta \ll 1$ but not 0 to allow for inflation. To illustrate why this is important, consider a generic inflationary potential $V_{\rm sr}$, where sr stands for slow-roll. If one considers all operators of five and six dimensions involving the inflaton, unless forbidden by some symmetry, these operators can contribute with $\mathcal{O}(1)$ corrections to the slow-roll parameters, prematurely ending inflation [55]. Then, for inflation to be successful, we must ensure that whatever the UV physics is at play, it does not induce such destructive terms. The situation is even more dangerous when it comes to *large-field models of inflation*, where the inflaton vacuum expectation value changes by an amount much larger than the Planck scale during inflation. Here Planck-suppressed terms of any dimension can contribute significantly to the slow-roll parameters, so one has to control infinitely many terms not to spoil inflation.

From a particle physics perspective, PGNBs are ubiquitous. They appear whenever an approximate global symmetry is broken. We may refer to these PGNBs as axions.

The first model, where axion plays the role of the inflaton [19] exploited a periodic potential

$$V(\varphi) = \Lambda^4 \left[1 - \cos\left(\frac{\varphi}{f}\right)\right] \tag{2.105}$$

to drive inflation. Here f is the axion decay constant and Λ is some non-perturbatively generated scale proportional to $e^{-1/\lambda}$, with λ being the gauge coupling. The shift symmetry (continuous) is valid at all orders in the perturbation theory, but it is generally broken by non-perturbative effects to a *discrete sub-group* $\varphi \to \varphi + 2\pi f$. Unfortunately, this model complies with observations only if $f \gtrsim M_{\rm Pl}$ [56]. This regime is problematic, since in the case of the PGNB, it means that the symmetry breaking occurs above the quantum gravity scale, where conventional quantum field theory (QFT) is presumably not valid [57, 58]. To avoid such issues, many extensions to axion models have been proposed (see e.g.[59, 60, 61, 62]).

The axion decay constant obviously plays an important role in any axion inflation model. The reasoning behind this is, that it controls the least-irrelevant shift-symmetric coupling, such as the five-dimensional coupling with the gauge fields $\varphi F\tilde{F}/f$. In any axion model this coupling is expected

and to be more precise it is manifest as an interaction term in the Lagrangian

$$\mathcal{L}_{\rm int} = -\frac{\alpha}{4f}\phi F^{\mu\nu}\tilde{F}_{\mu\nu}. \tag{2.106}$$

$F_{\mu\nu} \equiv \partial_\mu A_\nu - \partial_\nu A_\mu$ is the U(1) gauge field strength and $\tilde{F}_{\mu\nu} \equiv \epsilon^{\mu\nu\rho\sigma}F_{\rho\sigma}/2\sqrt{-g}$ is its dual. Here ϵ denotes the completely antisymmetric tensor. The dimensionless parameter α is order unity from the perspective of effective field theory, however in [59], it was shown to be larger for some realizations of axion inflation. To realize a controlled effective field theory it is natural to take $\alpha/f \gg M_{\rm Pl}$. In ref [59], a modified slow-roll mechanism was proposed: The gauge fields slow down the inflaton field φ even on steep potentials. This allows for an elongated duration of inflation. On the other hand ref [63] took a more conservative approach and showed that even in the standard slow-roll scenario, the coupling (2.106) can have a significant impact on the phenomenology of the model. We adopt this approach which is based on the following observation: The motion of the inflaton field amplifies the gauge field fluctuations δA, which in turn decay into inflaton perturbations via *inverse dacay* $\delta A + \delta A \to \delta\varphi$. This process also allows for excess production of primordial gravitational waves and large non-Gaussianities [27, 63, 64]. These studies also show, that for $\alpha/f \gtrsim 10^2 M_{\rm Pl}^{-1}$, the new source of perturbations dominates the standard vacuum fluctuations.

2.5.1 Gauge field production

As advertised, we must show how the gauge fields are produced during inflation. To meet this goal, we start with the action of a PGNB coupled to $U(1)$ gauge fields [27]

$$S = \int d^4x\sqrt{-g}\left[\frac{M_{\rm Pl}^2}{2}R - \frac{1}{2}g^{\mu\nu}\partial_\mu\phi\partial_\nu\phi - V(\phi) - \frac{1}{4}F_{\mu\nu}F^{\mu\nu} - \frac{\alpha}{4f}\phi F_{\mu\nu}\tilde{F}^{\mu\nu}\right], \tag{2.107}$$

where g is the determinant of the spatially flat FRLW metric. R is the Ricci scalar and $F, \tilde{F}$ are the gauge field strength and its dual (see equation (2.106)). As usual, the inflaton field is made up of the background and the fluctuating parts $\phi(\mathbf{x}, t) = \phi(t) + \delta\phi(\mathbf{x}, t)$.

In Appendix B we obtain the equations of motion for the gauge fields and the inflaton field by varying this action. As a result we obtain(B.7)[11](B.11) and (B.21)

$$\left(\vec{\nabla}\cdot\vec{A}\right)' = 0, \tag{2.108}$$

$$\vec{A}'' - \frac{\alpha}{f}\phi'\vec{\nabla}\times\vec{A} + \vec{\nabla}^2\vec{A} = 0, \tag{2.109}$$

$$\phi'' + 2\mathcal{H}\phi' - \nabla^2\phi + a^2\frac{dV}{d\phi} = a^2\frac{\alpha}{f}\vec{E}\cdot\vec{B}. \tag{2.110}$$

where $' \equiv \partial/\partial\tau$ and in analogy with the electric and the magnetic field, we have defined

$$\vec{B} = \frac{1}{a^2}\epsilon^{ijk}\partial_i A_k \equiv \frac{1}{a^2}\vec{\nabla}\times\vec{A}, \qquad \vec{E} = -\frac{1}{a^2}\partial_0 A_i \equiv -\frac{1}{a^2}\vec{A}'. \tag{2.111}$$

[11] Equation (B.7) is actually a constraint equation

Equations (2.108-2.110) are complemented with the 00 Einstein equation, which determines the gauge field contribution to the total energy density [63]

$$\mathcal{H}^2 = \frac{1}{3M_{\rm Pl}^2}\left[\frac{1}{2}(\phi')^2 + \frac{1}{2}\left(\vec{\nabla}\phi\right)^2 + a^2V(\phi) + \frac{a^2}{2}\left(\vec{E}^2 + \vec{B}^2\right)\right]. \tag{2.112}$$

Note, however, that these equations do not complete the treatment of perturbations, since one must also consider the metric fluctuations by using for example the ADM formalism. For our purposes, the equations presented will suffice (for more on why this is justified the reader is referred to [27]).

In equation (2.109), it is clear that the second term accounts for the gauge field production due to the motion of the inflaton field. The effect of the produced gauge fields is twofold: *i*) gauge fields source inflaton perturbations through equation (2.110) and *ii*) the gauge field backreacts on the background dynamics by equation (2.112), see Sec. 2.5.3.

2.5.2 Tachyonic amplification

The motion of the inflaton field causes instability in the gauge field fluctuations. To see this effect we turn to equation (2.109) and consider a homogeneous background $\phi(t)$. The Fourier decomposition of the gauge field reads

$$\vec{A}(\mathbf{x},\tau) = \int \frac{d^3k}{(2\pi)^{3/2}} \sum_{\lambda=\pm}\left[\vec{\varepsilon}_\lambda(\mathbf{k})a_\lambda(\mathbf{k})A_\lambda(k,\tau)e^{i\mathbf{k}\cdot\mathbf{x}} + \varepsilon^*_\lambda(\mathbf{k})a^\dagger_\lambda(\mathbf{k})A^*_\lambda(k,\tau)e^{-i\mathbf{k}\cdot\mathbf{x}}\right], \tag{2.113}$$

where λ here denotes different polarizations, $\vec{\varepsilon}_\lambda$ are the polarization vectors that obey the relations

$$\vec{k}\cdot\vec{\varepsilon}_\pm(\vec{k}) = 0, \qquad \vec{k}\times\vec{\varepsilon}_\pm = \mp ik\vec{\varepsilon}_\pm(\vec{k}), \qquad \vec{\varepsilon}_\pm(-\vec{k}) = \vec{\varepsilon}^*_\pm(\vec{k}), \qquad \vec{\varepsilon}^*_\lambda(\vec{k})\cdot\vec{\varepsilon}_{\lambda'}(\vec{k}) = \delta_{\lambda\lambda'}, \tag{2.114}$$

and the creation-annihilation operators obey the canonical commutation relations

$$[a_\lambda(\mathbf{k})a^\dagger_{\lambda'}(\mathbf{p})] = \delta_{\lambda\lambda'}\delta^{(3)}(\mathbf{k}-\mathbf{p}), \tag{2.115}$$

$$[a_\lambda(\mathbf{k})a_{\lambda'}(\mathbf{p})] = 0, \qquad [a^\dagger_\lambda(\mathbf{k})a^\dagger_{\lambda'}(\mathbf{p})] = 0. \tag{2.116}$$

Plugging (2.113) into the equation of motion (2.109), the modes $A_\pm$ will obey the following equation:

$$\left[\frac{d^2}{d\tau^2} + k^2 \pm \frac{2k\xi}{\tau}\right]A_\pm(\tau,k) = 0, \qquad \xi = \frac{\alpha\dot{\phi}}{2fH}, \tag{2.117}$$

where the dot denotes a derivative with respect to cosmic time. During inflation, the parameter ξ can be considered as a constant, since the evolution $\dot{\phi}$ is subleading in the slow-roll approximation[12]. Without loss of generality one can assume $\alpha > 0$ and $\dot{\phi} > 0$ and therefore $\xi > 0$. In this case, " $+$ " mode undergoes tachyonic instability and grows exponentially, while the " $-$ " mode gets suppressed.

[12] We will generalize to scale dependence of ξ in later sections.

This is clearer once we divide equation (2.117) by k^2 and identify $\omega_{\text{eff}}^2 = 1+2\xi/k\tau$. Since $\tau \in (-\infty; 0]$ during inflation $\omega_{\text{eff}}^2 < 0$ for $k\tau \lesssim 2\xi$ leads to tachyonic amplification of $A_+(\tau, k)$.

As usual, we require the solutions to be of the Bunch-Davies form at the beginning of inflation

$$A_\pm(\tau, k) = \frac{e^{-ik\tau}}{\sqrt{2k}}, \qquad k\tau \to -\infty. \tag{2.118}$$

Then the solutions of (2.117) satisfying this condition can be written in terms of the Coulomb functions [59]

$$A_\pm(\tau, k) = \frac{1}{\sqrt{2k}} \left(G_0(\pm\xi, -k\tau) + iF_0(\pm\xi, -k\tau)\right), \tag{2.119}$$

where G_0 and F_0 are the irregular and regular Coulomb functions respectively. In fig. 4 we see, that the plus mode dominates over the minus mode near the end of inflation[13].

We can make an approximation in the regime $2\xi \gg -k\tau$ and $e^{\pi\xi} \gg 1$

$$A_+(\tau, k) \simeq \sqrt{\frac{-2\tau}{\pi}} e^{\pi\xi} K_1(2\sqrt{-2\xi k\tau}), \tag{2.120}$$

where K_1 is the Bessel function of the second kind. The interval $(8\xi)^{-1} \lesssim -k\tau \lesssim 2\xi$ accounts for most of the power of the created gauge fields [63]. This can be seen in figure 5 where we have plotted the exact solution and a relatively tractable approximation

$$A_+(\tau, k) \simeq \frac{1}{\sqrt{2k}} \left(-\frac{k\tau}{2\xi}\right)^{1/4} e^{\pi\xi - 2\sqrt{-2\xi k\tau}}. \tag{2.121}$$

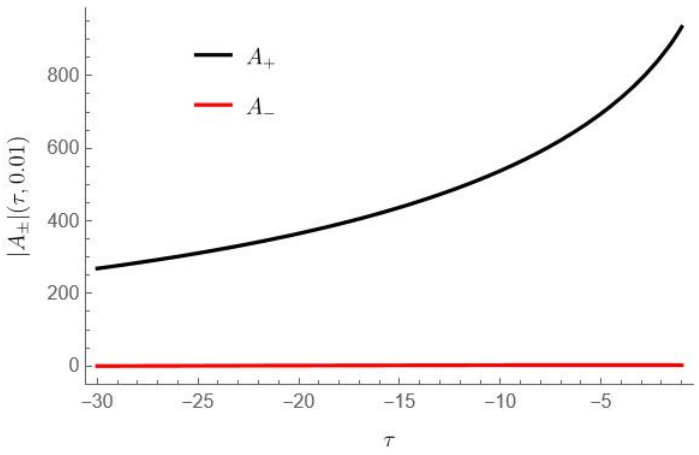

Figure 4: Behavior of the plus (black) and minus (red) modes at $\xi = 2$ and $k = 0.05$. The plus mode is absolutely dominant close to the end of inflation.

For our purposes, we will be using this approximation in the remainder of the text. In order to

[13] Although which mode is amplified is completely arbitrary and depends only on the overall sign of ξ

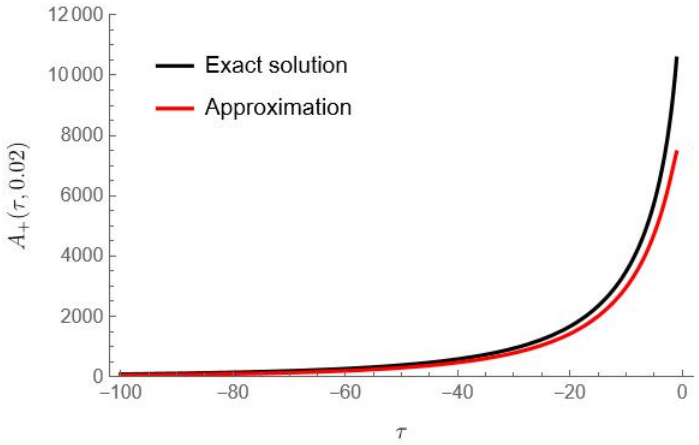

Figure 5: The exact (black) and the approximated (red) mode behavior in the interval $(8\xi)^{-1} \lesssim -k\tau \lesssim 2\xi$, where we have taken $\xi = 3$ and $k = 0.2$.

derive the environment correlation function we will also need its time derivative

$$A'_+(\tau, k) = \left(\frac{1}{4\tau} + \sqrt{\frac{2k\xi}{-\tau}}\right) A_+(\tau, k) \simeq \sqrt{\frac{2k\xi}{-\tau}} A_+(\tau, k). \tag{2.122}$$

2.5.3 Backreaction in the slow-roll Approximation

Since gauge fields undergo an exponential amplification near the end of inflation, it would be natural to investigate their backreaction on the homogeneous inflaton background.

We will use the mean-field equations (2.110, 2.112), that capture the backreaction of the produced gauge fields on the homogeneous inflaton background. Switching to physical time, we have

$$\begin{aligned} \ddot{\phi} + 3H\dot{\phi} + V_\phi &= \frac{\alpha}{f}\langle \vec{E} \cdot \vec{B} \rangle, \\ H^2 &= \frac{1}{3M_{\rm Pl}^2}\left[\frac{1}{2}(\dot{\phi})^2 + V(\phi) + \frac{1}{2}\langle \vec{E}^2 + \vec{B}^2 \rangle\right], \end{aligned} \tag{2.123}$$

where $V_\phi \equiv dV/d\phi$. Notice that the gradient terms have vanished, because these equations govern the backreaction on the homogeneous dynamics of $\phi(t)$ and $a(t)$.

Using eq. (2.113) and neglecting the negative mode altogether, we write

$$\begin{aligned} \langle \vec{E} \cdot \vec{B} \rangle &= -\frac{1}{a^4(\tau)} \int \frac{d^3k}{(2\pi)^{3/2}} \frac{d^3p}{(2\pi)^{3/2}} p \langle \left[\vec{\varepsilon}_+(\mathbf{k}) \cdot \vec{\varepsilon}_+(\mathbf{p}) a_+(\mathbf{k}) a_+^\dagger(\mathbf{p}) A'_+(\tau, k) A^*_+(\tau, p) e^{i(\mathbf{k}-\mathbf{p})\cdot\mathbf{x}} \right] \rangle \\ &= -\frac{1}{(2\pi)^2 a^4(\tau)} \int dk k^3 \partial_\tau |A_+(\tau, k)|^2, \end{aligned} \tag{2.124}$$

where in the first equation we only kept the non-vanishing expectation values.

This derivation can be trivially adopted to calculate $\langle \vec{E}^2 + \vec{B}^2 \rangle$, leading to

$$\frac{1}{2}\langle \vec{E}^2 + \vec{B}^2 \rangle = \frac{1}{(2\pi)^2 a^4} \int dk k^2 \left[|A'_+(\tau,k)|^2 + k^2 |A_+(\tau,k)|^2 \right]. \tag{2.125}$$

While evaluating these integrals, we can disregard the large momentum ($k > 2\xi aH$) modes as well, since these modes stay in their vacuum states and do not undergo tachyonic instability. This way one establishes a UV cutoff for the integrals in equations (2.124-2.125): $-k\tau < 2\xi$. However, since the gauge field production occurs mainly in the interval $(8\xi)^{-1} < k/(aH) < 2\xi$, we can extend the region of integration from 0 to ∞, since the gauge field production rapidly decreases outside this interval, so their contribution will be negligible. This way, we can approach the integrals analytically. Plugging equations (2.121), (2.122) into the integral in (2.124)

$$\int dk k^3 \partial_\tau |A_+(\tau,k)|^2 = e^{2\pi\xi} \int_0^\infty dk k^3 e^{-4\sqrt{2\xi k/aH}}. \tag{2.126}$$

We can make the change of variable $p = 2(2\xi k/aH)^{1/4}$, which leads to a Gaussian integral. Plugging this into (2.124) produces

$$\langle \vec{E}\cdot\vec{B} \rangle = -\frac{4}{(2\pi)^2 a^4(\tau)} e^{2\pi\xi} \left(\frac{aH}{32\xi}\right)^4 \int_0^\infty dp p^{15} e^{-p^2} \simeq -2.4\cdot 10^{-4} \left(\frac{H}{\xi}\right)^4 e^{2\pi\xi}. \tag{2.127}$$

The procedure for evaluating $1/2\langle \vec{E}^2 + \vec{B}^2 \rangle$ is exactly the same and it leads to

$$\frac{1}{2}\langle \vec{E}^2 + \vec{B}^2 \rangle \simeq 1.4\cdot 10^{-4} \frac{H^4}{\xi^3} e^{2\pi\xi}. \tag{2.128}$$

Backreaction effects are twofold. First, we consider the effect on the homogeneous Klein-Gordon equation (1st equation in (2.123)). It is trivial to show that to trust the usual slow-roll prescription $|3H\dot{\phi}| \simeq |-V_\phi| \gg \alpha/f \langle \vec{E}\cdot\vec{B} \rangle$ we must have

$$e^{\pi\xi}\xi^{-3/2} \ll 79 \frac{\dot{\phi}}{H^2}. \tag{2.129}$$

Second, since the gauge fields are involved in the Friedmann equation (2nd equation in (2.123)), to ensure that the potential dominates the background evolution of the universe we impose $3M_{\rm Pl}^2 H^2 \simeq V \gg \frac{1}{2}\langle \vec{E}^2 + \vec{B}^2 \rangle$, leading to

$$e^{\pi\xi}\xi^{-3/2} \ll 146 \frac{M_{\rm Pl}}{H}. \tag{2.130}$$

If these inequalities are satisfied, then the gauge field backreaction on the homogeneous background is negligible, which is a good approximation up to the near end of inflation.

Taking into account the standard result for the primordial power spectrum $\mathcal{P}^{1/2} = H^2/(2\pi\dot{\phi}) \simeq 5\cdot 10^{-5}$, one can obtain a bound for ξ, namely $\xi \leq 4.7$.

2.5.4 Power Spectrum

Even when (2.129) and (2.130) are satisfied the coupling ϕFF can still have a profound effect on the cosmological perturbations. Here we study the effect of the gauge field production on the scalar power spectrum following [27].

For perturbations equation (2.110) can be rewritten as

$$[\partial_\tau^2 + 2\mathcal{H}\partial_\tau - \nabla^2 + a^2 m^2]\delta\phi(\mathbf{x},\tau) = a^2\frac{\alpha}{f}\left(E\cdot B - \langle\vec{E}\cdot\vec{B}\rangle\right), \tag{2.131}$$

where $m^2 = V_{\phi\phi}$. The solution can be split into two independent parts. One is the standard solution of the homogeneous equation (zero source term) and the second one includes the source term

$$\delta\phi(\mathbf{x},\tau) = \delta\phi^{\text{vac}}(\mathbf{x},\tau) + \delta\phi^{\text{sourced}}(\mathbf{x},\tau). \tag{2.132}$$

The first term corresponds to the standard vacuum fluctuations, while the second term is produced through $\delta A + \delta A \to \delta\phi$ process. This term is actually highly non-Gaussian and may even dominate the standard vacuum fluctuations [63].

Next, we Fourier decompose (2.132)

$$\delta\phi(\mathbf{x},\tau) = \int \frac{d^3k}{(2\pi)^{3/2}}\frac{Q_{\mathbf{k}}(\tau)}{a(\tau)}e^{i\mathbf{k}\cdot\mathbf{x}}. \tag{2.133}$$

Notice, that the last term in (2.131) is proportional to $\delta^{(3)}(\mathbf{k})$ and thus has no effect on modes $\mathbf{k}\neq 0$. Then the EOM in Fourier space writes

$$\left[\partial_\tau^2 + k^2 + a^2m^2 - \frac{a''}{a}\right]Q_{\mathbf{k}}(\tau) = S_{\mathbf{k}}(\tau), \tag{2.134}$$

where

$$S_{\mathbf{k}}(\tau) \equiv a^3(\tau)\frac{\alpha}{f}\int\frac{d^3k}{(2\pi)^{3/2}}\vec{E}\cdot\vec{B}e^{i\mathbf{k}\cdot\mathbf{x}}. \tag{2.135}$$

From (2.132) it follows, that $Q \to Q^{\text{vac}} + Q^{\text{sourced}}$. The homogeneous part can be expanded as

$$Q_{\mathbf{k}}^{\text{vac}}(\tau) = b(\mathbf{k})\varphi_k(\tau) + b^\dagger(-\mathbf{k})\varphi_k^*(\tau), \tag{2.136}$$

where the ladder operators $b, b^\dagger$ satisfy

$$\left[b(\mathbf{k}), b^\dagger(\mathbf{p})\right] = \delta^{(3)}(\mathbf{k}-\mathbf{p}). \tag{2.137}$$

Notice, the homogeneous equations are the the ones considered in section 2.3.3, whose solutions can be written as

$$\varphi_k(\tau) = \frac{i}{2}\sqrt{\frac{\pi}{k}}\sqrt{-k\tau}H_\nu^{(1)}(-k\tau), \tag{2.138}$$

where we have chosen for convenience the arbitrary phase, such that the solution in the limit $-k\tau \to 0$ is real.

The vacuum modes can be employed in the Green function

$$G_k(\tau,\tau') = i\Theta(\tau-\tau')\left[\varphi_k(\tau)\varphi^*(\tau') - \varphi^*(\tau)\varphi(\tau')\right], \tag{2.139}$$

which obeys

$$\left[\partial_\tau^2 + k^2 + a^2m^2 - \frac{a''}{a}\right] G_k(\tau,\tau') = \delta(\tau-\tau'). \tag{2.140}$$

The sourced part of the solution then takes the following form

$$Q_{\mathbf{k}}^{\rm sourced}(\tau) = \int_{-\infty}^{0} d\tau' G_k(\tau,\tau') S_{\mathbf{k}}(\tau'). \tag{2.141}$$

According to our definitions the curvature perturbations on uniform density hypersurfaces (ζ in section 2.3.3) $\zeta = -\frac{H}{\dot\phi}\frac{Q_{\mathbf{k}}}{a}$.

We now have the ingredients to compute the correlation functions and ultimately, the power spectrum. The vacuum modes produce the standard result

$$\langle \zeta_{\mathbf{k}}^{\rm vac}\zeta_{\mathbf{k}'}^{\rm vac}\rangle = \frac{2\pi^2}{k^3}\mathcal{P}\,(-k\tau)^{n_s-1}\,\delta^{(3)}(\mathbf{k}-\mathbf{k}'), \tag{2.142}$$

where the *spectral index* is defined as $n_s = 1+3-2\nu = 1+\mathcal{O}(\varepsilon,\eta)$ and $\mathcal{P}^{1/2} \equiv H^2/2\pi\dot\phi$.

The extra part of the power spectrum comes from the sourced scalar perturbations. According to (2.141) the two-point function reads

$$\langle \zeta_{\mathbf{k}}^{\rm sourced}(\tau)\zeta_{\mathbf{k}}^{\rm sourced}(\tau')\rangle = \frac{H^2}{\dot\phi^2 a^2}\int d\tau' d\tau'' G_k(\tau,\tau')G_k(\tau,\tau'')\langle S_{\mathbf{k}}(\tau')S_{\mathbf{k}'}(\tau'')\rangle. \tag{2.143}$$

Now we make an important approximation. Namely, since we are interested in power spectra of superhorizon modes ($-k\tau \ll 1$), this allows us to rewrite the solution (2.138) as

$$\varphi_k(\tau) \simeq \frac{a(\tau)H}{\sqrt{2}k^{3/2}}(-k\tau)^{\frac{n_s-1}{2}}. \tag{2.144}$$

which is *real*. Using this we can rewrite (2.143) as

$$\langle \zeta_{\mathbf{k}}^{\rm sourced}(\tau)\zeta_{\mathbf{k}}^{\rm sourced}(\tau')\rangle \simeq \frac{2H^4}{\dot\phi^2}\frac{(-k\tau)^{n_s-1}}{k^3}\int_{-\infty}^{\tau} d\tau' d\tau''\,{\rm Im}\{\varphi_k(\tau')\}\,{\rm Im}\{\varphi_k(\tau'')\}\langle S_{\mathbf{k}}(\tau')S_{\mathbf{k}}(\tau'')\rangle, \tag{2.145}$$

where we have already used the fact that the integral vanishes for $\mathbf{k} \neq \mathbf{k}'$. The approximation (2.144) is used only for the modes that depend on τ; The rest of them are under the integral that ranges from $-\infty$ to τ, so we will not make the same approximation.

After explicit evaluation of the correlation function $\langle S_{\mathbf{k}}S_{\mathbf{k}'}\rangle$ we arrive at the following integral

expression

$$\langle \zeta_{\mathbf{k}}^{\rm sourced}(\tau)\zeta_{\mathbf{k}'}^{\rm sourced}(\tau)\rangle = \frac{\alpha^2 H^6 e^{4\pi\xi}}{2^8\pi^3 f^2\dot{\phi}^2}\frac{(-k\tau)^{n_s-1}}{k^3}\delta^{(3)}(\mathbf{k}+\mathbf{k}')\times$$
$$\times\int d^3q_*\left[1+\frac{|q_*|^2-\mathbf{q}_*\cdot\hat{z}}{|\mathbf{q}_*||\hat{z}-\mathbf{q}_*|}\right]^2\sqrt{|\mathbf{q}_*|}\sqrt{|\mathbf{q}_*-\hat{z}|}\left[\sqrt{|\mathbf{q}_*|}+\sqrt{|\mathbf{q}_*-\hat{z}|}\right]^2\times$$
$$\times I^2\left[2\sqrt{2\xi}\left(\sqrt{|\mathbf{q}_*|}+\sqrt{|\mathbf{q}_*-\hat{z}}\right)\right], \quad (2.146)$$

where $\mathbf{q}_* \equiv \mathbf{q}/|\mathbf{k}|$, we have put $\mathbf{k}||\hat{z}$ and

$$I[z] \equiv \sqrt{\frac{\pi}{2}}\int_{-k\tau}^{\infty} dx x^{3/2}\,{\rm Re}\left[H_\nu^{(1)}(x)\right]e^{-z\sqrt{x}}. \quad (2.147)$$

It should be noted, that in this treatment the slow-roll corrections are omitted and we are working in zeroth order in slow-roll.

The correlation function can be written conveniently as

$$\langle \zeta_{\mathbf{k}}^{\rm sourced}(\tau)\zeta_{\mathbf{k}'}^{\rm sourced}(\tau)\rangle \equiv \frac{2\pi^2}{k^3}(-k\tau)^{n_s-1}\mathcal{P}^2 f_2(\zeta)e^{4\pi\xi}\delta^{(3)}(\mathbf{k}+\mathbf{k}'), \quad (2.148)$$

where

$$f_2(\xi) = \frac{\xi^2}{8\pi}\int d^3q_*\left[1+\frac{|q_*|^2-\mathbf{q}_*\cdot\hat{z}}{|\mathbf{q}_*||\hat{z}-\mathbf{q}_*|}\right]^2\sqrt{|\mathbf{q}_*|}\sqrt{|\mathbf{q}_*-\hat{z}|}\left[\sqrt{|\mathbf{q}_*|}+\sqrt{|\mathbf{q}_*-\hat{z}|}\right]^2\times$$
$$\times I^2\left[2\sqrt{2\xi}\left(\sqrt{|\mathbf{q}_*|}+\sqrt{|\mathbf{q}_*-\hat{z}}\right)\right]. \quad (2.149)$$

This integral has to be evaluated numerically. For $\xi \gg 1$ we have [27]

$$f_2(\xi) \simeq \frac{7.5\times 10^{-5}}{\xi^6}, \qquad \xi \gg 1. \quad (2.150)$$

In terms of phenomenology, the most interesting interval is $2 \leq \xi \leq 3$. One can obtain a fit for $f(\xi)$ in this interval

$$f_2(\xi) \simeq \frac{3\cdot 10^{-5}}{\xi^{5.4}}, \qquad 2 \leq \xi \leq 3. \quad (2.151)$$

The power spectrum is related to the two-point function by

$$\langle \zeta_{\mathbf{k}}\zeta_{\mathbf{k}'}\rangle \equiv P_{\zeta\zeta}(k)\frac{2\pi^2}{k^3}\delta^{(3)}(\mathbf{k}+\mathbf{k}'). \quad (2.152)$$

In our case, there are two independent contributions coming from ζvac and ζ^{sourced}, hence

$$P_{\zeta\zeta}(k) = \mathcal{P}\left(\frac{k}{k_0}\right)^{n_s-1}\left[1+\mathcal{P}f_2(\xi)e^{4\pi\xi}\right]. \tag{2.153}$$

In Sec. 3.5.1 we compare this result with the one obtained using our adopted formalism.

3 Quantum Dechoerence in the Early Universe

In this section, we will introduce a general framework and concepts suited for decoherence. Our emphasis is on the master equations which allow us to study open quantum systems, i.e. quantum systems that interact with their environment. The reader may refer to [65, 66, 67] for a more exhaustive review. We then apply these concepts to the standard paradigmatic single-field model of inflation, as done in for example in refs [3, 2, 6, 7] and many more. Finally, we apply the developed formalism to axion inflation.

3.1 A brief introduction to decoherence

Quantum decoherence takes into account the fact that realistic physical systems usually interact with their environment (broadly defined). Quantum interactions induce entanglement between the system and large environmental degrees of freedom. These interactions affect the observables of a given quantum system[14], in such a way that the supposed quantum system loses coherence, the main source of quantum effects, such as interference. This is called the environment-induced *decoherence* and it is at the root of quantum-to-classical transition as is evident from our argument. Namely, since the quantum system has lost all its quantum properties, it now behaves classically. In other words, decoherence describes how interactions at the quantum level influence the statistics of the system.

The process of dynamical decoherence is very efficient. In fact, even if the interaction with the environment is weak, the system still becomes highly entangled with the environment degrees of freedom. This is an irreversible process, mainly due to the entanglement with enormous environmental degrees of freedom, which practically cannot be tracked.

Another property of decoherence is usually called environment-induced superselection. That is, the environment imposes robust preferred states for the system. Practically, this means, that the environment limits the physical observables on a given system.

Imagine photons scattering off of a body (see figure 6). In the classical picture when measuring an observable, such as momentum, photon scattering has a negligible effect, so we usually discard such contributions.

As for the quantum picture, every scattering event is associated with entangled pairs of photons and the object constituents. Such quantum correlations carry away coherence from the body, diminishing the properties of the quantum nature of the object. Note that decoherence is independent of photon momentum transfer. This means that the environment may not inflict any classical perturbation on the system but cause efficient decoherence. We stress, that nevertheless, decoherence may occur with classical processes, such as energy dissipation from the system, but it is a strictly quantum mechanism.

Interestingly, a definite environment is not needed. In fact, the thermal radiation and even the cosmic microwave background (CMB) are completely enough to realize decoherence. This shows just how ubiquitous decoherence is in the universe. In the cosmological setting, even with the most

[14] These are usually referred to as open quantum systems.

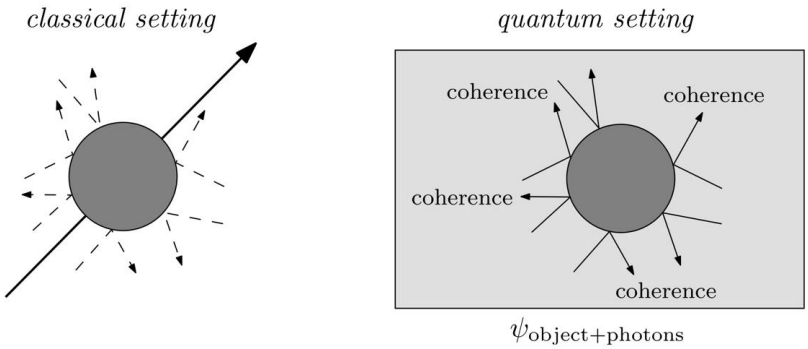

Figure 6: Figure borrowed from [65] for illustrative purposes. On the left: photons scattering on an object do not (or negligibly) change the classical observable, momentum, of the object. On the right: in the quantum picture every scattering event contributes to the decoherence of the constituents of the object.

minimalistic choice of environment, decoherence remains a barrier to observing any quantum imprint from the early universe [7, 9, 10].

3.2 Formal Tools

In this section, we will introduce the basic formalism, crucial for the study of decoherence. For exhaustive reviews, the reader may refer to [65, 66, 67, 68].

3.2.1 Density matrices

Quantum state vector $|\psi\rangle$ encodes maximum information regarding the state of the physical system. We can associate the density matrix, also called the density operator to the state vector $|\psi\rangle$

$$\hat{\rho} \equiv |\psi\rangle \langle\psi| \,. \tag{3.1}$$

We may express the state $|\psi\rangle$ as a superposition of states

$$|\psi\rangle = \sum_i a_i |\psi_i\rangle \,, \tag{3.2}$$

so that the density matrix can be rewritten accordingly

$$\hat{\rho} = \sum_{ij} a_i a_j |\psi_i\rangle \langle\psi_j| \,. \tag{3.3}$$

In the matrix representation of $\hat{\rho}$ the terms $i \neq j$ correspond to the off-diagonal terms, also known as interference terms that encapsulate decoherence, however, there is a subtlety associated with these terms. Namely, interference is to be understood with respect to a certain basis $\{|\psi_i\rangle\}$, however there always exists a basis in which the density matrix becomes diagonal. Disappearance of the

interfering matrix elements does not imply loss of quantum properties. Generally in a different basis interference will reappear, showing the persistent underlying coherence between these basis states.

This prompts the definition of the *pointer states* which are system states $|s_i\rangle$, such that when we consider interactions with the environment, if the initial combined state can be factorized $|s_i\rangle |E_i(0)\rangle$, the combined state at $t > 0$ can also be factorized $|s_i\rangle |E_i(t)\rangle$. From these states, *pointer observables* can be constructed

$$\hat{B} = \sum_i b_i |s_i\rangle \langle s_i| . \tag{3.4}$$

$|s_i\rangle$ are eigenstates of the interaction Hamiltonian $\hat{H}_{\text{int}}$, which means, that the pointer projectors $|s_i\rangle \langle s_i|$ commute with $\hat{H}_{\text{int}}$. We obtain the so-called *commutativity criterion*

$$\left[\hat{B}, \hat{H}_{\text{int}}\right] = 0. \tag{3.5}$$

Taking the trace of the density matrix is a common way to differentiate between the system and the environment. One can choose an orthonormal basis of states, e.g. $\{|\phi_i\rangle\}$, of the Hilbert space of the quantum system. The trace operation is defined as

$$Tr\{\hat{A}\} = \sum_i \langle \phi_i|\hat{A}|\phi_i\rangle , \tag{3.6}$$

where $\hat{A}$ is some operator. The trace operation does not depend on the chosen basis, which means that it can be evaluated using any orthonormal basis of the Hilbert space of a given system.

Trace is a cyclical operation, e.g.

$$Tr\{\hat{A}\hat{B}\hat{C}\} = Tr\{\hat{C}\hat{A}\hat{B}\} = Tr\{\hat{B}\hat{C}\hat{A}\}, \tag{3.7}$$

it is also linear

$$Tr\{\hat{A} + \hat{B}\} = Tr\{\hat{A}\} + Tr\{\hat{B}\}. \tag{3.8}$$

To see how useful the trace operation actually is, let us consider the following operator $\hat{A} = \hat{\rho}\hat{O}$, where ρ is the usual pure-state (the difference between the pure and mixed-state density matrices is explained below) and $\hat{O}$ is an operator corresponding to a physical observable being measured on the system. As before, we choose an orthonormal basis $|o_i\rangle$, that will correspond to eigenstates of the operator $\hat{O}$ with corresponding eigenvalues o_i. Then according to the definition of the trace operation, we have

$$Tr\{\hat{A}\} = \sum_i \langle o_i|(|\psi\rangle \langle\psi|)\hat{O}|o_i\rangle = \sum_i o_i |\langle o_i|\psi\rangle|^2. \tag{3.9}$$

However, it is evident, that according to the *Born rule*, $|\langle o_i|\psi\rangle|^2$ is the probability of the outcome o_i of the measurement. This means that we have obtained the expectation value of the observable $\hat{O}$. This is known as the *trace rule*

$$\langle\hat{O}\rangle = Tr\{\hat{\rho}\hat{O}\}. \tag{3.10}$$

If we choose $\hat{O}$ to be the identity operator, we get

$$Tr\{\hat{\rho}\} = 1. \tag{3.11}$$

3.2.2 Mixed States

It is easy to generalize the trace rule to non-pure, or mixed-state density matrices. The mixedness is linked to our ignorance of the state preparation and is thus associated with classical probabilities[15].

We denote $|\psi_i\rangle$ the possible pure states contained in the mixed state, and their respective probabilities p_i. Then the idea is simply weighting the expectation values $\langle\psi_i|\hat{O}|\psi_i\rangle$, that is

$$\langle\hat{O}\rangle = \sum_i p_i \langle\psi_i|\hat{O}|\psi_i\rangle . \tag{3.12}$$

To consistently describe the statistics of the system we can introduce the mixed-state density matrix

$$\hat{\rho} = \sum_i p_i |\psi_i\rangle \langle\psi_i| , \tag{3.13}$$

where $p_i \leq 0$ and $\sum_i p_i = 1$. It follows, that

$$\langle\hat{O}\rangle = Tr\{\hat{\rho}\hat{O}\}, \qquad Tr\{\hat{\rho}\} = 1. \tag{3.14}$$

We can introduce useful parameters quantifying the level of "mixedness". The pure-state density matrix, defined as $\hat{\rho} = |\psi\rangle \langle\psi|$ is a projection operator on the pure state $|\psi\rangle$, which immediately implies that

$$\hat{\rho}^2 = \hat{\rho}, \tag{3.15}$$

whereas if we take the mixed-state density matrix, we obtain a different result, namely

$$\hat{\rho}^2 = \sum_{ij} p_i p_j |\psi_i\rangle \langle\psi_i|\psi_j\rangle \langle\psi_j| , \tag{3.16}$$

where generally $\langle\psi_i|\psi_j\rangle \neq 0$, but even if this was the case (one can always choose a state basis in which the density matrix is diagonal), we still end up with

$$\hat{\rho}^2 = \sum_i (p_i)^2 |\psi_i\rangle \langle\psi_i| . \tag{3.17}$$

which is not equivalent to (3.15), since for mixed states p_i is strictly less thaan 1. This means that one can find out if the system is in a pure state, simply by checking if (3.15) holds.

Furthermore, we can actually quantify "mixedness". To see this we recall (3.13). Obviously if one of the probability values (e.g. p_1) is 1, then the rest are all 0, which means that we are absolutely

[15] If we consider a system prepared in either one of the two states $|\psi_1\rangle$ or $|\psi_2\rangle$, we can associate classical probabilities to these states since such ignorance can be quantified using classical probabilities.

certain that the system is prepared in some state $|\psi_1\rangle$. The opposite extreme is if the $\hat{\rho} \propto \hat{I}$, where $\hat{I}$ is the identity operator. In this case, we are absolutely ignorant about the quantum state, which means that every possible state is associated with the same value of probability. This corresponds to the maximal degree of ignorance.

A common measure of mixedness is the *purity*, defined as

$$\gamma \equiv Tr\{\hat{\rho}^2\}. \tag{3.18}$$

If $\gamma = 1$, the system is in a pure state (see equations (3.14-3.15)). If we examine the mixed state density matrix, by plugging (3.17) into (3.18), we obtain

$$\gamma = \sum_{i=1}^{N} p_i^2, \tag{3.19}$$

where N is the dimension of the system Hilbert space. For a maximally mixed state $p_i = 1/N$. Then $\sum_{i=1}^{N} 1/N^2 = N/N^2 = 1/N$, which is the lower bound of the sum in (3.19).

Another tool, commonly used for quantifying purity is the von Neumann entropy, which is basically a generalization of the notion of entropy from statistical mechanics to the density operator formalism. It can be written as

$$S(\hat{\rho}) \equiv -Tr\{\hat{\rho}\log_2\hat{\rho}\} \equiv -\sum_i \lambda_i \log_2 \lambda_i, \tag{3.20}$$

where λ_i are the eigenvalues of $\hat{\rho}$. $\lambda_i = 0$ is handled by defining $0\log_2 0 \equiv 0$.

Let us again analyze the extreme cases. First, if $\hat{\rho}$ is pure, then all $\lambda_i = 0$, except one. By our definition this means $S(\hat{\rho}) = -1\log_2 1 = 0$. On the other hand, in case of maximal mixing, all $\lambda_i = p_i = 1/N$, which leads to $S(\hat{\rho}) = \log_2 N$, which is the upper bound for the von Neumann entropy. The parallel between von Neumann entropy and the classically defined entropy is clear, namely, it is a measure of information or rather the measure of ignorance about the state of the system when the system has more than one state available.

3.2.3 The Reduced Density Matrix

Reduced density matrices play a key role in decoherence. The basic idea is to completely extract all the information from the system with little or no consideration of the specifics of the environment. This approach is crucial when the environment is inaccessible to the observer.

Consider a system $\mathcal{S}$, entangled to another system $\mathcal{E}$. If the observer can only measure the system $\mathcal{S}$, the appropriate object that allows the observer to extract all information from $\mathcal{S}$ is the *reduced density matrix*.

$$\hat{\rho}_{\mathcal{S}} \equiv Tr_{\mathcal{E}}\hat{\rho}, \tag{3.21}$$

where we have used the partial trace over the system $\mathcal{E}$. In other words, we have averaged over the degrees of freedom of the inaccessible system.

When studying decoherence it is crucial to identify the system and the environment. Usually, the environment is either uninteresting or practically impossible to completely measure. The reduced density matrices allow us to trace over the degrees of freedom of the environment of the composite density matrix and obtain complete statistics of the system of interest. The system-environment interaction is incorporated into the reduced density matrix, which, by definition, means the reduced density matrix is strictly mixed.

Let us confirm that we can obtain the expectation values by using the reduced density matrix instead of the composite one. In other words, let us show that the trace rule applies to the reduced density matrix.
Consider observables of $\mathcal{S}$, which can be written as $\hat{O} = \hat{O}_{\mathcal{S}} \otimes \hat{\mathbb{I}}_{\mathcal{E}}$, where "$\otimes$" is to be understood as a tensorial product and $\hat{\mathbb{I}}_{\mathcal{E}}$ is the identity operator acting on the Hilbert space of the environment. Let $\{|\psi_i\rangle\}$ and $\{|\phi_j\rangle\}$ be the orthonormal basis states of the system and environment Hilbert spaces respectively. Using (3.6), (3.14) and (3.21) we obtain

$$\begin{aligned}
\langle \hat{O} \rangle &= Tr\{\hat{\rho}\hat{O}\} = \\
&= \sum_{ij} \langle\psi_i| \langle\phi_j| \hat{\rho}(\hat{O}_{\mathcal{S}} \otimes \hat{\mathbb{I}}_{\mathcal{E}}) |\phi_j\rangle |\psi_i\rangle = \\
&= \sum_i \langle\psi_i| \left(\sum_j \langle\phi_j|\hat{\rho}|\phi_j\rangle \right) \hat{O}_{\mathcal{S}} |\psi_i\rangle = \\
&= \sum_i \langle\psi_i|(Tr_{\mathcal{E}}\hat{\rho})\hat{O}_{\mathcal{S}}|\psi_i\rangle \equiv \\
&\equiv \sum_i \langle\psi_i|\hat{\rho}_{\mathcal{S}}\hat{O}_{\mathcal{S}}|\psi_i\rangle = \\
&= Tr\{\hat{\rho}_{\mathcal{S}}\hat{O}_{\mathcal{S}}\}.
\end{aligned} \tag{3.22}$$

Finally, let us note that the concept of density matrices can in principle be generalized to any number of subsystems. Specifically the reduced density matrix for a system entangled with $N-1$ subsystems will be

$$\hat{\rho}_k = Tr_{1,\dots k-1,k+1,\dots N}\{\hat{\rho}\}. \tag{3.23}$$

If we want to evaluate the expectation value of the observable on the system k, one can show that the previous result simply generalizes to

$$\langle \hat{O} \rangle = Tr_k\{\hat{\rho}_k\hat{O}_k)\}. \tag{3.24}$$

3.2.4 System-Environment Bipartition

As we have seen in the previous sections, the definition of bipartition into a system and its environment is crucial to applying the reduced density formalism. In the context of inflation, we can

identify the perturbations observed on the CMB and the LSS as the system. These are the large scale perturbations ($0.005\text{Mpc}^{-1} \lesssim k \lesssim 0.2\text{Mpc}^{-1}$). The environment is poorly specified and usually inaccessible for observations. In the minimalist approach, one can simply identify the scales crossing the horizon later than the observed perturbations as the environment that decohere the large scale perturbations [7, 10]. In addition to the minimal scenario, one may consider other fields coupled to the system (see [2], Appendix B for an example) as the environment. As we will see in the context of axion inflation, the U(1)-axion coupling allows us to define the gauge fields as the environment.

For now, we may simply consider bipartition into two fields that compose the entire system $\Psi = \chi\mathcal{F}$. Let χ be the system and $\mathcal{F}$ the unobservable degrees of freedom that interact with the system, then the total action can be written as

$$S[\Psi] = S[\chi] + S[\mathcal{F}] + S_{\text{int}}[\chi;\mathcal{F}]. \tag{3.25}$$

The last term represents the interaction between the fields. For instance, it could describe the axion-U(1) gauge field interaction. The goal then is to obtain the statistics of the system χ by taking into account the impact of the environment $\mathcal{F}$.

3.2.5 Phase Space Representation - Wigner Function

The Wigner function is frequently used as a phase space representation of reduced density matrices in systems with continuous degrees of freedom.

Employing the system-environment bipartition, the quantum state is a function of variables (χ, p_χ) and $(\mathcal{F}, p_\mathcal{F})$, where p_χ and $p_\mathcal{F}$ are the conjugate momenta of the variables χ and $\mathcal{F}$ respectively. The Wigner function is then defined as the Wigner-Weyl transform of the composite density matrix

$$\begin{aligned} W[\chi, p_\chi; \mathcal{F}, p_\mathcal{F}] = \int dadb e^{-i(p_\chi a + p_\mathcal{F} b)} \times \\ \left(\left\langle \chi + \frac{a}{2}\right| \otimes \left\langle \mathcal{F} + \frac{b}{2}\right|\right) \hat{\rho} \left(\left|\chi - \frac{a}{2}\right\rangle \otimes \left|\mathcal{F} - \frac{b}{2}\right\rangle\right), \end{aligned} \tag{3.26}$$

where $|\chi\rangle$ and $|\zeta\rangle$ are the eigenstates of the position operators for the system and the environment respectively. Tracing out the environment is equivalent to the marginalization of the phase space of the environment and the reduced Wigner function reads

$$W_{\text{red}}[\chi, p_\chi] = \int d\mathcal{F} dp_\mathcal{F} W[\chi, p_\chi; \mathcal{F}, p_\mathcal{F}], \tag{3.27}$$

which is effectively the Wigner-Weyl transform of the reduced density matrix [69]. This explains how we can trace the environmental degrees of freedom out in phase-space or in the Hilbert space, according to which is more convenient for a given problem.

An expectation value of a quantum operator $\hat{A}$ can be computed by the phase-space average of

its weyl transform against the Wigner function

$$\langle \hat{A} \rangle = \int d\chi d\zeta dp_\chi dp_\zeta \tilde{A}(\chi, \zeta, p_\chi, p_\zeta) W[\chi, p_\chi; \zeta, p_\zeta], \tag{3.28}$$

which is why we may refer to the Wigner function as a *quasi-probability distribution function*.

3.3 Quantum Master Equations

In this section, we will introduce quantum master equations, which are the cornerstone of Open Quantum Systems (OQS). Usually, we are interested in a (relatively) small number of degrees of freedom that are surrounded by an environment (larger number of degrees of freedom). Master equations are a tool to model the dynamics of a system immersed in a larger environment.

First, we will clarify the formal side of master equations (see e.g. [65], [66], [70] for more extensive reviews). This section will serve as an intermediate step in applying the master equation formalism to cosmology.

3.3.1 General formalism

Generally, the total (time-dependent) Hamiltonian governing the evolution of the system+environment is

$$H(t) = H_S(t) \otimes \mathbb{I}_E + H_E \otimes \mathbb{I}_S + H_{\text{int}}, \tag{3.29}$$

where we have dropped the hats not to cluster notations unnecessarily. The first and the second terms in the equation act on the system and the environment Hilbert spaces respectively and H_{int} is the interaction Hamiltonian.

The composite system (S+E) is a closed system with unitary dynamics, which implies that we can evolve the system using a unitary operator, also called the propagator $U(t_0, t)$, i.e.,

$$|\psi(t)\rangle = U(t, t_0) |\psi(t_0)\rangle \tag{3.30}$$

where

$$U(t, t_0) = \mathcal{T} \exp\left[-i \int_{t_0}^{t} dt' H(t')\right], \tag{3.31}$$

where $\mathcal{T}$ is the time-ordering operator, which guarantees the time-dependent Hamiltonians are applied in a chronologically decreasing order[16].

In general, for time-dependent Hamiltonians, the total system evolution is governed by the *von Neumann equation*

$$\frac{\partial \hat{\rho}_{ES}(t)}{\partial t} = -i \left[H(t), \hat{\rho}_{SE}(t)\right], \tag{3.33}$$

[16] A time-independent Hamiltonian would correspond to a closed system and the propagator would be simplified to

$$U(t, t_0) = \exp\left[-iH(t - t_0)\right]. \tag{3.32}$$

where [..., ...] is the commutator and $\hat{\rho}_{SE}$ is the density operator of the combined system-environment. As we have seen in sec. 3.2.3, in order to study the system only, we must trace over the environment degrees of freedom

$$\frac{\partial \hat{\rho}_S}{\partial t} = -i\mathrm{Tr}_E\{[H(t), \hat{\rho}_{SE}]\}. \tag{3.34}$$

The formal solution can be written as an expansion, with every following term representing higher-order interactions

$$\hat{\rho}_S(t) = \hat{\rho}_S(t^0) - i\int_{t_0}^{t} dt' \mathrm{Tr}_E\{[H(t), \hat{\rho}_{SE}(t_0)]\} + (-i)^2 \int_{t_0}^{t} dt'' \mathrm{Tr}_E\{[H(t'), [H(t''), \hat{\rho}_{SE}(t_0)]]\} + \dots \tag{3.35}$$

We can rewrite the von Neumann equation compactly using the *Liouville-von Neumann super-operator*

$$\frac{\partial \hat{\rho}_{SE}(t)}{\partial t} = \mathcal{L}(t)\hat{\rho}_{SE}(t). \tag{3.36}$$

Once $\hat{\rho}_{SE}(t)$ is known at a given time, in principle taking the trace over environment degrees of freedom gives the final system state.

In practice solving equation (3.36) is very difficult if not impossible for the combined system S+E. Under some simplifying assumptions can be described by *dynamical maps*. In particular, let us assume, that the initial composite state is an uncorrelated product state

$$\hat{\rho}_{SE}(t_0) = \hat{\rho}_S(t_0) \otimes \hat{\rho}_E(t_0). \tag{3.37}$$

Since the composite system is closed, this state undergoes unitary evolution, and taking the trace, the procedure leads to

$$\hat{\rho}_S(t) = \mathrm{Tr}\{U(t, t_0)\hat{\rho}_S * t_0 \otimes \hat{\rho}_E(t_0)U(t, t_0)\}. \tag{3.38}$$

The evolution of ρ_S can now be described by a *dynamical map*, which solely acts on the initial state $\hat{\rho}_S(t_0)$

$$\rho_S(t) = \mathcal{V}(t, t_0)[\hat{\rho}(t_0)], \tag{3.39}$$

where $\mathcal{V}$ is completely positive and trace preserving (CPTP) and allows us to model the system evolution without also modeling the entire environment. Below is a diagram showing the action of a dynamical map:

$$\begin{array}{ccc} \hat{\rho}_S(t_0) \otimes \hat{\rho}_E(t_0) & \xrightarrow[\text{unitary evolution}]{} & U(t,t_0)\hat{\rho}_S \otimes \hat{\rho}_E U(t,t_0) \\ \Big\downarrow \mathrm{Tr}_E & & \mathrm{Tr}_E \Big\downarrow \\ \hat{\rho}_S(t_0) & \xrightarrow{\text{dynamical map}} & \mathcal{V}(t,t_0)[\hat{\rho}(t_0)] \end{array}$$

$\mathcal{V}$ is a map from the system reduced density operator space $S[\mathcal{H}_S]$ onto itself

$$\mathcal{V}(t,t_0) : S[\mathcal{H}_S] \longrightarrow S[\mathcal{H}_S]. \tag{3.40}$$

A dynamical map can be characterized by operators that act on the system Hilbert space. To show this we use the spectral decomposition for the environment density matrix

$$\hat{\rho}(t_0) = \sum_i \alpha_i \left|\phi_i\right\rangle \left\langle\phi_i\right|, \tag{3.41}$$

where $|\phi_i\rangle$ form an orthonormal basis in the environment Hilbert space $\mathcal{H}_E$ and α_i are non-negative numbers that satisfy $\sum_i \alpha_i = 1$. Plugging (3.41) into (3.38) we obtain

$$\mathcal{V}(t,t_0)\hat{\rho}_S(t_0) = \sum_{i,j} W_{ij}(t,t_0)\hat{\rho}_S(t_0)W_{ij}^\dagger(t,t_0), \tag{3.42}$$

where W are indeed operators in $\mathcal{H}_S$ and are defined as

$$W_{ij}(t,t_0) = \sqrt{\alpha_j}\left\langle\phi_i\right| U(t,t_0) \left|\phi_i\right\rangle. \tag{3.43}$$

and satisfies

$$\sum_{ij} W_{ij}^\dagger(t,t_0)W_{ij}(t,t_0) = \mathbb{I}_S. \tag{3.44}$$

Using the cyclical property of the trace it can easily be shown that this simply translates to

$$\mathrm{Tr}\{\mathcal{V}(t,t_0)\hat{\rho}_S(t_0)\} = \mathrm{Tr}\{\rho_S(t_0)\} = 1, \tag{3.45}$$

which proves the dynamical map preserves the trace of the density operator.

3.3.2 Born-Markov approximation

Next, we assume, that the system interacts with a large, memoryless environment and the strength of the said interaction is weak. This significantly simplifies the mathematical analysis of open quantum systems.

To be more precise, according to the *Born approximation*, the system does not alter much the

state of the environment due to two main assumptions: *i*) the environment is considered to be much larger than the system, for example, it could be a thermodynamic environment with an effectively infinite number of degrees of freedom. *ii*) the interactions between the system and the environment are weak. So while the (weak) interactions affect the system, the environment, being very large is practically unaltered by the evolution of the system.

These approximations can also be thought of in terms of characteristic timescales. Since the environment quickly returns to its original state after interacting with the environment, the environment correlation function decays quickly, usually in physical systems $C_E \propto \exp[-t/t_E]$, where t_E is the environment correlation time. If $t > t_E$, the environment correlation time decays quickly. On the other hand, the system retains correlations for a longer time t_S, meaning that $t_S \gg t_E$.

Combining these assumptions, we further approximate that the correlations between the system and the environment decay quickly, allowing us to write the full density matrix as a product state at all times

$$\hat{\rho}_{SE}(t) = \hat{\rho}_S(t) \otimes \hat{\rho}_E(t). \tag{3.46}$$

The weak coupling limit also entails the environment density matrix does not change in time $\hat{\rho}_E(t) = \hat{\rho}_E$.

These assumptions allow us to construct a dynamical map

$$\hat{\rho}_S(t) = \mathcal{V}(t, t_0)\hat{\rho}_S(t_0). \tag{3.47}$$

however, this map still depends on the initial time t_0 and we would like to construct a one-parameter dynamical map. To this end, we make the second major approximation, the *Markov approximation*. According to this approximation, the system retains no memory of past interactions. In other words, the dynamics of the system do not depend on any past instance and is only determined by the present state. The memory effects are completely neglected.

Quantum Markovian dynamics is described by a one-parameter dynamical map that satisfies the semi-group property

$$\mathcal{V}(t_1) \circ \mathcal{V}(t_2) = \mathcal{V}(t_1 + t_2). \tag{3.48}$$

The semi-group property ensures that there is no reverse dynamical map and this is expected since a system immersed in a large environment is prone to decoherence and/or dissipation, which are irreversible processes.

Given a quantum dynamical semi-group, it is always possible to find a linear operator $\mathcal{L}$, which is the semi-group generator

$$\mathcal{V}(t) = e^{\mathcal{L}t} \qquad \Rightarrow \qquad \mathcal{V}(t)\hat{\rho}_S(t_0) = \exp[\mathcal{L}t]\,\hat{\rho}_S(t_0). \tag{3.49}$$

Differentiating by time leads to a general form of a *Markovian master equation*

$$\frac{\partial \hat{\rho}_S(t)}{\partial t} = \mathcal{L}\hat{\rho}_S(t). \tag{3.50}$$

It is sometimes convenient to introduce *the dissipator*

$$\mathcal{D}(\hat{\rho}_S) = \sum_k \gamma_k \left(A_k \rho_S A_k^\dagger - \frac{1}{2} A_k^\dagger A_k \rho_S - \frac{1}{2} \hat{\rho}_S A_k^\dagger A_k \right), \tag{3.51}$$

where γ_k are positive real numbers and A_k are the so-called *Lindblad operators*, which act on the system Hilbert space and are specified by the physics of a given problem.

Equation (3.50) is sometimes written as

$$\frac{\partial \hat{\rho}_S(t)}{\partial t} = -i\left[H, \hat{\rho}_S(t)\right] + \mathcal{D}(\hat{\rho}_S(t)) \tag{3.52}$$

where H is not always the free system Hamiltonian. In the weak coupling limit, it is the Lamb-shift Hamiltonian [66]. The dissipator $\mathcal{D}$ describes irreversible processes, such as loss of coherence of the system state (decoherence) and energy dissipation.

We stress, that this the discussion in this chapter is purely formal. In Appendix C we derive the following equation (C.39)

$$\frac{d\rho_S}{dt} = i[\rho_S, H_S] - \frac{\gamma}{2} \int d^3x d^3y C_R(\mathbf{x}, \mathbf{y})[A(\mathbf{x}), [A(\mathbf{y}), \rho_S]], \tag{3.53}$$

which can be applied directly to early universe cosmology. The next chapter will be devoted to applying this equation to single-field scalar inflation mostly following [2].

3.4 Lindblad Formalism in Early Universe Cosmology

In this section, we discuss the implementation of the Lindblad equation in early universe cosmology as done by [2]. We will leave the environment as generic as possible until sec 3.4.6 where we specify an important type of environment which is the massive scalar field. We will see how decoherence changes the power spectrum and compare new results with observations. We will also see how to assess decoherence in the early universe using the Lindblad formalism.

3.4.1 The free Hamiltonian

The curvature perturbation encodes both the scalar metric perturbations and the inflaton field fluctuations. In the simplest case of free evolution, the Hamiltonian governing the curvature fluctuations takes the following form [50]

$$\hat{H}_v = \int_{\mathbb{R}} d^3\mathbf{k} \hat{H}_\mathbf{k} = \frac{1}{2} \int_{\mathbb{R}} d^3\mathbf{k} \left[\hat{p}_\mathbf{k} \hat{p}_\mathbf{k}^\dagger + \omega^2(\tau, \mathbf{k}) \hat{v}_\mathbf{k} \hat{v}_\mathbf{k}^\dagger \right], \tag{3.54}$$

where $\hat{p}_{\mathbf{k}} = \hat{v}'_{\mathbf{k}}$ is the conjugate momentum of the Fourier-transformed Mukhanov-Sasaki variable

$$\hat{v}_{\mathbf{k}}(\tau) = \int \frac{d^3\mathbf{k}}{(2\pi)^{3/2}} \hat{v}(\tau, \mathbf{x}) e^{-i\mathbf{k}\cdot\mathbf{x}}. \tag{3.55}$$

The Hamiltonian (3.54) describes parametric oscillators with frequency

$$\omega(\tau, \mathbf{k}) = k^2 - \frac{(a\sqrt{\varepsilon})''}{a\sqrt{\varepsilon}}, \tag{3.56}$$

where ε is the first slow-roll parameter $\varepsilon = 1 - \mathcal{H}'/\mathcal{H}^2$.

3.4.2 Canonical Quantization of Scalar Perturbations

Since $\hat{v}(\tau, \mathbf{x})$ is real, it follows from (3.55), that $\hat{v}^\dagger_{\mathbf{k}} = \hat{v}_{-\mathbf{k}}$. We proceed by decomposing $\hat{v}_{\mathbf{k}}$ and $\hat{p}_{\mathbf{k}}$ into real and imaginary parts [2]: $\hat{v}_{\mathbf{k}} = (\hat{v}^{\mathrm{R}}_{\mathbf{k}} + i\hat{v}^{\mathrm{I}}_{\mathbf{k}})/\sqrt{2}$ and $\hat{p}_{\mathbf{k}} = (\hat{p}^{\mathrm{R}}_{\mathbf{k}} + i\hat{p}^{\mathrm{I}}_{\mathbf{k}})/\sqrt{2}$, consequently $\hat{v}^{\mathrm{R}}_{\mathbf{k}} = \hat{v}^{\mathrm{R}}_{-\mathbf{k}}$, $\hat{v}^{\mathrm{I}}_{\mathbf{k}} = -\hat{v}^{\mathrm{I}}_{-\mathbf{k}}$, $\hat{p}^{\mathrm{R}}_{\mathbf{k}} = \hat{p}^{\mathrm{R}}_{-\mathbf{k}}$, $\hat{p}^{\mathrm{I}}_{\mathbf{k}} = -\hat{p}^{\mathrm{I}}_{-\mathbf{k}}$, so the operators $\hat{v}^{R}_{\mathbf{k}}$ and $\hat{p}^{I}_{\mathbf{k}}$ are Hermitian. It is evident that not all $\hat{v}_{\mathbf{k}}$ are independent degrees of freedom. Namely, we can quantize $\hat{v}^{\mathrm{R}}_{\mathbf{k}}$ and $\hat{v}^{\mathrm{I}}_{\mathbf{k}}$ on half of the Fourier space, meaning that $\mathbf{k} \in \mathbb{R}^{3+}$. Same goes for the conjugate variable $\hat{p}_{\mathbf{k}}$. The usual canonical commutation relations will read

$$[\hat{v}_{\mathbf{k}}, \hat{p}_{\mathbf{q}}] = i\delta^{(3)}(\mathbf{k} + \mathbf{q}), \tag{3.57}$$

and

$$[\hat{v}^\dagger_{\mathbf{k}}, \hat{p}_{\mathbf{q}}] = [\hat{v}_{\mathbf{k}}, \hat{p}^\dagger_{\mathbf{q}}] = i\delta^{(3)}(\mathbf{k} - \mathbf{q}). \tag{3.58}$$

Since we will be working with the density matrix, we note, that in the free theory the density matrix of perturbations $\hat{\rho}_v = |\Psi[v]\rangle \langle\Psi[v]|$ (here Ψ is the wave functional) factorizes

$$\hat{\rho}_v(\tau) = \prod_{\mathbf{k}\in\mathbb{R}^{3+}} \prod_{s=\mathrm{R,I}} \hat{\rho}^s_{\mathbf{k}}(\tau), \tag{3.59}$$

however, this expression will not hold for non-linear interactions.

As discussed in the previous chapter, evolution of the system is controlled by the Liouville-von Neumann equation, which is the equivalent of the Schrödinger equation but in the density matrix formalism

$$\frac{d\hat{\rho}_v}{d\tau} = -i\left[\hat{H}_v, \hat{\rho}_\nu\right]. \tag{3.60}$$

And if the state is factorizable, we can rewrite this equation in Fourier space. To this end let us take the time derivative of expression (3.59)

$$\frac{d\hat{\rho}_v}{d\tau} = \int_{\mathbb{R}^{3+}} d^3\mathbf{k} \left(\frac{d\hat{\rho}^{\mathrm{R}}_{\mathbf{k}}}{d\tau}\hat{\rho}^{\mathrm{I}}_{\mathbf{k}} + \hat{\rho}^{\mathrm{R}}_{\mathbf{k}}\frac{d\hat{\rho}^{\mathrm{I}}_{\mathbf{k}}}{d\tau}\right) \prod_{\mathbf{k}'\neq\mathbf{k}} \prod_{s=\mathrm{R,I}} \hat{\rho}^s_{\mathbf{k}'}(\tau). \tag{3.61}$$

using equation (3.54), we see that $\hat{H}_v = \sum_{s=\mathrm{I,R}} \int_{\mathbb{R}^{3+}} d^3\mathbf{k} \hat{H}^s_{\mathbf{k}}$. Then for the commutator in the

right-hand side of the equation (3.60), we get

$$\left[\hat{H}_v, \hat{\rho}_\nu\right] = \int_{\mathbb{R}^{3+}} d^3\mathbf{k} \left([\hat{H}^{\mathrm{R}}_{\mathbf{k}}, \hat{\rho}^{\mathrm{R}}_{\mathbf{k}}]\hat{\rho}^{\mathrm{I}}_{\mathbf{k}} + \hat{\rho}^{\mathrm{R}}_{\mathbf{k}}[\hat{H}^{\mathrm{I}}_{\mathbf{k}}, \hat{\rho}^{\mathrm{I}}_{\mathbf{k}}]\right) \prod_{\mathbf{k}'\neq\mathbf{k}} \prod_{s=\mathrm{R,I}} \hat{\rho}^{s}_{\mathbf{k}'}(\tau). \tag{3.62}$$

Using equation (3.60), equations (3.61) and (3.62) clearly imply that

$$\frac{d\hat{\rho}^{s}_{\mathbf{k}}}{d\tau} = -i[\hat{H}^{s}_{\mathbf{k}}, \hat{\rho}^{s}_{\mathbf{k}}], \tag{3.63}$$

meaning that in the absence of non-linear interactions, each Fourier subspace can be treated independently.

3.4.3 Adding the Environment

The free Hamiltonian (3.54) describes a closed system, in the sense that it does not involve any interaction terms. However, it is reasonable to think, that the primordial perturbations were constantly interacting with other sectors, at least gravitationally. Moreover, interactions with the standard model fields could have a significant role in subsequent reheating and the radiation-dominated epoch [2], [71]. Even if the other fields are absent, the perturbations outside our causal horizon and physics beyond the UV and IR cutoffs of the theory should be considered as the environment [7]. Therefore, it is sensible to consider the primordial perturbations as an open system interacting with an environment. Thus we can adopt methods used in Open Quantum Systems (OQS). Specifically, by partitioning the composite system into primordial perturbations (system) and the environment, which may vary from model to model, we can use the reduced density matrix of the system and trace the evolution using a master equation. The reduced density matrix of the system is defined by tracing out the environment degrees of freedom

$$\hat{\rho}_v = \mathrm{Tr}_E\{\hat{\rho}_{\mathrm{composite}}\}. \tag{3.64}$$

We also rewrite the total Hamiltonian

$$\hat{H} = \hat{H}_v \otimes \hat{\mathbb{I}}_{\mathrm{E}} + \hat{\mathbb{I}}_v \otimes \hat{H}_{\mathrm{E}} + g\hat{H}_{\mathrm{int}}, \tag{3.65}$$

where $\hat{H}_v$ is defined in (3.54), $\hat{H}_{\mathrm{E}}$ is the environment Hamiltonian, $\hat{H}_{\mathrm{int}}$ is the interaction Hamiltonian with a coupling g. $\hat{\mathbb{I}}_{v(E)}$ are the identity operators acting on the Hilbert spaces of the system or the environment respectively. If the system and the environment couple through local interactions only, then the interaction Hamiltonian can be expressed as

$$\hat{H}_{\mathrm{int}} = \int d^3\mathbf{x}\hat{A}(\tau, \mathbf{x}) \otimes \hat{R}(\tau, \mathbf{x}), \tag{3.66}$$

where $\hat{A}$ is an operator in the system's sector and $\hat{R}$ in the environment sector.

The effect of the environment will be encoded in a new, non-unitary term in the Liouville-

von Neumann equation and will lead to the so-called Lindblad equation. The construction of the Lindblad equation can be found in Appendix C. Here we simply quote the result

$$\frac{d\hat{\rho}_v}{d\tau} = -i[\hat{H}_v, \hat{\rho}_v] - \frac{\gamma}{2}\int d^3\mathbf{x}d^3\mathbf{y}C_R(\mathbf{x},\mathbf{y})\left[\hat{A}(\mathbf{x}),\left[\hat{A}(\mathbf{y}),\hat{\rho}_v\right]\right], \tag{3.67}$$

where we have omitted the time dependence for brevity. C_R is the same-time correlation function of the environment $\hat{R}$. Namely

$$C_R(\mathbf{x},\mathbf{y}) = \langle\hat{R}(\tau,\mathbf{x})\hat{R}(\tau,\mathbf{y})\rangle. \tag{3.68}$$

The coefficient γ is related to the coupling g between the system and the environment and the autocorrelation time τ_c of the environment $\hat{R}$.

$$\gamma = 2g^2\tau_c. \tag{3.69}$$

This parameter is generally time-dependent, so we adopt a power-law dependence on the scale factor [2]

$$\gamma = \gamma_*\left(\frac{a}{a_*}\right)^p, \tag{3.70}$$

where p is a free parameter and $*$ corresponds to a reference time, that we can conveniently take to be the time when the pivot scale $k_* = 0.05\text{Mpc}^{-1}$ crosses the Hubble radius, i.e. $k_* = a_*H_*$.

We assume that the environment is statistically homogeneous and isotropic, leading to $C_R(\mathbf{x},\mathbf{y}) \propto |\mathbf{x}-\mathbf{y}|$. Furthermore, in the Lindblad formalism, the environment correlation function is required to decay rapidly compared to the typical evolution time of the system. Usually the decay is exponential $\propto e^{-\tau/\tau_c}$. However, in order to make the mathematical analysis tractable, the top-hat approximation is made

$$C_R(\mathbf{x},\mathbf{y}) = \bar{C}_R\Theta\left(\frac{a|\mathbf{x}-\mathbf{y}|}{\ell_c}\right), \tag{3.71}$$

where $\Theta(x)$ is 1 if $x < 1$ and 0 otherwise. The presence of the scale factor in this expression is due to the fact that ℓ_c is the *physical* correlation length.

3.4.4 Quantum Mean Values

In order to extract information from the quantum state described by the density matrix $\hat{\rho}_v$, we can evaluate the quantum expectation values by means of the *trace rule*:

$$\langle\hat{O}\rangle = \text{Tr}\{\hat{\rho}_v\hat{O}\}, \tag{3.72}$$

where $\hat{O}$ is an operator acting on the Hilbert space of the system. We can use this method in case we are able to solve the Lindblad equation exactly and derive the $\hat{\rho}_v$ explicitly. However, in most cases, this is very difficult to achieve. In that case, we solve the equation of motion governing $\langle\hat{O}\rangle$ directly. Taking the temporal derivative of (3.72) and plugging in the Lindblad equation (3.67), we

get

$$\frac{d\langle\hat{O}\rangle}{d\tau} = \left\langle \frac{\partial\hat{O}}{\partial\tau} \right\rangle - i\left\langle \left[\hat{O}, \hat{H}_v\right] \right\rangle - \frac{\gamma}{2}\int d^3\mathbf{x}d^3\mathbf{y}C_R(\mathbf{x},\mathbf{y})\left\langle \left[\left[\hat{O}, \hat{A}(\mathbf{x})\right], \hat{A}(\mathbf{y})\right] \right\rangle, \tag{3.73}$$

where we have also taken into account a possible explicit time-dependence of the operator $\hat{O}$ through the first term on the right-hand side. Importantly, the third term, corresponding to the system-environment interaction can be rewritten in the Fourier space [2], leading to

$$\frac{d\langle\hat{O}\rangle}{d\tau} = \left\langle \frac{\partial\hat{O}}{\partial\tau} \right\rangle - i\left\langle \left[\hat{O}, \hat{H}_v\right] \right\rangle - \frac{\gamma}{2}(2\pi)^{3/2}\int d^3\mathbf{k}y\tilde{C}_R(\mathbf{k})\left\langle \left[\left[\hat{O}, \hat{A}_{\mathbf{k}}\right], \hat{A}_{-\mathbf{k}}\right] \right\rangle. \tag{3.74}$$

3.4.5 Power Spectrum

In previous sections, we have shown that the interactions with the environment are described by the addition of a non-unitary term to the evolution equation of the reduced density matrix $\hat{\rho}_v$. This term suppresses the off-diagonal elements of the density matrix and leads to decoherence. However, notice in the Lindblad equation (3.67), there is a unitary term as well coming from the free Hamiltonian of the system. If that term couples the evolution of the diagonal elements with the non-diagonal ones, the Lindblad term also has an effect on the diagonal elements of the density matrix. This changes the values of statistical observables such as the power spectrum, which is the point we would like to outline in this chapter.

Let us assume a linear coupling of the system to the environment. Hence $\hat{A}(\mathbf{x}) = \hat{v}(\mathbf{x})$. In this case, the Lindblad equation can be solved exactly, meaning that all of the matrix elements of $\hat{\rho}_v$ can be obtained explicitly. As stressed in 3.4.4 this means, that there are two ways to obtain the curvature power spectrum with reasonable effort [2], [4]. The first one amounts to solving the Lindblad equation exactly and then applying the trace rule to obtain the quantum mean values. In this case

$$P_{vv}(k) = \left\langle|\hat{v}_{\mathbf{k}}|^2\right\rangle = \left\langle(\hat{v}^s_{\mathbf{k}})^2\right\rangle = \mathrm{Tr}_v\{(\hat{v}^s_{\mathbf{k}})^2\hat{\rho}_v\} = \int d\hat{v}^s_{\mathbf{k}}\,\langle\hat{\rho}_{\mathbf{k}}|\hat{v}^s_{\mathbf{k}}|\hat{\rho}_{\mathbf{k}}\rangle\,(\hat{v}^s_{\mathbf{k}})^2, \tag{3.75}$$

with $s = \mathrm{I}, \mathrm{R}$ stand for the real and imaginary parts, and the convention of summing over repeated indices is adopted. The second method amounts to directly solving equation (3.74) when $\hat{O} = |\hat{v}_{\mathbf{k}}|^2$. The two methods are equivalent for the linear interactions, however at higher orders the first method is not applicable since no explicit solution to the Lindblad equation can be found in this case.

We highlight the main steps required for solving the Lindblad equation for linear interactions $\hat{A}(\mathbf{x}) = \hat{v}(\mathbf{x})$. But first, we derive the Lindblad equation in Fourier space. We will show, that much like the free evolution equation (3.60), the Lindblad equation also decouples into independent Lindblad equations for each Fourier subspace. Since the difference between the two equations is the non-unitary Lindblad term, it is enough to show that this term decouples for each Fourier subspace.

The Lindblad term for the linear interaction reads

$$\begin{aligned}\int d^3\mathbf{x}d^3\mathbf{y}C_R(\mathbf{x}-\mathbf{y})\left[\hat{v}(\mathbf{x}),[\hat{v}(\mathbf{y}),\hat{\rho}_v]\right] &= (2\pi)^{3/2}\int_{\mathbb{R}^3} d^3\mathbf{p}\tilde{C}_R(\mathbf{p})\left[\hat{v}^\dagger_{\mathbf{p}},[\hat{v}_{\mathbf{p}},\hat{\rho}_v]\right]\\ = \frac{(2\pi)^{3/2}}{2}\int_{\mathbb{R}} d^3\mathbf{p}\tilde{C}_R(\mathbf{p})\left(\left[\hat{v}^{\mathrm{R}}_{\mathbf{p}},\left[\hat{v}^{\mathrm{R}}_{\mathbf{p}},\hat{\rho}_v\right]\right]+\left[\hat{v}^{\mathrm{I}}_{\mathbf{p}},\left[\hat{v}^{\mathrm{I}}_{\mathbf{p}},\hat{\rho}_v\right]\right]-\left[\hat{v}^{\mathrm{I}}_{\mathbf{p}},\left[\hat{v}^{\mathrm{R}}_{\mathbf{p}},\hat{\rho}_v\right]\right]+\left[\hat{v}^{\mathrm{R}}_{\mathbf{p}},\left[\hat{v}^{\mathrm{I}}_{\mathbf{p}},\hat{\rho}_v\right]\right]\right),\end{aligned} \tag{3.76}$$

where we first Fourier-expanded the equal-time correlator C_R and the variables $\hat{v}$ and then we used the decomposition into the real and imaginary parts $\hat{v}_{\mathbf{p}} = (\hat{v}^{\mathrm{R}}_{\mathbf{p}} + i\hat{v}^{\mathrm{I}}_{\mathbf{p}})/\sqrt{2}$ as in sec. 3.4.2. If we split the integral over $\mathbb{R}^3$ into two parts $\mathbb{R}^{3+}$ and $\mathbb{R}^{3-}$, the last two terms will vanish because of relations $\hat{v}^{\mathrm{R}}_{\mathbf{p}} = \hat{v}^{R}_{-\mathbf{p}}$, $\hat{v}^{\mathrm{I}}_{\mathbf{p}} = -\hat{v}^{\mathrm{I}}_{-\mathbf{p}}$ and the fact that the environment correlation function does not depend on the sign of $\mathbf{p}$. On the other hand, the first two terms will be doubled, leading to

$$\begin{aligned}&\int d^3\mathbf{x}d^3\mathbf{y}C_R(\mathbf{x}-\mathbf{y})\left[\hat{v}(\mathbf{x}),[\hat{v}(\mathbf{y}),\hat{\rho}_v]\right] =\\ &= (2\pi)^{3/2}\int_{\mathbb{R}^{3+}} d^3\mathbf{p}\tilde{C}_R(\mathbf{p})\left(\left[\hat{v}^{\mathrm{R}}_{\mathbf{p}},\left[\hat{v}^{\mathrm{R}}_{\mathbf{p}},\hat{\rho}^{\mathrm{R}}_{\mathbf{p}}\right]\right]\hat{\rho}^{\mathrm{I}}_{\mathbf{p}}+\hat{\rho}^{\mathrm{R}}_{\mathbf{p}}\left[\hat{v}^{\mathrm{I}}_{\mathbf{p}},\left[\hat{v}^{\mathrm{I}}_{\mathbf{p}},\hat{\rho}^{\mathrm{I}}_{\mathbf{p}}\right]\right]\right)\prod_{\mathbf{p}'\neq\mathbf{p}}\prod_{s=\mathrm{R},\mathrm{I}}\hat{\rho}^{s}_{\mathbf{p}'},\end{aligned} \tag{3.77}$$

where we have we have assumed that the state is initially factorizable. The linearity of the interaction term preserves the fact that each Fourier mode evolves separately allowing us to write the Lindblad equation in Fourier space as

$$\frac{d\hat{\rho}^s_{\mathbf{k}}}{d\tau} = -i\left[\hat{H}^s_{\mathbf{k}},\hat{\rho}_{\mathbf{k}^s}\right] - \frac{\gamma}{2}(2\pi)^{3/2}\tilde{C}_R(\mathbf{k})\left[\hat{v}^s_{\mathbf{k}},\left[\hat{v}^s_{\mathbf{k}},\hat{\rho}^s_{\mathbf{k}}\right]\right], \tag{3.78}$$

where we notice, that the second term on the right-hand side must be homogeneous with a square of a comoving wavenumber in order to have the correct dimensions. This scale, denoted k_γ can be written as [2]

$$k_\gamma \equiv \sqrt{\frac{8\pi}{3}\bar{C}_R\ell_c^3\frac{\gamma_*}{a_*^3}}. \tag{3.79}$$

Equation (3.78) can be solved exactly for the linear interaction. First we define the eigenvectors $|v^s_{\mathbf{k}}\rangle$ of the operator $\hat{v}^s_{\mathbf{k}}$. These are defined so that they satisfy the following eigenvalue equation $\hat{v}^s_{\mathbf{k}}|v^s_{\mathbf{k}}\rangle = v^s_{\mathbf{k}}|v^s_{\mathbf{k}}\rangle$. We project equation (3.78) onto $\left\langle v^{s,(1)}_{\mathbf{k}}\right|$ and $\left|v^{s,(2)}_{\mathbf{k}}\right\rangle$ and use the free Hamiltonian $\hat{H}_v$ defined in (3.54) along with the definition of the momentum operator in the position basis,

$\hat{p}^s_{\mathbf{k}} = -i\partial/(\partial v^s_{\mathbf{k}})$. The result obtained in [2] reads:

$$\left\langle v^{s,(1)}_{\mathbf{k}} \right| \hat{\rho}^s_{\mathbf{k}} \left| v^{s,(2)}_{\mathbf{k}} \right\rangle = \frac{(2\pi)^{-1/2}}{\sqrt{|v_{\mathbf{k}}|^2 + \mathcal{J}_{\mathbf{k}}}} \exp\left[\frac{\left(v^{s,(1)}_{\mathbf{k}}\right)^2 + \left(v^{s,(2)}_{\mathbf{k}}\right)^2 + i\left(|v_{\mathbf{k}}|^2\right)' \left[\left(v^{s,(2)}_{\mathbf{k}}\right)^2 - [\left(v^{s,(1)}_{\mathbf{k}}\right)^2\right]}{4\left(|v_{\mathbf{k}}|^2 + \mathcal{J}_{\mathbf{k}}\right)} \right]$$
$$\times \exp\left[-\frac{\left[v^{s,(2)}_{\mathbf{k}} - v^{s,(1)}_{\mathbf{k}}\right]^2}{2\left(|v_{\mathbf{k}}|^2 + \mathcal{J}_{\mathbf{k}}\right)} \left(\mathcal{I}_{\mathbf{k}}\mathcal{J}_{\mathbf{k}} - \mathcal{K}^2_{\mathbf{k}} + |v'_{\mathbf{k}}|^2\mathcal{J}_{\mathbf{k}} + |v_{\mathbf{k}}|^2\mathcal{I}_{\mathbf{k}} - \left(|v_{\mathbf{k}}|^2\right)'\mathcal{K}_{\mathbf{k}}\right) \right.$$
$$\left. -\frac{i\mathcal{K}_{\mathbf{k}}}{2\left(|v_{\mathbf{k}}|^2 + \mathcal{J}_{\mathbf{k}}\right)} \left[\left(v^{s,(2)}_{\mathbf{k}}\right)^2 - \left(v^{s,(1)}_{\mathbf{k}}\right)^2\right] \right], \tag{3.80}$$

which is an exact solution of the Lindblad equation and where

$$\mathcal{I}_{\mathbf{k}}(\tau) \equiv 4(2\pi)^{3/2} \int_{-\infty}^{\tau} d\tau' \gamma(\tau') \tilde{C}_R(\mathbf{k}, \tau') \mathrm{Im}^2\{v_{\mathbf{k}}(\tau') v^{*'}_{\mathbf{k}}(\tau)\}, \tag{3.81}$$

$$\mathcal{J}_{\mathbf{k}}(\tau) \equiv 4(2\pi)^{3/2} \int_{-\infty}^{\tau} d\tau' \gamma(\tau') \tilde{C}_R(\mathbf{k}, \tau') \mathrm{Im}^2\{v_{\mathbf{k}}(\tau') v^{*}_{\mathbf{k}}(\tau)\}, \tag{3.82}$$

$$\mathcal{K} \equiv 4(2\pi)^{3/2} \int_{-\infty}^{\tau} d\tau' \gamma(\tau') \tilde{C}_R(\mathbf{k}, \tau') \mathrm{Im}\{v_{\mathbf{k}}(\tau') v^{*'}_{\mathbf{k}}(\tau)\} \mathrm{Im}\{v_{\mathbf{k}}(\tau') v^{*}_{\mathbf{k}}(\tau)\}. \tag{3.83}$$

It is worth mentioning that $v_{\mathbf{k}}(\tau)$ are the solutions of the free Mukhanov-Sasaki equation $v''_{\mathbf{k}} + \omega^2(k) v_{\mathbf{k}} = 0$, whose initial conditions are set to be the Bunch-Davies vacuum. This implies that our ability to set the initial conditions for the primordial perturbations to the Bunch-Davies vacuum is preserved by the Lindblad equation.

Because of the linearity of the interaction term, (3.80) still describes a Gaussian state. Moreover, we can show that by turning off the interaction ($\gamma = 0$) we recover the two-mode squeezed state, which is the standard solution when no interactions are involved. We put $\mathcal{I} = \mathcal{J} = \mathcal{K} = 0$, leading to

$$\left\langle v^{s,(1)}_{\mathbf{k}} \right| \hat{\rho}^s_{\mathbf{k}} \left| v^{s,(2)}_{\mathbf{k}} \right\rangle |_{\gamma=0} = \Psi(v^{s,(1)}_{\mathbf{k}}) \Psi^*(v^{s,(2)}_{\mathbf{k}}), \tag{3.84}$$

where

$$\Psi(v) = \left(\frac{1}{2\pi|v_{\mathbf{k}}|^2}\right)^{\frac{1}{4}} \exp\left[-\frac{1 - i|v_{\mathbf{k}}|^{2'}}{4|v_{\mathbf{k}}|^2} v^2 \right], \tag{3.85}$$

which we can rewrite using a new parameter $\Omega_{\mathbf{k}} \equiv -iv'_{\mathbf{k}}/(2v_{\mathbf{k}})$ as

$$\Psi(v) = \left[\frac{2\,\mathrm{Re}(\Omega_{\mathbf{k}})}{\pi}\right]^{\frac{1}{4}} e^{-\Omega_{\mathbf{k}} v^2}. \tag{3.86}$$

Indeed, this corresponds to the two-mode squeezed state, which is a pure state.

In (3.80) it is evident that the diagonal elements of the density matrix are modified by the presence of the environment. Namely, if we put $v^{s,(1)}_{\mathbf{k}} = v^{s,(2)}_{\mathbf{k}}$, we see, that the solution depends on $\mathcal{J}_{\mathbf{k}}$. This simply shows that the observable statistics of the system are modified by the presence of

the environment and since the state is still Gaussian, this modification is encapsulated entirely by the two-point correlation function.

To calculate the correlator, we recall (3.75). The integral is Gaussian and can be easily evaluated leading to

$$P_{vv}(k) = \langle|\hat{v}^s_{\mathbf{k}}|^2\rangle = \mathrm{Tr}\{(v^s_{\mathbf{k}})^2\hat{\rho}^s_v\} = \int_{-\infty}^{\infty} dv^s_{\mathbf{k}}\,\langle\hat{v}^s_{\mathbf{k}}|\hat{\rho}^s_{\mathbf{k}}|\hat{v}^s_{\mathbf{k}}\rangle = |v_{\mathbf{k}}|^2 + \mathcal{J}_{\mathbf{k}}, \tag{3.87}$$

where the first term is the usual result we get in the absence of interactions. Exploiting the well-known relation between the power spectrum and the two-point function

$$\langle\zeta_{\mathbf{k}}\zeta_{\mathbf{k}'}\rangle = \frac{2\pi^2}{k^3}P_{\zeta\zeta}\delta^{(3)}(\mathbf{k}+\mathbf{k}'), \tag{3.88}$$

and using the relation between the Mukhanov-Sasaki variable and the curvature perturbations $\zeta_{\mathbf{k}} = -Hv_{\mathbf{k}}/(a\dot{\phi})$ we get the combined curvature power spectrum

$$P_{\zeta\zeta} = \frac{k^3}{2\pi^2}\frac{H^2P_{vv}(k)}{a^2\dot{\phi}^2} = P^{\mathrm{standard}}_{\zeta\zeta}(1+\Delta P_{\mathbf{k}}), \tag{3.89}$$

where

$$\Delta P_{\mathbf{k}} \equiv \frac{\mathcal{J}_{\mathbf{k}}}{|v_{\mathbf{k}}|^2}. \tag{3.90}$$

Let us also recall, that the standard result is

$$P^{\mathrm{standard}}_{\zeta\zeta} = \mathcal{P}\left(\frac{k}{k_*}\right)^{n_s-1}, \tag{3.91}$$

where $n_s = 1+3-2\nu$, $\nu = 3/2+\varepsilon+\eta/2$, ϵ and η being the first and the second slow-roll parameters. We also used the definition

$$\mathcal{P}^{1/2} = \frac{H^2}{2\pi|\dot{\phi}|} \tag{3.92}$$

Alternative derivation of the power spectrum. The technique developed above is restricted only to interactions linear in the system variable, however, there is a more general way, that does not require solving the Lindblad equation explicitly. This can be done by focusing on the two-point correlators.

Recalling equation (3.74) and taking $\langle\hat{O}\rangle = \langle\hat{O}_{\mathbf{k}_1}\hat{O}_{\mathbf{k}_1}\rangle$, with $\hat{O} = \hat{v}_{\mathbf{k}_1}$ or $\hat{p}_{\mathbf{k}_2}$, we get the so-called

transport equations in ref. [6],

$$\frac{d}{d\tau}\langle\hat{v}_{\mathbf{k}_1}\hat{v}_{\mathbf{k}_2}\rangle = \langle v_{\mathbf{k}_1}\hat{p}_{\mathbf{k}_2} + \hat{p}_{\mathbf{k}_1}\hat{v}_{\mathbf{k}_2}\rangle, \tag{3.93}$$

$$\frac{d}{d\tau}\langle\hat{v}_{\mathbf{k}_1}\hat{p}_{\mathbf{k}_2}\rangle = \langle\hat{p}_{\mathbf{k}_1}\hat{p}_{\mathbf{k}_2}\rangle - \omega^2(k_2)\langle\hat{v}_{\mathbf{k}_1}\hat{v}_{\mathbf{k}_2}\rangle, \tag{3.94}$$

$$\frac{d}{d\tau}\langle\hat{p}_{\mathbf{k}_1}\hat{v}_{\mathbf{k}_2}\rangle = \langle\hat{p}_{\mathbf{k}_1}\hat{p}_{\mathbf{k}_2}\rangle - \omega^2(k_1)\langle\hat{v}_{\mathbf{k}_1}\hat{v}_{\mathbf{k}_2}\rangle, \tag{3.95}$$

$$\frac{d}{d\tau}\langle\hat{p}_{\mathbf{k}_1}\hat{p}_{\mathbf{k}_2}\rangle = -\omega^2(k_2)\langle\hat{p}_{\mathbf{k}_1}\hat{v}_{\mathbf{k}_2}\rangle - \omega^2(k_1)\langle\hat{v}_{\mathbf{k}_1}\hat{p}_{\mathbf{k}_2}\rangle + \gamma(2\pi)^{3/2}\tilde{C}_R(\mathbf{k}_1)\delta(\mathbf{k}_1+\mathbf{k}_2). \tag{3.96}$$

Notice the last term does depend on γ and C_R, however, since these equations are coupled, it actually affects all two-point functions. The Dirac delta ensures that the interaction with the environment preserves statistical homogeneity, i.e. it allows for solutions like

$$\langle\hat{O}_{\mathbf{k}_1}\hat{O}'_{\mathbf{k}_2}\rangle P_{OO'}(\mathbf{k}_1)\delta(\mathbf{k}_1+\mathbf{k}_2). \tag{3.97}$$

For the heavy scalar field, just as for the axion environment to be considered in future chapters, the correlator actually preserves statistical isotropy $\tilde{C}_R(\mathbf{k}) = \tilde{C}_R(k)$ so that the solutions can actually be both isotropic and homogeneous with $P_{OO'}$ depends on the modulus of the wavenumber.

This leads to three coupled differential equations that can be written as a third-order differential equation for P_{vv}:

$$P'''_{vv} + 4\omega^2 P'_{vv} + 4\omega'\omega P_{vv} = S_1 \tag{3.98}$$

where

$$S_1(k,\tau) = 2(2\pi)^{3/2}\gamma\tilde{C}_R(k). \tag{3.99}$$

It can be shown that (3.87) does solve equation (3.98).

Now all that is left is to evaluate $\Delta P_{\mathbf{k}}/|v_{\mathbf{k}}|^2$. Let us work at first order in the slow-roll parameters ε and η.

To proceed, two additional approximations are made: first, we are interested in the power spectrum at the end of inflation, so we take $-k\tau \ll 1$. Second, the environment correlation time t_c must be shorter than the typical time in which the system evolves. For the inflaton field that would be $\sim H^{-1}$. Furthermore, if the correlation time and length are similar (as in the case of a heavy scalar field as we will see in section 3.4.6), by the connection (E.13) this leads to $H\ell_c \ll 1$.

Imposing these limits, the dominant contribution depends on the parameter p. If $p > 3 + (2 + 2\nu)/(1+\varepsilon_*)$, where $\nu = 3/2 + \varepsilon_* + \eta_*/2$ with the star denoting that ε is evaluated when the pivot sale k_* crosses the horizon,

$$\Delta P_{\mathbf{k}}\big|_1 \simeq \frac{\pi 2^{-1-2\nu}}{\nu^2\Gamma^2(\nu)}\left(\frac{k_\gamma}{k_*})\right)^2\left(\frac{k}{k_*}\right)^{2\nu}\left(\frac{\eta}{\eta_*}\right)^{2+2\nu-(p-3)(1+\epsilon_*)}\left[\frac{2}{2-(p-3)(1+\varepsilon_*)}\right.$$
$$\left.-\frac{1}{2(1+\nu)-(p-3)(1+\varepsilon_*)}-\frac{1}{2(1+\nu)-(p-3)(1+\varepsilon_*)}\right]; \quad (3.100)$$

for $3+1/(1+\varepsilon_*)<p<3+(2+2\nu)/(1+\varepsilon_*)$ we have

$$\Delta P\big|_2 \simeq \frac{\sqrt{\pi}}{4}\left(\frac{k_\gamma}{k_*}\right)^2\left(\frac{k}{k_*}\right)^{(p-3)(1+\varepsilon_*)-2}\frac{\Gamma\left[\frac{(p-3)(1+\varepsilon_*)-1}{2}\right]\Gamma\left[1+\nu-\frac{(p-3)(1+\varepsilon_*)}{2}\right]}{\Gamma\left[\frac{(p-3)(1+\varepsilon_*)}{2}\right]\Gamma\left[\frac{(p-3)(1+\varepsilon_*)}{2}+\nu\right]}; \quad (3.101)$$

and finally, for $p<3+1/(1+\varepsilon_*)$,

$$\Delta P_{\mathbf{k}}\big|_3 \simeq \left(\frac{k_\gamma}{k_*}\right)^2\left(\frac{k}{k_*}\right)^{(p-3)(1-\varepsilon_*)(1+\varepsilon_*)+\varepsilon_*-2}\frac{(1+\varepsilon_*)^{1-(p-3)(1+\varepsilon_*)}}{2-2(p-3)(1+\varepsilon_*)}. \quad (3.102)$$

For consistency, these must also be expanded in slow-roll. At first order for the three cases $(i=1,2,3)$ we have

$$\Delta P_{\mathbf{k}}\big|_i \simeq \mathcal{A}_i(k)\left[1+\mathcal{B}_i\varepsilon_*+\mathcal{C}_i\varepsilon_*+(\mathcal{D}_i\varepsilon_*+\mathcal{E}_i\varepsilon_*)\ln\left(\frac{k}{k_*}\right)\right], \quad (3.103)$$

where for the three cases

$$\mathcal{A}_1(k)=\left(\frac{k_\gamma}{k_*}\right)^2\left(\frac{k}{k_*}\right)^3\left(\frac{\eta}{\eta_*}\right)^{2+2\nu-(p-3)(1+\varepsilon_*)}\frac{2}{(p-2)(p-5)(p-8)}, \quad (3.104)$$
$$\mathcal{B}_1=2\gamma_E+\ln 4-7+\frac{1}{2-p}+\frac{3}{8-p}+\frac{2}{5-p}, \quad (3.105)$$
$$\mathcal{C}=\gamma_E+\ln 2-2+\frac{6}{(p-2)(p-8)}, \qquad \mathcal{D}_1=2, \qquad \mathcal{E}_1=1; \quad (3.106)$$
$$\mathcal{A}_2(k)=\left(\frac{k_\gamma}{k_*}\right)^2\left(\frac{k}{k_*}\right)^{p-5}\frac{(6-p)\pi}{2^{6-p}(p-2)\sin(\pi p/2)\Gamma(p-3)}, \quad (3.107)$$
$$\mathcal{B}_2=-2\frac{(p-1)(p-3)}{(p-4)(p-2)}-\frac{1}{2}(p-5)\psi(4-\frac{p}{2})-\psi(-2+\frac{p}{2})-\frac{1}{2}(p-3)\psi(-\frac{3}{2}+\frac{p}{2}), \quad (3.108)$$
$$\mathcal{C}_2=\frac{1}{2}\psi\left(4-\frac{p}{2}\right)-\frac{1}{2}\psi\left(\frac{p}{2}\right), \qquad \mathcal{D}_2=p-3, \qquad \mathcal{E}_2=0; \quad (3.109)$$
$$\mathcal{A}_3(k)=\left(\frac{k_\gamma}{k_*}\right)^2\left(\frac{k}{k_*}\right)^{p-5}\frac{(H_*\ell_c)^{p-4}}{2(4-p)}, \quad (3.110)$$
$$\mathcal{B}_3=3-p+\frac{1}{4-p}+\ln(H_*\ell_c), \qquad \mathcal{C}_3=0, \qquad \mathcal{D}_3=1, \qquad \mathcal{E}_3=0. \quad (3.111)$$

where γ_E is the Euler constant and $\psi(z)$ is the digamma function. It is important to note, that only

in the third case do we see the dependence on the correlation length ℓ_c, which means that in this case the result depends on the form of the correlation function, hence the top-hat approximation in this case may not be accurate. However, in the first two cases, the form of the correlation function is irrelevant, so the top-hat approximation works just as well as a more physically justifiable form like an exponential decay $C_R \sim e^{-a|\mathbf{x}-\mathbf{y}|/\ell_c}$, for example.

It should be noted, that in the second and third case, the power spectrum settles to a stationary value at late times, whereas in the first case, the power spectrum evolves and is not frozen at large scales. This can be seen by rewriting $\mathcal{A}_1$ as

$$\mathcal{A}_1(k) = \left(\frac{k_\gamma}{k_*}\right)^2 \left(\frac{k}{k_*}\right)^3 \left(\frac{\eta}{\eta_*}\right)^{2+2\nu-(p-3)(1+\varepsilon_*)} \frac{2}{(p-2)(p-5)(p-8)} \exp\left[\Delta N_* \left(p-3-\frac{2(1+\nu)}{1+\varepsilon_*}\right)\right] \tag{3.112}$$

where $\Delta N_* = N - N_*$ is the number of e-folds passed since the pivot scale crosses the Hubble radius. Since we are considering the case in which $p > 3 + (2+\nu)/(1+\varepsilon_*)$, the sign of the exponential is positive, leading to the late-time enhancement of the power spectrum.

The CMB measurements suggest a scale-independent power spectrum. However, we have two branches, one of which is scale-dependent and one is not. The scale-dependent branch must be constrained so that it is beyond the observable scales. We introduce the transient scale k_t, at which the transition between the two branches occurs. This must be such that $\mathcal{A}_i(k_t) \sim 1$. This gives rise to

$$\left.\frac{k_t}{k_*}\right|_1 \simeq \left(\frac{k_\gamma}{k_*}\right)^{-2/3} \exp\left[-\frac{\Delta N_*}{3}\left(p-3-\frac{2(1+\nu)}{(1+\varepsilon)}\right)\right], \tag{3.113}$$

$$\left.\frac{k_t}{k_*}\right|_2 \simeq \left(\frac{k_\gamma}{k_*}\right)^{-\frac{2}{p-5}}, \tag{3.114}$$

$$\left.\frac{k_t}{k_*}\right|_3 \simeq \left(\frac{k_\gamma}{k_*}\right)^{-\frac{2}{p-5}} (H_*\ell_c)^{-\frac{p-4}{p-5}}, \tag{3.115}$$

where ΔN_* corresponds to $N - N_*$, but evaluated at the end of inflation, i.e. $N_{\text{end}} - N_*$.

In fig. 7 we see, that the corrections grow at small scales. In that case, we must ensure these scales are outside the observable window, $k_t \gg k_*$. Taking equation (3.113) into account, we obtain a constraint of the interaction strength at small scales,

$$\frac{k_\gamma}{k_*} \ll \exp\left[-\frac{\Delta N_*}{2}\left(p-8+3\varepsilon_*-\eta_*\right)\right]. \tag{3.116}$$

Similar treatment for the cases $i = 2$ and 3 leads to

$$\left.\frac{k_\gamma}{k_*}\right|_2 \ll 1 \tag{3.117}$$

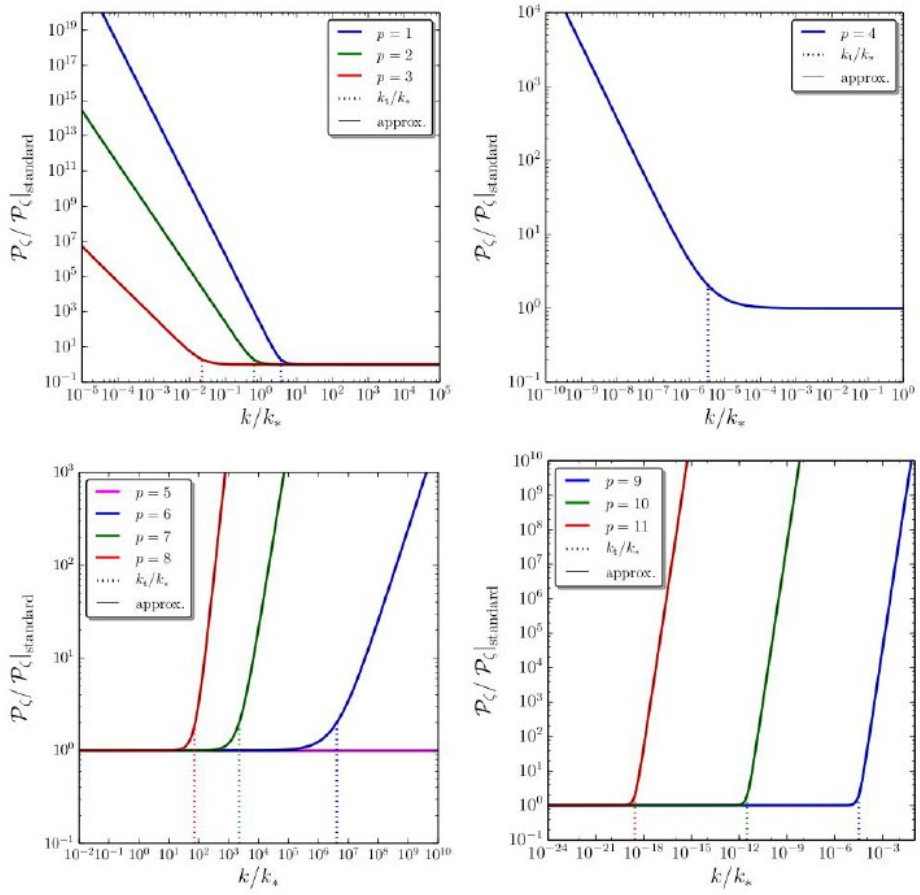

Figure 7: Comparison of the Power spectra for different values of p obtained numerically and using analytical approximations. The vertical dotted lines correspond to the transient scale k_t. The values chosen are $\varepsilon_* = 10^{-4}$, $\eta_* = 1 - 0.96 - 2\varepsilon_*$, $H_*\ell_c = 10^{-3}$, $k_\gamma/k = 10^{-3}$, and $\Delta N_* = 50$. [2].

and

$$\left.\frac{k_\gamma}{k_*}\right|_3 \ll (H_*\ell_c)^{\frac{4-p}{2}}. \tag{3.118}$$

The only case that does not constrain the interaction strength is $p = 5$, for which the power spectrum is scale-invariant.

3.4.6 Concrete example: heavy scalar field environment

Consider the inflaton field ϕ coupled to a much heavier scalar field ψ. The corresponding action reads

$$S = -\int d^4x\sqrt{-g}\left[\frac{1}{2}\partial^\mu\phi\partial_\mu\phi + V(\phi) + \frac{1}{2}\partial^\mu\psi\partial_\mu\psi + \frac{M^2}{2}\psi^2 + \lambda\mu^{4-n-m}\phi^n\psi^m\right], \tag{3.119}$$

where V is the potential, M is the mass of scalar field ψ, which is assumed to be larger than the Hubble scale $M \gg H$. λ is a small coupling constant and μ is the mass scale that appears in the power-law coupling between the two fields evolving in the de Sitter background.

According to (C.18), the action should be written in such a way that the quantum mean of the interacting term vanishes in the stationary configuration. This is done by adding and subtracting $\lambda\mu^{4-n-m}\langle\psi^m\rangle_{\rm st}\phi^n$,

$$S = -\int d^4x\sqrt{-g}\Bigg[\frac{1}{2}\partial^\mu\phi\partial_\mu\phi + V(\phi) + \frac{1}{2}\partial^\mu\psi\partial_\mu\psi + \frac{M^2}{2}\psi^2 + \lambda\mu^{4-n-m}\phi^n\langle\psi^m\rangle + \lambda\mu^{4-m-n}\phi^n(\psi^m - \langle\psi^m\rangle_{\rm st})\Bigg]. \quad (3.120)$$

The 4th term can be added to the potential forming

$$V_{\rm eff} = V(\phi) + \lambda\mu^{4-n-m}\phi^n\langle\psi^m\rangle. \quad (3.121)$$

We can now easily identify the interaction Hamiltonian

$$\hat{H}_{\rm int} = \lambda\mu^{4-m-n}a^4\int d^3x\hat{\phi}^n(\tau,\mathbf{x})\hat{\psi}^m(\tau,\mathbf{x}). \quad (3.122)$$

Assuming that $V_{\rm eff}(\phi) = m^2\phi^2/2$ in Fourier space we can write

$$S_\phi = \frac{1}{2}\int d\tau\int_{\mathbb{R}^3} d^3k\left[v'_{\mathbf{k}}v'^*_{\mathbf{k}} - \left(k^2 - \frac{a''}{a} + ma^2\right)v_{\mathbf{k}}v_{\mathbf{k}*}\right], \quad (3.123)$$

where $v(\tau,\mathbf{x}) \equiv a(\tau)\phi(\tau,\mathbf{x})$. In case $m = 0$ we recover the action for the curvature perturbations if the metric perturbations are ignored. This means that we can identify $v(\tau,\mathbf{x})$ with the Mukhanov-Sasaki variable in the uniform curvature gauge.

The interaction Hamiltonian now reads

$$H_{\rm int} = \lambda\mu^{4-m-n}a^{4-n}\int d^3x v^n(\tau,\mathbf{x})\left[\psi^m(\tau,\mathbf{x}) - \langle\psi^m\rangle_{\rm st}\right]. \quad (3.124)$$

Looking back at equations (3.65)-(3.66) we can identify the system and the environment part of the interaction Hamiltonian: $A = v^n$ and $R = \psi^m - \langle\psi^m\rangle_{\rm st}$. The effective coupling constant then reads $g = \lambda\mu^{4-n-m}$, and according to (C.40) $\gamma = 2g^2\tau_c$, where now τ_c is the conformal correlation time and is related to the physical correlation time by $t_c = a\tau_c$, the ansatz (3.70) is satisfied if

$$\gamma_* = 2t_c\lambda^2\mu^{8-2n-2m}a_*^{7-2n}, \quad (3.125)$$

and $p = 7 - 2n$.

As mentioned before, the crucial part after identifying the environment is deriving its correlation

function. This can be done by point-splitting renormalization in the small separation limit $\epsilon \equiv [(t_1 - t_2)^2 - a^2(\mathbf{x}_1 - \mathbf{x}_2)^2]/4 \ll \min(1/H^2, 1/M^2)$. Here we simply quote the result in [2]:

$$C_R(t_1, \mathbf{x}_1; t_2, \mathbf{x}_2) = \left[(2m-1)!! - \sigma(m)[(m-1)!!]^2\right] \left(\frac{37}{504\pi^2}\frac{H^6}{M^4}\right)^m \times \\ \times \left[1 - \frac{m^2(2m-3)!!}{(2m-1)!! - \sigma(m)[(m-1)!!]^2}\frac{M^2\Sigma\epsilon^2}{2}\right], \quad (3.126)$$

where $\sigma(m)$ is 1 if m is even and 0 if m is odd and $\Sigma = \pm 1$ depending on whether the separation between the two points $(t_1, \mathbf{x}_1)$ and $(t_2, \mathbf{x}_2)$ is spacelike or timelike. It should be noted that in deriving the correlation function one eventually needs to evaluate $\langle\psi^m\rangle_{\rm st}$. In this construction the result is

$$\langle\psi^m\rangle_{\rm st} = \sigma(m)(m-1)!! \left(\frac{37}{504\pi^2}\frac{H^6}{M^4}\right)^{m/2}. \quad (3.127)$$

It is now possible to identify $\bar{C}_R$, the correlation time t_c and the correlation length ℓ_c, specifically

$$\bar{C}_R = \left[(2m-1)!! - \sigma(m)[(m-1)!!]^2\right] \left(\frac{37}{504\pi^2}\frac{H^6}{M^4}\right)^m, \quad (3.128)$$

$$t_c = \ell_c = 2\sqrt{2}\sqrt{\frac{(2m-1)!! - \sigma(m)[(m-1)!!]^2}{m^2(2m-3)!!}}\frac{1}{M}. \quad (3.129)$$

By plugging this into (3.125) we obtain

$$\gamma_* = 4\sqrt{2}\sqrt{\frac{(2m-1)!! - \sigma(m)[(m-1)!!]^2}{m^2(2m-3)!!}}\frac{\lambda^2}{M}\mu^{8-2n-2m}a_*^{7-2n}. \quad (3.130)$$

It should be noted that under this construction, the scalar field ψ is considered to be a test particle (this is not a necessary requirement). The idea is that the contribution of ψ to the energy budget of the universe is negligible. The Friedmann equation $\rho = 3M_{\rm Pl}^2H^2$ leads to the following condition

$$M^2\langle\psi^2\rangle_{\rm st} \ll 3M_{\rm Pl}^2H^2. \quad (3.131)$$

If we now use equation (3.127) for $m = 2$ we can write

$$\frac{M^2\langle\psi^2\rangle_{\rm st}}{3M_{\rm Pl}^2H^2} = \frac{37}{1512\pi^2}\frac{H^4}{M^2M_{\rm Pl}^2}. \quad (3.132)$$

By our assumption $M \gg H$ and from observational bounds $H/M_{\rm Pl} \lesssim 10^{-5}$, hence the condition (3.131) is satisfied.

Second, if we take ϕ to be the inflaton field, we must ensure, that the correction to $V(\phi)$ presented in equation (3.121) is small so that it does not spoil slow-roll inflation. In this case, as we have seen

in equation (2.39), $3M_{\rm Pl}^2H^2 \simeq V(\phi)$. Then the condition reads

$$\lambda\mu^{4-n-m}\langle\psi^m\rangle_{\rm st}\phi^n \ll 3M_{\rm Pl}^2H^2. \tag{3.133}$$

This also guarantees that we can use perturbation theory to assess the effect of the environment on the system. By plugging in (3.127) we obtain

$$\sigma(m)(m-1)!!\left(\frac{37}{504\pi^2}\frac{H^6}{M^4}\right)^{m/2}\lambda\frac{\mu^{4-n-m}\phi^n H^{3m-2}}{M_{\rm Pl}M^{2m}} \ll 1. \tag{3.134}$$

The constraint here actually depends on the value of ϕ, which is specified once a concrete model of inflation is considered.

Third, the interaction term must not affect much the behavior of the environment

$$\lambda\mu^{4-n-m}\phi^n\psi^m \ll M^2\psi^2. \tag{3.135}$$

Since we have assumed ψ is a test field, the condition (3.131) readily ensures that (3.135) is satisfied. Using (3.127) we get

$$\frac{\lambda\mu^{4-m-n}\phi^n\langle\psi^m\rangle_{\rm st}}{M^2\langle\psi^2\rangle{\rm st}} = (m-1)!!\left(\frac{37}{504\pi^2}\right)^{\frac{m}{2}-1}\lambda\frac{\mu^{4-m-n}\phi^n}{H^{6-3m}M^{2m-2}}. \tag{3.136}$$

Lastly, we need to ensure, that when the environment is in the stationary state, $R = \psi^m - \langle\psi^m\rangle_{\rm st}$, it has autocorrelation time that is smaller than the typical evolution time of the system. Since the system is a light scalar field, we expect it to evolve at timescales of order $\tilde{T}_A = H^{-1}$. According to (3.128) the environment correlation time $t_c \sim 1/M$, so that

$$\frac{t_c}{\tilde{T}_A} \sim \frac{H}{M}, \tag{3.137}$$

and since by our initial assumption the environment is massive ($M \ll H$), this condition is always satisfied.

Power spectrum constraints. For $n = 1$, interaction with the heavy scalar field environment the parameter $p = 5$, or to be more precise (see ref [2]) $p = 5 - 6m\varepsilon_*$. Combining the standard expression to the power spectrum with equations (3.89) and (3.101), one obtains

$$P_{\zeta\zeta} = \frac{H_*\left(1+\frac{\pi}{6}\frac{k_\gamma^2}{k_*^2}\right)}{8\pi^2\varepsilon M_{\rm Pl}^2}\left[1+Q\left(\frac{k_\gamma}{k_*},\frac{k}{k_*},\varepsilon_*,\eta_*,m\right)\right]. \tag{3.138}$$

First, notice the amplitude depends on k_γ/k_*, so if we assume the tensor perturbations are unaffected by the environment, the tensor-to-scalar ratio $r = P_{hh}/P_{\zeta\zeta}$, where P_{hh} is the tensor

power spectrum, now writes

$$r = \frac{r|_{\rm standard}}{1 + \frac{\pi}{6}\frac{k_\gamma^2}{k_*^2}}, \tag{3.139}$$

where $r|_{\rm standard} = 16\varepsilon_*$. If $k_\gamma/k_* \ll 1$, the standard result is recovered, however when this is not the case the tensor-to-scalar ratio becomes smaller.

Second, the spectral index $n_s \equiv 1 + d\ln P_{\zeta\zeta}/d\ln k$ also changes

$$n_s = n_s|_{\rm standard} - \frac{\frac{\pi}{6}\frac{k_\gamma^2}{k_*^2}}{1 + \frac{\pi}{6}\frac{k_\gamma^2}{k_*^2}}(6m-2)\varepsilon_*. \tag{3.140}$$

For $k_\gamma/k_* \ll 1$, the standard result is recovered, however if $k_\gamma/k_* \gg 1$ one obtains $n_s \simeq n|_{\rm standard} - (6m-2)\varepsilon_*$. The shift is negative, at least for $m > 1/3$.

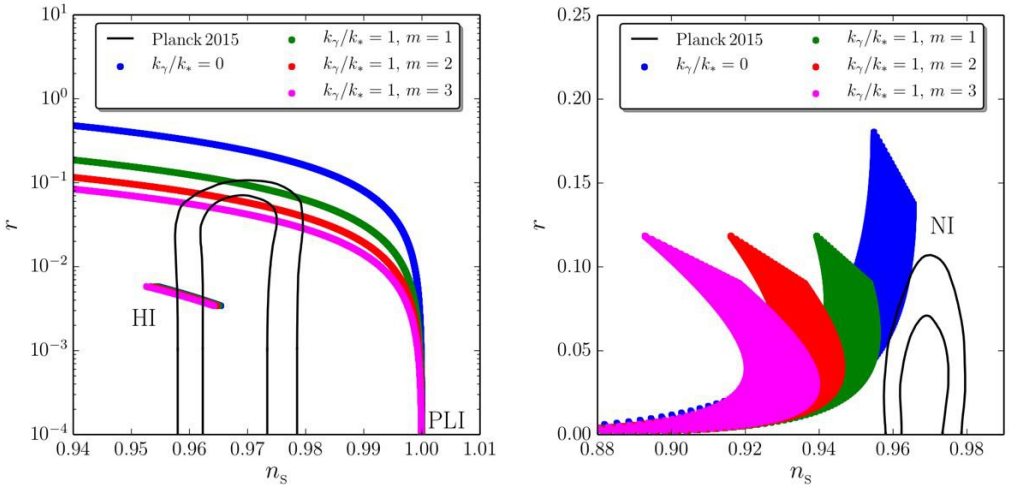

Figure 8: Spectral index n_s and the tensor-to-scalar ratio r for various values of k_γ/k_* and m, for different models of single-field inflation: Higgs inflation ("HI"), power-law inflation ("PLI"), and natural inflation ("'Ni"). The blue color corresponds to the standard results without decoherence and other colors describe the result when decoherence is present. The black lines correspond to the one and two-sigma contours obtained from Planck 2015 data. [2].

The comparison of these findings with data is shown in Fig. 8, which shows how decoherence affects the compatibility of three scenarios (Higgs inflation, natural inflation, power-law inflation) with data.

- Decoherence has almost no effect on the observables of Higgs inflation.
- Natural inflation is already disfavoured by data and decoherence makes it even worse.
- Power-law inflation was disfavoured by data, however, decoherence cures this and as m increases it agrees with data even better.

3.4.7 Decoherence

We move to quantifying decoherence of the inflaton perturbations due to the environment, i.e. gauge fields. Specifically, the non-unitary term in the Lindblad equation (3.78) suppresses the off-diagonal elements of the reduced density matrix.

In the case of linear interactions with the environment, the Lindblad equation can be solved exactly and leads to Eq. (3.80).

We consider an off-diagonal element of the density matrix, with a distance from the diagonal $\Delta v_{\mathbf{k}}$. Then according to equation (3.80)

$$\left|\left\langle v^s_{\mathbf{k}}+\frac{\Delta v_{\mathbf{k}}}{2}\right|\hat{\rho}^s_{\mathbf{k}}\left|v^s_{\mathbf{k}}-\frac{\Delta v_{\mathbf{k}}}{2}\right\rangle\right| = |\left\langle v^s_{\mathbf{k}}\right|\hat{\rho}^s_{\mathbf{k}}\left|v^s_{\mathbf{k}}\right\rangle|\exp\left[-\frac{\delta_{\mathbf{k}}+\frac{1}{4}}{2}\frac{\Delta v^2_{\mathbf{k}}}{P_{vv}(k)}\right], \tag{3.141}$$

where we have used (3.87) for $P_{vv}(k)$ and introduced the *decoherence parameter*

$$\delta_{\mathbf{k}} \equiv \mathcal{I}_{\mathbf{k}}\mathcal{J}_{\mathbf{k}} - \mathcal{K}^2_{\mathbf{k}} + |v'_{\mathbf{k}}|^2\mathcal{J}_{\mathbf{k}} + |v_{\mathbf{k}}|^2\mathcal{I}_{\mathbf{k}} - |v_{\mathbf{k}}|^{2'}\mathcal{K}_{\mathbf{k}}. \tag{3.142}$$

We have separated the 1/4 term from the decoherence parameter since it is present even in the free theory, whereas if we turn off the interactions, $\delta_{\mathbf{k}} = 0$ (see equations (3.81-3.83)). Hence, $\delta_{\mathbf{k}}$ is the environment contribution to the suppression of the non-diagonal elements.

Heuristically, since 1/4 corresponds to the standard decrease of the off-diagonal elements it makes sense to compare it with the contribution coming from $\delta_{\mathbf{k}}$. If $\delta_k \gg 1$, it means that the environment strongly suppresses the off-diagonal elements, so the environment-induced decoherence is dominating.

Moreover, the state purity is defined as the trace of the reduced density matrix squared, $\mathrm{Tr}\{\hat{\rho}^{s2}_{\mathbf{k}}\}$ and it is one of the simplest measures of decoherence. Using equation (3.80), we can write it as a Gaussian integral and obtain

$$\mathrm{Tr}\{\hat{\rho}^{s2}_{\mathbf{k}}\} = \int_{-\infty}^{\infty} dv^{s,(1)}_{\mathbf{k}} \int_{-\infty}^{\infty} dv^{s,(2)}_{\mathbf{k}} |\left\langle v^{s,(1)}_{\mathbf{k}}\right|\hat{\rho}^s_{\mathbf{k}}\left|v^{s,(2)}_{\mathbf{k}}\right\rangle|^2 = \frac{1}{\sqrt{1+4\delta_{\mathbf{k}}}} \tag{3.143}$$

which implies that when $\delta_{\mathbf{k}} \ll 1$, the purity is 1. On the other hand when $\delta_{\mathbf{k}} \gg 1$, the purity decreases. Decoherence can be considered complete if $\mathrm{Tr}\{\hat{\rho}^s_{\mathbf{k}}\} \to 0$, or in terms of the decoherence parameter $\delta_{\mathbf{k}} \gg 1$. We shall adopt this criterion in what follows.

First, we notice, that some of the terms in equation (3.142) are quadratic in γ, since $\mathcal{I}, \mathcal{J}, \mathcal{K}$ are actually linear in γ. However, the Lindblad equation was derived in the linear order in γ, so we can neglect higher order terms, leading to

$$\delta_{\mathbf{k}}(\tau) \simeq |v_{\mathbf{k}}|^2\mathcal{I}_{\mathbf{k}} + |v'_{\mathbf{k}}|^2\mathcal{J}_{\mathbf{k}} - |v_{\mathbf{k}}|^{2'}\mathcal{K}_{\mathbf{k}}. \tag{3.144}$$

$\mathcal{I}, \mathcal{J}$ and $\mathcal{K}$ can be computed by taking the relevant integrals (3.81)-(3.83).

If we require that decoherence is complete (very large $\delta_{\mathbf{k}}$) by the end of inflation we get the

following condition

$$\frac{k_\gamma}{k_*} \gg \begin{cases} (H_*\ell_c)^{\frac{1-(p-3)(1+\varepsilon_*)}{2}} & \text{if} \quad p < 3 + \frac{2-2\nu}{1+\varepsilon_*} \\ e^{\left(\frac{1-\nu}{1+\varepsilon_*} - \frac{p-2}{2}\right)\Delta_{N_*}} & \text{if} \quad p > 3 + \frac{2-2\nu}{1+\varepsilon_*}. \end{cases} \tag{3.145}$$

Combining these with the upper bounds on k_γ/k_* obtained before, we can see the range of possible values that comply with both bounds. The analysis is summarized in figure 9.

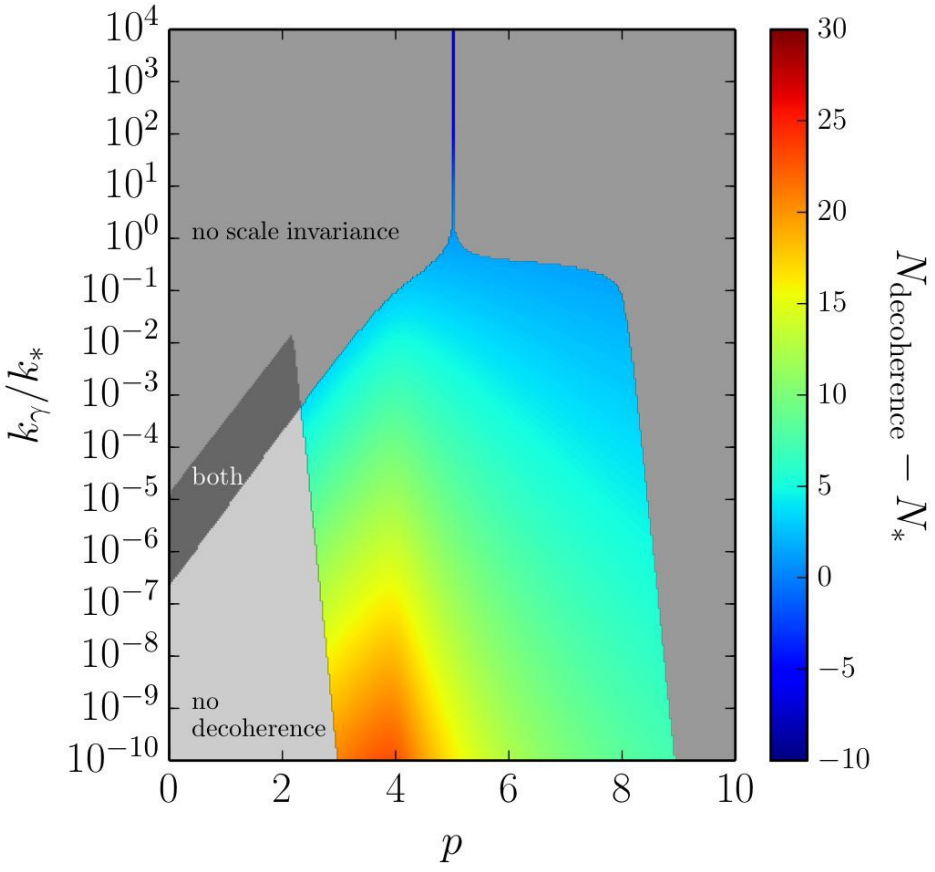

Figure 9: Regions of parameter space $(p, k_\gamma/k_*)$ depicting the validity of parameter values. The coloured regions correspond to values for which decoherence is complete and the scale invariance preserved. The light gray region depicts parameter values that are not allowed due to insufficient decoherence. Medium gray color depicts invalid values due to violation of scale invariance and the dark gray region is where both conditions are violated. Decoherence is assumed to be complete for $\delta_{\mathbf{k}} > 10$, and quasi scale invariance is assumed to be preserved if $|n_s - \bar{n}_s| < 5\sigma_{n_s}$, where $\bar{n}_s \simeq 0.96$ and $\sigma_{n_s} \simeq 0.006$ are the mean value and the standard deviation of the spectral index as measured by Planck. [2].

An important feature of figure 9 is the thin vertical line at $p = 5$, which derives from the scale-invariance of the Lindblad term associated with this particular value. Note, that this is indeed the value we obtain for heavy scalar fields (Sec. 3.4.6).

3.5 Lindblad formalism in axion inflation

The goal now is to apply the formalism introduced in the previous chapter to axion models of inflation, which we discussed at some length in section 2.5.

Let us rewrite the action of the model for clarity

$$S = \int d^4x\sqrt{-g}\left[\frac{M_{\rm Pl}^2}{2}R - \frac{1}{2}g^{\mu\nu}\partial_\mu\phi\partial_\nu\phi - V(\phi) - \frac{1}{4}F_{\mu\nu}F^{\mu\nu} - \frac{\alpha}{4f}\phi F_{\mu\nu}\tilde{F}^{\mu\nu}\right]. \tag{3.146}$$

where $M_{\rm Pl}$ is the Planck mass, R is the Ricci scalar, $F_{\mu\nu} \equiv \partial_\mu A_\nu - \partial_\nu A_\mu$ is the U(1) gauge field strength and $\tilde{F}^{\mu\nu} \equiv \epsilon^{\mu\nu\rho\sigma}F_{\rho\sigma}/2\sqrt{-g}$ is its dual. Here ϵ denotes the Levi-Civita tensor. f is the axion decay constant and α is the adimensional coupling constant, which is expected to be $\sim O(1)$. The axion inflaton field ϕ embodies the shift symmetry, hence the axion is invariant under a (slightly broken) symmetry $\phi \longrightarrow \phi + const.$. The dimension of f can easily be obtained by comparing the last term in the action with others. This yields $[f] = [M]$.

We will apply the Lindblad equation to this model by identifying the gauge fields as the environment and the inflaton field as the system.

First, notice that the coupling between the system and the environment is yet again linear in the system sector. This means that we can use the same form of the solution to the Lindblad equation as (3.80), at least at lowest-order in the perturbations. However, of course, the correlation function C_R (3.68) and the γ (3.69) parameter will be specific to the model at hand.

As in the case of the heavy scalar field, in the stationary configuration of the environment, the expectation value (EV) of the interacting term must vanish, so we would like to write the interaction action as

$$S_{\rm int} = \int d^4x\sqrt{-g}\frac{\alpha}{4f}\phi\left(F_{\mu\nu}\tilde{F}^{\mu\nu} - \langle F_{\mu\nu}\tilde{F}^{\mu\nu}\rangle_{\rm stat}\right). \tag{3.147}$$

Notice, that the new term $\langle F_{\mu\nu}\tilde{F}^{\mu\nu}\rangle_{\rm stat}$ corresponds to (2.127). This would translate to a corresponding shift in the potential

$$\bar{V}_{\rm eff} = \bar{V}(\phi) + \frac{\alpha}{4f}\phi\langle F_{\mu\nu}\tilde{F}^{\mu\nu}\rangle_{\rm stat}, \tag{3.148}$$

where we have introduced bars so as not to confuse the notations with the previous chapter.

We again define $\hat{v}(\tau, \mathbf{x}) = a(\tau)\phi(\mathbf{x}, \tau)$. This will be useful since it will correspond to the Mukhanov-Sasaki variable in the uniform curvature gauge. In appendix B we showed that $F_{\mu\nu}\tilde{F}^{\mu\nu} = 4a^{-4}\partial_\tau\vec{A}\cdot(\vec{\nabla}\times\vec{A})$ (see Eq. (B.16)). Then, the corresponding interaction Hamiltonian reads

$$H_{\rm int} = \frac{\alpha}{af}\int d^3x\hat{v}(\tau)\left(\partial_\tau\vec{A}\cdot(\vec{\nabla}\times\vec{A}) - \langle\partial_\tau\vec{A}\cdot(\vec{\nabla}\times\vec{A})\rangle_{\rm stat}\right). \tag{3.149}$$

We can identify this Hamiltonian as the one in (C.38):

$$gH_{\rm int} = g\int d^3\mathbf{x}A(t, \mathbf{x})\otimes R(t, \mathbf{x}), \tag{3.150}$$

where g is the coupling, $A(\eta, \mathbf{x})$ represents the system and $R(t, \mathbf{x})$ the environment. As seen from the expression the interaction is local. By analogy

$$A(\tau, \mathbf{x}) = \hat{v}(\tau, \mathbf{x}), \qquad R(\tau, \mathbf{x}) = \left(\partial_\tau \vec{A} \cdot (\vec{\nabla} \times \vec{A}) - \langle \partial_\tau \vec{A} \cdot (\vec{\nabla} \times \vec{A}) \rangle_{\text{stat}}\right). \tag{3.151}$$

Then we immediately see $g = \frac{\alpha}{af}$.[17]

According to (C.39), $\gamma = 2g^2\tau_c$, where τ_c is the autocorrelation time for the environment. Notice, that we are using the conformal autocorrelation time τ_c instead of conventional physical t_c, which is constant. The two are connected by the relation $t_c = \tau_c a(\tau)$.

To continue we consider the form given by Eq. (3.70) for γ

$$\gamma = \gamma_* \left(\frac{a}{a_*}\right)^p. \tag{3.152}$$

Then,

$$\gamma = 2\frac{\alpha^2}{a^2 f^2}\frac{t_c}{a} \qquad \Rightarrow \qquad \gamma_* = \frac{2\alpha^2 t_c}{a_*^3 f^2}, \tag{3.153}$$

where we have obtained $p = -3$ for this model. As mentioned in the previous chapter, this indicates, that the top-hat approximation may not be good enough and one may need a more complicated, albeit more physical form of the correlation function. To this end, we would like to evaluate the gauge field correlation function, but also make the top-hat approximation to see if it can still be used.

Therefore, we need to evaluate the following correlation $a^4(\tau')a^4(\tau'')\langle(\vec{B}\cdot\vec{E})(\mathbf{k},\tau')(\vec{B}\cdot\vec{E})(\mathbf{k},\tau'')\rangle$. In Appendix D it is shown, that this leads to the following form of the correlation function

$$\begin{aligned} C_R(k,\tilde{\tau}) &= \frac{1}{16}\frac{k^5}{(2\pi)^3} e^{4\pi\xi} \times \\ \times \int d^3p \left|1 + \frac{|\mathbf{p}|^2 - \hat{z}\cdot\mathbf{p}}{|\mathbf{p}||\hat{z}-\mathbf{p}|}\right|^2 |\mathbf{p}|^2 \left(1 + \frac{|\hat{z}-\mathbf{p}|^{1/2}}{|\mathbf{p}|^{1/2}}\right) & e^{-\sqrt{\kappa}\left(\sqrt{|\mathbf{p}|}+\sqrt{|\hat{z}-\mathbf{p}|}\right)}, \end{aligned} \tag{3.154}$$

where $\mathbf{p}$ is adimensional, $\hat{z}$ is a unit vector along $\mathbf{k}$ and we have defined $\kappa = -32\xi k\tilde{\tau}$, with $2\tilde{\tau} = \tau' + \tau''$. It is clear already from this result, that the Markovian approximation is likely not a good one in this case since it clearly violates our starting assumption of stationary environment[18]. In fact, the environment is evolving as the gauge fields get amplified because of the background dynamics. This suggests that the Lindblad formalism may not be applicable and that a more accurate treatment would involve non-Markovian master equations (see e.g., [72]).

Nevertheless, we proceed with the Lindblad equation for reasons of tractability and with a pragmatic justification: we will measure the success of the approach by comparing our results for the power spectrum, with those already present in the literature, and if we find that the two are

[17] Notice that g is time-dependent.

[18] The correlation function in this case cannot be written as a function of a difference $|\tau' - \tau''|$, which is a necessary condition to derive the Lindblad equation (see Appendix C).

in agreement, we will deem the Lindblad formalism as an acceptable approximation within this particular context.

The integral (3.154) above can be evaluated numerically by fitting formulae[19]. As for the fit, we would like to have a result for $2 \leq \xi \leq 3$, which is the most interesting range in terms of phenomenology (see Sec. 2.5). The fit leads to

$$C_R(k,\tilde{\tau}) = \frac{367}{16}\frac{k^5}{(2\pi)^3}e^{4\pi\xi}e^{0.11\cdot 2^8\xi k\tilde{\tau}} \qquad 2 \leq \xi \leq 3; \tag{3.155}$$

Using this form of the correlation function, we can identify an effective (conformal) correlation time $|\tau_c| \equiv (0.11 \cdot 2^8 \xi k)^{-1}$. One of the novelties in this work is in fact the scale dependence of the correlation time. In this particular case, we see that the shorter modes decohere more efficiently compared to longer modes (we will quantify this in the following sections).

As mentioned in 3.4.6, the conformal correlation time is related to the cosmic correlation time by $t_c = a\tau_c$, which immediately implies that $t_c = (\beta\xi k_{\rm phys})$, where $k_{\rm phys} = k/a$ and $\beta = 0.11 \cdot 2^8$.

Furthermore, let us make the following observation: at first order in slow-roll

$$\xi = \frac{\alpha M_{\rm Pl}}{f}\sqrt{\frac{\varepsilon}{2}}, \tag{3.156}$$

where we have used the definition of $\xi = 2\alpha\dot{\phi}/fH$ and $\varepsilon = \dot{\phi}^2/2M_{\rm Pl}^2H^2$. Since all modes of astrophysical interest today had crossed the horizon during inflation, we can evaluate ξ at the horizon crossing ($k = aH$). This amounts to evaluating the slow-roll parameter at the horizon crossing and we can write $\varepsilon|_{k=aH} = -\dot{H}/k_{\rm phys}^2$ and by plugging this into the expression for the correlation time t_c, we obtain

$$t_c = \frac{1}{\beta\xi H}. \tag{3.157}$$

Notice, that the correlation time is smaller when $\xi \gg 1$. This is because as ξ grows the environment looks more and more like a thermal bath, whose characteristic is a small correlation time. In any case, the requirement that the correlation time needs to be smaller than the typical timescale in which the system evolves is satisfied for $\xi \geq \mathcal{O}(1)$, since the system - the inflaton field - evolves with the characteristic time $\sim H^{-1}$.

In Appendix D we have also computed the environment (physical) correlation length

$$\ell_c = \frac{\beta\xi}{H}. \tag{3.158}$$

Note, that this implies, that for values of $\xi \gtrsim (0.11 \cdot 2^8)^{-1}$ the correlation length can become super-Hubble, so the correlations are not spatially local, but this is not necessarily a contradiction; e.g. In Sec. 3.4.6 the correlation time and the correlation length are similar, so it is rightfully expected that the correlation length *must* be shorter than the Hubble radius because the Lindblad formalism imposes a short correlation time. However, if the correlation length is different compared to the

[19] Although an analytical expression can be found in Appendix D for $\xi \gg 1$.

correlation time, which is precisely the case studied in this thesis, the correlation length can take larger values.

Using the exponential form for the environment correlation function characterizes the physics well, but is less tractable analytically for the purposes of our future discussions, which is why we also use the top-hat approximation

$$C_R(k,\tilde{\tau}) = \frac{367}{16(2\pi)^3}k^5 e^{4\pi\xi} \times \Theta\left(\frac{\tilde{\tau}}{\tau_c}\right), \tag{3.159}$$

where

$$\Theta\left(\frac{\tilde{\tau}}{\tau_c}\right) = \begin{cases} 1 & \tilde{\tau} < \tau_c \\ 0 & \tilde{\tau} \geq \tau_c, \end{cases} \tag{3.160}$$

and $|\tau_c| \equiv (0.11 \cdot 2^8 \xi k)^{-1}$ is the environment autocorrelation time. The use of the top-hat approximation is twofold. First, since the calculations can be done analytically, we obtain more insight into the physics and how the interplay of different parameters affects the final results. Second, as stated by [2], in certain regimes the top-hat approximation cannot be trusted and one needs to resort to more physical forms (like the exponential) of the correlation function. Having both forms, we will be able to explicitly check the validity of the top-hat approximation by comparing the final results obtained using both approaches.

Let us conclude by specifying the conditions, under which our model is compatible with the base assumptions, such as the Born approximation used to derive the Lindblad equation.

First, we must notice, that $\bar{V}_{\text{eff}}(\phi)$ contains the inflationary potential and a correction. To ensure that the new term does not spoil slow-roll inflation, we must make sure the correction is small compared to the original potential. In slow-roll approximation $\bar{V}(\phi) \simeq 3H^2 M_{\text{Pl}}^2$. If we recall the equation (2.127), the requirement, that $\bar{V}(\phi) \gg \frac{\alpha}{4f}\phi\langle F_{\mu\nu}\tilde{F}^{\mu\nu}\rangle_{\text{stat}}$ is equivalent to

$$0.2 \cdot 10^{-4}\frac{\alpha}{f}\phi\frac{H^2}{M_{\text{Pl}}^2}\frac{e^{2\pi\xi}}{\xi^4} \ll 1. \tag{3.161}$$

It is not very clear what this bound entails, however, we can use $\xi = \frac{\alpha M_{\text{Pl}}}{f}\sqrt{\varepsilon/2}$ to rewrite this bound in a clearer form

$$0.2 \cdot 10^{-4}\frac{H^2}{M_{\text{Pl}}^2}\frac{\phi}{M_{\text{Pl}}}\sqrt{\frac{2}{\varepsilon}}\frac{e^{2\pi\xi}}{\xi^3} \ll 1. \tag{3.162}$$

If we assume $\varepsilon = 10^{-3}$ (which is within the current observational bounds, see [73]), from the condition that the backreaction is negligible, (2.130), *at most* $e^{2\pi\xi}\xi^3 = 10^3 M_{\text{Pl}}^2/H^2$. So the largest value the LHS can possibly take is $\mathcal{O}(1)\phi/M_{\text{Pl}}$. This translates to

$$\frac{\phi}{M_{\text{Pl}}} \ll 1. \tag{3.163}$$

Whether this bound is satisfied or not will depend solely on the specific value of ϕ in a given model. In large field models, this bound is manifestly violated, however small-field models would comply

with this bound.

The second requirement is that the interaction term must not affect the environment much. In terms of the action (3.146), the condition reads

$$\frac{\alpha}{f}\phi F_{\mu\nu}\tilde{F}^{\mu\nu} \ll F_{\mu\nu}F^{\mu\nu}. \tag{3.164}$$

If we use the mean field approximation, using equations (2.127) and (2.128) we obtain

$$\frac{\alpha}{f}\phi \ll 0.58. \tag{3.165}$$

While this bound suggests a small value of the coupling α/f, again, this depends on the specific value of ϕ in a given model. Using (3.156) we can also rewrite this inequality in the following manner

$$\xi\frac{\phi}{M_{\rm Pl}} \ll 0.38\sqrt{\varepsilon}. \tag{3.166}$$

In large-field models of inflation, where ϕ can take values $\gtrsim M_{\rm Pl}$, this bound requires a very small value of ξ. Hence, we can only use the Lindblad formalism in case we have a small field model, where $\phi \ll M_{\rm Pl}$.

3.5.1 Power Spectrum in the Lindblad Formalism

In this section, we compute the power spectrum using the Lindblad formalism, which we compare to the standard results (e.g., ref [27]). We do this in two different ways: *i*) we use the complete form of the environment correlation function (3.154) and obtain the power spectrum numerically, *ii*) we approximate the environment correlator using a top-hat ansatz (3.159) and proceed analytically.

In Appendix E, we use the top-hat anzats ($C_R \propto \Theta(\tau/\tau_c)$) to compute the correction to the power-spectrum analytically. We rewrite equation (E.23) as

$$\begin{aligned}\Delta P_{\mathbf{k}} = \frac{\mathcal{J}_{\mathbf{k}}}{|v_{\mathbf{k}}|^2} = -\sqrt{\frac{2}{\pi}}\frac{367e^{4\pi\xi}}{32}\left(\frac{H}{M_{\rm Pl}}\right)^2\frac{2\xi}{\varepsilon}\left(\frac{k}{k_*}\right)^{-3\varepsilon}\frac{1}{\beta}\Gamma^2(1-\nu)\frac{\sin^2(\pi\nu)}{\pi^2\nu^2}\times \\ \left\{\frac{1}{4^\nu(1-\alpha+2\nu)}\left[(\beta\xi)^{(\varepsilon-1)(1+\alpha+2\nu)} - \left(\frac{k}{k_*}\right)^{1+\alpha+2\nu}\exp\left[-(N-N_*)\frac{1+\alpha+2\nu}{1+\varepsilon}\right]\right]\right. \\ + \frac{2^{-4\nu}(-k\tau)^{4\nu}}{4^{-\nu}(1-\alpha-2\nu)}\left[(\beta\xi)^{(\varepsilon-1)(1+\alpha-2\nu)} - \left(\frac{k}{k_*}\right)^{1+\alpha-2\nu}\exp\left[-(N-N_*)\frac{1+\alpha-2\nu}{1+\varepsilon}\right]\right] \\ \left. - 2\frac{2^{-2\nu}(-k\tau)^{2\nu}}{1+\alpha}\left[(\beta\xi)^{(\varepsilon-1)(1+\alpha)} - \left(\frac{k}{k_*}\right)^{1+\alpha}\exp\left[-(N-N_*)\frac{1+\alpha}{1+\varepsilon}\right]\right]\right\},\end{aligned} \tag{3.167}$$

where we have used the equation (E.13) and

$$-k\tau = \left(\frac{-k\tau}{-k_*\tau_*}\right)(-k_*\tau_*) \simeq \left(\frac{k}{k_*}\right)\left(\frac{a}{a_*}\right)^{-\frac{1}{1+\varepsilon}} = \left(\frac{k}{k_*}\right)e^{-\frac{1}{1+\varepsilon}(N-N_*)}, \tag{3.168}$$

where $N - N_*$ is the number of e-folds passed since a pivot scale k_* crossed the Hubble radius. The time domain that we are interested in is when $N > N_*$[20]. The time-dependent part in Eq. (3.167) gets exponentially suppressed and the correction to the power spectrum is effectively constant in time. In this limit, it is clear, that the second term in Eq. (3.167) dominates the rest. Note also, that this expression was obtained after taking two important approximations: First, since we are interested in superhorizon scales, $-k\tau \ll 1$. Second, since we are interested in $\xi \geq \mathcal{O}(1)$, then by our identification of the conformal correlation time $\tau_c = (\beta\xi k)^{-1}$, it is clear, that $-k\tau_c \ll 1$.

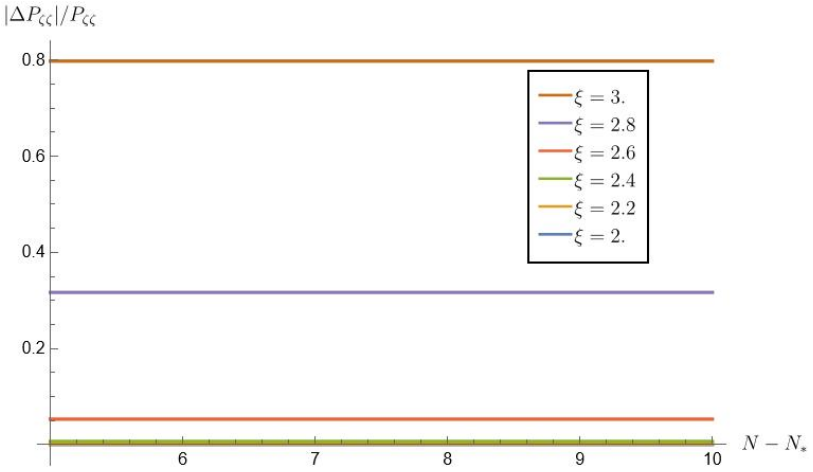

Figure 10: time dependence of the relative difference between the top-hat result (3.167) for the power spectrum using the Lindblad formalism and the standard result (2.153) is depicted for different values of ξ. The time dependence becomes negligible as one approaches $N > N_*$ as expected. This plot is obtained for $k = k_*$, $\mathcal{P} = 2.1 \times 10^{-9}$, $\varepsilon = 10^{-3}$, $\eta = 2 \times 10^{-2}$ and $H/M_{\rm Pl} = 10^{-5}$.

In ref. [27] they have derived the correction to the power spectrum due to the presence of the gauge fields in axion inflation (see Sec. 2.5). A comparison of the latter with our results is depicted in Fig 10, where the y-axis is the relative difference $|\Delta P_{\zeta\zeta}|/P_{\zeta\zeta}$ (notice $\Delta P_{\zeta\zeta}$ is the difference between the power spectrum obtained in this thesis and the power spectrum in ref [27], not to be mistaken with $\Delta P_{\mathbf{k}}$ defined in (3.90)) and the x-axis corresponds to $N - N_*$. It is clear, that, at least when considering the top-hat approximation of the gauge field correlation function, as ξ increases, the relative error $|\Delta P_{\zeta\zeta}|/P_{\zeta\zeta}$ between the two results increases. In particular, the relative difference crosses the 10% threshold at $\xi = 2.63$ (see also Fig. 11) and reaches as much as 80% near $\xi = 3$.

This naturally prompts us to check what happens if we do not use the top-hat approximation

[20]Note, that we cannot treat the regime $N < N_*$, since in that case, the second term in each line of Eq. (3.167) becomes larger than the first one, which is forbidden since we are using the top-hat ansatz that imposes a cutoff (see how the boundaries of the integrals (E.11)-(E.12) were obtained) and we need $-k\tau \ll 1$.

and use equation (3.154) instead. We may proceed by plugging it into (3.82):

$$\mathcal{J}_{\mathbf{k}}(\tau) = \frac{\delta^{(3)}(\mathbf{k}+\mathbf{k}')}{4}\frac{k^5}{(2\pi)^{3/2}}e^{4\pi\xi}\int_{-\infty}^{\tau} d\tau'\gamma(\tau')\mathrm{Im}^2\{v_{\mathbf{k}}(\tau')v^*_{\mathbf{k}}(\tau)\}\times$$
$$\times\int d^3p\left|1+\frac{|\mathbf{p}|^2-\hat{z}\cdot\mathbf{p}}{|\mathbf{p}||\hat{z}-\mathbf{p}|}\right|^2|\mathbf{p}|^2\left(1+\frac{|\hat{z}-\mathbf{p}|^{1/2}}{|\mathbf{p}|^{1/2}}\right)e^{-\sqrt{\kappa}\left(\sqrt{|\mathbf{p}|}+\sqrt{|\hat{z}-\mathbf{p}|}\right)}. \tag{3.169}$$

In Appendix E, we have derived an expression for $\mathcal{J}_{\mathbf{k}}$, (E.25), similar to the top-hat approximation. The correction to the power spectrum can obtained by dividing this expression by $|v_{\mathbf{k}}|^2$. The resulting power spectrum is compared to (2.153) in figure 11. This plot suggests, that even though the relative difference is quite large in both cases for $\xi \gtrsim 2.7$, using the full integral form of the environment correlator slightly alleviates the tension between our results and the standard power spectrum available in the literature.

We note, however, that this does not yet mean, that our approach is unreliable for $\xi > 2.7$, since in order to derive equation (2.153), a series of approximations were used, so we are practically comparing approximations, that are bound to have error-bars.

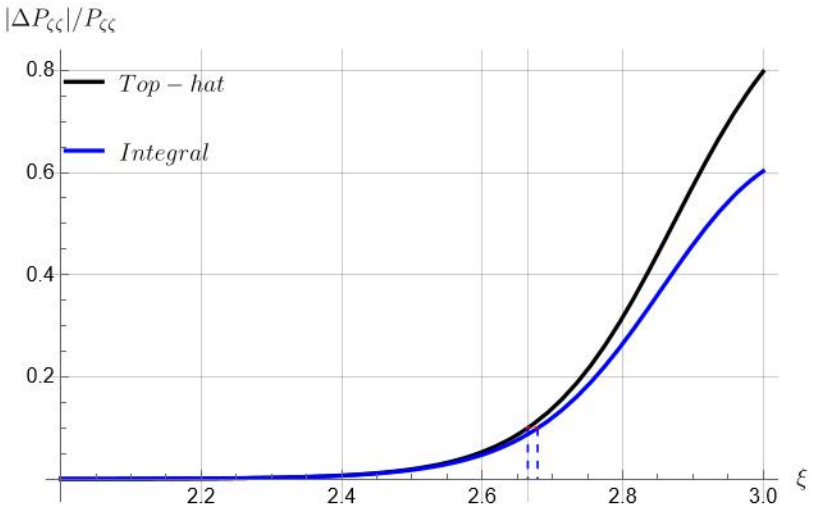

Figure 11: The power spectrum derived using the integral (blue) and the top-hat(black) forms are compared to the power spectrum in [27]. The dashed lines correspond to the 10% error threshold, which are very close. This plot is obtained for $k = k_*$, $\mathcal{P} = 2.1\times10^{-9}$, $\varepsilon = 10^{-3}$, $\eta = 1-0.96-2\varepsilon$ and $H/M_{\mathrm{Pl}} = 10^{-5}$.

Alternative derivation. We notice, that the integrals $\mathcal{J}_{\mathbf{k}}$ and (2.143) are quite similar, therefore, we may follow along the same line and derive the correction using the same approximations as in [27]. This will allow us to put the Lindblad formalism to the test more rigorously.

As we have done in section 2.5.4, we write

$$v_{\mathbf{k}}(\tau) = i\sqrt{\frac{\pi}{4k}}\sqrt{-k\tau}H^{(1)}_{\nu}(-k\tau), \tag{3.170}$$

where $H_\nu^{(1)}$ is the Hankel function of the first kind. We are interested in the late-time power spectrum when $-k\tau \to 0$[21]. In this approximation

$$v_{\mathbf{k}}(\tau) = \frac{1}{\sqrt{2}}\frac{aH}{k^{3/2}}(-k\tau)^{\frac{n_s-1}{2}}. \tag{3.171}$$

We can rewrite equation (3.169):

$$\mathcal{J}_{\mathbf{k}}(\tau) = \frac{\delta^{(3)}(\mathbf{k}+\mathbf{k}')}{4}\frac{k^5}{(2\pi)^{3/2}}e^{4\pi\xi}\int d^3p \left|1+\frac{|\mathbf{p}|^2-\hat{z}\cdot\mathbf{p}}{|\mathbf{p}||\hat{z}-\mathbf{p}|}\right|^2 |\mathbf{p}|^2\left(1+\frac{|\hat{z}-\mathbf{p}|^{1/2}}{|\mathbf{p}|^{1/2}}\right) I(\xi,|\mathbf{p}|,|\hat{z}-\mathbf{p}|), \tag{3.172}$$

where we have defined

$$I(\xi,|\mathbf{p}|,|\hat{z}-\mathbf{p}|) \equiv \int_{-\infty}^{\tau} d\tau'\gamma(\tau')\mathrm{Im}^2\{v_{\mathbf{k}}(\tau')v_{\mathbf{k}}^*(\tau)\}e^{-\sqrt{\kappa}(\sqrt{|\mathbf{p}|}+\sqrt{|\hat{z}+\mathbf{p}|})}. \tag{3.173}$$

Recall that in our model the factor $\gamma(\tau)$ is given by (C.40)

$$\gamma(\tau) = \frac{2\alpha^2 t_c}{f^2 a^3}. \tag{3.174}$$

Using this equation with (3.171), we get

$$I(\xi,|\mathbf{p}|,|\hat{z}-\mathbf{p}|) \simeq \frac{\alpha^2 t_c}{f^2}\frac{a^2(\tau)H^2}{k^3}(-k\tau)^{n_s-1}\times \\ \times\int_{-\infty}^{\tau} d\tau' a^{-3}(\tau')\mathrm{Im}^2\{v_{\mathbf{k}}(\tau')\}e^{-\sqrt{\kappa}(\sqrt{|\mathbf{p}|}+\sqrt{|\hat{z}+\mathbf{p}|})}. \tag{3.175}$$

It is crucial to note that we do not use the approximation (3.171) on $v_{\mathbf{k}}(\tau')$ since τ' is the integration variable. Nevertheless, we may use the complete solution (3.170), leading to

$$I \simeq \frac{\pi\alpha^2 t_c}{4f^2}\frac{a^2(\tau)H^5}{k^3}(-k\tau)^{n_s-1}\int_{-\infty}^{\tau} d\tau'\tau'^4\mathrm{Re}^2\{H_\nu^{(1)}(-k\tau')\}e^{-\sqrt{\kappa}(\sqrt{|\mathbf{p}|}+\sqrt{|\hat{z}+\mathbf{p}|})}. \tag{3.176}$$

Finally, we make a change of variable $x = -k\tau$, leaving us with

$$I \simeq \frac{\pi\alpha^2 t_c}{4f^2}\frac{a^2(\tau)H^5}{k^3}(-k\tau)^{n_s-1}\frac{1}{k^5}\int_{x}^{\infty} dx' x'^4 Re^2\{H_\nu^{(1)}(x')\}e^{-4\sqrt{2\xi}\sqrt{x'}(\sqrt{|\mathbf{p}|}+\sqrt{|\hat{z}-\mathbf{p}|})}. \tag{3.177}$$

Since we are interested only in super-horizon modes, $-k\tau \to 0$, we may set the lower limit of the integral to zero. It is now evident that we can put $\nu = 3/2$, since the slow-roll corrections will not affect the scale dependence, but only the amplitude of the power spectrum by a negligible amount.

[21] Notice that in fact, we have chosen the arbitrary phase such that $v_{\mathbf{k}}(\tau)$ will be real in the limit $-k\tau \ll 1$.

This leads to

$$I \simeq \frac{\alpha^2 t_c}{2f^2}\frac{a^2(\tau)H^5}{k^3}(-k\tau)^{n_s-1}\frac{1}{k^5}\int_0^\infty dx' x'^3\left(\frac{\sin^2(x')}{x'^2}-\frac{\sin(2x')}{x'}+\cos^2(x')\right)\times \\ \times e^{-4\sqrt{2\xi}\sqrt{x'}(\sqrt{|\mathbf{p}|}+\sqrt{|\hat{z}-\mathbf{p}|})}. \quad (3.178)$$

The integral presented here must be carried out numerically, and for future convenience, we denote it simply by $J(4\sqrt{2\xi}(\sqrt{|\mathbf{p}|}+\sqrt{|\hat{z}-\mathbf{p}|})$. We now rewrite the curvature power spectrum as follows

$$P_{\zeta\zeta} = P_{\zeta\zeta}^{\text{standard}}\left(1+\underbrace{2\pi\mathcal{P}f(\xi)e^{4\pi\xi}Ht_c}_{\Delta P_{\mathbf{k}}}\right), \quad (3.179)$$

where

$$f(\xi) = \frac{\xi}{\beta\sqrt{2\pi}}\int d^3p\left|1+\frac{|\mathbf{p}|^2-\hat{z}\cdot\mathbf{p}}{|\mathbf{p}||\hat{z}-\mathbf{p}|}\right|^2|\mathbf{p}|^2\left(1+\frac{|\hat{z}-\mathbf{p}|^{1/2}}{|\mathbf{p}|^{1/2}}\right)J(4\sqrt{2\xi}(\sqrt{|\mathbf{p}|}+\sqrt{|\hat{z}-\mathbf{p}|})). \quad (3.180)$$

Generally, we need to evaluate the integral (3.180) numerically. However, if we consider a large argument for J, which automatically means large ξ, a simplification is reached. Namely, in (3.178), only small values of x will contribute since for larger values the integral goes to zero exponentially. For what follows, we denote the argument of J by u

$$J(u) \simeq \frac{5}{18}\int_0^\infty dx' x'^7 e^{-u\sqrt{x'}}. \quad (3.181)$$

We can simply change the integration variable to $y = x'^{1/4}$ leading to a Gaussian integral

$$J(u) \simeq \frac{10}{9}\int_0^\infty dy y^{31}e^{-uy^2} = \frac{726485760000}{u^{16}}, \qquad u \gg 1. \quad (3.182)$$

Indeed if $\sqrt{|\mathbf{p}|}+\sqrt{|\hat{z}-\mathbf{p}|} \simeq \mathcal{O}(1)$ this approximation holds true for large values of ξ. Then, the rest of the integral can be evaluated numerically and we find

$$f(\xi) \simeq \frac{30}{\xi^6}. \quad (3.183)$$

The regime $2 \leq \xi \leq 3$ is the most interesting regime phenomenologically, so it is interesting to at least have a numerical fit

$$f(\xi) = 0.75\cdot 10^{-4}\xi^{-6.4}, \qquad 2 \leq \xi \leq 3. \quad (3.184)$$

We compare our results to [27] in figure 12. We see that for lower values of ξ the two results are in good agreement. Interestingly, it appears, that the Lindblad formalism starts to fail as we increase ξ as before. In figures 11 and 12 the 10% threshold of validity is crossed at around the same value,

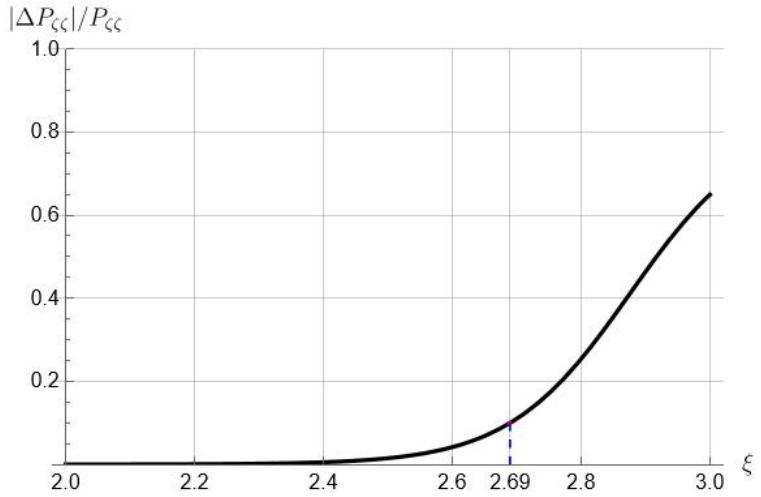

Figure 12: The relative error $|\Delta P_{\zeta\zeta}|/P_{\zeta\zeta}$ between the power spectrum obtained using the Lindblad formalism and the standard one found in the literature (see [27]). The results are in good agreement (below 10 % relative error) for values of ξ from 2 to 2.7, which is marked by the blue dashed line. The plot is evaluated for $\mathcal{P} = 2.1 \times 10^{-9}$.

$\xi \simeq 2.7$. We speculate, that this is because as we increase ξ, we effectively increase the coupling α/f with the environment, as described by Eq. (3.156). The tension arises because in deriving the Lindblad equation, one of the key assumptions is that the coupling between the system and the environment is weak. Hence, if we increase the interaction strength, the environment backreaction becomes important and the Lindblad approximation fails.

3.5.2 Decoherence

We follow the analysis done in Sec. 3.4.7 and apply it to our current construction. Recalling, that the decoherence parameter, at linear order in γ can be written as (3.142)

$$\delta_{\mathbf{k}}(\tau) \simeq |v_{\mathbf{k}}|^2 \mathcal{I}_{\mathbf{k}} + |v'_{\mathbf{k}}|^2 \mathcal{J}_{\mathbf{k}} - |v_{\mathbf{k}}|^{2'} \mathcal{K}_{\mathbf{k}}. \tag{3.185}$$

For axion inflation, Appendix E contains explicit forms of the constituents of this equation. We consider first the top-hat approximation since this leads to an approximate analytical expression that can be interpreted physically.

After many cancellations, in the slow-roll approximation, the resulting expression is

$$\delta_{\mathbf{k}}^{(\text{top-hat})}(\tau) = \frac{367}{16\sqrt{2\pi}} \frac{\xi e^{4\pi\xi}}{\beta \sin^2(\pi\nu)} \left(\frac{H}{M_{\text{Pl}}}\right)^2 \frac{2}{\varepsilon} \left(\frac{k}{k_*}\right)^{-3\varepsilon} \left[I_1(\nu) + I_1(-\nu) - 2I_2(\nu)\cos(\pi\nu)\right], \tag{3.186}$$

where I_1 and I_2 are given by (E.11-E.12). Note, that the integral has a cutoff at $-k\tau_c$ produced by the top-hat form of the environment correlation function. In the limit $-k\tau, -k\tau_c \ll 1$, the integrals I_1 and I_2 is also obtained in Appendix A (E.18-E.19). Through simple analysis, one concludes that among the three terms present in the above equation, the second term ($\propto I_1(-\nu)$) gives the

dominant contribution. This observation allows us to write an approximate analytical expression for the decoherence parameter, yielding

$$\delta_{\mathbf{k}}^{(\text{top-hat})} \simeq \frac{1}{\sqrt{2\pi}} \frac{367 e^{4\pi\xi}}{16 \sin^2(\pi\nu)} \left(\frac{\alpha H}{f}\right)^2 \left(\frac{k}{k_*}\right)^{-3\varepsilon} \times \left\{ \frac{1}{4^{-\nu}(1+\alpha-2\nu)\Gamma^2(1-2\nu)} \left[(\beta\xi)^{(1+\varepsilon)(1+\alpha-2\nu)} - \left(\frac{k}{k_*}\right) e^{-(N-N_*)\left(\frac{1+\alpha-2\nu}{1+\varepsilon}\right)} \right] \right\}. \quad (3.187)$$

This way we can interpret the behavior of the decoherence parameter. According to (3.187), for $N > N_*$ regime, the time dependence of $\delta_{\mathbf{k}}$ quickly becomes negligible due to the exponential suppression. The decoherence parameter reaches a constant value, as seen in the left panel in Fig. 13. We argue, that this is expected since the gauge fields are amplified close to the horizon crossing of a given mode k. This implies, that the scalar perturbations effectively decouple from the environment, hence the purity (see equation (3.143)) of the state remains unaltered.

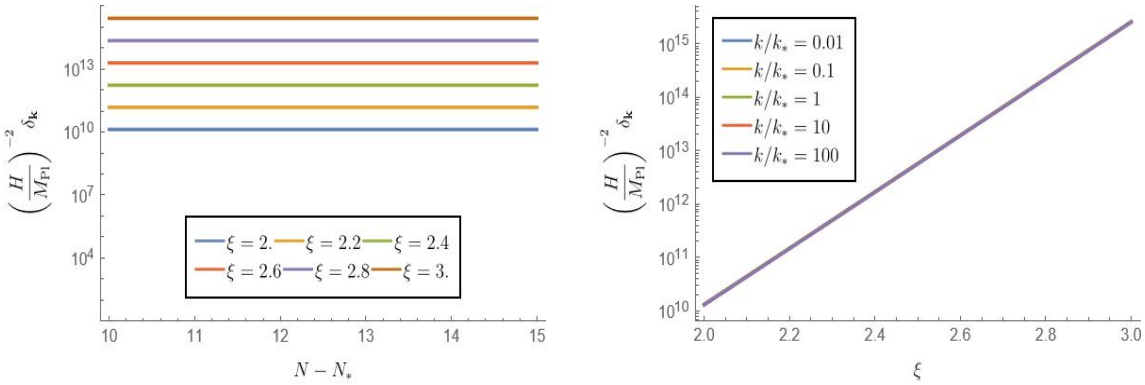

Figure 13: The decoherence parameter (rescaled by $(H/M_{\rm Pl})^{-2}$) is evaluated using the top-hat form of the environment correlation function. In these plots: (left) the decoherence parameter is plotted as a function of time (here number of e-folds) for given values of the parameter ξ for $k = k_*$. (right) Decoherence parameter is plotted against the parameter ξ for $N - N_* = 15$ for various values of k/k_*.

Next, we use the integral form of the environment correlation function (3.154). Using the expressions (E.24-E.26) we may construct the decoherence parameter similar to (3.186)

$$\delta_{\mathbf{k}}^{(\text{integral})}(\tau) = \frac{1}{16\sqrt{2\pi}} \frac{\xi e^{4\pi\xi}}{\beta \sin^2(\pi\nu)} \left(\frac{H}{M_{\rm Pl}}\right)^2 \frac{2}{\varepsilon} \left(\frac{k}{k_*}\right)^{-3\varepsilon} \left[F_1(\nu) + F_1(-\nu) - 2F_2(\nu)\cos(\pi\nu)\right], \quad (3.188)$$

where F_1 and F_2 are defined in Appendix E, Eqs. (E.27)-(E.28). We produce a fit for these functions that read

$$F_1(\nu) = 1.15 \cdot 10^{-6} \cdot \xi^{-0.57} \qquad F_1(-\nu) = 312 \cdot \xi^{-0.51} \qquad F_2(\nu) = -9.76 \cdot 10^{-5} \cdot \xi^{-0.41}. \quad (3.189)$$

The result, which we deem as more reliable compared to the previous one, is plotted in figure 14. The values of the decoherence parameter are shifted compared to the top-hat case by $\sim 10^3 \div 10^4$.

This result shows a more critical difference between the two approaches.

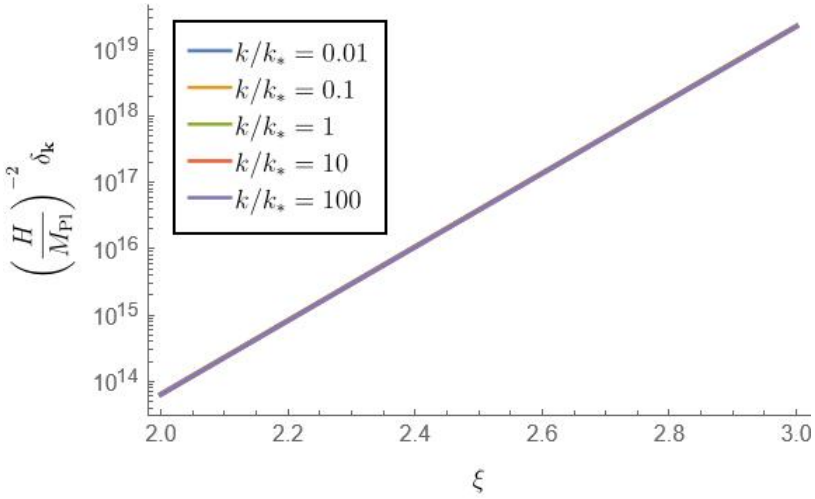

Figure 14: The decoherence parameter (rescaled by $(H/M_{\rm Pl})^{-2}$) evaluated using the integral form of the environment correlation function for various values of k/k_*. The result is practically scale-independent as the lines on the plot are indistinguishable. To obtain the plot, we have fixed $\varepsilon = 10^{-3}$ and $\eta = 1 - 0.96 - 2\varepsilon$.

In order to reach successful decoherence we require $\mathrm{Tr}\{\hat{\rho}_{\mathbf{k}}^{(s)2}\} \ll 1$, or equivalently $\delta_{\mathbf{k}} \gg 1$. We compare this result to observational constraints. According to [73] the upper bound on the energy scale of inflation is equivalent to an upper bound $H < 2.5 \times 10^{-5} M_{\rm Pl}$, or equivalently $M_{\rm Pl}^2/H^2 > 6.25 \times 10^{10}$. The top hat approach (Fig. 13) results in a saturation of this bound for values $\xi \approx 2$, leading to largely incomplete decoherence. On the other hand, using the integral form of the gauge field correlation function allows for a large amount of decoherence for all values $2 < \xi < 3$. This shows, that in our case the top-hat approximation should be taken with a grain of salt since it can lead to dangerous conclusions.

3.5.3 Accounting for the scale dependence of ξ

As we have noted before, ξ is not really a constant during inflation, in fact, it is expected to increase as inflation proceeds. This is because the value of $\dot{\phi}$ increases and H decreases (for a detailed work utilizing this effect see e.g. [74, 75]). On the other hand, this means that ξ also depends on scale. The specific form of the dependence is given by [76]

$$\xi = \xi_* \left[1 + \frac{\eta_*}{2} \log\left(\frac{k}{k_*}\right)\right], \tag{3.190}$$

where ξ_* is the value taken when the pivot scale ($k_* = 0.05$ Mpc^{-1}) crosses the horizon. The current upper bound is $\xi_* \leq 2.3$ [17]. Even though the dependence appears to be weak, we would like to know how this affects both the power spectrum and the decoherence parameter.

The results are presented in Fig. 15. On the left side we see, the relative difference between our results and (2.153). Notice, that for both the top-hat approximation and the integral form the

relative difference starts to deviate (meaningfully) from 0 around $k \approx k_*$. The increasing relative error is consistent with the previous result, since large k corresponds to large ξ. The two curves closely follow each other, but at small scales (large k) the difference between the two approaches is more pronounced.

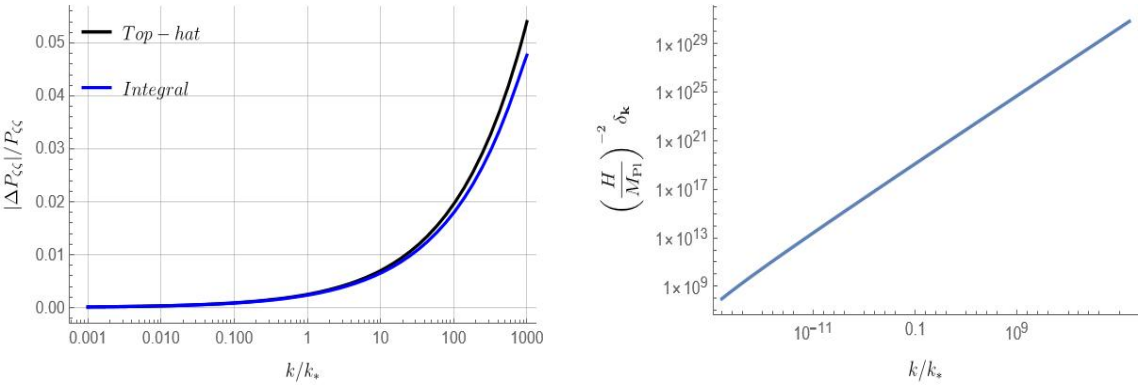

Figure 15: (Left) Power spectrum, evaluated by using Eq. (3.190) is compared to (2.153). (Right) The decoherence parameter (rescaled by $H^2/M_{\rm Pl}^2$) is obtained likewise for very large and very small scales. The plots are obtained for $\varepsilon = 10^{-3}$, $\eta = 1 - 0.96 - 2\varepsilon$, $\mathcal{P} = 2.1 \cdot 10^{-9}$ and for the power spectrum we have fixed $H^2/M_{\rm Pl}^2$.

On the right side we have evaluated the decoherence parameter on scales ranging from very large to very small. To do this, however, we made a new fit for the correlation function, since restricting to $2 < \xi < 3$ does not produce any meaningful results[22]. Instead, we considered a larger interval to encompass all the scales ($0.1 \leq \xi \leq 8$). We see that as we move to larger scales, decoherence gets weaker. While the large values of ξ are arguably inconsistent with the Born-Markov approximations, it is still interesting to see which scales do not decohere according to our prescription. The observational bounds on the Hubble parameter during inflation ($M_{\rm Pl}^2/H^2 > 6.25 \cdot 10^{10}$) suggests, that at very large scales, $k/k_* \lesssim 10^{-15}$, decoherence is insufficient.

This is expected in our construction since as ξ increases with scale k, the interaction strength effectively becomes larger, increasing the effect of decoherence on smaller scales. So the correlation structure is such, that there are quantum correlations on large scales that are less affected by decoherence, while smaller scales suffer larger decoherence.

Another important point is that the region of insufficient decoherence is well outside the observable scales, meaning, that, for example, for the scales probed on the CMB decoherence is complete.

Notice that we have evaluated the power spectrum near the end of inflation, but we also used $\varepsilon \ll 1$, which may be a gross oversimplification, since the end of inflation is characterized by the slow-roll parameters becoming $\mathcal{O}(1)$, so the scale dependence may be more significant, however for the scope of this thesis, we neglect the evolution of ε.

[22] Importantly when making a new fit, we also change the correlation time by a numerical factor. For values $0.1 \leq \xi < 8$, which we have used for the fit the physical correlation time is $t_c = (0.35 \cdot 2^5 \xi H)^{-1}$. One can easily verify that for the mentioned values of ξ, the $t_c < H^{-1}$ still holds.

4 Traces of "Quantumness" from the Early Universe

In this section, we overview the challenges associated with differentiating between classical and quantum correlations from the early universe. We introduce the cosmological Bell inequalities following [8] where we conclude that any violation of the Bell inequalities is likely unattainable from data.

We then connect the Bell inequalities with other measures of quantum correlations such as quantum discord and state-separability [77].

Finally, we expand on the quantum discord and calculate it for the case of axion inflation.

4.1 CMB Bell inequalities

As we have seen in Sec. 2.4 the initial quantum fluctuations are placed in the *squeezed state* at the end of inflation. These states are highly entangled and therefore, highly non-classical. One draws the conclusion, that, at least if the inflationary mechanism truly describes the physical reality of the early universe, the correlations observed on the CMB must be characterized by the quantum theory. However, it has been shown (see, e.g. [49]) that at the level of the power spectrum (or the curvature two-point function $\langle\hat{\zeta}(\tau,\mathbf{x})\hat{\zeta}(\tau,\mathbf{y})\rangle$), the classical stochastic theory works just as well. In the same reference, it was found, that due to the fact that the quantum state is highly discordant, the correlation functions $\langle\hat{\zeta}(\tau,\mathbf{x})\hat{\zeta}'(\tau,\mathbf{y}) + \hat{\zeta}(\tau,\mathbf{x})\hat{\zeta}(\tau,\mathbf{y})\rangle$ and $\langle\hat{\zeta}'(\tau,\mathbf{x})\hat{\zeta}'(\tau,\mathbf{y})\rangle$ deviate from their classical counterparts significantly.

The measurement of quantum entanglement of the inflationary squeezed state has been done using the quantum discord [49], and the resulting discord reads

$$\delta(\mathbf{k},-\mathbf{k}) = \cosh^2 r_k \log_2(\cosh^2 r_k) - \sinh^2 r_k \log_2(\sinh^2 r_k) \simeq \frac{2}{\ln 2} r_k - 2\frac{1}{\ln 2} + \mathcal{O}(e^{-2r_k}). \tag{4.1}$$

So large squeezing corresponds to large quantum discord which means the quantum correlations become more pronounced.

The difficulty in measuring any quantum signatures from the early universe is also due to the fact, that the quantum mechanical phase space of cosmic perturbations is made up of two non-commuting variables - the growing ($\hat{\zeta}$) and the decaying mode ($\hat{\zeta}'$). As the name suggests, one of the modes rapidly decays, making any attempts to measure quantities related to its amplitude, such as the correlators defined above, hopeless. So according to the standard scenario, we cannot measure "quantumness" using the commutator of the phase space variables[23].

Yet, there are reasons to establish Bell CMB experiments [78, 79]. Specifically, we note the three most obvious reasons

- The validity of the statement that observing the decaying mode amplitude is hopeless is vague, in the sense, that we would like to assess how severe this problem is when establishing Bell experiments;

[23] Although, it should be noted, that higher order correlators, such as the four-point correlation function cannot be reproduced by any classical state, even at the level of the growing mode.

- The power spectrum measures correlations for a single wavenumber $\mathbf{k}$, while typically in Bell experiments include modes $\mathbf{k}$ *and* $-\mathbf{k}$;
- In non-minimal cases the decaying mode can be accessible [79, 80].

As we shall see, the Bell inequalities are violated, even when one mode decays.

The key question is, how do we extract Bell inequalities from CMB observations? and can it even be done in practice?

4.1.1 CMB Bell experiment with pseudo-spin operators

Let us first write down the Hamiltonian for the scalar perturbations

$$\hat{H} = \int_{\mathbb{R}^3} d^3\mathbf{k} \left[\frac{k}{2} \left(\hat{c}_{\mathbf{k}} \hat{c}^{\dagger}_{\mathbf{k}} + \hat{c}_{-\mathbf{k}} \hat{c}^{\dagger}_{-\mathbf{k}} \right) - \frac{i}{2} \frac{z'}{z} \left(\hat{c}_{\mathbf{k}} \hat{c}_{-\mathbf{k}} - \hat{c}^{\dagger}_{-\mathbf{k}} \hat{c}^{\dagger}_{\mathbf{k}} \right) \right], \tag{4.2}$$

where $\hat{c}$ and $\hat{c}^{\dagger}$ are the annihilation and the creation operators respectively. They satisfy $[\hat{c}_{\mathbf{k}}, \hat{c}^{\dagger}_{\mathbf{p}}] = \delta(\mathbf{k} - \mathbf{p})$. $z \equiv aM_{\rm Pl}\sqrt{2\varepsilon}$, as before. The creation and annihilation operators are related to the curvature perturbations $\hat{\zeta}_{\mathbf{k}}$ through $\hat{v}_{\mathbf{k}} = (\hat{c}_{\mathbf{k}} + c_{-\mathbf{k}})/\sqrt{2k}$ and $\hat{p}_{\mathbf{k}} = -i\sqrt{k/2}(\hat{c}_{\mathbf{k}} - \hat{c}^{\dagger}_{-\mathbf{k}})$ by $\hat{\zeta}_{\mathbf{k}} = \hat{v}_{\mathbf{k}}/z$ and $\hat{\zeta}'_{\mathbf{k}} = \hat{p}_{\mathbf{k}}/z$. We can now introduce the quantities $\hat{q}_{\mathbf{k}} = (\hat{c}_{\mathbf{k}} + \hat{c}^{\dagger}_{\mathbf{k}})/\sqrt{2k}$ and $\hat{\pi}_{\mathbf{k}} = -i\sqrt{k/2}(\hat{c}_{\mathbf{k}} - \hat{c}^{\dagger}_{\mathbf{k}})$, which are advantageous in the sense, that they do not mix $\mathbf{k}$ modes with $-\mathbf{k}$ modes like $\hat{\zeta}$. One may look at them as the position and the momentum at the scale $\mathbf{k}$.

Typically, when constructing the Bell experiment, one deals with discrete variables, however, $\hat{\zeta}$, or the Mukhanov-Sasaki operator $\hat{v}$, are complex variables, with continuous spectra. To apply the concepts of Bell experiments in this case, one can define the *pseudos-spin operators*.

Banaszek-Wodkiewitz pseudo-spin operators [81]. One possible way is by defining the following operators

$$\hat{s}_x(\mathbf{k}) = \sum_{n=0}^{\infty} \left(|2n_{\mathbf{k}} + 1\rangle \langle 2n_{\mathbf{k}}| + |2n_{\mathbf{k}}\rangle \langle 2n_{\mathbf{k}} + 1| \right) \tag{4.3}$$

$$\hat{s}_y(\mathbf{k}) = \sum_{n=0}^{\infty} \left(|2n_{\mathbf{k}}\rangle \langle 2n_{\mathbf{k}} + 1| - |2n_{\mathbf{k}} + 1\rangle \langle 2n_{\mathbf{k}}| \right) \tag{4.4}$$

$$\hat{s}_z(\mathbf{k}) = \sum_{n=0}^{\infty} \left(|2n_{\mathbf{k}} + 1\rangle \langle 2n_{\mathbf{k}} + 1| - |2n_{\mathbf{k}}\rangle \langle 2n_{\mathbf{k}}| \right) \tag{4.5}$$

and similar expressions for $-\mathbf{k}$. The states $|n_{\mathbf{k}}\rangle$ are the eigenvectors of the particle number operator. These operators satisfy the usual $SU(2)$ commutation relations, and if one defines $\mathbf{n} = (\sin\theta_n \cos\phi_n, \sin\theta_n \sin\phi_n, \cos\theta_n)$, one gets $(\mathbf{n} \cdot \hat{\mathbf{s}})^2 = \hat{\mathbb{I}}$, so that the outcome of the Hermitian operator $\mathbf{n} \cdot \hat{\mathbf{s}}$ is ± 1. From this point, it is possible to proceed with analogy with the standard way of constructing the Bell inequality [8]. The Bell operator in this construction is

$$\hat{\mathcal{B}}(\mathbf{k}, -\mathbf{k}) = \mathbf{n}\cdot\hat{\mathbf{s}}(\mathbf{k}) \otimes \mathbf{m}\cdot\hat{\mathbf{s}}(-\mathbf{k}) + \mathbf{n}\cdot\hat{\mathbf{s}}(\mathbf{k}) \otimes \mathbf{m}'\cdot\hat{\mathbf{s}}(-\mathbf{k}) + \mathbf{n}'\cdot\hat{\mathbf{s}}(\mathbf{k}) \otimes \mathbf{m}\cdot\hat{\mathbf{s}}(-\mathbf{k}) - \mathbf{n}'\cdot\hat{\mathbf{s}}(\mathbf{k}) \otimes \mathbf{m}'\cdot\hat{\mathbf{s}}(-\mathbf{k}), \tag{4.6}$$

where $\mathbf{n}'$, $\mathbf{m}$, and $\mathbf{m}'$ are also unit vectors. Then taking the mean value of $\hat{\mathcal{B}}$ in the two-mode squeezed state, one obtains

$$\langle 2MSS|\hat{\mathcal{B}}(\mathbf{k},-\mathbf{k})|2MSS\rangle = 2\sqrt{\langle 2MSS|\,\hat{s}_z(\mathbf{k})\otimes\hat{s}_z(-\mathbf{k})\,|2MSS\rangle^2 + \langle 2MSS|\,\hat{s}_x(\mathbf{k})\otimes\hat{s}_x(-\mathbf{k})\,|2MSS\rangle^2}. \tag{4.7}$$

where $|2MSS\rangle$ is the two-mode squeezed state and can be written as

$$|2MSS\rangle = \frac{1}{\cosh r_k}\sum_{n=0}^{\infty} e^{-2in\varphi_k}\tanh^n r_k\,|n_{\mathbf{k}}, n_{-\mathbf{k}}\rangle \tag{4.8}$$

and one can easily check that Eq. (4.7) can be written as

$$\langle 2MSS|\hat{\mathcal{B}}(\mathbf{k},-\mathbf{k})|2MSS\rangle = 2\sqrt{1+\tanh(2r_k)\cos(2\varphi_k)}. \tag{4.9}$$

On superhorizon scales $r_k \to \infty$ and $\varphi_k \to -\pi/2$. Hence $\langle 2MSS|\hat{\mathcal{B}}(\mathbf{k},-\mathbf{k})|2MSS\rangle \to 2\sqrt{2}$, which means the Bell inequality is violated. This is known as the Cirel'son bound and it represents the maximal value the Bell operator can take. As expected from the large discord, the CMB is placed in a highly quantum state that maximally violates the Bell inequality.

Gour-Khanna-Mann-Revzen pseudo-spin operators [82, 83]. The choice of the pseudo-spin operators is not unique. Cosmological Bell inequalities can be studied using the GKMR operators. To see this, let us define

$$|\mathcal{E}_{\mathbf{k}}\rangle = \frac{1}{\sqrt{2}}\left(|q_{\mathbf{k}}\rangle + |-q_{\mathbf{k}}\rangle\right), \tag{4.10}$$

$$|\mathcal{O}_{\mathbf{k}}\rangle = \frac{1}{\sqrt{2}}\left(|q_{\mathbf{k}}\rangle - |-q_{\mathbf{k}}\rangle\right). \tag{4.11}$$

Using these we can construct

$$\hat{S}_x = \int_0^{\infty} dq_{\mathbf{k}}\left(|\mathcal{E}_{\mathbf{k}}\rangle\langle\mathcal{O}_{\mathbf{k}}| + |\mathcal{O}_{\mathbf{k}}\rangle\langle\mathcal{O}_{\mathbf{k}}|\right), \tag{4.12}$$

$$\hat{S}_y = i\int_0^{\infty} dq_{\mathbf{k}}\left(|\mathcal{O}_{\mathbf{k}}\rangle\langle\mathcal{E}_{\mathbf{k}}| - |\mathcal{E}_{\mathbf{k}}\rangle\langle\mathcal{O}_{\mathbf{k}}|\right), \tag{4.13}$$

$$\hat{S}_z = -\int_0^{\infty} dq_{\mathbf{k}}\left(|\mathcal{E}_{\mathbf{k}}\rangle\langle\mathcal{E}_{\mathbf{k}}| - |\mathcal{O}_{\mathbf{k}}\rangle\langle\mathcal{O}_{\mathbf{k}}|\right). \tag{4.14}$$

When constructing the Bell operator, one obtains the same equation (4.7) with $\langle 2MSS|\hat{S}_z(\mathbf{k})\otimes\hat{S}_z(-\mathbf{k})|2MSS\rangle = 1$ and a more complicated form for the second term

$$\langle 2MSS|\,\hat{S}_x(\mathbf{k})\hat{S}_x(-\mathbf{k})\,|2MSS\rangle = \frac{2}{\pi}\arctan\left[\frac{2\tanh(r_k)\cos(2\varphi_k)}{\sqrt{\tanh^4(r_k) - 2\tanh^2(r_k)\cos(4\varphi_k)+1}}\right]. \tag{4.15}$$

In Fig. 16 it is clear, that for various values of φ_k, the Bell inequality violation is slightly weaker

than the BW case. On superhorizon scales again, we have $r_k \to \infty$ and $\phi_k \to -\pi/2$, which leads again to the saturation of the Cirel'son bound, $\langle 2MSS|\, \hat{\mathcal{B}}_{\rm GKMR}(\mathbf{k}, -\mathbf{k})\, |2MSS\rangle \to 2\sqrt{2}$.

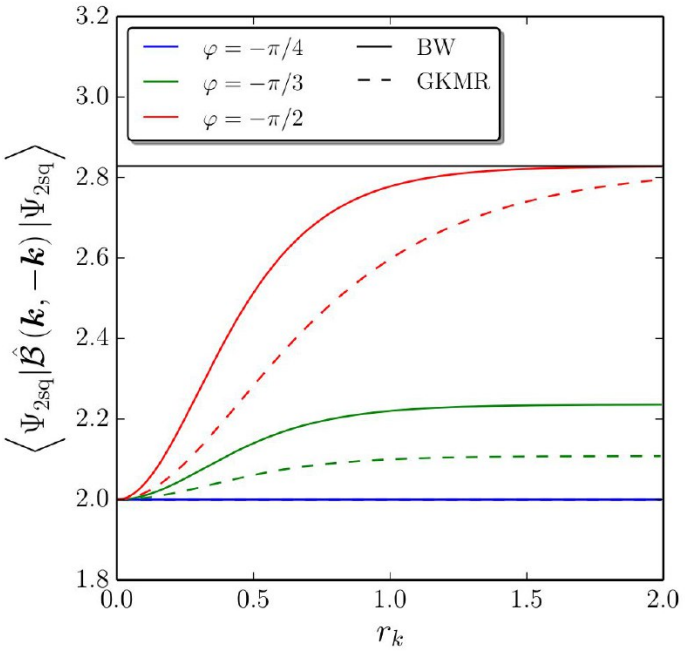

Figure 16: Mean value of the Bell operator using the BW pseudo-spin operators (solid lines) and the GKMR operators (dashed lines) as a function of the squeezing parameter for various values of φ_k. The horizontal blue line corresponds to $\varphi_k = -\pi/4$ since in both BW and GKMR case the second term in (4.7) vanishes. The black horizontal line corresponds to the Cirel'son bound.

In Ref. [8] another possibility is discussed using the Larson spin operators which we do not discuss here.

4.1.2 Can we measure the pseudo-spin operators?

The answer to this question is probably no and here's why. Let us consider the temperature anisotropy operator

$$\frac{\widehat{\delta T}}{T}(\theta, \phi) = \sum_{l=2}^{\infty} \sum_{m=-l}^{m=l} \hat{a}_{lm} Y_{lm}(\theta, \phi), \tag{4.16}$$

which is an observable. Here $\hat{a}_{lm}$ is are non-Hermitian operators. We can connect the temperature anisotropies with the curvature operator $\hat{\zeta}_{\mathbf{k}}$ by utilizing the Sachs-Wolfe effect

$$\frac{\delta T}{T}(\mathbf{e}) = \int \frac{d\mathbf{k}}{(2\pi)^{3/2}} \left[F(\mathbf{k}) + i\mathbf{k}\cdot\mathbf{e}G(\mathbf{k})\right] e^{-i\mathbf{k}\cdot\mathbf{e}(\tau_{\rm ss}-\tau_0)+i\mathbf{k}\cdot\mathbf{x}_0}, \tag{4.17}$$

where F and G are the form factors that track the post-inflationary evolution of the perturbations. Importantly, the form factors are proportional to $\hat{\zeta}_{\mathbf{k}}(\tau_{\rm end})$ evaluated at the end of inflation:

$$\frac{\delta T}{T}(\mathbf{e}) = \int \frac{d\mathbf{k}}{(2\pi)^{3/2}} \left[F(\mathbf{k}) + i\mathbf{k}\cdot\mathbf{e}G(\mathbf{k})\right] \hat{\zeta}_{\mathbf{k}}(\tau_{\rm end}) e^{-i\mathbf{k}\cdot\mathbf{e}(\tau_{\rm lss}-\tau_0)+i\mathbf{k}\cdot\mathbf{x}_0}. \tag{4.18}$$

The operators $\widehat{\delta T}/T(\mathbf{e})$ and $\widehat{\delta T}/T(\mathbf{e}')$ will commute, since $\left[\hat{\zeta}_{\mathbf{k}}, \hat{\zeta}_{\mathbf{p}}\right] = 0$[24].

Let us now construct the position operator using the curvature perturbations. This can easily be done and leads to

$$\hat{q}_{\mathbf{k}} = \frac{z}{2}\left(\hat{\zeta}_{\mathbf{k}} + \hat{\zeta}_{-\mathbf{k}}\right) + \frac{z}{2k}\left(\zeta'_{\mathbf{k}} - \zeta'_{-\mathbf{k}}\right). \tag{4.19}$$

So the knowledge of $\hat{\zeta}$ is not sufficient to understand $\hat{q}$. However, we can neglect the decaying mode, so that the measurement of $\hat{\zeta}$ translates to the measurement of $\hat{q}$. If we have measured $\hat{q}$, then it is possible to measure the spin operators only if they commute with $\hat{q}$, since in cosmology unlike in the lab situations, we cannot perform a new measurement, so any operator that does not commute with $\hat{q}$ cannot be measured. This is exactly the case for all the considered spin operators. Namely, at least two of the spin operators do not commute with $\hat{q}$, rendering measurements of Bell inequalities impossible.

Hence, we conclude, that measuring the pseudo-spin operator is probably not possible due mostly to the nature of the experiment in cosmology, which cannot be repeated.

4.2 Comparing different measures of quantumness

As mentioned before, Bell inequalities are not the only measures of "quantumness". Any genuine quantum signatures of inflationary fluctuations can significantly improve our understanding of fundamental issues, like the need to quantize gravity or how exactly classicality emerges [6, 8].

The problem of measuring quantumness is not new in physics and is important in many areas. For example, in quantum computing, maintaining quantumness is crucial as a computational resource [84]. The same goes for quantum cryptography [85, 86].

This led to various notions of "quantumness". We distinguish two main approaches. *i*) study the correlations between a system and the environment and see if it can be reproduced by classical random variables. This method leads to different measures such as the Bell inequalities [87] (as discussed above), non-separability of states [88], quantum discord [89, 90, 91], etc.. *ii*) making use of the phase space representation of quantum mechanics. This leads for example, to non-positivity of the Wigner function or the absence of P-representation as signals of quantumness [92, 93].

These measures can be related, depending on the circumstances. For example, it is well known, that if we consider pure states, the quantum discord reduces to entanglement entropy [91] which vanishes for separable states. On the other hand, all non-separable states violate the Bell inequality [88]. But if the states are mixed, the connections become more vague.

[24] We note that in principle there is also another contribution proportional to the decaying mode, but we neglect it since it is weak.

We follow [77] to relate different criteria of quantumness for special (but ubiquitous in many areas of physics) states and see how these criteria respond to decoherence. Specifically, two continuous degrees of freedom are studied in the two-mode squeezed states (see section 2.4.1) and we compare three measures of quantumness: the Bell inequality, quantum discord, and non-separability.

4.2.1 Gaussian two-mode squeezed states

Let us consider two continuous degrees of freedom q_1, q_2 and their conjugate momenta p_1, p_2. These variables can be combined into the phase-space vector $\hat{\mathbf{R}}^{1/2} = (q_1, q_2, p_1, p_2)^T$ with $[q_i, p_j] = i\delta_{ij}$ and whose quantum state is described by a density matrix $\hat{\rho}$. The Wigner function of the Gaussian state is Gaussian (See the formal definitions in Sec. 3.2), hence all information about the state can be extracted from the covariance matrix

$$\Gamma_{ab} = \langle\{\hat{R}_a, \hat{R}_b\}\rangle, \tag{4.20}$$

where $\{,\}$ stands for the anti-commutator. The Wigner function can be written as

$$W(\mathbf{R}_{1/2}) = \frac{1}{\pi^2\sqrt{|\Gamma|}} \exp\left[-\hat{\mathbf{R}}^T_{1/2}\gamma\hat{\mathbf{R}}_{1/2}\right], \tag{4.21}$$

where $|\Gamma|$ is the determinant of the covariance matrix. Let us recall the definition of purity $p \equiv \mathrm{Tr}\{\hat{\rho^2}\}$. The state is considered pure if $p = 1$ and mixed if $p < 1$. For Gaussian states, purity can be written in terms of the determinant of the covariance matrix as [94]

$$p = \frac{1}{\sqrt{|\Gamma|}}. \tag{4.22}$$

Two-mode squeezed vacua (TMSV) are states, whose covariance is determined exclusively by two squeezing parameters r and φ (See section 2.4.1 for more details of the squeezing formalism)[95]

$$\Gamma = \begin{pmatrix} \Gamma_{11} & \Gamma_{12} \\ \Gamma_{21} & \Gamma_{22} \end{pmatrix}, \tag{4.23}$$

where

$$\Gamma_{11} = \Gamma_{22} \equiv \cosh(2r)\mathbb{I}_2, \tag{4.24}$$

and

$$\Gamma_{12} = \Gamma_{21} \equiv -\sinh(2r)\begin{pmatrix} \cos 2\varphi & \sin 2\varphi \\ \sin 2\varphi & -\sin 2\varphi \end{pmatrix}. \tag{4.25}$$

Thus, having determined the squeezing parameters, one can use equation (4.22) to evaluate state purity. It should be stressed, that the two-mode squeezed vacua lose quantum properties by the effect of decoherence [96, 97]. We only consider two-mode thermal squeezed states, whose covariance

matrix is

$$\Gamma = \frac{\Gamma^{TMSV}}{\sqrt{p}}. \tag{4.26}$$

These states are ubiquitous in physics, including cosmology, for example, when the primordial perturbations are linearly coupled with the environment while preserving homogeneity [98].

Under the canonical transformation $\hat{\mathbf{R}} \to \mathbf{T}\hat{\mathbf{R}}$, where $\mathbf{T}$ is a symplectic matrix which preserves the commutation relations, the covariance matrix obeys $\Gamma \to \mathbf{T}\Gamma\mathbf{T}^T$. This implies the covariance matrix depends on the canonical variables describing the system. For instance, there exists a partition, in which the covariance matrix is block-diagonal

$$\Gamma^D = \frac{1}{\sqrt{p}}\mathrm{diag}(\Gamma^{\mathrm{OMSV}}, \Gamma^{\mathrm{OMSV}}), \tag{4.27}$$

where

$$\Gamma^{\mathrm{OMSV}} \equiv \begin{pmatrix} \Gamma_{qq} & \Gamma_{qp} \\ \Gamma_{pq} & \Gamma_{pp} \end{pmatrix}, \tag{4.28}$$

and

$$\Gamma_{qq} = \left[\cosh(2r) - \cos(2\varphi)\sinh(2r)\right], \tag{4.29}$$

$$\Gamma_{qp} = \gamma_{pq} = -\sin(2\varphi)\sinh(2r), \tag{4.30}$$

$$\Gamma_{pp} = \left[\cosh(2r) + \cos(2\varphi)\sinh(2r)\right]. \tag{4.31}$$

So that the Wigner function can be factorised $W(q_1^D, p_1^D, q_2^D, p_2^D) = W(q_1^D, p_1^D)W(q_2^D, p_2^D)$. In this partition, the quantum state is a product of two uncorrelated one-mode squeezed states. Then it is obvious that the quantumness criteria, which characterize the correlations between two sub-systems depends on the chosen partition. Usually, there is a preferred basis of operators chosen by the form of the interaction which corresponds to separately measurable physical quantities. We nevertheless use the partition (4.27). The Wigner functions can be represented as ellipses on phase space (see fig. 17). the squeezing parameter r controls the eccentricity of the ellipse, while φ is the angle between the semi-minor axis and the q_i axis.

4.2.2 quantumness criteria

We distinguish three criteria of quantumness.

Quantum Discord. Quantum discord is comprised of two measures of correlations between sub-systems that coincide in the classical limit but may differ for quantum correlations. The first measure called the *mutual entropy*, is the sum of the von-Neumann entropy of both sub-systems minus the entropy of the entire system. The second measure is the entanglement entropy, defined as the entropy of a sub-system minus the entropy of the same sub-system once all other sub-systems have been measured, where an extremisation is performed over the possible ways to measure the other subsystems. Denoted by $\mathcal{D}$, for the Gaussian states quantum discord can be expressed by the local symplectic invariants of the covariance matrix, which means that the discord is invariant under

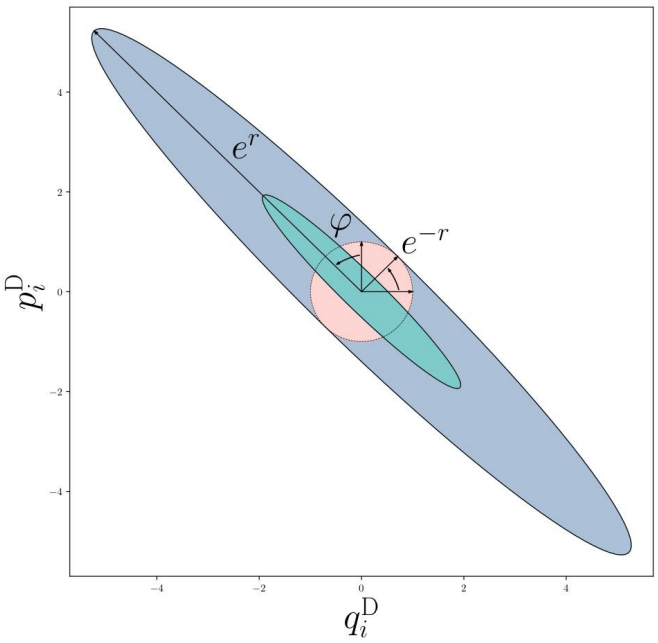

Figure 17: Contours of the Wigner function W in phase space. The red circle corresponds to the pure vacuum state $p = 1$ and $r = 0$, and the green ellipse is still a pure state ($p = 1$) but slightly squeezed with $r = 1$ along the $\varphi = \pi/4$ direction. The Blue ellipse has purity $p = e^{-4}$ and its semi-minor axis is the same as for the vacuum state. Figure taken from [77].

local sympletic transformations that mix q_i with p_i, but not with q_j or p_j.

$$\mathcal{D}(p, r) = f[\sigma(p, r)] = 2f[p^{-1/2}] + f\left[\frac{\sigma(p, r) + p^{-1}}{\sigma(p, r) + 1}\right], \tag{4.32}$$

where for $x \geq 1$

$$f(x) \equiv \left(\frac{x+1}{2}\right)\log_2\left(\frac{x+1}{2}\right) - \left(\frac{x-1}{2}\right)\log_2\left(\frac{x-1}{2}\right), \tag{4.33}$$

and

$$\sigma(p, r) = \frac{\cosh(2r)}{\sqrt{p}}. \tag{4.34}$$

The quantum discord depends only on p and r. This is because the local sympletic invariance allows for φ to be changed arbitrarily by performing a phase-space rotation in each sector, so the final result is independent of φ.

It should be noted, that for pure states quantum discord, entanglement entropy, and mutual entropy coincide up to numerical factors. While this guarantees the correlated pure states have quantum correlations, quantum discord does not add any value to the analysis and is usually not taken into account since entanglement entropy is simply easier to compute. The true advantage of the quantum discord becomes transparent when we consider mixed states instead.

Bell Inequality. The GKMR operators, found in Sec. 4.1 can be written as

$$\hat{\sigma}_x^i = \int_{-\infty}^{\infty} \mathrm{sign}(q_i)\, |q_i\rangle \langle q_i|\, dq_i, \tag{4.35}$$

$$\hat{\sigma}_y^i = -i \int_{-\infty}^{\infty} \mathrm{sign}(q_i)\, |q_i\rangle \langle -q_i|\, dq_i, \tag{4.36}$$

$$\hat{\sigma}_z^i = -\int_{-\infty}^{\infty} |q_i\rangle \langle -q_i|\, dq_i. \tag{4.37}$$

These operators obey the $SU(2)$ commutation relations $[\hat{\sigma}_\mu^i, \hat{\sigma}_\nu^j] = 2i\epsilon_{\mu\nu\lambda}\hat{\sigma}_\lambda^i \delta^{ij}$, where $\epsilon_{\mu\nu\lambda}$ is the totally anti-symmetric tensor. The Bell inequality can be constructed using these operators

$$\langle \hat{B} \rangle = 2\sqrt{\langle \hat{\sigma}_z^1 \hat{\sigma}_z^2 \rangle^2 + \langle \hat{\sigma}_x^1 \hat{\sigma}_x^2 \rangle} \leq 2. \tag{4.38}$$

The operators $\hat{\sigma}_\mu^1$ and $\hat{\sigma}_\mu^2$ act on different sectors. This means, that the Weyl transform of their product factorizes $\widetilde{\sigma_\mu^1 \sigma_\nu^2} = \widetilde{\sigma}_\mu^1 \widetilde{\sigma}_\nu^2$. The Weyl transforms can be shown to yield

$$\widetilde{\sigma_x^i} = \mathrm{sign}(q_i), \qquad \tilde{\sigma_z^i} = -\pi\delta(q_i)\delta(p_i). \tag{4.39}$$

We can now evaluate the expectation values

$$\langle \hat{\sigma}_z^i \hat{\sigma}_z^j \rangle = p, \qquad \langle \hat{\sigma}_x^i \hat{\sigma}_z^j \rangle = -\frac{2}{\pi} \arcsin[|\cos(2\varphi)| \tanh(2r)]. \tag{4.40}$$

Plugging these into equation (4.38) we obtain

$$\langle \hat{B} \rangle = 2\sqrt{p^2 + \frac{4}{\pi^2} \arcsin^2[|\cos(2\varphi)| \tanh(2r)]}. \tag{4.41}$$

Non-separability. A state is considered to be separable in a certain partition if we can write its density matrix as a statistical mixture of products of the density matrices of the sub-systems

$$\hat{\rho} = \sum_i \alpha_i \hat{\rho}_1^i \bigotimes \hat{\rho}_2^i, \tag{4.42}$$

where α_i are real. For Gaussian states, it has been shown [99], that the so-called Peres-Hordenski criterion is a necessary and sufficient way to tell if the state is separable. We cite the resulting condition on separability for the Gaussian state with the covariance (4.26) found in [77]:

$$e^{-2r} \geq \sqrt{p}. \tag{4.43}$$

As for the partition (4.27), the state is always separable.

4.2.3 Comparing quantumness criteria

Let us compare the three criteria of quantumness introduced above. First of all, the squeezing angle φ can be fixed by rotating the direction of the measurement in the phase space. To maximize the Bell inequality, we fix it to $\varphi = 0$. Then all three criteria depend only on purity p and the squeezing parameter r as depicted in Fig. 18. The color in the figure corresponds to different values of the quantum discord, while the black and white lines are the thresholds of the Bell inequality and the state (non-)separability.

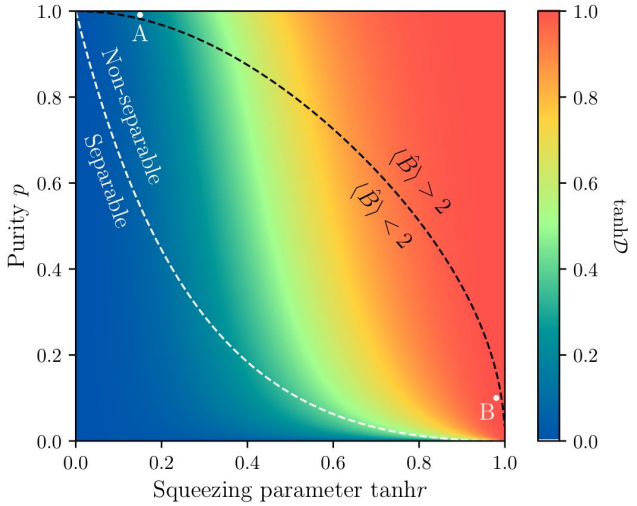

Figure 18: Hyperbolic tangent of the quantum discord as a function of the purity p and the hyperbolic tangent of the squeezing parameter r using equation (4.92). The black and white dashed curves correspond to the thresholds of the Bell inequality (see (4.41)) and the state (non-)separability (see (4.43)) respectively. The figure is taken from [77].

All the criteria are equivalent for $p = 1$ except for the vacuum state $r = 0$. Namely, all pure states have a non-vanishing quantum discord, the state is non-separable and the Bell inequality is violated. We also see that non-separability is necessary but not sufficient for the violation of the Bell inequality. Also, the states with low discord are separable.

This plot is also useful for understanding the interplay of the squeezing parameter and decoherence (characterized by purity in this context). Namely, as we know, the squeezed states are highly quantum and it is interesting to see how it responds to decoherence. As the squeezing parameter r increases, the state with fixed purity p becomes more quantum, in the sense, that it crosses the non-separability and Bell inequality thresholds while moving into an increasingly discordant state. Instead, if we also vary p, it becomes evident, that we need more decoherence (less values of p) as r increases to obtain a classical state[25].

[25]The term classical is used since the three measures of the quantumness criteria cannot distinguish these states from classical states.

Figure 18 also requires some comments about the values of quantum discord. The plot shows that the discord can take large or small values even after crossing both the non-separability and the Bell inequality thresholds. Compare the points A and B in the plot; The Bell inequality is violated at A, however, the quantum discord takes on low values. On the other hand, at point B the Bell inequality is not violated, but the discord is large. This suggests that the numerical value of the quantum discord does not have a clear interpretation, at least in this case and compared to the other criteria we have considered.

4.3 Quantumness From Axion Inflation: Discord and Decoherence

We would like to expand the topic of quantum discord. This chapter is largely inspired by [6]. We first delve into the formal structure of Gaussian states and discuss some notions from the previous chapter in a more rigorous and detailed way, then we apply the formalism to axion models of inflation, utilizing our construction from Ch. 3.

4.3.1 Partitions

As mentioned in the previous chapter, evaluating measures of quantumness depends on the chosen partition. To understand why, we start by partitioning a system into sub-parts and look for quantum correlations.

We want to characterize our system by Hermitian operators, satisfying the canonical commutation relations. For instance, for a system of n particles, we can choose the position $\hat{q}_i$ and momenta $\hat{\pi}_i$, where i=1,. . . , n and $[\hat{q}_i, \hat{\pi}_j] = i\delta_{ij}$. The quantum state of the system is an element of the Hilbert space

$$\mathcal{E} = \bigotimes_{i=1,\dots,n} \mathcal{E}_i. \tag{4.44}$$

To characterize the system, we can introduce a vector

$$\hat{R} = (\hat{q}_1, \hat{\pi}_1, \dots, \hat{q}_n, \hat{\pi}_n)^T. \tag{4.45}$$

The canonical commutation relations associated with the components of $\hat{R}$ can be written compactly as

$$\left[\hat{R}_a, \hat{R}_b\right] = iJ^{(n)}_{ab}, \tag{4.46}$$

where J is a block-diagonal matrix

$$J^{(n)} = \begin{pmatrix} J^{(1)} & & \\ & \ddots & \\ & & J^{(1)} \end{pmatrix}, \qquad J^{(1)} = \begin{pmatrix} 0 & 1 \\ -1 & 0 \end{pmatrix}. \tag{4.47}$$

One can equivalently describe the system using the creation-annihilation operators since

$$\hat{q}_i = \frac{1}{\sqrt{2}}(\hat{c}_i + \hat{c}_i^\dagger) \qquad \hat{\pi} = -\frac{i}{\sqrt{2}}(\hat{c}_i - \hat{c}_i^\dagger). \tag{4.48}$$

and a corresponding vector

$$\hat{C} = \left(\hat{c}_1, \dots, \hat{c}_i, \dots \hat{c}_n, \hat{c}_1^\dagger, \dots \hat{c}_i^\dagger, \dots \hat{c}_n^\dagger\right)^T. \tag{4.49}$$

Notice that the components are not gathered according to their numerical labels as before. To gather such terms, we may use the *permutation matrix* $P^{(n)}$, such that

$$\hat{\tilde{C}} = P^{(n)} \cdot \hat{C} = \left(\hat{c}_1, \hat{c}_1^\dagger \dots \hat{c}_i, \hat{c_i}^\dagger \dots, \hat{c}_n, \hat{c}_n^\dagger\right). \tag{4.50}$$

This will be useful since the relation between $\hat{R}$ and $\hat{C}$ is linear and thus can be written as $\hat{R} = M^{(n)} \cdot \hat{C}$. To establish $M^{(n)}$ we first write $\hat{R} = \bar{M}^{(n)} \cdot \hat{\tilde{C}}$, where $\bar{M}^{(n)}$ is now obviously a block-diagonal matrix,

$$\bar{M}^{(n)} = \begin{pmatrix} \bar{M}^{(1)} & & \\ & \ddots & \\ & & M^{(1)} \end{pmatrix}, \qquad \bar{M}^{(1)} = \frac{1}{\sqrt{2}} \begin{pmatrix} 1 & 1 \\ -i & i \end{pmatrix}. \tag{4.51}$$

Since $P^{(n)}$ is orthogonal, $\bar{M}^{(n)} = P^{(n)} \cdot M^{(n)} \quad \Rightarrow \quad M^{(n)} = \bar{M}^{(n)} \cdot P^{(n)T}$. The final expression allows us to calculate $M^{(n)}$ using $\bar{M}^{(n)}$ established above. Let us also notice, that $\bar{M}^{(1)}\bar{M}^{(1)\dagger} = \mathbb{I}_2 \quad \Rightarrow \quad \bar{M}^{(n)}\bar{M}^{(n)\dagger} = \mathbb{I}_n$, which automatically guarantees $M^{(n)}M^{(n)\dagger} = \mathbb{I}_n$. We can write down the commutation relations using vectors $\hat{C}$ as

$$\left[\hat{C}_a, \hat{C}_b\right] = \Omega^{(n)}_{ab}, \qquad \Omega^{(n)} = iM^{(n),-1}J^{(n)}M^{(n),-1,T} = \begin{pmatrix} 0 & \mathbb{I}_n \\ -\mathbb{I}_n & 0 \end{pmatrix}. \tag{4.52}$$

We can always partition into two subsets as long as $n \geq 2$. For instance, if we take $n = 4$, $\hat{R} = (\hat{q}_1, \hat{\pi}_1, \hat{q}_2, \hat{\pi}_2, \hat{q}_3, \hat{\pi}_3\hat{q}_4, \hat{\pi}_4)^T$, we may choose $\hat{R}_A = (\hat{q}_1, \hat{\pi}_1, \hat{q}_2, \hat{\pi}_2)^T$ and $\hat{R}_B = (\hat{q}_3, \hat{\pi}_3\hat{q}_4, \hat{\pi}_4)^T$, which is by definition a partition. We may as well choose to assemble $\hat{R}$ by combining components with all possible combinations of numeric labels associated with the position and the momenta. Choosing a partition corresponds to a canonical transformation that preserves the commutator structure. So, $\hat{R} \to \hat{R}' = T\hat{R}$, where T must be real so that $\hat{R}'$ is kept Hermitian. T must also be such that $\left[\hat{R}'_a, \hat{R}'_b\right] = \left[\hat{R}_a, \hat{R}_b\right]$. Also, (4.46) implies $TJT^T = J$, which defines a symplectic matrix T, whose determinant must be 1 (as is true for any symplectic matrix). The same applies to $\hat{C}$. Namely, $S\Omega S^T = \Omega$, where $S = M^{-1}TM = M^TTM$, which implies $\det|S| = 1$. Another important

observation is, that the partition $\hat{C}$ has the property $\hat{C}^\dagger = A \cdot \hat{C}$, where

$$A = \begin{pmatrix} 0 & \mathbb{I}_n \\ \mathbb{I}_n & 0 \end{pmatrix} \tag{4.53}$$

. Then, since $\hat{R} = M \cdot \hat{C}$, we get $M = M^* A$. Now, by definition $S = M^{-1} T M$, so that its complex conjugate can easily be found to be

$$S^* = ASA \tag{4.54}$$

We should note that the local canonical transformations within the partitions do not mix the subsystems, so they do not represent a change in partition.

For two partitions to share the same vacuum state, S must not mix the creation and annihilation operators. The way that $\hat{C}$ is established implies S is block-diagonal. On the other hand, according to (4.54), the blocks must be complex conjugates to each other

$$S = \begin{pmatrix} s^{(n)} & 0 \\ 0 & s^{(n)*} \end{pmatrix}. \tag{4.55}$$

Since S is sympletic, $s^{(n)} s^{(n)\dagger} = \mathbb{I}_n$, which means $s^{(n)}$ belong to the unitary group. We may conclude that the space of partitions is the group $U(n)$. Any parametrization of that group is a reparametrization of all partitions. For example, if we take $n = 2$, the matrices of $U(2)$ can be written as

$$S^{(2)} = \begin{pmatrix} e^{i\alpha} \cos\theta & -e^{i\delta} \sin\theta \\ e^{i\beta} \sin\theta & r^{i(\delta+\beta-\alpha)\cos\theta} \end{pmatrix}. \tag{4.56}$$

where $\alpha, \beta\delta$ and θ are arbitrary real parameters, that determine the partition. In other words, they are changing these parameter amounts to changing partitions. We can now rewrite the symplectic matrix T in terms of these parameters

$$T = \begin{pmatrix} \cos\alpha\cos\theta & -\sin\alpha\cos\theta & -\cos\delta\sin\theta & \sin\delta\sin\theta \\ \sin\alpha\cos\theta & \cos\alpha\cos\theta & -\sin\delta\sin\theta & -\cos\delta\sin\theta \\ \cos\beta\sin\theta & -\sin\beta\sin\theta & \cos(\alpha-\beta-\delta)\cos\theta & \sin(\alpha-\beta-\delta)\cos\theta \\ \sin\beta\sin\theta & \cos\beta\sin\theta & -\sin(\alpha-\beta-\delta)\cos\theta & \cos(\alpha-\beta-\delta)\cos\theta \end{pmatrix}. \tag{4.57}$$

The 4-parameter symplectic matrices that change partitions form an isomorphic group to the more general symplectic group $\mathrm{Sp}(4,\mathbb{R})$, which is 10-dimensional for 4×4 matrices. In agreement with the $U(n)$ group structure

$$T^{1/2\to 1'/2'} = T^{1/2\to 1''/2''} \cdot T^{1''/2''\to 1'/2'} \tag{4.58}$$

and

$$T^{1/2\to 1'/2'} = \left(T^{1'/2'\to 1/2}\right)^{-1}. \tag{4.59}$$

Example: scalar field with a quadratic Hamiltonian. Let us now recall the free Hamilto-

nian (3.54) defined in Ch. 3

$$\hat{H}_v = \int_{\mathbb{R}} d^3\mathbf{k}\hat{H}_\mathbf{k} = \frac{1}{2}\int_{\mathbb{R}} d^3\mathbf{k}\left[\hat{p}_\mathbf{k}\hat{p}^\dagger_\mathbf{k} + \omega^2(\tau,\mathbf{k})\hat{v}_\mathbf{k}\hat{v}^\dagger_\mathbf{k}\right]. \tag{4.60}$$

To keep the discussion generic, we shall not specify ω, which encodes the physics of a given setup, and τ is to be understood as a generic time variable. In the said chapter, we made a canonical transformation that allowed us to proceed using Hermitian operators

$$\hat{v}^{\mathrm{R}}_\mathbf{k} = \frac{\hat{v}_\mathbf{k} + \hat{v}^\dagger_\mathbf{k}}{\sqrt{2}}; \qquad \hat{v}^{\mathrm{I}}_\mathbf{k} = \frac{\hat{v}_\mathbf{k} - \hat{v}^\dagger_\mathbf{k}}{i\sqrt{2}}; \qquad \hat{p}^{\mathrm{R}}_\mathbf{k} = \frac{\hat{p}_\mathbf{k} + \hat{p}^\dagger_\mathbf{k}}{\sqrt{2}}; \qquad \hat{p}^{\mathrm{I}}_\mathbf{k} = \frac{\hat{p}_\mathbf{k} - \hat{p}^\dagger_\mathbf{k}}{i\sqrt{2}}. \tag{4.61}$$

One can easily check that the commutation relations are unchanged. We can rewrite the Hamiltonian in terms of $\hat{v}^{\mathrm{R}}$ and $\hat{p}^{\mathrm{I}}$:

$$\hat{H}_v = \int_{\mathbb{R}^{3+}} d^3\mathbf{k} \sum_{s=\mathrm{R,I}} \hat{H}^s_\mathbf{k} = \frac{1}{2}\int_{\mathbb{R}^{3+}} d^3\mathbf{k} \sum_{s=\mathrm{R,I}} \left[(\hat{p}^s_\mathbf{k})^2 + \omega^2(\tau,\mathbf{k})(\hat{v}^s_\mathbf{k})^2\right]. \tag{4.62}$$

The advantage of this last parametrization is that the Hamiltonian is sum separable. In other words, the Hamiltonian describes independent parametric oscillators. If the initial state of the system can be factorized, it remains factorized at any later time, so the dynamics does not generate any entanglement between different subspaces.

In the lab, Bell experiments partitioning appears to be trivial: one can spatially separate the systems, which is a natural partition because Bell experiments are designed to test locality. For quantum fields, the situation is less obvious. If one considers two spatially distant regions, one would have to deal with mixed states since observing the field at two distinct locations implies tracing over all field configurations in all other locations. This is where Fourier space is extremely useful, since different Fourier subspaces are uncoupled. This way, the state mixing effect of the environment-induced decoherence is isolated from that of the effect coming from the aforementioned effective mixing effect.

In Fourier space, however, there is no obvious way to partition the system. For example, one could construct operators for a single mode

$$\hat{q}_\mathbf{k} = \frac{1}{\sqrt{2k}}\left(\hat{c}_\mathbf{k} + \hat{c}^\dagger_\mathbf{k}\right) \qquad \hat{\pi}_\mathbf{k} = -i\sqrt{\frac{k}{2}}\left(\hat{c}_\mathbf{k} - \hat{c}^\dagger_\mathbf{k}\right), \tag{4.63}$$

where notice that compared to (4.48), we have included additional factors of k to maintain correct dimensions. These equations, along with Eq. (4.61), define different partitions. Namely, a partition between imaginary and real sectors and $\mathbf{k}/-\mathbf{k}$ sectors, both with correlations of different nature and amounts.

We can conveniently form a vector using different partitions (see Eq. (4.45)). For example, in

the case of the R/I partition, we get

$$\hat{R}_{\mathrm{R/I}} = \left(k^{1/2}\hat{v}^R_{\mathbf{k}}, k^{-1/2}\hat{p}^R_{\mathbf{k}}, k^{1/2}\hat{v}^I_{\mathbf{k}}, k^{-1/2}\hat{p}^I_{\mathbf{k}}\right)^T \tag{4.64}$$

where the first two entries correspond to the first subsystem, and the second two correspond to the second subsystem. The commutation relations are non-vanishing only between the first and the second, along with the third and the fourth entries. If we choose the $\pm\mathbf{k}$ partition, we can construct a similar vector

$$\hat{R}_{\pm\mathbf{k}} = \left(k^{1/2}\hat{q}_{\mathbf{k}}, k^{-1/2}\hat{\pi}_{\mathbf{k}}, k^{1/2}\hat{q}_{-\mathbf{k}}, k^{-1/2}\hat{\pi}_{-\mathbf{k}}\right). \tag{4.65}$$

We focus on partitions that are linearly related to the reference partition R/I

$$\hat{R}_{1/2} = T^{\mathrm{R/I}\to 1/2}\hat{R}_{R/I} \tag{4.66}$$

This way, the quadratic nature of the Hamiltonian density is preserved. Since we want different parametrisations to have the same vacuum state, the matrix $T^{\mathrm{R/I}\to 1/2}$ corresponds to (4.57), which depends on 4 parameters, α, β, δ and θ. We can set $\alpha = 0, \beta = 3\pi/2 + 2\theta$, and $\delta = \pi/2$ to obtain a one-parameter subset of partitions

$$T^{\mathrm{R/I}\to 1/2}(\theta) = \begin{pmatrix} \cos\theta & 0 & 0 & 0 \\ 0 & \cos\theta & -\sin\theta & 0 \\ \sin\theta\sin(2\theta) & \sin\theta\cos(2\theta) & \cos\theta\cos(2\theta) & -\cos\theta\sin(2\theta) \\ -\sin\theta\cos(2\theta) & \sin\theta\sin(2\theta) & \cos\theta\sin(2\theta) & \cos\theta\cos(2\theta). \end{pmatrix} \tag{4.67}$$

So the rotations by θ correspond to different partitions. For $\theta = 0$, we get $T^{\mathrm{R/I}} = \mathbb{I}_4$ and the partition is unchanged. Notice also, that for $\theta = -\pi/4$, we move to $\pm\mathbf{k}$ partition. This subclass is enough to see how partitioning affects the final results; hence, for simplicity, we will focus mainly on the one-parameter partitions.

4.3.2 Covariance matrix

The Hamiltonian, being quadratic, the dynamics allows for Gaussian states as solutions. In this context by Gaussian we mean, that the Wigner function is Gaussian. As we already know, the Gaussian states are characterized by the two-point functions (see Eq. (4.20)) and upon a change of partition $\Gamma' = T\Gamma T^T$.

For the R/I partition, the two sectors will have the same reduced Hamiltonian and the two sectors decouple. The complete covariance matrix will have the form (recall the block diagonal partition in Ch. 4.2)

$$\Gamma^{\mathrm{R/I}} = \begin{pmatrix} \Gamma_{11} & \Gamma_{12} & 0 & 0 \\ \Gamma_{12} & \Gamma_{22} & 0 & 0 \\ 0 & 0 & \Gamma_{11} & \Gamma_{12} \\ 0 & 0 & \Gamma_{12} & \Gamma_{22} \end{pmatrix}. \tag{4.68}$$

which depends only on three parameters

$$\Gamma_{11} = 2k\langle(\hat{v}_{\mathbf{k}}^{\mathrm{R}})^2\rangle = 2k\langle(\hat{v}_{\mathbf{k}}^{\mathrm{I}})^2\rangle = k\langle\{\hat{v}_{\mathbf{k}}, \hat{v}_{\mathbf{k}}^{\dagger}\}\rangle, \tag{4.69}$$

$$\Gamma_{12} = \Gamma_{21} = \langle\hat{v}_{\mathbf{k}}^{\mathrm{R}}\hat{p}_{\mathbf{k}}^{\mathrm{R}} + \hat{p}_{\mathbf{k}}^{\mathrm{R}}\hat{v}_{\mathbf{k}}^{\mathrm{R}}\rangle = \langle\hat{v}_{\mathbf{k}}^{\mathrm{I}}\hat{p}_{\mathbf{k}}^{\mathrm{I}} + \hat{p}_{\mathbf{k}}^{\mathrm{I}}\hat{v}_{\mathbf{k}}^{\mathrm{I}}\rangle = \langle\hat{v}_{\mathbf{k}}\hat{p}_{\mathbf{k}}^{\dagger} + \hat{p}_{\mathbf{k}}\hat{v}_{\mathbf{k}}^{\dagger}\rangle \tag{4.70}$$

$$\Gamma_{22} = \frac{2}{k}\langle(\hat{p}_{\mathbf{k}}^{\mathrm{R}})^2\rangle = \frac{2}{k}\langle(\hat{p}_{\mathbf{k}}^{\mathrm{I}})^2\rangle = \frac{1}{k}\langle\{\hat{p}_{\mathbf{k}}, \hat{p}_{\mathbf{k}}^{\dagger}\}\rangle \tag{4.71}$$

A generic form for a 4×4 covariance matrix is

$$\Gamma = \begin{pmatrix} \Gamma_A & \Gamma_C \\ \Gamma_C & \Gamma_{B.} \end{pmatrix} \tag{4.72}$$

where Γ_A, Γ_B and Γ_C are 2×2 matrices. By using $\Gamma' = T\Gamma T^T$ and Eq. (4.67), we can obtain the representation of the covariance matrix in different partitions. Explicit evaluation gives

$$\Gamma_A = \begin{pmatrix} \Gamma_{11}\cos^2\theta + \Gamma_{22}\sin^2\theta & \Gamma_{12}\cos(2\theta) \\ \Gamma_{12}\cos(2\theta) & \Gamma_{22}\cos^2\theta + \Gamma_{11}\sin^2\theta \end{pmatrix}, \tag{4.73}$$

$$\Gamma_B = \begin{pmatrix} \Gamma_B|_{11} & \Gamma_B|_{12} \\ \Gamma_B|_{21} & \Gamma_B|_{22} \end{pmatrix}, \tag{4.74}$$

$$\Gamma_C = \begin{pmatrix} \frac{1}{2}(\Gamma_{11} - \Gamma_{22})\sin^2(2\theta) + \frac{1}{2}\Gamma_{12}\sin(4\theta) & -\frac{1}{4}(\Gamma_{11} - \Gamma_{22})\sin(4\theta) + \Gamma_{12}\sin^2\theta \\ -\frac{1}{4}(\Gamma_{11} - \Gamma_{22})\sin(4\theta) + \Gamma_{12}\sin^2(2\theta) & -\frac{1}{2}(\Gamma_{11} - \Gamma_{22})\sin^2(2\theta) - \frac{1}{2}\Gamma_{12}\sin(4\theta) \end{pmatrix}. \tag{4.75}$$

where

$$\Gamma_B|_{11} = \frac{1}{2}\Gamma_{11} + \frac{1}{2}\Gamma_{22} + \frac{1}{2}(\Gamma_{11} - \Gamma_{22})\cos(2\theta)\cos(4\theta) - \Gamma_{12}\cos(2\theta)\sin(4\theta), \tag{4.76}$$

$$\Gamma_B|_{12} = \Gamma_B|_{21} = \Gamma_{12}\cos(2\theta)\cos(4\theta) + \frac{1}{2}(\Gamma_{11} - \Gamma_{22})\cos(2\theta)\sin(4\theta), \tag{4.77}$$

$$\Gamma_B|_{22} = \frac{1}{2}\Gamma_{11} + \frac{1}{2}\Gamma_{22} - \frac{1}{2}(\Gamma_{11} - \Gamma_{22})\cos(2\theta)\cos(4\theta) + \Gamma_{12}\cos(2\theta)\sin(4\theta). \tag{4.78}$$

4.3.3 Quantum discord for Gaussian homogeneous states

Classical Correlations. Consider two systems A and B, with possible configurations $\{a_i\}$ and $\{b_j\}$. Probabilities associated with these configurations are p_i and p_j respectively. Measure of uncertainty about the configuration of a system is described by the von Neumann entropy

$$S(A) = -\sum_i p_i \log_2(p_i) \tag{4.79}$$

and similar for the system B. The joint uncertainty of the systems A and B is

$$S(AB) = -\sum_{ij} p_{ij} \log_2(p_{ij}), \tag{4.80}$$

where p_{ij} is the probability of finding A in configuration a_i and B in b_i.

The mutual information is defined as

$$\mathfrak{I}(A,B) = S(A) + S(B) - S(A,B). \tag{4.81}$$

If A and B are uncorrelated, i.e. $p_{ij} = p_i p_j$, $\mathfrak{I} = 0$. This can easily be shown using the fact, that $\sum_{i(j)} p_{i(j)} = 0$.

We can further generalize p_{ij} using Baye's theorem $p_{ij} = p_j p_{i|j}$, where $p_{i|j}$ is the probability of finding A in a_i, given that B is already found in b_i. Then the mutual information becomes

$$\mathfrak{I} = -\sum_i p_i \log_2(p_i) + \sum_{ij} p_j p_{i|j} \log_2(p_{i|j}). \tag{4.82}$$

The last quantity on the RHS will be denoted as $S(A|B)$ from now on. The above equation prompts for an alternative expression for mutual information

$$\mathfrak{J} = S(A) - S(A|B). \tag{4.83}$$

Note, that for classical systems $\mathfrak{I} = \mathfrak{J}$

Quantum correlations. We have to define similar quantities for quantum systems. Since using the density matrix formalism, the information on the system A is given by $\hat{\rho}_A = \mathrm{Tr}_B\{\hat{\rho}_{A,B}\}$, the von Neumann entropy in this case can be expressed as

$$S(A) = -\mathrm{Tr}\{\rho_A \log_2(\rho_A)\}. \tag{4.84}$$

Of course, the same holds for the system B and the combination AB. To complete the analogy we also need $S(A|B)$. To obtain this entropy measure we define a complete set of projectors Π_j, which projects on a quantum state $|b_j\rangle$: $\hat{\Pi}_j = \mathbb{I}_A \otimes |b_j\rangle\langle b_j|$. Notice, just as a complete basis of states $|b_i\rangle$ is not unique, neither is the complete set of projectors $\hat{\Pi}_j$. Probability of finding B in b_j is given by $p_j = \mathrm{Tr}\{\hat{\rho}\hat{\Pi}_j\}$ and the measurement of B that results in configuration b_j is given by $\hat{\rho} \to \hat{\Pi}_j\hat{\rho}\hat{\Pi}_j/p_j$. Therefore, we now introduce

$$\hat{\rho}_{A|\hat{\Pi}_j} = \mathrm{Tr}_B\left(\frac{\hat{\Pi}_j\hat{\rho}\hat{\Pi}_j}{p_j}\right). \tag{4.85}$$

Then in terms of the conditional entropy $S(A|B) = \sum_j p_j S(\hat{\rho}_{A|\hat{\Pi}_j})$. Then, we can define $\mathfrak{I}$ and $\mathfrak{J}$ in the same exact manner.

Quantum discord is defined as

$$\mathfrak{D}(A,B) = \min_{\{\hat{\Pi}_j\}} \left[\mathfrak{I}(A,B) - \mathfrak{J}(a,B)\right], \tag{4.86}$$

where we minimize over all possible complete sets of projectors, so that a non-vanishing discord signals a genuine quantum correlation in *any basis*.

The von Neumann entropy for Gaussian states can be written as

$$S(\hat{\rho}) = \sum_{i=1}^{n} f(\sigma_i), \tag{4.87}$$

where $f(x)$ is defined for $x \geq 1$ and is given by

$$f(x) = \left(\frac{x+1}{2}\right)\log_2\left(\frac{x+1}{2}\right) - \left(\frac{x-1}{2}\right)\log_2\left(\frac{x-1}{2}\right), \tag{4.88}$$

and σ_i are the sympletic eigenvalues of the covariance matrix, which depends on the choice of partition, and, therefore θ. The expression for $\sigma(\theta)$ reads

$$\sigma(\theta) = \sqrt{(\Gamma_{11}\Gamma_{22} - \Gamma_{12}^2)\cos^2(2\theta) + \left(\frac{\Gamma_{11}+\Gamma_{22}}{2}\right)^2 \sin^2(2\theta)}. \tag{4.89}$$

and the mutual information $\mathfrak{I}$ can be written as [6]

$$\mathfrak{I} = 2f[\sigma(\theta)] - 2f[\sigma(0)]. \tag{4.90}$$

As for the mutual information $\mathfrak{J}$, using the *singular-value decomposition theorem*, one can show that it is given by the following expression [6]

$$\max_{\{\hat{\Pi}_i\}} \mathfrak{J} = f[\sigma(\theta)] - f\left[\frac{\sigma^2(0)+\sigma(\theta)}{1+\sigma(\theta)}\right]. \tag{4.91}$$

So by subtracting the expressions for the mutual information we obtain the quantum discord

$$\mathfrak{D}(\theta) = f[\sigma(\theta)] - 2f[\sigma(0)] + f\left[\frac{\sigma^2(0)+\sigma(\theta)}{1+\sigma(\theta)}\right]. \tag{4.92}$$

As expected, to find quantum discord of a system, the knowledge of the covariance matrix in any partition will suffice. Additionally, it is evident, that for the R/I partition the quantum discord is zero.

4.3.4 The case of axion inflation

We now move on to calculating the discord for axion inflation. So we look at how the decohering effect of the gauge fields on the axion fluctuations influence the quantum discord of the system.

First off, let us quote the results for the quantum discord in the absence of an environment [6]. Notice, from Eq. (4.89), $\sigma(0) = \det|\Gamma^s|$, which for pure states is always 1. Hence quantum discord reduces to

$$\mathfrak{D}(\theta) = f[\sigma(\theta)]. \tag{4.93}$$

The parameter $\sigma(\theta)$ can be expressed in terms of the squeezing parameters

$$\sigma(\theta) = \sqrt{1 + \sinh^2(2r_k)\sin^2(2\theta)}, \tag{4.94}$$

where r_k is the squeezing parameter. What this indicates was expected, since as we have mentioned, different partitions induce a mixing effect, which translates to larger entanglement between the system degrees of freedom.

It is therefore interesting to see how much environment induced decoherence may be sufficient to erase traces of "quantumness", which prompts us to study this effect in axion inflation.

In case of the axion inflation, the environment is made up of gauge fields and we already have the solution for the state of our system. Since the state (3.80) is Gaussian, one can readily apply the formalism developed above to inflation. We shall study the case of axion inflation. Notice, that in Sec. 3 we have used the I/R partition throughout for convenience.

Since Gaussian states are completely characterized by their covariance matrix, we first evaluate the entries of Γ^s, where as usual $s = R, I$. Using Eq. (4.64) and (4.20) we get

$$\Gamma^s = \begin{pmatrix} 2k\langle(\hat{v}^s_{\mathbf{k}})^2\rangle & \langle\hat{v}^s_{\mathbf{k}}\hat{p}^s_{\mathbf{k}} + \hat{p}^s_{\mathbf{k}}\hat{v}^s_{\mathbf{k}}\rangle \\ \langle\hat{v}^s_{\mathbf{k}}\hat{p}^s_{\mathbf{k}} + \hat{p}^s_{\mathbf{k}}\hat{v}^s_{\mathbf{k}}\rangle & \frac{2}{k}\langle(\hat{p}^s_{\mathbf{k}})^2\rangle \end{pmatrix}. \tag{4.95}$$

So we need to evaluate the two-point correlators. According to Eq. (3.87), the first correlator

$$\langle(\hat{v}^s_{\mathbf{k}})^2\rangle = P_{vv} = |v_{\mathbf{k}}|^2 + \mathcal{J}_{\mathbf{k}}. \tag{4.96}$$

The other correlators can also be evaluated by performing a similar, albeit more involved integrals. The results read

$$\langle\hat{v}^s_{\mathbf{k}}\hat{p}^s_{\mathbf{k}} + \hat{p}^s_{\mathbf{k}}\hat{v}^s_{\mathbf{k}}\rangle = |v_{\mathbf{k}}|^{2\prime} + 2\mathcal{K}_{\mathbf{k}}, \tag{4.97}$$

$$\langle(\hat{p}^s_{\mathbf{k}})^2\rangle = |v'_{\mathbf{k}}|^2 + \mathcal{I}_{\mathbf{k}}. \tag{4.98}$$

The purity of the Gaussian state is related to the determinant of its covariance matrix by (4.22). However, as we have shown in Eq. (3.143), the purity can be expressed using the decoherence parameter $p = 1/\sqrt{1+4\delta_{\mathbf{k}}}$. As a consistency check let us show, that the determinant of our covariance matrix really boils down to $1 + 4\delta_{\mathbf{k}}$:

$$\begin{aligned} \det|\gamma^s| = 4\langle(\hat{v}^s_{\mathbf{k}})^2\rangle\langle(\hat{p}^s_{\mathbf{k}})^2\rangle - \langle\hat{v}^s_{\mathbf{k}}\hat{p}^s_{\mathbf{k}} + \hat{p}^s_{\mathbf{k}}\hat{v}^s_{\mathbf{k}}\rangle = 4(|v_{\mathbf{k}}|^2|v'_{\mathbf{k}}|^2 + |v_{\mathbf{k}}|^2\mathcal{I}_{\mathbf{k}} + |v'_{\mathbf{k}}|^2\mathcal{J}_{\mathbf{k}} + \mathcal{I}_{\mathbf{k}}\mathcal{J}_{\mathbf{k}}) - \\ - \left(\left(|v_{\mathbf{k}}|^{2\prime}\right)^2 + 4|v_{\mathbf{k}}|^{2\prime}\mathcal{K}_{\mathbf{k}} + 4\mathcal{K}^2_{\mathbf{k}}\right) = 1 + 4(\mathcal{I}_{\mathbf{k}}\mathcal{J}_{\mathbf{k}} - \mathcal{K}^2_{\mathbf{k}} + |v'_{\mathbf{k}}|^2\mathcal{J} + |v_{\mathbf{k}}|^2\mathcal{I}_{\mathbf{k}} - |v_{\mathbf{k}}|^{2\prime}\mathcal{K}_{\mathbf{k}}) = \\ = 1 + 4\delta_{\mathbf{k}}, \end{aligned} \tag{4.99}$$

where we have used the Wronskian condition $v_{\mathbf{k}}v^{*\prime}_{\mathbf{k}} - v^*_{\mathbf{k}}v'_{\mathbf{k}} = i$.

The quantity $\sigma(\theta)$ can be expressed in terms of the two-point functions (4.96)-(4.98) by plugging these expressions into (4.89).

An analogue to (4.94) was used in [6] to calculate decoherence in the presence of an environment

$$\sigma(\theta) = \lambda_k^{1/2}\sqrt{1+\sinh^2(2r_k)\sin^2(2\theta)} \tag{4.100}$$

where $\lambda_k \equiv \det|\gamma^s|$ and r_k are the effective squeezing parameters and θ is the partition angle. The additional squeezing parameter λ_k appears since the determinant of the covariance matrix is no longer one due to the presence of the environment.

By equating Eq. (4.100) with (4.89) the effective squeezing parameter r_k can be expressed in terms of the covariance matrix. Namely,

$$r_k = \frac{1}{2}\sinh^{-1}\left(\sqrt{\frac{1}{\det|\Gamma^s|}\left(\frac{\Gamma_{11}+\Gamma_{22}}{2}\right)^2 - 1}\right). \tag{4.101}$$

The next step is to plug in the expressions (4.96)-(4.98) into this equation. This way it is possible to see the influence of the model parameters, such as ξ for the axion inflation, on the squeezing parameter r_k. We proceed and find

$$r_k = \frac{1}{2}\sinh^{-1}\left(\sqrt{\frac{1}{1+4\delta_{\mathbf{k}}}\left[k^2\left(|v_{\mathbf{k}}|^2+\mathcal{J}_{\mathbf{k}}\right)^2 + 2\left(|v_{\mathbf{k}}|^2+\mathcal{J}_{\mathbf{k}}\right)\left(|v'_{\mathbf{k}}|^2+\mathcal{I}_{\mathbf{k}}\right) + \frac{1}{k^2}\left(|v'_{\mathbf{k}}|^2+\mathcal{I}_{\mathbf{k}}\right)^2\right] - 1}\right). \tag{4.102}$$

Approximations similar to the ones used in Ch. 3 can be used[26]. First, the terms proportional to γ^2 can be neglected since the Lindblad equation was derived at first order in γ. Second, out of the remaining terms the dominant terms can be identified from Eqns. (E.20)-(E.21) and (E.24)-(E.25)

$$r_k \simeq \frac{1}{2}\sinh^{-1}\left\{\left(\frac{\pi^2}{16\sin^4(\pi\nu)}\frac{1}{1+4\delta_{\mathbf{k}}}\left(\frac{k}{k_*}\right)^{-4\nu-2} e^{\frac{2}{1+\varepsilon}(N-N_*)(2\nu+1)}\times\right.\right.$$
$$\left.\left.\left[\left(\frac{1}{2}+\nu\right)\frac{2^\nu}{\Gamma(1+\nu)}+\frac{2^{\nu+1}}{}\right]^4\times\left[1+\frac{2}{\pi}\frac{e^{4\pi\xi}}{64}\left(\frac{H}{M_{\rm Pl}}\right)^2\frac{2}{\varepsilon}\left(\frac{k}{k_*}\right)^{-3\varepsilon}\frac{\xi}{\beta}F_1\right]-1\right)^{1/2}\right\}, \tag{4.103}$$

where Γ here represents the Gamma function and must not be confused with the covariance matrix. F_1 is defined by Eq. (E.27).

Equation (4.103) is plotted on Fig. 19, which indicates, that the squeezing parameter decreases with increasing ξ. Since state squeezing enhances the quantum correlations, this behavior should be compared to decoherence (Fig. 14), which, instead increases with increasing ξ. In both cases increasing the production rate of the gauge fields has the effect of decreasing "quantumness".

Another feature we see on Fig. 19 is that r_k increases with scale, meaning, that the larger scales become more squeezed than the smaller scales. This is in total agreement with the expectation in the literature (e.g.[28]), because the decaying mode decreases rapidly on superhorizon scales (See

[26] In what follows the integral form of the environment correlation function will be used.

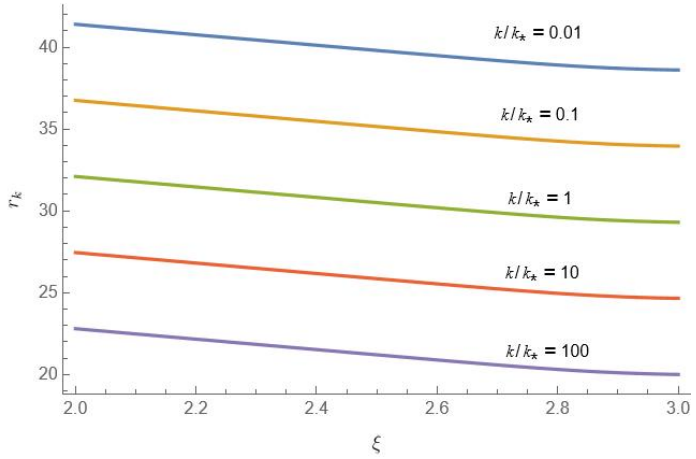

Figure 19: The generalized squeezing parameter evaluated for different scales as a function of ξ according to Eq. (4.103). This plot was obtained for $\varepsilon = 10^{-3}$, $\eta = 1 - 0.96 - 2\varepsilon$ and $H/M_{\rm Pl} = 10^{-5}$.

also Eq. (2.93)).

By plugging Eq. (4.103) into (4.100) and (4.92) we obtain quantum discord, which is plotted in Fig. 20 for two different partitions corresponding to $\theta = 0.01$ and $\theta = -\pi/4$. The plots show dependence of quantum discord $\mathfrak{D}$ on ξ and k/k_*. As expected, the result depends on the partition angle. Namely, we see that the quantum discord is larger for the $\pm\mathbf{k}$ partition.

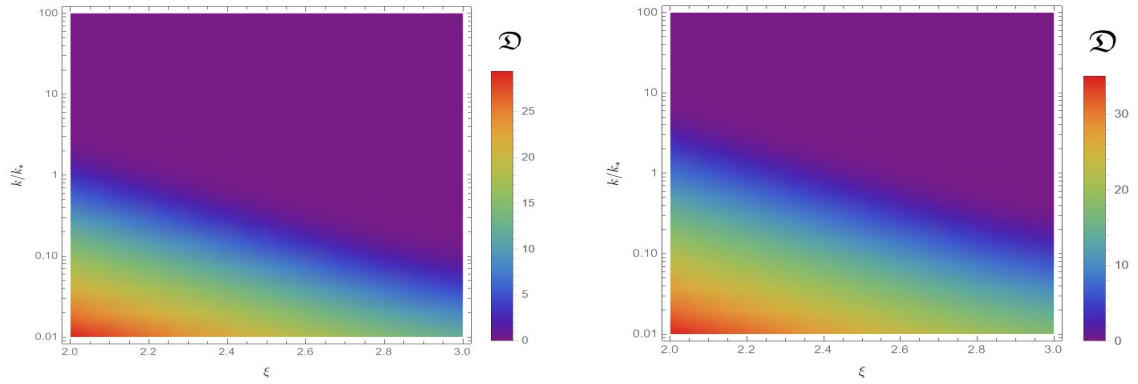

Figure 20: Quantum discord as a function of scale and ξ for two different partitions specified by $\theta = 0.01$ (left) and $\theta = -\pi/4$ (right). The bright colors indicate large discord, while the regions covered in purple correspond to near-zero discord. This heat map was obtained for $\varepsilon = 10^{-3}$, $\eta = 1 - 0.96 - 2\varepsilon$ and $H/M_{\rm Pl} = 10^{-5}$.

Discord increases for large scales and small ξ. This behavior can be compared both to quantum decoherence and state squeezing. First, in Sec. 3.5.2 we showed that decoherence increases with larger gauge field production, i.e. large ξ and in 3.5.3, we also showed that it decreases with increasing comoving scale. As for the state squeezing, which in some sense has an opposite effect on quantum correlations compared to decoherence, we see that the squeezing amplitude r_k decreases with ξ and increases with scale k/k_*. Therefore the quantum discord shown in Fig. 20 is in complete agreement

with previous results. Moreover, it highlights the competition between the state squeezing and decoherence mentioned in Sec. 4.2.

A word of caution is due when interpreting quantum discord. An interesting feature of the heat maps produced above is that if we fix ξ, we get both highly discordant and almost zero-discord results within observable scales. However, as we discussed in Sec. 4.2, the numerical value of quantum discord may contradict the results given by other measures of quantumness, such as Bell inequalities and state separability, so a conclusive assessment would require complementing the quantum discord with other measures.

5 Conclusion

In this thesis, we have studied the quantum-to-classical transition in the early universe. Namely, we have seen how the initial quantum fluctuations can evolve into classical states. We discussed the prospect of detecting any traces of "quantumness" and introduced its measures, such as the CMB Bell inequality and quantum discord. Moreover, we applied the concepts of open quantum systems to axion inflation models to study decoherence in this model. Below, we summarize the key points of each chapter.

After motivating the main study of this thesis in chapter 1, we study inflation in chapter 2, where we discuss the standard cosmological setup and introduce inflation as the leading mechanism that solves the shortcomings of the Hot Big Bang cosmology. We formally derive the scalar perturbations from inflation and confront the problem of quantum-to-classical transition using the squeezed state formalism. We also touch upon decoherence, which, along with state squeezing, is a mechanism by which the classicality of the current cosmological observables, like CMB or LSS, can be explained. Afterward, we study axion inflation, which is the model that is mainly studied under the scope of open quantum systems (OQS) theory in later chapters. We focused on the phenomenology of axion inflation and ultimately derived the power spectrum while taking the axion-U(1) gauge field coupling into account.

Chapter 3 tackles quantum decoherence of primordial fluctuations. We use the master equation formalism to assess decoherence during inflation. Specifically, we use the simplest kind of master equation, the Lindblad equation (C.39). We apply the formalism developed in [2] to axion inflation to understand how decoherence affects the model parameters. An important step in this thesis is to identify the environment and compute its equal time correlation function, which was done in Appendix D. We made a numerical fit to an exponential and retrieved the effective correlation time t_c and correlation length ℓ_c. One of the novel features of our work is the scale-dependent correlation time. We also derive bounds that allow us to use the Lindblad formalism and conclude that the validity of our approach depends on the explicit model and the value of ϕ in that model.

Since the exponential form of the environment correlation function can lead to intractable expressions, in order to continue analytically, we also make the top-hat approximation (3.159) and use both to check for consistency in the rest of the analysis. While the rest of the work is done using the Lindblad formalism, there is another point regarding the environment correlation function that requires a clear explanation. Namely, the correlation function (3.154) increases as we approach the end of inflation $\tau \to 0$, which is in stark contrast with the assumption of stationarity that was used in Appendix C to derive the Lindblad equation. Yet, we did not abandon the Lindblad formalism and used the power spectrum as a sort of test: If by using the Lindblad formalism, we can reproduce the results for the power spectrum in the literature, we deem it acceptable to use. In Sec. 3.5.1, we found that indeed, for values up to $\xi \simeq 2.7$, the relative difference between our results and the standard result (2.153) is within 10% accuracy by using both the top-hat approximation and the entire integral form of the environment correlation function. Notice, that since the current upper bound on ξ_* is 2.3 [17], the Lindblad formalism seems to be accurate within the current observa-

tional bounds. In both cases, for smaller values of ξ, the Lindblad formalism is remarkably accurate. However, the accuracy appears to decrease with increasing ξ. This is expected since increasing ξ effectively increases the axion-gauge field coupling, which means that the backreaction effects become significant, and the Lindblad formalism starts to fail altogether. The error significantly increases for larger ξ and reaches 60% for the integral form of the correlation function and 80% for the top-hat ansatz.

We continued by quantifying quantum decoherence in axion inflation. The results obtained using the top-hat ansatz and the complete integral form of the environment correlator turned out to be drastically different, with values of the decoherence parameters (see Eq. (3.142)) differing by as much as $10^3 \div 10^4$. Moreover, the top-hat solution predicts insufficient decoherence for values $\xi \simeq 2$, which appears to put a lower bound on the interaction strength. However, this is not really the case since the integral form, which is more accurate, predicts that decoherence is sufficient for all values of interest $2 < \xi < 3$. Another important point is that decoherence increases with increasing ξ (see Fig. 14), which is also expected because the enhanced production of gauge fields should have a greater decohering effect.

Finally, in 3.5.3, noticing that ξ is not a constant, we once again analyzed the power spectrum and the decoherence parameter using the scale-dependent expression for ξ. The power spectrum remains in good agreement with the standard result in the literature but starts to deviate on small scales. As for decoherence, using the current bound on the Hubble rate during inflation $H/M_{\rm Pl} \lesssim 2.5 \cdot 10^{-5}$, we obtained that for scales $k/k_* \leq 10^{-15}$, where $k_* = 0.05{\rm Mpc}^{-1}$ decoherence is insufficient. Needless to say, these scales are far beyond what the current instruments can probe. However, in contrast with a heavy scalar environment, where if anything, decoherence increases at large scales, we find that the structure of decoherence in axion inflation such that erasure of quantum correlations is more pronounced on smaller scales compared to their larger counterparts.

Chapter 4 shows the obstructions one faces when it comes to detecting any traces of quantumness, however large, from the early universe. If we neglect decoherence, the emergent squeezed state is considered highly quantum, but detecting its quantum nature using something like the CMB Bell experiment appears to be doomed partially because the decaying mode is inaccessible for current-day probes, but more importantly because unlike experiments performed in the lab, the experiments in cosmology cannot be repeated. We also compare different measures of quantumness for Gaussian states. The quantum discord or the state separability can also be used to differentiate quantum and classical states and are compared in Fig. 18.

For the case of axion inflation, quantum discord is evaluated in Sec. 4.3. According to Fig. 20 discord decreases for increased gauge field production, which is logically consistent with the fact that decoherence increases and that the squeezing parameter decreases with ξ. This is also the case for scale dependence. Namely, discord increases on large scales, while decoherence decreases and squeezing amplitude increases with scale.

Outlook

Here, we present some of the possible future directions of research based on the content of this thesis

- As we have already noticed, the gauge field correlation function appears to grow as we reach the end of inflation, suggesting that the environment cannot be regarded as stationary, which violates one of the base assumptions used to derive the Lindblad equation. While we have circumvented this problem in a pragmatic way by comparing the power spectrum obtained within our framework with the standard one present in the literature, a more precise analysis can be done using non-Markovian master equations [72] such as the time-convolutionless (TCL) master equation. It should be stressed that this approach would make the analysis far more complicated compared to using the Lindblad equation.

- In Sec. 4, we have introduced some measures of "quantumness", such as the Bell inequalities or the quantum discord, which can, in principle, be utilized in cosmology. It would be interesting to extend the work done in this thesis by computing these measures for axion inflation. In principle, this can be done, because due to the linearity of the coupling in the system sector, the final state of the said system is still Gaussian. Analytical techniques developed for continuous-variable quantum information can be directly applied.

- A natural extension of our work is to treat higher-order correlation functions, such as the bispectrum, trispectrum, and so on. Recent observations of CMB have suggested possible hints of parity-odd signatures, though these remain tentative and require further confirmation. Such features could, in principle, originate from parity-violating interactions in the early universe — as predicted by axion inflation models through the coupling $\phi F\tilde{F}$. Studying higher-order primordial correlation functions within this framework is, therefore, especially compelling. A promising future direction would be to apply the open quantum systems formalism to such scenarios in order to explore how parity-violating quantum correlations evolve and potentially decohere during inflation.

- As stressed at the end of Sec. 4.3.4, for a more complete assessment, quantum discord must be complemented with other measures of quantumness. A potential extension to the work done in this thesis could be to work out the regimes in which the Bell inequality is violated, or when the states remain separable. This would shed more light on our current result for quantum discord.

Acknowledgements

I am most thankful to my supervisor, Prof. Nicola Bartolo, whose influence started shaping my research path early on, when I took his course on the cosmology of the early universe. Having long, lively discussions ever since I started research, had a profound impact on the development of my thesis.

I would also like to thank Prof. Daniele Bertacca for the stimulating discussions regarding my thesis and for pointing out issues that required further attention.

Many thanks to the Cosmo group at the University of Padova. I've had ample opportunities to discuss topics related to my thesis work on the weekly meetings.

Outside of academia, I would like to thank my family and friends for giving me the will to pursue my passion. And lastly, to Mariam, thank you for being my greatest supporter.

Appendices

A Relation between the Heisenberg and Schrödinger pictures

In the main text, we have defined the squeezing parameters in the Schrödinger picture. However, since the physics described by the Heisenberg representation is the same as the one described by the Schrödinger picture, we would like to make a connection and try to relate the mode functions, typically used in the Heisenberg picture, with the squeezing parameters, introduced in the main text using the Schrödinger picture (see refs. [29, 28]).

We start by introducing the *Heisenberg picture operators* $\hat{v}(\mathbf{x},\tau)$ and $\hat{p}(\mathbf{x},\tau)$, which can be written as

$$\begin{aligned}\hat{v}(\mathbf{x},\tau) &= \hat{\mathcal{U}}^{\dagger}(\tau,\tau_0)\hat{v}(\mathbf{x},\tau_0)\hat{\mathcal{U}}(\tau,\tau_0) = \int \frac{d^3k}{(2\pi)^{3/2}} e^{i\mathbf{k}\cdot\mathbf{x}} \left(u^{*}_{\mathbf{k}}(\tau)\hat{a}_{\mathbf{k}} + u_{-\mathbf{k}}(\tau)\hat{a}^{\dagger}_{-\mathbf{k}}\right), \\ \hat{p}(\mathbf{x},\tau) &= \mathcal{U}^{\dagger}(\tau,\tau_0)\hat{p}(\mathbf{x},\tau_0)\hat{\mathcal{U}}(\tau,\tau_0) = \int \frac{d^3k}{(2\pi)^{3/2}} e^{i\mathbf{k}\cdot\mathbf{x}} \left(w^{*}_{\mathbf{k}}(\tau)\hat{a}_{\mathbf{k}} + w_{-\mathbf{k}}(\tau)a^{\dagger}_{-\mathbf{k}}\right).\end{aligned} \tag{A.1}$$

The mode functions $u_{\mathbf{k}}(\tau)$ and $w_{\mathbf{k}}(\tau)$ obey the Heisenberg equations of motion. These equations have the following form

$$\begin{aligned}u'_{\mathbf{k}} &= w_{\mathbf{k}} + \frac{z'}{z}u_{\mathbf{k}}, \\ w'_{\mathbf{k}} &= -k^2 u_{\mathbf{k}} - \frac{z'}{z}w_{\mathbf{k}}\end{aligned} \tag{A.2}$$

and equations correspond to the configuration and conjugate momentum variables of the field theory given by the Hamiltonian (2.75). We impose the initial conditions corresponding to the (right oriented) moving wave $u_{\mathbf{k}}(\tau_0) = \sqrt{2k}$ and $w_{\mathbf{k}}(\tau_0) = i\sqrt{k/2}$. The solution to equations (A.2) are now uniquely defined for all times. At the inintial time, one obtains the Schrödinger picture operators given by (2.76). At later times we have

$$\begin{aligned}\hat{v}_{\mathbf{k}}(\tau) &= \frac{1}{\sqrt{2k}}\left(\hat{a}_{\mathbf{k}}(\tau) + \hat{a}^{\dagger}_{-\mathbf{k}}(\tau)\right), \\ \hat{p}_{\mathbf{k}}(\tau) &= -i\sqrt{\frac{k}{2}}\left(\hat{a}_{\mathbf{k}}(\tau) - \hat{a}^{\dagger}_{-\mathbf{k}}(\tau)\right),\end{aligned} \tag{A.3}$$

where $\hat{a}_{\mathbf{k}}(\tau)$ and $\hat{a}^{\dagger}_{\mathbf{k}}(\tau)$ are the Heisenberg picture (thus time-dependent) creation and annihilation operators

$$\begin{aligned}\hat{a}_{\mathbf{k}}(\tau) \equiv \hat{\mathcal{U}}^{\dagger}(\tau,\tau_0)\hat{a}_{\mathbf{k}}(\tau_0)\hat{\mathcal{U}}(\tau,\tau_0) &= \hat{\mathcal{R}}^{\dagger}[\theta_{\mathbf{k}}]\hat{\mathcal{S}}^{\dagger}[r_{\mathbf{k}},\varphi_{\mathbf{k}}]\hat{a}_{\mathbf{k}}\hat{\mathcal{S}}[r_{\mathbf{k}},\varphi_{\mathbf{k}}]\hat{\mathcal{R}}[\theta_{\mathbf{k}}] \\ &= \cosh r_{\mathbf{k}} e^{-i\theta_{\mathbf{k}}} a_{\mathbf{k}} - \sinh r_{\mathbf{k}} e^{i(\theta_{\mathbf{k}}+2\varphi_{\mathbf{k}})} a^{\dagger}_{\mathbf{k}}.\end{aligned} \tag{A.4}$$

Then plugging this into equation (A.3), we get

$$\begin{aligned}\hat{v}_{\mathbf{k}}(\tau) = \frac{1}{\sqrt{2k}}\Big[a_{\mathbf{k}}\left(\cosh r_{\mathbf{k}} e^{-i\theta_{\mathbf{k}}} - \sinh r_{\mathbf{k}} e^{-i(\theta_{\mathbf{k}}+2\varphi_{\mathbf{k}})}\right) \\ + a^{\dagger}_{-\mathbf{k}}\left(\cosh r_{\mathbf{k}} e^{i\theta_{\mathbf{k}}} - \sinh r_{\mathbf{k}} e^{i(\theta_{\mathbf{k}}+2\varphi_{\mathbf{k}})}\right)\Big].\end{aligned} \tag{A.5}$$

$$\begin{aligned}\hat{p}_{\mathbf{k}}(\tau) = -i\sqrt{\frac{k}{2}}\Big[a_{\mathbf{k}}\left(\cosh r_{\mathbf{k}} e^{-i\theta_{\mathbf{k}}} - \sinh r_{\mathbf{k}} e^{-i(\theta_{\mathbf{k}}+2\varphi_{\mathbf{k}})}\right) \\ + a^{\dagger}_{-\mathbf{k}}\left(\cosh r_{\mathbf{k}} e^{i\theta_{\mathbf{k}}} - \sinh r_{\mathbf{k}} e^{i(\theta_{\mathbf{k}}+2\varphi_{\mathbf{k}})}\right)\Big].\end{aligned} \tag{A.6}$$

By simply comparing these equations to (A.1), we obtain a connection between the Schrödinger picture variables and the Heisenber picture mode functions

$$\begin{aligned}u_{\mathbf{k}}(\tau) &= \frac{1}{\sqrt{2k}}\left(\cosh r_{\mathbf{k}} e^{i\theta_{\mathbf{k}}} - \sinh r_{\mathbf{k}} e^{-i(\theta_{\mathbf{k}}+2\varphi_{\mathbf{k}})}\right), \\ w_{\mathbf{k}}(\tau) &= i\sqrt{\frac{k}{2}}\left(\cosh r_{\mathbf{k}} e^{i\theta_{\mathbf{k}}} + \sinh r_{\mathbf{k}} e^{i(\theta_{\mathbf{k}}+2\varphi_{\mathbf{k}})}\right).\end{aligned} \tag{A.7}$$

After some algebra one can easily reproduce the equations of motion (2.93) by solving the Hamilton's equations.

B Axion and gauge field equations of motion

Let us vary the action (3.146) with respect to A^0. Recalling the definition of a functional derivative

$$\frac{\delta f}{\delta g} \equiv \frac{\partial f}{\partial g} - \partial_\mu\left(\frac{\partial f}{\partial(\partial_\mu g)}\right), \tag{B.1}$$

then in our case

$$\frac{\partial \mathcal{L}}{\partial A_0} - \partial_\rho\left(\frac{\partial \mathcal{L}}{\partial(\partial_\rho A_0)}\right) = 0. \tag{B.2}$$

Since the action depends only on the derivatives of the gauge field, the first term is zero. Let us continue with the second term. We first calculate the term in the round brackets and then apply the derivative.

$$\begin{aligned}\frac{\partial \mathcal{L}}{\partial(\partial_\rho A_0)} = \sqrt{-g}\frac{\partial}{\partial(\partial_\rho A_0)}\left[-\frac{1}{4}F^{\mu\nu}F_{\mu\nu} - \frac{\alpha}{4f}\phi\tilde{F^{\mu\nu}}F_{\mu\nu}\right] = \\ = \sqrt{-g}\left[-(\partial^\rho A^0 - \partial^0 A^\rho)\right],\end{aligned} \tag{B.3}$$

where we have used

$$\frac{\partial(\partial_\alpha A_\beta)}{\partial(\partial_\sigma A_\gamma)} = \delta^\sigma_\alpha \delta^\gamma_\beta. \tag{B.4}$$

Notice the derivative of the second term vanished because

$$\epsilon^{\mu\nu\alpha\beta}[\delta^{\mu\rho}\delta^{\nu 0}(\partial_\alpha A_\beta - \partial_\beta A_\alpha) + \delta^{\nu\rho}\delta^{\mu 0}(\partial_\beta A_\alpha - \partial_\alpha A_\beta) + (\mu\nu \leftrightarrow \alpha\beta)] = 4[\nabla \times \vec{A} - \nabla \times \vec{A}] = 0, \tag{B.5}$$

where we have used the definition of a vector product $A \times B = \epsilon^{ijk} A_i B_k$[27].

Then applying the derivative

$$\partial_\rho \left[-(\partial_\rho A_0 - \partial_0 A_\rho)\right] = a^4[\nabla^2 A_0 - \partial_0(\vec{\nabla} \cdot \vec{A})] = [\nabla^2 A^0 - \partial_0(\vec{\nabla} \cdot \vec{A})] = 0. \tag{B.6}$$

Since we are not considering charger particles,

$$(\vec{\nabla} \cdot \vec{A})' = 0. \tag{B.7}$$

which means that $\vec{\nabla} \cdot \vec{A}$ is constant in time and we can set it to zero.

Gauge field equation of motion. Now we vary the action WRT the vector A_i. Following the procedure above

$$\partial_\rho \left[\frac{\partial \mathcal{L}}{\partial(\partial_\rho A_i)}\right] = 0 \tag{B.8}$$

leads to

$$\partial_\rho \left[\frac{\partial S}{\partial(\partial_\rho A_i)}\right] = \partial_\rho \left[-(\partial_\rho A_i - \partial_i A_\rho) + \frac{2\alpha}{f}\phi(\epsilon^{\rho i\alpha\beta}\partial_\alpha A_\beta + \epsilon^{\mu\nu\rho i}\partial_\mu A_\nu)\right]. \tag{B.9}$$

Where we have used $F^{\mu\nu}F_{\mu\nu} = g^{\alpha\mu}g^{\beta\nu}F_{\alpha\beta}F_{\mu\nu}$ and equation B.4. Then finally, after plugging $\rho = 0$ and $\rho = j$, we get

$$\underbrace{-\vec{A}'' + \frac{\alpha}{f}\phi'\vec{\nabla} \times \vec{A} + \frac{\alpha}{f}\phi\left(\vec{\nabla} \times \vec{A}\right)'}_{\rho=0} + \underbrace{\vec{\nabla}^2\vec{A} - \frac{\alpha}{f}\phi\left(\vec{\nabla} \times \vec{A}\right)'}_{\rho=j} = 0. \tag{B.10}$$

Finally, the equation of motion for the gauge field reads:

$$\vec{A}'' - \frac{\alpha}{f}\phi'\vec{\nabla} \times \vec{A} + \vec{\nabla}^2\vec{A} = 0. \tag{B.11}$$

Inflaton equation of motion. Varying the action WRT ϕ leads to

$$\frac{\partial \mathcal{L}}{\partial \phi} - \partial_\rho\left(\frac{\partial \mathcal{L}}{\partial(\partial_\rho \phi)}\right) = 0. \tag{B.12}$$

Let us compute the first term

$$\frac{\partial \mathcal{L}}{\partial \phi} = -\sqrt{-g}\left[\frac{\partial V}{\partial \phi} + \frac{\alpha}{4f}\tilde{F}^{\mu\nu}F_{\mu\nu}\right]. \tag{B.13}$$

[27] Repeated indices are summed over throughout the appendix.

Claim: If we define

$$\vec{B} = \frac{1}{a^2}\epsilon^{ijk}\partial_i A_k \equiv \frac{1}{a^2}\vec{\nabla}\times\vec{A}, \qquad \vec{E} = -\frac{1}{a^2}\partial_0 A_i \equiv -\frac{1}{a^2}\vec{A}', \tag{B.14}$$

in analogy with electromagnetism, we then get $\tilde{F}^{\mu\nu}F_{\mu\nu} = -4\vec{E}\cdot\vec{B}$.
Proof:

$$\tilde{F}^{\mu\nu}F_{\mu\nu} = \frac{1}{2a^4}\epsilon^{\mu\nu\alpha\beta}\left[\partial_\alpha A_\beta \partial_\mu A_\nu - \partial_\alpha A_\beta \partial_\nu A_\mu - \partial_\beta A_\alpha \partial_\mu A_\nu + \partial_\beta A_\alpha \partial_\nu A_\mu\right]. \tag{B.15}$$

The completely antisymmetric tensor is zero if two of its indices coincide, therefore, one of the indices must be temporal. For example, if $\mu = 0$, then $\nu\alpha, \beta$ must be spatial indices, which we will denote as i, j, k respectively

$$\tilde{F}^{0i}F_{0i} = \frac{1}{2a^4}\epsilon^{0ijk}\left[\partial_j A_k \partial_0 A_i - \partial_k A_j \partial_0 A_i\right] = \frac{1}{a^4}\dot{\vec{A}}\left(\vec{\nabla}\times\vec{A}\right) = -\vec{B}\cdot\vec{E}. \tag{B.16}$$

It is trivial to show that switching the temporal index to ν, α and β yield the same result. Therefore by summing these terms we finally get

$$\tilde{F}^{\mu\nu}F_{\mu\nu} = -4\vec{B}\cdot\vec{E}. \tag{B.17}$$

Using (B.17) we immediately see that

$$\frac{\partial\mathcal{L}}{\partial\phi} = -a^4\left[\frac{\partial V}{\partial\phi} - \frac{\alpha}{f}\vec{E}\cdot\vec{B}\right]. \tag{B.18}$$

As for the second term in B.12,

$$\begin{aligned}\partial_\rho\left(\frac{\partial\mathcal{L}}{\partial(\partial_\rho\phi)}\right) &= \partial_\rho\left(\frac{a^4}{2}\frac{\partial}{\partial(\partial_\rho\phi)}(g^{\mu\nu}\partial_\mu\phi\partial_\nu\phi)\right) = \\ &= \partial_\rho\left(\frac{a^4}{2}(g^{\rho\nu}\partial_\nu\phi + g^{\mu\rho}\partial_\mu\phi)\right) = \partial_\rho(a^4 g^{\mu\rho}\partial_\mu\phi) = \sqrt{-g}\Box\phi.\end{aligned} \tag{B.19}$$

where we have used the general definition of the D'Alambertian in curved spacetimes. Expanding it out explicitly

$$\Box\phi = \frac{1}{a^4}\partial_0\left(a^4\left(-\frac{1}{a^2}\right)\partial_0\phi\right) + \frac{1}{a^4}\partial_i(a^4\frac{1}{a^2}\partial_i\phi) = -\frac{2}{a^3}a'\phi' - \frac{1}{a^2}\phi'' + \frac{1}{a^2}\nabla^2\phi. \tag{B.20}$$

Finally the equation of motion reads

$$\phi'' + 2\mathcal{H}\phi' - \nabla^2\phi + a^2\frac{dV}{d\phi} = a^2\frac{\alpha}{f}\vec{E}\cdot\vec{B}. \tag{B.21}$$

C Derivation of the Lindblad equation

We follow ref [2] and derive the Lindblad equation, that can be implemented directly in a cosmological scenario.

A combined Hilbert space of the system ("S") and the environment("E") is a tensorial product of the separate Hilbert spaces $\mathcal{H} = \mathcal{H}_S \otimes \mathcal{H}_E$. Thus the full Hamiltonian can be written as

$$H = H_0 + H_{\text{int}} = H_S \otimes I_E + H_E \otimes I_S + gH_{\text{int}}, \tag{C.1}$$

with H_S acting on the Hilbert space of our system and H_E on the environment, both being parts of the free Hamiltonian H_0. $I_{S(E)}$ being identity operators acting in corresponding Hilbert spaces. g plays the role of the coupling between the system and the environment and H_{int} describes the interactions.

As we have seen in Sec. 3.3, evolution of the density matrix $\hat{\rho}$ is governed by the Liouville-von Neumann equation

$$\frac{d\hat{\rho}}{dt} = -i[H, \hat{\rho}]. \tag{C.2}$$

Moving to the interaction picture, we can factor out the time dependence due to the free Hamiltonian from ρ. To do this we can introduce[28]

$$\begin{aligned} \tilde{\rho}(t) &= U^\dagger(t)\hat{\rho}(t)U(t), \\ \tilde{H}_{\text{int}}(t) &= U^\dagger(t)H_{\text{int}}U(t). \end{aligned} \tag{C.3}$$

where $U(t) = e^{-i\int_o^t dt' H_0(t')}$ is the unitary evolution operator. Then the time evolution of this operator is given by

$$\frac{dU(t)}{dt} = -iH_0(t)U(t), \tag{C.4}$$

so that

$$\begin{aligned} \frac{d\tilde{\rho}}{dt} = iH_0\tilde{\rho}(t) - iU^\dagger(t)[H, \rho(t)]U(t) - i\tilde{\rho}(t)H_0 = i[H_0, \tilde{\rho}(t)] - i(U^\dagger(t)\rho(t)U(t)U^\dagger(t)HU(t)+ \\ +U^\dagger(t)HU(t)U^\dagger(t)\rho(t)U(t)) = \cancel{i[\tilde{H_0}, \rho(t)]} - \cancel{i[H_0, \tilde{\rho}(t)]} - ig[\tilde{H}_{\text{int}}, \tilde{\rho}(t)]. \end{aligned} \tag{C.5}$$

We can formally integrate this, yielding

$$\tilde{\rho}(t + \Delta t) = \tilde{\rho}(t) - ig\int_t^{t+\Delta t} dt'[\tilde{H}_{\text{int}}(t'), \tilde{\rho}(t')], \tag{C.6}$$

[28] By equations C.3, the evolution of the states is governed by H_{int}, whereas the evolution of the operators will be governed by H_0.

which we expanding iteratively

$$\tilde{\rho}(t+\Delta t) = \tilde{\rho}(t) - ig\int_t^{t+\Delta t} dt'[\tilde{H}_{\text{int}}(t'), \tilde{\rho}(t)] + \\ (-ig)^2 \int_t^{t+\Delta t} dt' \int_t^{t'} dt''[\tilde{H}_{\text{int}}(t'), [\tilde{H}_{\text{int}}(t''), \tilde{\rho}(t)]] + \mathcal{O}(g^3). \tag{C.7}$$

Here we have neglected higher order terms by imposing the Born approximation (weak coupling). Switching the dependence of $\tilde{\rho}$ with respect to t in the second term of the sum by t'' yields a correction of a higher order in g, which we are neglecting since we are focusing on up to second order expansion in g, hence

$$\tilde{\rho}(t+\Delta t) - \tilde{\rho}(t) = -ig\int_t^{t+\Delta t} dt'[\tilde{H}_{\text{int}}(t'), \tilde{\rho}(t)] + \\ (-ig)^2 \int_t^{t+\Delta t} dt' \int_t^{t'} dt''[\tilde{H}_{\text{int}}(t'), [\tilde{H}_{\text{int}}(t''), \tilde{\rho}(t'')]] + \mathcal{O}(g^3). \tag{C.8}$$

Since the interaction should not have any significant effect on the environment, we can restrict ourselves to the *reduced density matrix* (see section 3.2.3):

$$\tilde{\rho}_S(t) = Tr_E\{\tilde{\rho}(t)\}, \tag{C.9}$$

where the environment degrees of freedom have been traced out. We rewrite (C.8) as

$$\tilde{\rho}_S(t+\Delta t) - \tilde{\rho}_S(t) = -ig\int_t^{t+\Delta t} dt' Tr_E\{[\tilde{H}_{\text{int}}(t'), \tilde{\rho}(t)]\} + \\ (-ig)^2 \int_t^{t+\Delta t} dt' \int_t^{t'} dt'' Tr_E\{[\tilde{H}_{\text{int}}(t'), [\tilde{H}_{\text{int}}(t''), \tilde{\rho}(t'')]]\} + \mathcal{O}(g^3). \tag{C.10}$$

In practice, we can also define a reduced density matrix for the environment in the same way: $\tilde{\rho}_E = Tr_S\{\tilde{\rho}(t)\}$, however this does not always mean that $\tilde{\rho}(t) = \tilde{\rho}_S(t) \otimes \tilde{\rho}_E(t)$, but in fact

$$\tilde{\rho}(t) = \tilde{\rho}_S(t) \otimes \tilde{\rho}_E(t) + g^p \tilde{\rho}(t)_{corr}. \tag{C.11}$$

Here p is an integer. The last term characterizes interactions between the environment and the system, that is if we start from a situation, in which the density operators can be factorized and $\rho(t)_{corr} = 0$, we will obtain the non-zero correlation term only if we switch on the interaction.

Claim: $Tr_E\{\tilde{\rho}_{corr}\} = 0 = Tr_S\{\tilde{\rho}_{corr}\}$.
Proof: Lets focus on $Tr_S\{\tilde{\rho}_{corr}\} = 0$, the second relation can be shown in the same manner. utilizing the fact that $Tr_S\{\tilde{\rho}_E(t)\} = \tilde{\rho}_E(t)$ and the normalization $Tr\{\tilde{\rho}(t)\} = Tr_S Tr_E(\tilde{\rho}(t)) = 1$, we have:

$$Tr_S\{\tilde{\rho}(t)\} = Tr_S\{\tilde{\rho}_S(t)\}\tilde{\rho}_E(t) + g^p Tr_S\{\tilde{\rho}_{corr}(t)\} = \tilde{\rho}_E(t) + g^p Tr_S\{\tilde{\rho}_{corr}(t)\} \tag{C.12}$$

however, as defined before $Tr_S\{\rho(t)\} = \rho_E$, which leads to $Tr_S\{\rho_{corr}(t)\} = 0$.

(C.11)→ (C.10):

$$\begin{aligned}
\tilde{\rho}_S(t+\Delta t) - \tilde{\rho}_S(t) = -ig\int_t^{t+\Delta t} dt' Tr_E\{[\tilde{H}_{\text{int}}(t'), \tilde{\rho}_S(t)\otimes\tilde{\rho}_E(t)]\} - \quad \text{(A)}\\
-ig^{p+1}\int_t^{t+\Delta t} dt' Tr_E\{[\tilde{H}_{\text{int}}(t'), \tilde{\rho}_{corr}(t)]\} + \quad \text{(B)}\\
(-ig)^2\int_t^{t+\Delta t} dt'\int_t^{t'} dt'' Tr_E\{[\tilde{H}_{\text{int}}(t'), [\tilde{H}_{\text{int}}(t''), \tilde{\rho}_E(t'')\otimes\tilde{\rho}_S(t'')]]\} + \quad \text{(C)}\\
+(-ig)^{p+2}\int_t^{t+\Delta t} dt'\int_t^{t'} dt'' Tr_E\{[\tilde{H}_{\text{int}}(t'), [\tilde{H}_{\text{int}}(t''), \tilde{\rho}_{corr}(t'')]]\} + \mathcal{O}(g^3). \quad \text{(D)}
\end{aligned} \tag{C.13}$$

Now we assume the interacting Hamiltonian of the form

$$H_{int}(t) = A(t)\otimes R(t), \tag{C.14}$$

where A acts on $\mathcal{H}_S$ and R on $\mathcal{H}_E$. Then $U(t)$ can be factorized: $U(t) = U_S\otimes U_E$ [29].

Let us evaluate the term (A). In this term we have[30]

$$\begin{aligned}
Tr_E\{[\tilde{H}_{\text{int}}(t'), \tilde{\rho}_S(t)\otimes\tilde{\rho}_E(t)]\} = \tilde{A}(t')\tilde{\rho}_S(t)\otimes Tr_E\{\tilde{R}(t')\tilde{\rho}_{E(t)}\} +\\
\tilde{\rho}_S(t)\tilde{A}(t')\otimes Tr_E\{\tilde{\rho}_E(t)\tilde{R}(t')\} = [\tilde{A}(t'), \tilde{\rho}_S(t)]Tr\{\tilde{R}(t')\tilde{\rho}_E(t)\}
\end{aligned} \tag{C.16}$$

because of the cyclic property of the trace.

Let us now make some approximations:

1. The influence of the interaction is negligible for the environment $\longrightarrow \tilde{\rho}_E(t) \simeq \tilde{\rho}_E \equiv \tilde{\rho_E}$ in the interaction picture, which is not to say that ρ is time-independent, however in the typical time-frame in which the system evolves due to interactions the evolution of the environment two-point correlation function decays rapidly.

[29] Equation (C.14) is introduced without the tildes, however we can trivially show that it also holds for the associated quantities with tildes. Namely,

$$\tilde{H}_{\text{int}}(t) = (U_S^\dagger\otimes U_E^\dagger)(A\otimes R)(U_S\otimes U_E) = (U_S^\dagger A U_S)\otimes(U_E^\dagger R U_E) = \tilde{A}\otimes\tilde{R} \tag{C.15}$$

.

[30] A and ρ_S come out of the trace obviously and operators acting on different Hilbert spaces will commute.

2. Stationary state for the environment $\Rightarrow H_E$ is not explicitly time dependent and $[\tilde{\rho}_E, H_E] = 0$. Then by the definition of the evolution operator U_E, we immediately get $[\rho_E, U_E] = 0$. This also implies that $\rho_E(t) = e^{-iH_E t}\tilde{\rho}_E e^{iH_E t}$, which means that $\rho_E = \tilde{\rho}_E$. On the other hand this means that $[\rho_E, H_E] = 0$.

   Now we can write

$$\tilde{\rho}_E = \sum_n p_n |n\rangle \langle n| , \tag{C.17}$$

   where $|n\rangle$ are eingenvectors of H_E, with eingenvalue E_n, and p_n is a real constant.[31]

3. the mean value of the environment part of the Hamiltonian vanishes, namely

$$\langle R \rangle = Tr_E\{R\tilde{\rho}_E\} = 0. \tag{C.18}$$

   This means that Ⓐ $= 0$. Notice that this also means that $\langle \tilde{R} \rangle = 0$. Namely using the cyclic property of the trace along with the fact that $\tilde{\rho}_E$ commutes with U_E

$$\begin{aligned} Tr_E\{\tilde{R}\tilde{\rho}_E\} = Tr_E\{U_E^\dagger R U_E \tilde{\rho}_E\} = Tr_E\{U_E \tilde{\rho}_E U_E^\dagger R\} = \\ = Tr_E\{\tilde{\rho}_E U_E U_E^\dagger R\} = Tr_E\{\tilde{\rho}_E R\} = 0. \end{aligned} \tag{C.19}$$

   Now, going back to eq. (C.13) and noticing that the LHS should be proportional to g^p at leading order in g, since in the absence of interaction $\tilde{\rho}_S$ does not evolve in the interaction picture. Then since the RHS is proportional to g of order $p+1, 2$ and $p+2$, the only possibility left is to identify $p = 2$.

   Out of the three terms left over, the dominant one is obviously Ⓒ, so

$$\tilde{\rho}_S(t+\Delta t) - \tilde{\rho}_S(t) \simeq (-ig)^2 \int_t^{t+\Delta t} dt' \int_t^{t'} dt'' Tr_E\{[\tilde{H}_{\text{int}}(t'), [\tilde{H}_{\text{int}}(t''), \tilde{\rho}_E \otimes \tilde{\rho}_S(t'')]]\}. \tag{C.20}$$

4. Eq. (C.20) is valid at leading order in g, which is why the fourth approximation must be made. Namely the interaction should evolve the system perturbatively. We can see how the trace in

[31] One can easily see that in fact $\tilde{\rho}_E H_E - H_E \tilde{\rho}_E \propto E_n - E_n = 0$

(C.20) can be rewritten using equation (C.14) and again the cyclicity of the trace operation:

$$\begin{aligned}
&Tr_E\{[\tilde{H}_{\text{int}}(t'),[\tilde{H}_{\text{int}}(t''),\tilde{\rho}_E\otimes\tilde{\rho}_S(t'')]]\} = \\
&= \tilde{A}(t')\tilde{A}(t'')\tilde{\rho}_S(t'')Tr_E\{\tilde{R}(t')\tilde{R}(t'')\tilde{\rho}_E\} - \tilde{A}(t')\tilde{\rho}_S(t'')\tilde{A}(t'')Tr_E\{\tilde{R}(t')\tilde{\rho}_E\tilde{A}(t'')\}- \\
&-\tilde{A}(t'')\tilde{\rho}_S(t'')\tilde{A}(t')Tr_E\{\tilde{R}(t'')\tilde{\rho}_E\tilde{A}(t')\} + \tilde{\rho}_S(t'')\tilde{A}(t'')\tilde{A}(t')Tr_E\{\tilde{\rho}_E\tilde{R}(t'')\tilde{R}(t')\} = \\
&= \tilde{A}(t')\tilde{A}(t'')\tilde{\rho}_S(t'')Tr_E\{\tilde{\rho}_E\tilde{R}(t')\tilde{R}(t'')\} - \tilde{A}(t')\tilde{\rho}_S(t'')\tilde{A}(t'')Tr_E\{\tilde{\rho}_E\tilde{R}(t'')\tilde{R}(t')\}- \\
&-\tilde{A}(t'')\tilde{\rho}_S(t'')\tilde{A}(t')Tr_E\{\tilde{\rho}_E\tilde{R}(t')\tilde{R}(t'')\} + \tilde{\rho}_S(t'')\tilde{A}(t'')\tilde{A}(t')Tr_E\{\tilde{\rho}_E\tilde{R}(t'')\tilde{R}(t')\} = \\
&= \left(\tilde{A}(t')\tilde{A}(t'')\tilde{\rho}_S(t'') - \tilde{A}(t'')\tilde{\rho}_S(t'')\tilde{A}_S\right)C_R(\tau)+ \\
&+ \left(\tilde{\rho}_S(t'')\tilde{A}(t'')\tilde{A}(t') - \tilde{A}(t\rho)_S(t'')\tilde{A}(t'')\right)C_R(-\tau),
\end{aligned} \tag{C.21}$$

where we have introduced the correlation function of the environment

$$C_R(t',t'') = C_R(\tau) = Tr_E\{\tilde{\rho}_E\tilde{R}(t')\tilde{R}(t'')\}. \tag{C.22}$$

Environment being stationary, we can actually show that the two-point function depends on $\tau = t' - t''$ only:

$$\begin{aligned}
C_R(t',t'') &= Tr_E\{\tilde{\rho}_E e^{iH_E t'}\tilde{R}(0)e^{-iH_E t'}e^{iH_E t''}\tilde{R}(0)e^{-iH_E t''}\} = \\
&= Tr_E\{\tilde{\rho}_E e^{iH_E t''}e^{iH_E \tau}\tilde{R}(0)e^{-iH_E \tau}\tilde{R}(0)e^{-iH_E t''}\} = \\
&= Tr_E\{\tilde{\rho}_E e^{iH_E t''}\tilde{R}(\tau)\tilde{R}(0)e^{-iH_E t''}\} = \\
&= Tr_E\{\tilde{\rho}_E\tilde{R}(\tau)\tilde{R}(0)\} \equiv C_R(\tau),
\end{aligned} \tag{C.23}$$

where we used the cyclicity of the trace along with the commutation relation $[\rho_E, H_E] = 0$. We can put the correlator in a more explicit form. We can use (17) and write

$$\begin{aligned}
C_R(\tau) &= \sum_m \langle m|\left(\sum_n p_n|n\rangle\langle n|\tilde{R}(\tau)\tilde{R}(0)\right)|m\rangle = \\
&= \sum_{/n}\sum_m p_n\delta_{mn}\langle n|\tilde{R}(\tau)\tilde{R}(0)|m\rangle = \\
&\sum_n p_n\langle n|\tilde{R}(\tau)\tilde{R}(0)|n\rangle = \\
&= \sum_n p_n\langle n|e^{iH_E\tau}\tilde{R}(0)e^{-iH_E\tau}\tilde{R}(0)|n\rangle = \\
&= \sum_{n,m,p,q} p_n\langle n|e^{iH_E\tau}|m\rangle\langle m|\tilde{R}(0)|p\rangle\langle p|e^{-iH_E\tau}|q\rangle\langle q|\tilde{R}(0)|n\rangle = \\
&= \sum_{n,p} p_n e^{i(E_n-E_p)\tau}|\langle n|\tilde{R}(0)|p\rangle|^2,
\end{aligned} \tag{C.24}$$

where we have used the properties of the Kronecker delta twice. Particularly, one can imme-

diately see that $C_R(-\tau) = C_R^*(\tau)$. In the limit where the environment contains (an alsmost) continuous number of energy levels, destructive interference occurs and quickly drives $C_R(\tau)$ to zero within a characteristic time t_c, $C_R(\tau) \simeq C(0)e^{-\tau/t_c}$.

Using (C.21), we can make a further simplification

$$\begin{aligned}\int_t^{t+\Delta t} dt' \int_t^{t'} dt'' Tr_E\{[\tilde{H}_{\text{int}}(t'), [\tilde{H}_{\text{int}}(t''), \tilde{\rho}_E(t'') \otimes \tilde{\rho}_S(t'')]]\} = \\ = \int_t^{t+\Delta t} dt' \int_t^{t'} dt'' \Big(\Big[\tilde{A}(t')\tilde{A}(t'')\tilde{\rho}_S(t'') - \tilde{A}(t'')\tilde{\rho}_S(t'')\tilde{A}(t')\Big] C_R(t'-t'') - \\ - \Big[\tilde{A}(t')\tilde{\rho}(t'')\tilde{A}(t'')\tilde{A}(t')\Big] C_R(t''-t')\Big).\end{aligned} \tag{C.25}$$

We can reparametrize the integration domain using t' and $\tau = t' - t''$. τ obviously takes on values from 0 to Δt because if we fix t'' to be equal to t the maximum value acquired by τ within the previous domain is $\tau = t + \Delta t - t = \Delta t$. Once τ is fixed the t' obviously varies from $t + \tau$ to $t + \Delta t$:

$$\int_t^{t+\Delta t} dt' \int_t^{t'} dt'' = \int_0^{\Delta t} d\tau \int_{t+\tau}^{t+\Delta t} dt'. \tag{C.26}$$

We can consider an extended integration domain, however it should be noted that because of the existence of the two point functions in (25) the integrand vanishes for $\tau \gg t_c$, so the integrand support is limited by this condition. Let us extend the integrand in the following way[32]

$$\int_0^{\infty} d\tau \int_t^{t+\Delta t} dt'. \tag{C.27}$$

Where the upper bound on τ has been extended to ∞ and the lower bound on t' to t.

5. In the limit where $t_c \ll \Delta t$, the new integration domains imposed by extending the previous one contribute negligibly to the entire integral. Hence the fifth assumption

$$t_c \ll \Delta t, \tag{C.28}$$

which means that the *enviromnent* correlation time must be much shorter than the evolution time of the density matrix. Under this assumption we get

$$\begin{aligned}\tilde{\rho}_S(t+\Delta t) - \tilde{\rho}_S(t) \simeq \\ -g^2 \int_0^{\infty} d\tau \int_t^{t+\Delta t} dt' \Big([\tilde{A}(t')\tilde{A}(t'-\tau)\tilde{\rho}_S(t'-\tau) - \tilde{A}(t'-\tau)\tilde{\rho}_S(t'-\tau)\tilde{A}(t')\Big] C_R(\tau) - \\ - \Big[\tilde{A}(t')\tilde{\rho}(t'-\tau)\tilde{A}(t'-\tau)\tilde{A}(t') - \tilde{\rho}_S(t'-\tau)\tilde{A}(t'-\tau)\tilde{A}(t')\Big] C_R(-\tau)\Big).\end{aligned} \tag{C.29}$$

[32] This will render the computation much easier and will not change the outcome significantly

If Δt is smaller than the time-frame in which A varies[33], $\tilde{A}(t') \simeq \tilde{A}(t)$ and $\tilde{A}(t'-\tau) \simeq \tilde{A}(t-\tau)$. The integral WRT t' can now be taken trivially. Furthermore, we can divide both sides by Δt to finally obtain the time derivative; On the RHS Δt will actually cancel with the one coming from the integration by t'

$$\begin{aligned}\frac{\Delta\tilde{\rho}_S}{\Delta t} = -g^2 \int_0^\infty d\tau \Big(\left[\tilde{A}(t)\tilde{A}(t-\tau)\tilde{\rho}_S(t) - \tilde{A}(t-\tau)\tilde{\rho}_S(t)\tilde{A}(t)\right] C_R(\tau) - \\ - \left[\tilde{A}(t)\tilde{\rho}(t)\tilde{A}(t-\tau)\tilde{A}(t) - \tilde{\rho}_S(t)\tilde{A}(t-\tau)\tilde{A}(t)\right] C_R(-\tau)\Big),\end{aligned} \tag{C.30}$$

where we have also used the fact that since the variation of $\tilde{\rho}_S$ between t and $t+\Delta t$ is of order g^2 and the RHS is already of that order, we can simply write $\tilde{\rho}(t)$ because the corrections arising from this change gives rise to higher order terms which we can neglect.

We can define

$$\begin{aligned}L_1(t) &\equiv g^2 \int_0^\infty d\tau C_R(\tau)\tilde{A}(t-\tau), \\ L_2(t) &\equiv g^2 \int_0^\infty d\tau C_E^*(\tau)\tilde{A}(t-\tau) = L_1^\dagger,\end{aligned} \tag{C.31}$$

where we have used $C_R(-\tau) = C_R^*(\tau)$. The last equation holds if in fact $\tilde{A}$ is Hermitian. Before we plug these definitions into (C.30), note that under the fifth assumption $L_1(t)$ and $L_2(t)$ can be simplified. Specifically, because the correlation function decays as $\propto e^{-|\tau|/t_c}$, the integrals above are dominated by the contribution of a finite interval $\tau \in [0\,, \text{few } t_c]$. Since $\tilde{A}$ varies on timescales much longer than Δt (recall $\Delta t \gg t_c$), it will obviously not vary much within this interval. This allows us to perform the integral analytically:

$$L_1(t) = g^2 \int_0^\infty d\tau C_R(0) e^{-|\tau|/t_c}\tilde{A}(t) = g^2\tilde{A}(t)C_R(0)t_c \tag{C.32}$$

and the same for $L_2(t)$. Then we get

$$\begin{aligned}\frac{d\tilde{\rho}_S}{dt} &= -g^2 C_R(0)t_c\Big(\tilde{A}(t)\tilde{A}(t)\tilde{\rho}_S(t) - \tilde{A}(t)\tilde{\rho}_S(t)\tilde{A}(t) - \tilde{A}(t)\rho_S(t)\tilde{A}(t) - \tilde{\rho}_S(t)\tilde{A}(t)\tilde{A}(t)\Big) = \\ &= -g^2 C_R(0)t_c\left(\tilde{A}(t)[\tilde{A}(t), \tilde{\rho}_S(t)] - [\tilde{A}(t), \tilde{\rho}_S(t)]\tilde{A}(t)\right) = \\ &= -g^2 C_R(0)t_c[\tilde{A}(t), [\tilde{A}(t), \tilde{\rho}_S(t)]].\end{aligned} \tag{C.33}$$

By going back to the standard picture we re-obtain the free evolution term; in particular,

$$\frac{d\hat{\rho}_S}{dt} = i[\hat{\rho}_S, H_S] - g^2 C_R(0)t_c[A, [A, \hat{\rho_S}]]. \tag{C.34}$$

This is called the *Lindblad equation*.

[33] This, in turn means, that A should vary on timescales much larger than the autocorrelation time of the environment (see eq. (28)).

It can be generalized easily by considering a more generic interaction Hamiltonian

$$H_{\text{int}} = \sum_i A_i(t) \otimes R_i(t). \tag{C.35}$$

The environment correlator in this case will be defined as

$$C_{R,ij}(t,t') = Tr_E\{\tilde{\rho}_E \tilde{R}_i(t)\tilde{R}_j(t')\}. \tag{C.36}$$

And naturally, the Lindblad equation will take the following form

$$\frac{d\rho_S}{dt} = i[\rho_S, H_S] - g^2 \sum_{i,j} C_{R,ij}(0) t_{c,ij} [A_i, [A_j, \rho_S]] \tag{C.37}$$

where in addition to the assumptions made before, we also imposed $C_{R,ij} = C_{R,ji}$.

Furthermore, we can consider continuous parameters $\mathbf{x}$ and $\mathbf{y}$, instead of i and j that leads to the interacting Hamiltonian of the form

$$H_{\text{int}} = \int d^3\mathbf{x} A(t,\mathbf{x}) \otimes R(t,\mathbf{x}), \tag{C.38}$$

that will modify (C.37):

$$\frac{d\rho_S}{dt} = i[\rho_S, H_S] - \frac{\gamma}{2} \int d^3x d^3y C_R(\mathbf{x},\mathbf{y}) [A(\mathbf{x}), [A(\mathbf{y}), \rho_S]], \tag{C.39}$$

where

$$\gamma = 2g^2 t_c, \tag{C.40}$$

because any dependence of t_c on $\mathbf{x}$ and $\mathbf{y}$ can be absorbed into $C_R(\mathbf{x},\mathbf{y})$.

D Gauge field correlator

In Appendix C we found that the environment correlation function plays a crucial role in the Lindblad equation. Given the coupling $\phi\tilde{F}F$, we identify the gauge fields as the environment as we did in sec. 3.5 (see equation (3.151)). First, we notice that the Fourier transform of the last term in (3.151), $\langle \partial_\tau \vec{A} \cdot (\vec{\nabla} \times \vec{A}) \rangle_{\text{stat}}$ is proportional to $\delta^{(3)}(\mathbf{k})$ and so it will not affect modes with $\mathbf{k} \neq 0$[34]. Therefore, we need to compute $a^4(\tau')a^4(\tau'')\langle (\vec{B}\cdot\vec{E})(\mathbf{k},\tau')(\vec{B}\cdot\vec{E})(\mathbf{k},\tau'')\rangle \equiv \langle j_{\mathbf{k}}(\tau') j_{\mathbf{k}'}(\tau'')\rangle$. Let us write $j_{\mathbf{k}(\tau')}$

[34] According to [27], the right-hand-side of the first equation in 2.123 will not source any $\mathbf{k} \neq 0$ perturbations and since we are interested in the latter, we may neglect it in deriving the power spectrum all together.

more explicitly

$$
\begin{gathered}
j_{\mathbf{k}}(\tau') = \int \frac{d^3x}{(2\pi)^{3/2}} [\nabla \times \vec{A}(\mathbf{x},\tau')] \cdot [\partial_0 \vec{A}(\mathbf{x},\tau')] e^{i\mathbf{k}\cdot\mathbf{x}} = \\
\int \frac{d^3x}{(2\pi)^{3/2}} \frac{d^3q}{(2\pi)^{3/2}} \frac{d^3q'}{(2\pi)^{3/2}} e^{-i(\mathbf{k}-\mathbf{q}-\mathbf{q}')\cdot\mathbf{x}} q(\vec{\varepsilon}(\mathbf{q}) \cdot \vec{\varepsilon}(\mathbf{q}')) \times \\
\left(a(\mathbf{q})A(\tau',q) + a^\dagger(-\mathbf{q})A^*(\tau',q)\right)\left(a(\mathbf{q}')A'(\tau',q') + a^\dagger(-\mathbf{q}')A'^*(\tau',q')\right)
\end{gathered}
\tag{D.1}
$$

Finally, using the properties of the delta function, the triple integral simplifies to

$$
\begin{gathered}
j_{\mathbf{k}}(\tau') = \int \frac{d^3q}{(2\pi)^3} q \left(\vec{\varepsilon}(\mathbf{q}) \cdot \vec{\varepsilon}(\mathbf{k}-\mathbf{q})\right) \times \\
[a(\mathbf{q})A(\tau',|\mathbf{q}|)a(\mathbf{k}-\mathbf{q})A'(\tau',|\mathbf{k}-\mathbf{q}|) + a(\mathbf{q})A(\tau',|\mathbf{q}|)a^\dagger(\mathbf{q}-\mathbf{k})A'^*(\tau',|\mathbf{q}-\mathbf{k}|) + \\
a^\dagger(-\mathbf{q})A^*(\tau',|\mathbf{q}|)a(\mathbf{k}-\mathbf{q})A'(\tau',|\mathbf{k}-\mathbf{q}|) + a^\dagger(-\mathbf{q})A^*(\tau',|\mathbf{q}|)a^\dagger(\mathbf{q}-\mathbf{k})A'^*(\tau',|\mathbf{q}-\mathbf{k}|)].
\end{gathered}
\tag{D.2}
$$

Now that we have the explicit form, we can calculate the correlation function

$$
\begin{gathered}
\langle j_{\mathbf{k}}(\tau') j_{\mathbf{k}'}(\tau'')\rangle = \int \frac{d^3q}{(2\pi)^{3/2}} \frac{d^3q'}{(2\pi)^{3/2}} qq' |\vec{\varepsilon}(\mathbf{q})\vec{\varepsilon}(\mathbf{k}-\mathbf{q})||\vec{\varepsilon}(\mathbf{q}')\vec{\varepsilon}(\mathbf{k}'-\mathbf{q}')| \times \\
\langle [a(\mathbf{q})A(\tau',|\mathbf{q}|)a(\mathbf{k}-\mathbf{q})A'(\tau',|\mathbf{k}-\mathbf{q}|) + a(\mathbf{q})A(\tau',|\mathbf{q}|)a^\dagger(\mathbf{q}-\mathbf{k})A'^*(\tau',|\mathbf{q}-\mathbf{k}|) + \\
a^\dagger(-\mathbf{q})A^*(\tau',|\mathbf{q}|)a(\mathbf{k}-\mathbf{q})A'(\tau',|\mathbf{k}-\mathbf{q}|) + a^\dagger(-\mathbf{q})A^*(\tau',|\mathbf{q}|)a^\dagger(\mathbf{q}-\mathbf{k})A'^*(\tau',|\mathbf{q}-\mathbf{k}|)] \times \\
[a(\mathbf{q}')A(\tau'',|\mathbf{q}'|)a(\mathbf{k}'-\mathbf{q}')A'(\tau'',|\mathbf{k}'-\mathbf{q}'|) + a(\mathbf{q}')A(\tau'',|\mathbf{q}'|)a^\dagger(\mathbf{q}'-\mathbf{k}')A'^*(\tau'',|\mathbf{q}'-\mathbf{k}'|) + \\
a^\dagger(-\mathbf{q}')A^*(\tau'',|\mathbf{q}'|)a(\mathbf{k}'-\mathbf{q}')A'(\tau'',|\mathbf{k}'-\mathbf{q}'|) + a^\dagger(-\mathbf{q}')A^*(\tau'',|\mathbf{q}'|)a^\dagger(\mathbf{q}'-\mathbf{k}')A'^*(\tau'',|\mathbf{q}'-\mathbf{k}'|)]\rangle.
\end{gathered}
\tag{D.3}
$$

It can be confirmed, that the only terms surviving after the contractions are the following

$$
\begin{gathered}
\langle \overbrace{a(\mathbf{q})\overbrace{a(\mathbf{k}-\mathbf{q})\overbrace{a^\dagger(-\mathbf{q}')a^\dagger(\mathbf{q}'-\mathbf{k}')}}}\rangle + \langle \overbrace{a(\mathbf{q})\overbrace{a(\mathbf{k}-\mathbf{q})\overbrace{a^\dagger(-\mathbf{q}')a^\dagger(\mathbf{q}'-\mathbf{k}')}}}\rangle = \\
\langle a(\mathbf{q})a^\dagger(-\mathbf{q}')\rangle\langle a(\mathbf{k}-\mathbf{q})a^\dagger(\mathbf{q}'-\mathbf{k}')\rangle + \langle a(\mathbf{q})a^\dagger(\mathbf{q}'-\mathbf{k}')\rangle\langle a(\mathbf{k}-\mathbf{q})a^\dagger(-\mathbf{q}')\rangle = \\
\delta^{(3)}(\mathbf{q}+\mathbf{q}')\delta^{(3)}(\mathbf{k}-\mathbf{q}-\mathbf{q}'+\mathbf{k}') + \delta^{(3)}(\mathbf{q}-\mathbf{q}'+\mathbf{k}')\delta^{(3)}(\mathbf{k}-\mathbf{q}+\mathbf{q}').
\end{gathered}
\tag{D.4}
$$

which simply leads to

$$
\begin{gathered}
\langle j_k(\tau') j_{k'}(\tau'')\rangle = \frac{\delta^{(3)}(\mathbf{k}+\mathbf{k}')}{4} \int \frac{d^3q}{(2\pi)^3} |\mathbf{q}| \left|1 + \frac{|\mathbf{q}|^2 - \mathbf{k}\cdot\mathbf{q}}{|\mathbf{q}||\mathbf{k}-\mathbf{q}|}\right|^2 \times \\
\Big[|\mathbf{q}|A'(\tau',q)A(\tau',|\mathbf{k}-\mathbf{q}|)A^*(\tau'',q)A'^*(\tau'',|\mathbf{k}-\mathbf{q}|) + \\
|\mathbf{k}-\mathbf{q}|A'(\tau',q)A(\tau,|\mathbf{k}-\mathbf{q})A^*(\tau'',|\mathbf{q}-\mathbf{k}|)A'^*(\tau'',q)\Big],
\end{gathered}
\tag{D.5}
$$

where we have used the relations

$$|\vec{\varepsilon}(\mathbf{q})\cdot\vec{\varepsilon}(\mathbf{k}-\mathbf{q})|^2=\frac{1}{4}\left|1+\frac{|\mathbf{q}|^2-\mathbf{k}\cdot\mathbf{q}}{|\mathbf{q}||\mathbf{k}-\mathbf{q}|}\right|^2,\qquad \vec{\varepsilon}(-\mathbf{k})=\vec{\varepsilon^*}(\mathbf{k}). \tag{D.6}$$

We proceed by plugging expressions (2.121) and (2.122) into (D.5)

$$\begin{aligned}\langle j_k(\tau')j_{k'}(\tau'')\rangle=\frac{\delta^{(3)}(\mathbf{k}+\mathbf{k}')}{16}e^{4\pi\xi}\int\frac{d^3q}{(2\pi)^3}|\mathbf{q}|\left|1+\frac{|\mathbf{q}|^2-\mathbf{k}\cdot\mathbf{q}}{|\mathbf{q}||\mathbf{k}-\mathbf{q}|}\right|^2\left[|\mathbf{q}|+|\mathbf{q}|^{1/2}|\mathbf{k}-\mathbf{q}|^{1/2}\right]\times\\ \times e^{-4\sqrt{-2\xi\tilde{\tau}}\left(\sqrt{|\mathbf{q}|}+\sqrt{|\mathbf{k}-\mathbf{q}|}\right)},\end{aligned} \tag{D.7}$$

where we define $2\tilde{\tau}=\tau'+\tau''$. Now we change the integration variable to $\mathbf{p}=\mathbf{q}/|\mathbf{k}|$ and let $\mathbf{k}||\hat{z}$. which leads to

$$\begin{aligned}\langle j_k(\tau')j_{k'}(\tau'')\rangle=\frac{\delta^{(3)}(\mathbf{k}+\mathbf{k}')}{16}\frac{k^5}{(2\pi)^3}e^{4\pi\xi}\times\\ \times\int d^3p\left|1+\frac{|\mathbf{p}|^2-\hat{z}\cdot\mathbf{p}}{|\mathbf{p}||\hat{z}-\mathbf{p}|}\right|^2|\mathbf{p}|^2\left(1+\frac{|\hat{z}-\mathbf{p}|^{1/2}}{|\mathbf{p}|^{1/2}}\right)e^{-\sqrt{\kappa}\left(\sqrt{|\mathbf{p}|}+\sqrt{|\hat{z}-\mathbf{p}|}\right)},\end{aligned} \tag{D.8}$$

where $\kappa=-2^5\xi\tilde{\tau}|\mathbf{k}|$. Evaluating this integral is highly non-trivial and requires numerical techniques. However, one can make a numerical fit for the range of values of ξ, that are relevant in terms of observations. In particular the range $2\leq\xi\leq 3$ is of particular interest, since it both complies with observations and dominates gauge production. Let $I(\xi)$ denote the integral in the equation above. After fitting the integral in (D.8) reads

$$I(\kappa)\simeq 367\times e^{-0.88\kappa},\qquad 2\leq\xi\leq 3. \tag{D.9}$$

We notice here, although it is quite clear from equation (D.7), that as expected, due to the dynamical nature of the background in which the fields evolve, assuming the environment to be stationary is an erroneous assumption. We see, this in the temporal behavior of the correlation function, whose exponential suppression appears to be weakening as we approach $\tau\longrightarrow 0$.

Nevertheless, one may identify an effective correlation time $\tau_c=(0.88\cdot 2^5\xi|\mathbf{k}|)^{-1}$ which leads to $I\propto\exp(\tilde{\tau}/\tau_c)$. This makes sense physically, since shorter wavelengths evolve faster. Notice, that the scale-dependent correlation time is a novelty in our model.

It will prove useful to calculate the correlation function for the case of large ξ. First, we notice, that for $\xi\gg 1$, the integrand is highly peaked at at $|\mathbf{p}|\ll 1$. We expand the integrand, keeping only the leading order terms

$$\langle j_k(\tau')j_{k'}(\tau'')\rangle = \frac{\delta^{(3)}(\mathbf{k}+\mathbf{k}')}{16}\frac{k^5}{(2\pi)^3}e^{4\pi\xi}\times$$
$$\times 2\pi\int_0^\pi d\theta\sin\theta\int_0^\infty dpp^4(p+1)^2(1-\cos\theta)^2(1+2p\cos\theta)\left(1+\frac{1}{\sqrt{p}}-\frac{\sqrt{p}}{2}\cos\theta\right)e^{-\sqrt{\kappa}(1+\sqrt{p})} =$$
$$= \frac{\pi\delta^{(3)}(\mathbf{k}+\mathbf{k}')}{8}\frac{k^5}{(2\pi)^3}e^{4\pi\xi}120960\pi e^{-\sqrt{\kappa}}\times$$
$$= \frac{\left(-257400\kappa^{3/2}+660\kappa^{5/2}+9\kappa^{7/2}+\kappa^4+90\kappa^3-18810\kappa^2-4684680\kappa-43243200\sqrt{\kappa}-302702400\right)}{\kappa^{17/2}}. \tag{D.10}$$

According to this expression, the power spectrum is suppressed by powers of κ, but more importantly, it is suppressed by an exponential $e^{-\sqrt{\kappa}}$.

For the Lindblad formalism, we will only require the equal-time correlation function of the environment. This is largely due to the Markovian approximation embedded in the Lindblad equation (see AppendixC).

Equation (2.121) is a good approximation for $(8\xi)^{-1}\lesssim -k\tau\lesssim 2\xi$. Hence in deriving (D.8), we must require a common region of integration space in (D.5), for which both functions A_+ can be approximated by (2.121). This automatically ensures that (2.122) is a good approximation. The requirements read (we following the analysis of [27]):

$$\frac{1}{8\xi}\lesssim -|\mathbf{q}|\tau'\lesssim 2\xi \qquad \Rightarrow \qquad \frac{1}{8\xi}\lesssim |\mathbf{p}|u\lesssim 2\xi, \tag{D.11}$$

$$\frac{1}{8\xi}\lesssim -|\mathbf{k}-\mathbf{q}|\tau'\lesssim 2\xi \qquad \Rightarrow \qquad \frac{1}{8\xi}\lesssim |\hat{z}-\mathbf{p}|u\lesssim 2\xi, \tag{D.12}$$

where $u=-k\tau'$ and $\mathbf{p}=\mathbf{q}/|\mathbf{k}|$ as before. We know that u extends from 0 to ∞ for super-horizon modes that are relevant for phenomenology. This means that for any value of $\mathbf{p}$ there exists a value of u, such that either $A_+(\tau',|\mathbf{p}|)$ or $A_+(\tau',|\hat{z}-\mathbf{p}|)$ is maximal so that it can be approximated by (2.121). On the other hand, this approximation must be valid for both modes in order to proceed. For the same u, this can only happen if $|\mathbf{p}|\simeq|\hat{z}-\mathbf{p}|$. Then the approximation in (2.121) can be used safely in the entire integration region in (D.8) if the integrand is highly peaked at $|\mathbf{p}|\simeq\mathcal{O}(1)$. We have checked explicitly that this is indeed the case.

In Appendix C, we derived a generic Lindblad equation in terms of the usual laboratory time t. In the cosmological context, this time corresponds to the cosmic time. However, one may write the cosmological Lindblad equation using some arbitrary time label (in our case the conformal time τ). In that case eq. (C.40) reads $\gamma=2g^2\tau_c$. As in section 3.4.6, one obtains the physical correlation time $t_c=a(\tau)\tau_c=(0.11\cdot 2^8\xi k_{\rm phys})^{-1}$, where $k_{\rm phys}=|\mathbf{k}|/a$. Notice also, that for a given physical scale, the correlation time decreases as ξ^{-1}, which means that more gauge field production enlarges the environment, making it act more and more like a thermal bath[35].

[35] In principle, the the correlation function for the case of large ξ (see equation(D.10)) also primarily decays expo-

Correlation function in real space. Let us Fourier transform the gauge field correlation function for ξ ranging from 2 to 3.

$$C_R(r,\tau) = \frac{367}{16}\frac{e^{4\pi\xi}}{(2\pi)^3}\int \frac{d^3k}{(2\pi)^3}k^5 e^{-\lambda k}e^{-i\mathbf{k}\cdot\mathbf{r}}, \tag{D.13}$$

where $\lambda \equiv -0.11\cdot 2^8\xi\tau > 0$ since $-\infty \leq \tau \leq 0$. We may use spherical coordinates to evaluate the integral.

$$\begin{aligned} 2\pi\int_0^\infty dk k^7 e^{-\lambda k}\int_0^\pi d\theta \sin(\theta)e^{-ikr\cos(\theta)} &= \frac{4\pi}{r}\int dk k^6 e^{-\lambda k}\sin(kr) \\ &= 4\pi\left[\frac{720}{(\lambda^2+r^2)^7}\left(7\lambda^6 - 35\lambda^4 r^2 + 21\lambda^2 r^4 - r^6\right)\right], \end{aligned} \tag{D.14}$$

where in the first equation we used the change of variables $d\theta \longrightarrow d\cos(\theta)$ to evaluate the angular integral. The second integral is listed in chapter 3 of ref [100]. Rewriting the environment correlation function

$$C_R(r,\tau) = 33030 \times \frac{e^{4\pi\xi}}{(2\pi)^5}\left[\frac{7\lambda^6 - 35\lambda^4 r^2 + 21\lambda^2 r^4 - r^6}{(\lambda^2+r^2)^7}\right]. \tag{D.15}$$

Using this expression, even though it is not an exponential decay, one can roughly estimate the effective correlation length of the environment. Namely, we see, that the correlation function decays quickly, dominated by $(\lambda^2+r^2)^7$. Thus, the correlation function decays significantly when $r \sim |\lambda|$, which we will identify as the correlation length l_c. Of course this would be the comoving length, but the physical correlation length is easily extracted using $\tau = -(aH)^{-1}$, resulting in $\ell_c = 0.11\cdot 2^8\xi/H$.

E The slow-roll approximation

The density matrix given in (3.80), can be computed explicitly if we can compute the integrals (3.81)-(3.83) exactly. To this end, we employ the slow-roll approximation. This allows us to obtain $\mathcal{I}_\mathbf{k}, \mathcal{J}_\mathbf{k}$ and $\mathcal{K}_\mathbf{k}$ which will be used to assess decoherence for axion models of inflation. In what follows we shall retain first-order slow-roll corrections.

$v_\mathbf{k}(\tau)$ in (3.80) are solutions of the following Mukhanov-Sasaki equation

$$\frac{d^2 v^s_\mathbf{k}}{d\tau^2} + \omega^2(k)v^s_\mathbf{k} = 0, \tag{E.1}$$

where at first order in the slow-roll parameters $\omega^2 \simeq k^2 - 2[1+3(2\varepsilon_* + \eta_*)/4]/\tau^2$ with ε_* and η_* being the first and the second slow-roll parameters evaluated at the time of horizon crossing of the pivot scale k_*. The full solution of this equation, normalized to the Bunch-Davies vacuum in the sub-Hubble limit is given by

$$v_\mathbf{k} = \frac{1}{2}\sqrt{\frac{\pi}{k}}\sqrt{-k\tau}H^{(2)}_\nu(-k\tau)e^{-i\frac{\pi}{2}\left(\nu+\frac{1}{2}\right)}, \tag{E.2}$$

nentially, so one could identify the correlation time to be $t_c = (0.11\cdot 2^8\xi k_{\rm phys})^{-1}$.

where $H_\nu^{(2)}(-k\tau)$ is the Henkel function of the second kind of order ν, with $\nu = 3/2 + \varepsilon_* + \eta_*/2$. In order to compute the integrals (3.81)-(3.83) we restrict our analysis to the regime $2 \geq \xi \geq 3$, where the gauge field correlation function is given by (3.159)

$$\tilde{C}_R(k, k', \tilde{\tau}) = \frac{\delta^{(3)}(\mathbf{k} + \mathbf{k}')}{16(2\pi)^3} k^5 e^{4\pi\xi} 367 \times \Theta\left(\frac{\tilde{\tau}}{\tau_c}\right). \tag{E.3}$$

and finally, at first order in the slow-roll parameters, the scale factor scales like $a \propto \tau^{-1-\varepsilon_*}$. Combining this with (C.40) gives

$$\gamma = \gamma_* \left(\frac{\tau}{\tau_*}\right)^{3(1+\varepsilon_*)}. \tag{E.4}$$

To work with the Henkel function in (E.2), we will use the following relations that allow us to express $H_\nu^{(2)}$ in terms of the Bessel function of the first kind J_ν:

$$H_\nu^{(2)}(x) = J_\nu(x) - iY_\nu(x), \tag{E.5}$$

$$\frac{dH_\nu^{(2)}(x)}{dx} = \frac{\nu}{x} H_\nu^{(2)} - H_{\nu+1}^{(2)}(x), \tag{E.6}$$

where

$$Y_\nu(x) = \frac{J_\nu \cos(\pi\nu) - J_{-\nu}(x)}{\sin(\pi\nu)}. \tag{E.7}$$

We are now ready to calculate $\mathcal{I}_\mathbf{k}$, $\mathcal{J}_\mathbf{k}$, and $\mathcal{K}_\mathbf{k}$. Since the calculation of all three parameters is similar, and $\mathcal{J}_\mathbf{k}$ is the simplest among the three to calculate, we present the derivation of $\mathcal{J}_\mathbf{k}$ as an example.

By plugging (E.2), (E.3) and (E.4) into (3.82) we obtain

$$J_\mathbf{k} = 4(2\pi)^{3/2} \gamma_* \tau_*^{-3(1+\varepsilon_*)} k^5 e^{4\pi\xi} 367(-k\tau) \frac{\pi^2}{256(2\pi)^{3/2} k^2} \times \int_{-\infty}^{\tau} d\tau' \tau'^{3(1+\varepsilon_*)} (-k\tau') \Theta\left(\frac{\tau'}{\tau_c}\right) \mathrm{Im}^2\{H_\nu^{(2)}(-k\tau') H_\nu^{(2)*}(-k\tau)\}. \tag{E.8}$$

Next we use the relations (E.5-E.7) to get

$$\mathrm{Im}^2\{H_\nu^{(2)}(-k\tau') H_\nu^{(2)*}(-k\tau)\} = \frac{1}{\sin^2(\pi\nu)} \big[J_\nu^2(-k\tau') J_{-\nu}^2(-k\tau) + J_{-\nu}^2(-k\tau') J_\nu^2(-k\tau) - 2J_\nu(-k\tau') J_{-\nu}(-k\tau') J_\nu(-k\tau) J_{-\nu}(-k\tau)\big]. \tag{E.9}$$

We plug this back and change the integration variable $\tau' \to -k\tau'$, which finally gives

$$\mathcal{J}_\mathbf{k} = \sqrt{2\pi} \frac{367 e^{4\pi\xi}}{128 k \sin^2(\pi\nu)} \left(\frac{H}{M_{\rm Pl}}\right)^2 \frac{2}{\varepsilon} \left(\frac{k}{k_*}\right)^{-3\varepsilon} \frac{\xi(-k\tau)}{\beta} \times \left[J_{-\nu}^2(-k\tau) I_1(\nu) + J_\nu^2(-k\tau) I_1(\nu) - 2J_{-\nu}(-k\tau) J_\nu(-k\tau) I_2(\nu)\right], \tag{E.10}$$

where $\beta = 0.11 \cdot 2^8$ and we have defined

$$I_1(\nu) = \int_{-k\tau}^{-k\tau_c} dx x^\alpha J_\nu^2(x), \tag{E.11}$$

and

$$I_2(\nu) = \int_{-k\tau}^{-k\tau_c} dx x^\alpha J_\nu(x) J_{-\nu}(x), \tag{E.12}$$

where $\alpha \equiv 3(1+\varepsilon_*)+1$. The upper limits on these integrals correspond to the time when the corresponding physical wavelength a/k crosses the correlation length of the environment ℓ_c. At leading order in the slow roll parameters, this condition reads

$$-k\tau_c = (1+\varepsilon_*)(H_*\ell_c)^{\varepsilon_*-1}\left(\frac{k}{k_*}\right)^{\varepsilon_*}. \tag{E.13}$$

One can check the validity of this equation explicitly at zeroth order in slow-roll parameters. Indeed our definition for the correlation length and the correlation time gives this precise result.

$\mathcal{I}_{\mathbf{k}}$ and $\mathcal{K}_{\mathbf{k}}$ can be computed in a similar fashion, resulting in the following expressions

$$\begin{aligned}\mathcal{I}_{\mathbf{k}} = -\sqrt{2\pi}\frac{367e^{4\pi\xi}}{128\sin^2(\pi\nu)}k\left(\frac{H}{M_{\rm Pl}}\right)^2\frac{2}{\varepsilon}\left(\frac{k}{k_*}\right)^{-3\varepsilon}\frac{\xi(-k\tau)^{-1}}{\beta}\times \\ \left\{\left[\left(\frac{1}{2}+\nu\right)J_{-\nu}(-k\tau)+(-k\tau)J_{-\nu-1}(-k\tau)\right]^2 I_1(\nu)+\left[\left(\frac{1}{2}+\nu\right)J_\nu(-k\tau)-\right.\right. \\ \left.-(-k\tau)J_{\nu+1}(-k\tau)\right]^2 I_1(-\nu)-2\left[\left(\frac{1}{2}+\nu\right)J_{-\nu}(-k\tau)+(-k\tau)J_{-\nu-1}(-k\tau)\right]\times \\ \left.\times\left[\left(\frac{1}{2}+\nu\right)J_\nu(-k\tau)-(-k\tau)J_{\nu+1}(-k\tau)\right]I_2(\nu)\right\},\end{aligned} \tag{E.14}$$

$$\begin{aligned}\mathcal{K}_{\mathbf{k}} = \sqrt{2\pi}\frac{367e^{4\pi\xi}}{128\sin^2(\pi\nu)}\left(\frac{H}{M_{\rm Pl}}\right)^2\frac{2}{\varepsilon}\left(\frac{k}{k_*}\right)^{-3\varepsilon}\frac{\xi}{\beta}\times \\ \times\left\{J_\nu(-k\tau)\left[\left(\frac{1}{2}+\nu\right)J_\nu(-k\tau)-(-k\tau)J_{\nu+1}(-k\tau)\right]I_1(\nu)+J_{-\nu}(-k\tau)\left[\left(\frac{1}{2}+\nu\right)J_{-\nu}(-k\tau)+\right.\right. \\ \left.(-k\tau)J_{-\nu-1}(-k\tau)\right]I_1(-\nu)-\left[(-k\tau)J_{-\nu}(-k\tau)J_{\nu+1}(-k\tau)-(-k\tau)J_\nu(-k\tau)J_{-\nu-1}(-k\tau)-\right. \\ \left.\left.-2\left(\frac{1}{2}+\nu\right)J_\nu(-k\tau)J_{-\nu}(-k\tau)\right]I_2(\nu)\right\}.\end{aligned} \tag{E.15}$$

The integrals $I_1(\nu)$ and $I_2(\nu)$ are of the Weber-Schafheitlin type and can be expressed in terms

of the generalized hypergeometric functions [2]:

$$I_1(\nu) = \frac{1}{4^\nu(1+\alpha+2\nu)\Gamma^2(1+\nu)}\times \left\{(-k\tau_c)^{1+\alpha+2\nu}\,{}_pF_q\left[\frac{1}{2}+\nu, \frac{1+\alpha}{2}+\nu; 1+\nu, \frac{3+\alpha}{2}+\nu, 1+2\nu; -(-k\tau_c)^2\right] - (-k\tau)^{1+\alpha+2\nu}\,{}_pF_q\left[\frac{1}{2}+\nu, \frac{1+\alpha}{2}+\nu; 1+\nu, \frac{3+\alpha}{2}+\nu; -(-k\tau)^2\right]\right\}, \quad \text{(E.16)}$$

$$I_2(\nu) = \frac{\sin(\pi\nu)}{\pi\nu(1+\alpha)}\times \left\{(-k\tau_c)^{1+\alpha}\,{}_pF_q\left[\frac{1}{2}, \frac{1+\alpha}{2}; \frac{3+\alpha}{2}, 1-\nu, 1+\nu; -(-k\tau_c)^2\right] - (-k\tau)^{1+\alpha}\,{}_pF_q\left[\frac{1}{2}, \frac{1+\alpha}{2}; \frac{3+\alpha}{2}, 1-\nu, 1+\nu; -(-k\tau)^2\right]\right\}. \quad \text{(E.17)}$$

These expressions are exact, but they lack insight due to their complicated form. For this reason, two approximations can be made [2]. The first limit comes from the regime we are considering, namely $2 \lesssim \xi \lesssim 3$. Since by our definition the (conformal) correlation time is $\tau_c = (0.11 \cdot 2^8 \xi k)^{-1}$, we immediately see, that for values $\xi \gtrsim \mathcal{O}(1)$, we have $-k\tau_c \ll 1$.[36] The second approximation consists of considering the above expressions when the physical wavelength a/k has crossed well outside the Hubble radius H^{-1}. This regime is important since all modes of astrophysical interest today were outside the horizon near the end of inflation. This condition is expressed as $-k\tau \ll 1$. Using these approximations would mean expanding the hypergeometric functions in (E.16) and (E.17) in the small third arguments. The outcome can be written as follows

$$I_1(\nu) \simeq \frac{1}{4^\nu(1+\alpha+2\nu)\Gamma^2(1+\nu)}\left[(-k\tau_c)^{1+\alpha+2\nu} - (-k\tau)^{1+\alpha+2\nu}\right], \quad \text{(E.18)}$$

$$I_2(\nu) \simeq \frac{\sin(\pi\nu)}{\pi\nu(1+\alpha)}\left[(-k\tau_c)^{1+\alpha} - (-k\tau)^{1+\alpha}\right]. \quad \text{(E.19)}$$

In order to assess decoherence, we need to calculate the decoherence parameter $\delta_{\mathbf{k}}(\tau) \simeq |v_{\mathbf{k}}|^2\mathcal{I}_{\mathbf{k}} + |v'_{\mathbf{k}}|^2\mathcal{J}_{\mathbf{k}} - |v_{\mathbf{k}}|^{2'}\mathcal{K}_{\mathbf{k}}$ (see section 3.4.7). Here we also present $|v_{\mathbf{k}}|^2$, $|v'_{\mathbf{k}}|^2$ and $|v_{\mathbf{k}}|^{2'}$ at first order in slow roll:

$$|v_{\mathbf{k}}|^2 = \frac{\pi}{4\sin^2(\pi\nu)}\frac{(-k\tau)}{k}\left(J_\nu^2(-k\tau) + J_{-\nu}^2(-k\tau) - 2J_\nu(-k\tau)J_{-\nu}(-k\tau)\cos(\pi\nu)\right), \quad \text{(E.20)}$$

[36] Note, that according to (E.13) this also implies $H_*\ell_c \gg 1$. On the contrary, for the massive scalar field environment, Ref. [2] used $H_*\ell_c \ll 1$, which can be traced back to the fact, that in case of the gauge field environment the correlation time is actually larger than the Hubble scale.

$$|v_{\mathbf{k}}'|^2 = \frac{\pi k}{4\sin^2(\pi\nu)}(-k\tau)^{-1}\Bigg\{\left(\frac{1}{2}+\nu\right)^2\left(J_\nu^2(-k\tau)-2J_\nu(-k\tau)J_{-\nu}(-k\tau)\cos(\pi\nu)+J_{-\nu}^2(-k\tau)\right)$$
$$+(-k\tau)^2\left(J_{\nu+1}^2(-k\tau)+2J_{\nu+1}(-k\tau)J_{-\nu-1}(-k\tau)\cos(\pi\nu)+J_{-\nu-1}^2(-k\tau)\right)$$
$$-2\left(\frac{1}{2}+\nu\right)(-k\tau)\big[J_\nu(-k\tau)J_{\nu+1}(-k\tau)-(J_{-\nu}(-k\tau)J_{\nu+1}(-k\tau)-J_\nu(-k\tau)J_{-\nu-1}(-k\tau))\cos(\pi\nu)$$
$$-J_{-\nu}(-k\tau)J_{-\nu-1}(-k\tau)\big]\Bigg\}, \quad \text{(E.21)}$$

$$|v_{\mathbf{k}}|^{2'} = -\frac{\pi}{4\sin^2(\pi\nu)}\Bigg\{\left(J_\nu^2(-k\tau)+2(-k\tau)J_\nu(-k\tau)\left[\frac{\nu}{-k\tau}J_\nu(-k\tau)-J_{\nu+1}(-k\tau)\right]\right)$$
$$+\left(-J_{-\nu}^2(-k\tau)+2(-k\tau)J_{-\nu}(-k\tau)\left[J_{-\nu-1}-\frac{\nu}{(-k\tau)}J_{-\nu}(-k\tau)\right]\right)-2\Bigg(J_\nu(-k\tau)J_{-\nu}(-k\tau)\cos(\pi\nu)$$
$$-(-k\tau)\left[\frac{\nu}{(-k\tau)}J_\nu(-k\tau)-J_{\nu+1}(-k\tau)\right]J_{-\nu}(-k\tau)\cos(\pi\nu)-(-k\tau)J_\nu(-k\tau)\left[J_{-\nu-1}-\frac{\nu}{(-k\tau)}J_{-\nu}(-k\tau)\right]\cos(\pi\nu)\Bigg)\Bigg\}, \quad \text{(E.22)}$$

When computing the decoherence parameter, many cancellations occur leading to $\delta_{\mathbf{k}} \propto [I_1(\nu) + I_1(-\nu) - 2I_2(\nu)\cos(\pi\nu)]$, see (3.186). It can be shown through simple analysis that the dominant term comes from $I_1(-\nu)$.

As we have seen in equation (3.89), the correction to the power spectrum corresponds exactly to $\mathcal{J}_{\mathbf{k}}/|v_{\mathbf{k}}|^2$. We apply the same approximations, $-k\tau_c \ll 1$ and $-k\tau \ll 1$ to (E.10) and (E.20) that leads to

$$\frac{\mathcal{J}_{\mathbf{k}}}{|v_{\mathbf{k}}|^2} = -\sqrt{\frac{2}{\pi}}\frac{367e^{4\pi\xi}}{32}\left(\frac{H}{M_{\rm Pl}}\right)^2\frac{2}{\varepsilon}\left(\frac{k}{k_*}\right)^{-3\varepsilon}\frac{\xi}{\beta}\Gamma^2(1-\nu)\frac{\sin^2(\pi\nu)}{\pi^2\nu^2}\times$$
$$\Bigg\{\frac{1}{4^\nu(1-\alpha+2\nu)}\left[(-k\tau_c)^{1+\alpha+2\nu}-(-k\tau)^{1+\alpha+2\nu}\right]+\frac{2^{-4\nu}(-k\tau)^{4\nu}}{4^{-\nu}(1-\alpha-2\nu)}\left[(-k\tau_c)^{1+\alpha-2\nu}-(-k\tau)^{1+\alpha-2\nu}\right]$$
$$-2\frac{2^{-2\nu}(-k\tau)^{2\nu}}{1+\alpha}\left[(-k\tau_c)^{1+\alpha}-(-k\tau)^{1+\alpha}\right]\Bigg\}. \quad \text{(E.23)}$$

It will also be interesting, to consider a more complicated form of correlation function (D.8) which should be more precise compared to the top-hat approximation. Following this direction, however, means that abandoning the prospect of an analytical solution. Yet, exploring this complicated version of the correlation function will allow us to compare it with the top-hat approximation used before. It is easy to confirm, the functions $\mathcal{I}, \mathcal{J}$ and $\mathcal{K}$ are quite similar to those seen before, which

is expected, since we only change the form of the correlation function

$$\mathcal{I}_{\mathbf{k}} = \sqrt{2\pi}\frac{e^{4\pi\xi}}{128\sin^2(\pi\nu)}k\left(\frac{H}{M_{\rm Pl}}\right)^2\frac{2}{\varepsilon}\left(\frac{k}{k_*}\right)^{-3\varepsilon}\frac{\xi(-k\tau)^{-1}}{\beta}\times$$
$$\left\{\left[\left(\frac{1}{2}+\nu\right)J_{-\nu}(-k\tau)+(-k\tau)J_{-\nu-1}(-k\tau)\right]^2F_1(\nu)+\left[\left(\frac{1}{2}+\nu\right)J_{\nu}(-k\tau)-\right.\right.$$
$$-(-k\tau)J_{\nu+1}(-k\tau)\Big]^2F_1(-\nu)-2\left[\left(\frac{1}{2}+\nu\right)J_{-\nu}(-k\tau)+(-k\tau)J_{-\nu-1}(-k\tau)\right]\times$$
$$\left.\times\left[\left(\frac{1}{2}+\nu\right)J_{\nu}(-k\tau)-(-k\tau)J_{\nu+1}(-k\tau)\right]F_2(\nu)\right\}, \quad \text{(E.24)}$$

$$\mathcal{J}_{\mathbf{k}} = \sqrt{2\pi}\frac{e^{4\pi\xi}}{128k\sin^2(\pi\nu)}\left(\frac{H}{M_{\rm Pl}}\right)^2\frac{2}{\varepsilon}\left(\frac{k}{k_*}\right)^{-3\varepsilon}\frac{\xi(-k\tau)}{\beta}\times$$
$$\times\left[J^2_{-\nu}(-k\tau)F_1(\nu)+J^2_{\nu}(-k\tau)F_1(\nu)-2J_{-\nu}(-k\tau)J_{\nu}(-k\tau)F_2(\nu)\right], \quad \text{(E.25)}$$

$$\mathcal{K}_{\mathbf{k}} = \sqrt{2\pi}\frac{e^{4\pi\xi}}{128\sin^2(\pi\nu)}\left(\frac{H}{M_{\rm Pl}}\right)^2\frac{2}{\varepsilon}\left(\frac{k}{k_*}\right)^{-3\varepsilon}\frac{\xi}{\beta}\times$$
$$\times\left\{J_{\nu}(-k\tau)\left[\left(\frac{1}{2}+\nu\right)J_{\nu}(-k\tau)-(-k\tau)J_{\nu+1}(-k\tau)\right]F_1(\nu)+J_{-\nu}(-k\tau)\Big[\left(\frac{1}{2}+\nu\right)J_{-\nu}(-k\tau)+\right.$$
$$(-k\tau)J_{-\nu-1}(-k\tau)\Big]F_1(-\nu)-\Big[(-k\tau)J_{-\nu}(-k\tau)J_{\nu+1}(-k\tau)-(-k\tau)J_{\nu}(-k\tau)J_{-\nu-1}(-k\tau)-$$
$$\left.-2\left(\frac{1}{2}+\nu\right)J_{\nu}(-k\tau)J_{-\nu}(-k\tau)\Big]F_2(\nu)\right\}, \quad \text{(E.26)}$$

where

$$F_1(\nu) = \int d^3p\left|1+\frac{|\mathbf{p}|^2-\hat{z}\cdot\mathbf{p}}{|\mathbf{p}||\hat{z}-\mathbf{p}|}\right|^2|\mathbf{p}|^2\left(1+\frac{|\hat{z}-\mathbf{p}|^{1/2}}{|\mathbf{p}|^{1/2}}\right)\int_{-k\tau}^{\infty}dx x^{\alpha}J^2_{\nu}(x)e^{-\sqrt{\kappa}\left(\sqrt{|\mathbf{p}|}+\sqrt{|\hat{z}-\mathbf{p}|}\right)}, \quad \text{(E.27)}$$

$$F_2(\nu) = \int d^3p\left|1+\frac{|\mathbf{p}|^2-\hat{z}\cdot\mathbf{p}}{|\mathbf{p}||\hat{z}-\mathbf{p}|}\right|^2|\mathbf{p}|^2\left(1+\frac{|\hat{z}-\mathbf{p}|^{1/2}}{|\mathbf{p}|^{1/2}}\right)\int_{-k\tau}^{\infty}dx x^{\alpha}J_{\nu}(x)J_{-\nu}(x)e^{-\sqrt{\kappa}\left(\sqrt{|\mathbf{p}|}+\sqrt{|\hat{z}-\mathbf{p}|}\right)}, \quad \text{(E.28)}$$

with x and α defined as in equations (E.11-E.12). We can evaluate these integrals numerically by fitting, see Sec. 3.5.3.

References

[1] Alan H Guth. Inflationary universe: A possible solution to the horizon and flatness problems. *Physical Review D*, 23(2):347, 1981.

[2] Jerome Martin and Vincent Vennin. Observational constraints on quantum decoherence during inflation. *Journal of Cosmology and Astroparticle Physics*, 2018(05):063, 2018.

[3] Jérôme Martin and Vincent Vennin. Non gaussianities from quantum decoherence during inflation. *Journal of Cosmology and Astroparticle Physics*, 2018(06):037, 2018.

[4] Aoumeur Daddi Hammou and Nicola Bartolo. Cosmic decoherence: primordial power spectra and non-gaussianities. *Journal of Cosmology and Astroparticle Physics*, 2023(04):055, 2023.

[5] Jessie de Kruijf and Nicola Bartolo. The effect of quantum decoherence on inflationary gravitational waves. *Journal of Cosmology and Astroparticle Physics*, 2024(11):041, 2024.

[6] Jérôme Martin, Amaury Micheli, and Vincent Vennin. Discord and decoherence. *Journal of Cosmology and Astroparticle Physics*, 2022(04):051, 2022.

[7] CP Burgess, R Holman, Greg Kaplanek, Jerome Martin, and Vincent Vennin. Minimal decoherence from inflation. *Journal of Cosmology and Astroparticle Physics*, 2023(07):022, 2023.

[8] Jerome Martin and Vincent Vennin. Obstructions to bell cmb experiments. *Physical Review D*, 96(6):063501, 2017.

[9] CP Burgess, R Holman, and D Hoover. On the decoherence of primordial fluctuations during inflation. *arXiv preprint astro-ph/0601646*, 2006.

[10] Francescopaolo Lopez and Nicola Bartolo. Quantum signatures and decoherence during inflation from deep subhorizon perturbations. *arXiv preprint arXiv:2503.23150*, 2025.

[11] Goran Lindblad. On the generators of quantum dynamical semigroups. *Communications in mathematical physics*, 48:119–130, 1976.

[12] Vittorio Gorini, Andrzej Kossakowski, and Ennackal Chandy George Sudarshan. Completely positive dynamical semigroups of n-level systems. *Journal of Mathematical Physics*, 17(5):821–825, 1976.

[13] Fernando C Lombardo and Diana Lopez Nacir. Decoherence during inflation: The generation of classical inhomogeneities. *Physical Review D—Particles, Fields, Gravitation, and Cosmology*, 72(6):063506, 2005.

[14] Elliot Nelson. Quantum decoherence during inflation from gravitational nonlinearities. *Journal of Cosmology and Astroparticle Physics*, 2016(03):022, 2016.

[15] D Boyanovsky. Effective field theory during inflation: Reduced density matrix and its quantum master equation. *Physical Review D*, 92(2):023527, 2015.

[16] Rémi Adam, Peter AR Ade, N Aghanim, Y Akrami, MIR Alves, F Argüeso, M Arnaud, F Arroja, Mark Ashdown, J Aumont, et al. Planck 2015 results-i. overview of products and scientific results. *Astronomy & Astrophysics*, 594:A1, 2016.

[17] PAR Ade, N Aghanim, M Arnaud, F Arroja, Mark Ashdown, J Aumont, Carlo Baccigalupi, Mario Ballardini, AJ Banday, RB Barreiro, et al. Planck 2015 results-xx. constraints on inflation. *Astronomy & Astrophysics*, 594:A20, 2016.

[18] Peter AR Ade, N Aghanim, M Arnaud, F Arroja, M Ashdown, J Aumont, C Baccigalupi, M Ballardini, AJ Banday, RB Barreiro, et al. Planck 2015 results-xvii. constraints on primordial non-gaussianity. *Astronomy & Astrophysics*, 594:A17, 2016.

[19] Katherine Freese, Joshua A Frieman, and Angela V Olinto. Natural inflation with pseudo nambu-goldstone bosons. *Physical Review Letters*, 65(26):3233, 1990.

[20] Nina K Stein and William H Kinney. Natural inflation after planck 2018. *Journal of Cosmology and Astroparticle Physics*, 2022(01):022, 2022.

[21] Eva Silverstein and Alexander Westphal. Monodromy in the cmb: gravity waves and string inflation. *Physical Review D—Particles, Fields, Gravitation, and Cosmology*, 78(10):106003, 2008.

[22] Nemanja Kaloper and Lorenzo Sorbo. A natural framework for chaotic inflation. *Physical review letters*, 102(12):121301, 2009.

[23] Nemanja Kaloper, Albion Lawrence, and Lorenzo Sorbo. An ignoble approach to large field inflation. *Journal of Cosmology and Astroparticle Physics*, 2011(03):023, 2011.

[24] Jihn E Kim, Hans Peter Nilles, and Marco Peloso. Completing natural inflation. *Journal of Cosmology and Astroparticle Physics*, 2005(01):005, 2005.

[25] Mohamed M Anber and Lorenzo Sorbo. N-flationary magnetic fields. *Journal of Cosmology and Astroparticle Physics*, 2006(10):018, 2006.

[26] Peter Adshead and Mark Wyman. Natural inflation on a steep potential with classical non-abelian gauge fields. *Physical review letters*, 108(26):261302, 2012.

[27] Neil Barnaby, Ryo Namba, and Marco Peloso. Phenomenology of a pseudo-scalar inflaton: naturally large nongaussianity. *Journal of Cosmology and Astroparticle Physics*, 2011(04):009, 2011.

[28] David Polarski and Alexei A Starobinsky. Semiclassicality and decoherence of cosmological perturbations. *Classical and Quantum Gravity*, 13(3):377, 1996.

[29] Andreas Albrecht, Pedro Ferreira, Michael Joyce, and Tomislav Prokopec. Inflation and squeezed quantum states. *Physical Review D*, 50(8):4807, 1994.

[30] Peter Coles and Francesco Lucchin. *Cosmology: The origin and evolution of cosmic structure*. John Wiley & Sons, 2003.

[31] Edward Kolb. *The early universe*. CRC press, 2018.

[32] David H Lyth and Andrew R Liddle. *The primordial density perturbation: Cosmology, inflation and the origin of structure*. Cambridge university press, 2009.

[33] Steven Weinberg. *Cosmology*. OUP Oxford, 2008.

[34] NV Krishnendu and Frank Ohme. Testing general relativity with gravitational waves: An overview. *Universe*, 7(12):497, 2021.

[35] Daniel Baumann. Tasi lectures on inflation. *arXiv preprint arXiv:0907.5424*, 2009.

[36] Stephen W Hawking. The development of irregularities in a single bubble inflationary universe. *Physics Letters B*, 115(4):295–297, 1982.

[37] Alexei A Starobinsky. Dynamics of phase transition in the new inflationary universe scenario and generation of perturbations. *Physics Letters B*, 117(3-4):175–178, 1982.

[38] Alan H Guth and So-Young Pi. Fluctuations in the new inflationary universe. *Physical Review Letters*, 49(15):1110, 1982.

[39] M Chiara Guzzetti, Nicola Bartolo, Michele Liguori, and Sabino Matarrese. Gravitational waves from inflation. *La Rivista del Nuovo Cimento*, 39:399–495, 2016.

[40] H Dieter Zeh. On the interpretation of measurement in quantum theory. *Foundations of Physics*, 1(1):69–76, 1970.

[41] Michel Brune, E Hagley, J Dreyer, X Maitre, Abdelhamid Maali, Ch Wunderlich, Jean-Michel Raimond, and Serge Haroche. Observing the progressive decoherence of the "meter" in a quantum measurement. *Physical review letters*, 77(24):4887, 1996.

[42] LP Grishchuk and Yu V Sidorov. Squeezed quantum states of relic gravitons and primordial density fluctuations. *Physical Review D*, 42(10):3413, 1990.

[43] Ivan Agullo, Béatrice Bonga, and Patricia Ribes Metidieri. Does inflation squeeze cosmological perturbations? *Journal of Cosmology and Astroparticle Physics*, 2022(09):032, 2022.

[44] VV Dodonov. Nonclassical'states in quantum optics: asqueezed'review of the first 75 years. *Journal of Optics B: Quantum and Semiclassical Optics*, 4(1):R1, 2002.

[45] Julien Lesgourgues, David Polarski, and Alexei A Starobinsky. Quantum-to-classical transition of cosmological perturbations for non-vacuum initial states. *Nuclear Physics B*, 497(1-2):479–508, 1997.

[46] Claus Kiefer, David Polarski, and Alexei A Starobinsky. Quantum-to-classical transition for fluctuations in the early universe. *International Journal of Modern Physics D*, 7(03):455–462, 1998.

[47] Claus Kiefer, Julien Lesgourgues, David Polarski, and Alexei A Starobinsky. The coherence of primordial fluctuations produced during inflation. *Classical and Quantum Gravity*, 15(10):L67, 1998.

[48] Claus Kiefer and David Polarski. Why do cosmological perturbations look classical to us? *Advanced science letters*, 2(2):164–173, 2009.

[49] Jerome Martin and Vincent Vennin. Quantum discord of cosmic inflation: Can we show that cmb anisotropies are of quantum-mechanical origin? *Physical Review D*, 93(2):023505, 2016.

[50] Viatcheslav F Mukhanov, Hume A Feldman, and Robert Hans Brandenberger. Theory of cosmological perturbations. *Physics reports*, 215(5-6):203–333, 1992.

[51] Thomas Colas. *Open Effective Field Theories for primordial cosmology: dissipation, decoherence and late-time resummation of cosmological inhomogeneities*. PhD thesis, Université Paris-Saclay, 2023.

[52] Nicholas David Birrell and Paul Charles William Davies. Quantum fields in curved space. 1984.

[53] Jérôme Martin, Christophe Ringeval, Roberto Trotta, and Vincent Vennin. The best inflationary models after planck. *Journal of Cosmology and Astroparticle Physics*, 2014(03):039, 2014.

[54] Fred C Adams, J Richard Bond, Katherine Freese, Joshua A Frieman, and Angela V Olinto. Natural inflation: Particle physics models, power-law spectra for large-scale structure, and constraints from the cosmic background explorer. *Physical Review D*, 47(2):426, 1993.

[55] Enrico Pajer and Marco Peloso. A review of axion inflation in the era of planck. *Classical and Quantum Gravity*, 30(21):214002, 2013.

[56] Christopher Savage, Katherine Freese, and William H Kinney. Natural inflation: Status after wmap 3-year data. *Physical Review D—Particles, Fields, Gravitation, and Cosmology*, 74(12):123511, 2006.

[57] Tom Banks, Michael Dine, Patrick J Fox, and Elie Gorbatov. On the possibility of large axion decay constants. *Journal of cosmology and astroparticle physics*, 2003(06):001, 2003.

[58] Renata Kallosh, Andrei Linde, Dmitri Linde, and Leonard Susskind. Gravity and global symmetries. *Physical Review D*, 52(2):912, 1995.

[59] Mohamed M Anber and Lorenzo Sorbo. Naturally inflating on steep potentials through electromagnetic dissipation. *Physical Review D—Particles, Fields, Gravitation, and Cosmology*, 81(4):043534, 2010.

[60] Nima Arkani-Hamed, Hsin-Chia Cheng, Paolo Creminelli, and Lisa Randall. Extranatural inflation. *Physical review letters*, 90(22):221302, 2003.

[61] Savas Dimopoulos, Shamit Kachru, John McGreevy, and Jay G Wacker. N-flation. *Journal of Cosmology and Astroparticle Physics*, 2008(08):003, 2008.

[62] Richard Easther and Liam McAllister. Random matrices and the spectrum of n-flation. *Journal of cosmology and astroparticle physics*, 2006(05):018, 2006.

[63] Neil Barnaby and Marco Peloso. Large non-gaussianity in axion inflation. *Physical review letters*, 106(18):181301, 2011.

[64] Neil Barnaby, Enrico Pajer, and Marco Peloso. Gauge field production in axion inflation: Consequences for monodromy, non-gaussianity¡? format?¿ in the cmb, and gravitational waves at interferometers. *Physical Review D—Particles, Fields, Gravitation, and Cosmology*, 85(2):023525, 2012.

[65] Decoherence Schlosshauer. the quantum-to-classical transition. *The Frontiers Collection (Springer-Verlag, 2007)*, 2007.

[66] Heinz-Peter Breuer and Francesco Petruccione. *The theory of open quantum systems*. Oxford University Press, USA, 2002.

[67] Maximilian Schlosshauer. The quantum-to-classical transition and decoherence. *arXiv preprint arXiv:1404.2635*, 2014.

[68] Maximilian Schlosshauer. Quantum decoherence. *Physics Reports*, 831:1–57, 2019.

[69] Thomas Colas, Julien Grain, and Vincent Vennin. Four-mode squeezed states: two-field quantum systems and the symplectic group sp (4, r). *The European Physical Journal C*, 82(1):6, 2022.

[70] Angel Rivas and Susana F Huelga. *Open quantum systems*, volume 10. Springer, 2012.

[71] Peter Adshead, John T Giblin Jr, Timothy R Scully, and Evangelos I Sfakianakis. Gauge-preheating and the end of axion inflation. *Journal of Cosmology and Astroparticle Physics*, 2015(12):034, 2015.

[72] Thomas Colas, Julien Grain, and Vincent Vennin. Benchmarking the cosmological master equations. *The European Physical Journal C*, 82(12):1085, 2022.

[73] Y. Akrami et al. Planck 2018 results. X. Constraints on inflation. *Astron. Astrophys.*, 641:A10, 2020.

[74] Jessica L Cook and Lorenzo Sorbo. Particle production during inflation and gravitational waves detectable by ground-based interferometers. *Physical Review D—Particles, Fields, Gravitation, and Cosmology*, 85(2):023534, 2012.

[75] Nicola Bartolo, Chiara Caprini, Valerie Domcke, Daniel G Figueroa, Juan Garcia-Bellido, Maria Chiara Guzzetti, Michele Liguori, Sabino Matarrese, Marco Peloso, Antoine Petiteau, et al. Science with the space-based interferometer lisa. iv: Probing inflation with gravitational waves. *Journal of Cosmology and Astroparticle Physics*, 2016(12):026, 2016.

[76] P Daniel Meerburg and Enrico Pajer. Observational constraints on gauge field production in axion inflation. *Journal of Cosmology and Astroparticle Physics*, 2013(02):017, 2013.

[77] Jérôme Martin, Amaury Micheli, and Vincent Vennin. Comparing quantumness criteria. *Europhysics Letters*, 142(1):18001, 2023.

[78] David Campo and Renaud Parentani. Inflationary spectra and violations of bell inequalities. *Physical Review D—Particles, Fields, Gravitation, and Cosmology*, 74(2):025001, 2006.

[79] Juan Maldacena. A model with cosmological bell inequalities. *Fortschritte der Physik*, 64(1):10–23, 2016.

[80] Samuel M Leach, Misao Sasaki, David Wands, and Andrew R Liddle. Enhancement of superhorizon scale inflationary curvature perturbations. *Physical Review D*, 64(2):023512, 2001.

[81] Konrad Banaszek and Krzysztof Wódkiewicz. Testing quantum nonlocality in phase space. *Physical review letters*, 82(10):2009, 1999.

[82] M Revzen, PA Mello, A Mann, and LM Johansen. Bell's inequality violation with non-negative wigner functions. *Physical Review A—Atomic, Molecular, and Optical Physics*, 71(2):022103, 2005.

[83] G Gour, FC Khanna, A Mann, and M Revzen. Optimization of bell's inequality violation for continuous variable systems. *Physics Letters A*, 324(5-6):415–419, 2004.

[84] Richard Jozsa and Noah Linden. On the role of entanglement in quantum-computational speed-up. *Proceedings of the Royal Society of London. Series A: Mathematical, Physical and Engineering Sciences*, 459(2036):2011–2032, 2003.

[85] Artur K Ekert. Quantum cryptography based on bell's theorem. *Physical review letters*, 67(6):661, 1991.

[86] Stefano Pironio, Antonio Acín, Serge Massar, A Boyer de La Giroday, Dzmitry N Matsukevich, Peter Maunz, Steven Olmschenk, David Hayes, Lefroy Luo, T Andrew Manning, et al. Random numbers certified by bell's theorem. *Nature*, 464(7291):1021–1024, 2010.

[87] John F Clauser, Michael A Horne, Abner Shimony, and Richard A Holt. Proposed experiment to test local hidden-variable theories. *Physical review letters*, 23(15):880, 1969.

[88] Reinhard F Werner. Quantum states with einstein-podolsky-rosen correlations admitting a hidden-variable model. *Physical Review A*, 40(8):4277, 1989.

[89] Leah Henderson and Vlatko Vedral. Classical, quantum and total correlations. *Journal of physics A: mathematical and general*, 34(35):6899, 2001.

[90] Harold Ollivier and Wojciech H Zurek. Quantum discord: a measure of the quantumness of correlations. *Physical review letters*, 88(1):017901, 2001.

[91] Anindita Bera, Tamoghna Das, Debasis Sadhukhan, Sudipto Singha Roy, Aditi Sen De, and Ujjwal Sen. Quantum discord and its allies: a review of recent progress. *Reports on Progress in Physics*, 81(2):024001, 2017.

[92] Marco G Genoni, Mattia L Palma, Tommaso Tufarelli, Stefano Olivares, MS Kim, and Matteo GA Paris. Detecting quantum non-gaussianity via the wigner function. *Physical Review A—Atomic, Molecular, and Optical Physics*, 87(6):062104, 2013.

[93] Josef Weinbub and DK Ferry. Recent advances in wigner function approaches. *Applied Physics Reviews*, 5(4), 2018.

[94] Gerardo Adesso, Sammy Ragy, and Antony R Lee. Continuous variable quantum information: Gaussian states and beyond. *Open Systems & Information Dynamics*, 21(01n02):1440001, 2014.

[95] Bonny L Schumaker and Carlton M Caves. New formalism for two-photon quantum optics. ii. mathematical foundation and compact notation. *Physical Review A*, 31(5):3093, 1985.

[96] Eric Joos and H Dieter Zeh. The emergence of classical properties through interaction with the environment. *Zeitschrift für Physik B Condensed Matter*, 59:223–243, 1985.

[97] Wojciech H Zurek. Pointer basis of quantum apparatus: Into what mixture does the wave packet collapse? *Physical review D*, 24(6):1516, 1981.

[98] David Campo and Renaud Parentani. Decoherence and entropy of primordial fluctuations. i. formalism and interpretation. *Physical Review D—Particles, Fields, Gravitation, and Cosmology*, 78(6):065044, 2008.

[99] Rajiah Simon. Peres-horodecki separability criterion for continuous variable systems. *Physical Review Letters*, 84(12):2726, 2000.

[100] Izrail Solomonovich Gradshteyn and Iosif Moiseevich Ryzhik. *Table of integrals, series, and products*. Academic press, 2014.